

significantly predict MSI-L from MSS. More importantly, in multivariate analysis, beta-catenin, CK20 and Cdx2 were independent predictors of MSI-L and together strongly discriminating (AUC=0.82). These features could be combined into a single score and visualized as an algorithm for the prediction of MSI-L. The parameter estimates from logistic regression analysis were used as weights for each marker then a total score and probability of MSI-L were obtained.

Conclusions: These results suggest that in contrast to MSS, MSI-L cancers may not frequently arise through deregulation of WNT pathway signaling. In addition, a simple combined score of beta-catenin, CK20 and Cdx2 may be useful as a predictive algorithm for the MSI-L status.

Genitourinary

779 KRAS Mutation Is Present in a Small Subset of Primary Urinary Bladder Adenocarcinomas

RE Alexander, A Lopez-Beltran, R Montironi, GT MacLennan, GR Chen, KM Post, SA Bilbo, JD Sen, K Meehan, A Cornwell, L Cheng. Indiana University School of Medicine, Indianapolis, IN; Cordoba University, Cordoba, Spain; Polytechnic University of the Marche Region (Ancona), United Hospitals, Ancona, Italy; Case Western Reserve University, Cleveland, OH; First Affiliated Hospital of Wenzhou Medical College, Wenzhou, China.

Background: The realization that the presence of KRAS mutations is a near absolute contraindication to the use of EGFR-targeted therapies in colonic adenocarcinoma and non-small cell lung carcinoma has significantly altered the clinical management of individual patients with these types of cancer. The aim of this study is to determine whether KRAS mutations occur in primary bladder adenocarcinoma and/or urothelial carcinoma with glandular differentiation.

Design: Twenty cases of primary bladder adenocarcinoma were identified. Clinical histories and hematoxylin and eosin slides of each case were reviewed to confirm primary bladder origin. An additional 5 cases of urothelial carcinoma with significant degree of glandular differentiation were included. DNA was extracted from formalin-fixed paraffin embedded tissue, amplified with Shifted Assay Termination (STA) technology. The STA reaction recognizes wild type or mutant target sequences and selectively extends detection primers with 1 to 20 labeled nucleotides. This extension is repeated 20 times to enrich the mutation signal. The enriched mutation signals are then detected by capillary electrophoresis fragment analysis. The PCR amplification products were analyzed on an ABI-3130XL analyzer with GeneMapper® software (Applied Biosystems® Inc., Foster City, CA). Analysis included 6 different mutations on codon 12 (G12C, G12V, G12S, G12D, G12R, G12A) and codon 13 (G13C, G13V, G13S, G13D, G13R, G13A) along with negative and positive controls. 55 cases of colonic adenocarcinomas were also analyzed.

Results: Two of twenty (10%) cases of primary urinary bladder adenocarcinoma were found to contain a KRAS mutation. Both cases exhibited G13D mutations on codon 13. None of the 5 cases of urothelial carcinoma with glandular differentiation displayed KRAS mutation. Eighteen (33%) of 55 cases of colonic adenocarcinoma contained a KRAS mutation.

Conclusions: KRAS mutations are present in a small subset of primary urinary bladder adenocarcinomas, suggesting a possible role in tumorigenesis. KRAS mutations do not provide a means of distinguishing between primary urinary bladder adenocarcinoma and primary colonic adenocarcinoma.

780 Gleason Pattern 5 Is Frequently Underdiagnosed on Prostate Needle Core Biopsy

T Al-Hussain, MS Nagar, JI Epstein. The Johns Hopkins Hospital, Baltimore.

Background: The current study assesses underdiagnosing Gleason pattern 5 on biopsy and discuss the potential consequences for patient management.

Design: We retrieved 300 consecutive prostate biopsy cases from our consultation files from 2009-2010 in which we identified Gleason pattern 5. All cases were diagnosed by one expert GU pathologist, and were sent in as a final diagnosis, where the outside pathologist was not requesting consultation as a result of difficulty with the diagnosis. Cases typically were sent for consultation at the request of the patient or the outside treating physician.

Results: Table compares Gleason grades rendered upon expert review (EXP) compared to those at the outside institutions (OS).

	OS 3+3=6	OS3+4=7	OS4+3=7	OS3+5=8	OS5+3=8	OS4+4=8
EXP3+5=8	2 (6.5%)	15 (48.4%)	1 (3.2%)	10 (32.2%)	0	1 (3.2%)
EXP5+3=8	0	0	4 (44.5%)	0	3 (33.3%)	1 (11.1%)
EXP4+5=9	1 (0.8%)	11 (8.8%)	21 (16.8%)	3 (2.4%)	1 (0.8%)	51 (40.8%)
EXP5+4=9	0	1 (1.4%)	5 (7.0%)	2 (2.8%)	1 (1.4%)	24 (33.3%)
EXP5+5=10	0	0	0	1 (1.6%)	1 (1.6%)	8 (12.7%)

	OS4+5=9	OS5+4=9	OS5+5=10	Total
EXP3+5=8	2 (6.5%)	0	0	31 (100%)
EXP5+3=8	1 (11.1%)	0	0	9 (100%)
EXP4+5=9	33 (26.4%)	4 (3.2%)	0	125 (100%)
EXP5+4=9	23 (31.9%)	15 (20.8%)	1 (1.4%)	72 (100%)
EXP5+5=10	19 (30.1%)	8 (12.7%)	26 (41.3%)	63 (100%)

Of the 300 cases, 203 cases (68%) were under-graded, 93 cases (31%) were graded the same, and 4 cases (1%) were overgraded relative to the grade assigned by the expert pathologist. In 146 (48.7%) of the cases, Gleason Pattern 5 was not identified by the outside pathologists. Of the 146 cases, the outside Gleason score was ≤ 7 in 61 (20.3%) and 4+4=8 in 85 (28.4%) of the cases. Even when the tumor was diagnosed

at our institution as Gleason score 5+5=10, only 26 (41.3%) were diagnosed as the same by the outside pathologists.

Conclusions: Gleason pattern 5 is commonly underdiagnosed by outside pathologists compared to an expert GU pathologist. One explanation is a hesitancy of pathologists to render the worst grade pattern possible and its adverse implications on prognosis and treatment. Another explanation is that some cases may have consisted of mostly pattern 4, less pattern 3 (or vice versa), and tertiary pattern 5. According to the ISUP modified grade, Gleason score on biopsy is derived by adding the most prevalent and highest grade patterns as opposed to the most and 2nd most common patterns. Not using the ISUP modified grading system could have accounted for at most 36/146 (24.7%) of the cases where Gleason pattern 5 was not recorded by the outside pathologists. Recognition of undergrading pattern 5 is the first step to improving its grading in the future by diverse educational means.

781 De-Differentiated Tubulocystic Carcinoma of the Kidney: A Series of 3 Cases with FISH Analysis

T Al-Hussain, L Cheng, S Zhang, JI Epstein. The Johns Hopkins Hospital, Baltimore; Indiana University School of Medicine, Indianapolis.

Background: Tubulocystic renal cell carcinoma (RCC) is relatively rare and was first described as a low grade variant of collecting duct carcinoma. This variant was not recognized in the 2004 WHO classification and only received its current name in 2009 in a series of 39 cases from 7 large institutions. It is low grade with only 2/17 cases with follow-up in this prior series developing metastases. Its relationship to collecting duct carcinoma is controversial and recent studies have linked it with papillary RCC. Only 1 case from 2011 describes a sarcomatoid tubulocystic RCC.

Design: 3 consult cases of de-differentiated tubulocystic RCC were identified. FISH was performed on 2 cases with available material.

Results: Two lesions measuring 9.5 cm. and 3.8 cm. were described as partly solid and cystic. One case was grossly a 14.0 cm cyst with a granular lining. Microscopically, all had classic areas of circumscribed tubulocystic RCC occupying 30%, 80%, and 90% of the tumor. 2 cases had small components of papillary RCC and 1 case a central large cystic component. In 2 cases, a proliferation of small tubules infiltrated away from the main mass with typical features of collecting duct carcinoma. In the 3rd case, a focus of sarcomatoid carcinoma was seen adjacent to the tubulocystic RCC. In 2 cases, tumor invaded peri-renal tissue. The 3rd case was organ confined with vascular invasion. 1 patient died 9 months post-operatively with metastases to the abdominal wall and femur. The 2nd case developed metastases to retroperitoneal nodes 3 years post-operatively. The 3rd patient was lost to follow-up.

Tumor Pattern	Chromosome 7	Chromosome 17	Chromosome Y
Case 1. Tubulocystic	Disomy	Trisomy	Loss
Case 1. De-differentiated	Disomy	Trisomy	Disomy
Case 2. Tubulocystic	Disomy	Trisomy	Disomy
Case 2. De-differentiated	Disomy	Trisomy	Disomy

Conclusions: This is the first series and only the 2nd report of de-differentiated tubulocystic RCC. FISH results showed some features that are seen with papillary RCC in both the tubulocystic and dedifferentiated components and with one exception showed identical cytogenetic findings between the 2 components. Morphologically, in 2 cases the de-differentiated areas were also indistinguishable from collecting duct carcinoma suggesting a relationship between the 2 entities. De-differentiated tubulocystic RCC increases the risk of aggressive behavior above that of usual tubulocystic RCC.

782 Virtual Karyotype of Renal Carcinoid Tumors by SNP Microarrays

RW Allan, JA Jeung, D Cao, AV Parwani, LD Truong, FA Monzon. University of Florida College of Medicine, Gainesville, FL; Washington University School of Medicine, St. Louis, MO; University of Pittsburgh School of Medicine, Pittsburgh, PA; The Methodist Hospital Research Institute, Weill Cornell Medical College of Cornell University, Houston, TX.

Background: Renal carcinoid tumors (RCT) are rare neoplasms. Unlike carcinoid tumors at other anatomic site, scarce data are available on the genetic changes in RCT. We sought to determine if there were characteristic chromosomal copy number changes in RCT using SNP arrays on archival formalin-fixed paraffin embedded (FFPE) tissue blocks.

Design: We obtained demographic, clinicopathologic information and archival FFPE tissue blocks from 5 patients with RCT from multiple institutions. DNA from the FFPE tissue blocks was analyzed with 250K Nsp SNP microarrays (Affymetrix, Santa Clara, CA). Virtual karyotypes were obtained detailing the genomic imbalances and loss of heterozygosity (LOH).

Results: The average age was 56 years (Male:Female 2:3). Tumors invaded perinephric adipose tissue (n=5), lymph nodes (n=3) or presented with metastatic disease (n=2, both liver). Three renal carcinoid tumors showed no chromosomal abnormalities (NCA). One tumor showed focal deletions in 3q [-3q(q21.31-q26.32)]. One tumor, an atypical carcinoid, showed multiple chromosomal abnormalities including loss of 3p and other chromosomal losses [-1(p31.1-p31.1), -1(p22.3-p11.2), -3(p26.3-q11.2), -10(q21.2-q26.3), -10(q21.1-q21.1), -11(q14.3-q23.3), -13, -16(q13-q24.3)].

Conclusions: Most renal carcinoid tumors showed no chromosomal abnormalities by SNP microarrays (3/5 tumors). Chromosomal abnormalities of chromosome 3 (3q or 3q loss) were present in the 2/5 tumors and one tumor (atypical carcinoid) showed complex abnormalities (loss 3p, additional chromosome losses). Loss of 3p is of interest as this is characteristic of clear cell (conventional) renal cell carcinoma. VHL mutation analysis in this tumor is underway. With the exception of more complex chromosomal changes being present in an atypical carcinoid, in the remaining tumors there was no difference between NCA tumors and those with no chromosomal abnormalities. A larger study of these rare tumors may identify recurrent abnormalities that may associated with clinical behavior.

783 Subcellular Localization of Gli-1 Correlates with Histologic Type, Grade and Stage of Renal Cell Carcinoma (RCC)

RN Al-Rohil, K-A Kim, J Garbaini, CE Sheehan, RP Kaufman, JS Ross, A Haymer-Buchan. Albany Medical College, Albany, NY.

Background: Hedgehog (Hh) pathway signaling is important in embryonic development and stem cell renewal and leads to activation of glioma associated oncogene 1 (Gli-1), which transcriptionally regulates target genes. Although Hh pathway reactivation has been described in RCC, Gli-1 protein expression has not been evaluated as a prognostic factor for the disease.

Design: Tissue sections from 145 formalin-fixed, paraffin-embedded RCCs (119 Clear Cell [CC], and 26 other types) were immunostained by an automated method (Ventana Medical Systems Inc., Tucson, AZ) using goat polyclonal GLI-1 antibody (Santa Cruz Biotech, Santa Cruz, CA). Nuclear (nGli), membranous (mGli), and cytoplasmic (cGli) immunoreactivity based on intensity and distribution was semiquantitatively scored and the results were correlated with clinical and morphologic variables.

Results: nGli-1 overexpression was noted in 54 (57%) tumors and correlated with tumor type (42% CCs vs 15% others, $p=0.008$), low grade (80% G1 vs 54% G2 vs 29% G3 vs 0% G4, $p<0.0001$ overall; 80% G1 vs 59% G2 vs 26% G3 vs 0% G4, $p<0.0001$ CCs), early stage (52% I vs 31% II vs 38% III vs 0% IV, $p=0.038$ CCs) and lengthened survival (44% alive vs 20% expired, $p=0.008$ overall; 51% alive vs 21% expired, $p=0.004$ CCs). mGli-1 overexpression was noted in 83 (57%) tumors and correlated with tumor type (69% CCs vs 4% others, $p<0.0001$) and low grade (100% G1 vs 72% G2 vs 57% G3 vs 15% G4, $p<0.0001$ overall; 100% G1 vs 79% G2 vs 69% G3 vs 20% G4, $p<0.0001$ CCs) and showed a trend toward correlation with lengthened survival (74% alive vs 58% expired, $p=0.08$ CCs). cGli-1 overexpression was noted in 69 (48%) tumors and correlated with tumor type (85% others vs 39% CCs, $p<0.0001$) and high grade (80% G4 vs 52% G3 vs 37% G2 vs 0% G1, $p=0.001$ overall, 73% G4 vs 49% G3 vs 29% G2 vs 0% G1, $p=0.002$ CCs). On multivariate analysis, high tumor grade ($p=0.003$) and advanced stage ($p=0.018$) independently predicted overall survival.

Conclusions: nGli-1 and mGli-1 overexpression characterize CC RCC and are associated with favorable prognostic features in RCC including low tumor grade, early pathologic stage and longer survival. In contrast, cGli-1 overexpression is associated with non-CC RCC and unfavorable prognostic factors such as high grade. Further study of the subcellular expression of Gli-1 in RCC is indicated.

784 Interrogation of ERG Gene Rearrangements in Prostate Cancer Identifies Novel Signatures Relative to Disease Progression and with Prognostic Implications

M Alshalfaj, LH Teng, LF Petersen, A Bakkar, A Al-Mami, S Liu, C Brenner, M Dolph, FY Feng, R Alhaji, TA Bismar. University of Calgary, Calgary, AB, Canada; Calgary Laboratory Services and University of Calgary, Calgary, AB, Canada; University of Michigan, Ann Arbor, MI.

Background: ERG gene rearrangements have been proposed to be reflective of specific molecular subtype of prostate cancer (PCA) with its prognostic implication. Herein, we investigated gene expression differences between those two classes of tumors to identify potential genetic targets and pathways.

Design: 6144 informative genes belonging to 46 castration resistant PCA samples were interrogated using the DASL platform. We used bioinformatic approach to identify significant dysregulated genes based on their ERG status (assessed by FISH).

Results: The employed method identified a group of 16 differentially expressed genes between ERG rearranged (19 samples) and ERG non-rearranged tumors (27 samples). We then were able to narrow down those genes to a 10 gene model which was the most accurate to predict prostate tissue sample classification relative to ERG status (77%). Several tumor suppressor genes as well as genes associated with cell growth, apoptosis and cancer metastasis were among the most significant deregulated genes between the two groups. Several of the genes described have never been characterized or have been poorly described in association with prostate cancer. Furthermore, we validated this model using Q-PCR and protein expression using progression TMA. The multi-gene model was also able to confirm significant prognostic value in prostate cancer beyond those of ERG alone when tested on public datasets.

Conclusions: ERG rearrangements tumors represent distinct subclass of PCA that is associated with downregulation of genes related to cell adhesion, and cell motility. This group as well shows downregulation of several tumor suppressor genes. As this represent a distinct subclass of tumors proposed to be associated with more aggressive behavior, analyzing and comparing the genes identified in this study with other genes associated with PCA could lead to better understanding of the molecular mechanism behind the aggressive behavior of ERG rearranged tumors. Furthermore, as the gene panel list identified showed significant association related to patients' prognosis in other tumor types, characterization of those genes could proof significant players in identifying pathways related to cancer progression in general and will help us to identify potential new targets for cancer therapy across several tumor types.

785 Relation of Primary Gleason Pattern 3 or 4 in Prostate Needle Biopsy to Pathological Stage and Progression after Radical Prostatectomy

A Amin, JI Epstein. The Johns Hopkins Hospital, Baltimore.

Background: It is still controversial if Gleason score 4+3=7 on prostate biopsy has a worse prognosis than 3+4=7 in predicting pathological stage and biochemical recurrence, especially if the number of positive cores is accounted for. Older studies predated the modified Gleason grading system established in 2005.

Design: In order to determine whether the breakdown of Gleason score 7 into 3+4 vs. 4+3 has prognostic significance in the modern era, we retrospectively studied 1791 cases of Gleason score 7 on prostate biopsy with corresponding radical prostatectomy performed at our institution between 2004-2010. 99.6% of radical prostatectomy

specimens were serially sectioned and submitted in entirety; in prostates >80 gms, the entire peripheral zone was submitted with representative sections of the anterior region involved by nodular hyperplasia.

Results: Of total 1791 patients, 1267 cases (70.7%) had a Gleason score 3+4=7 on biopsy, compared to 524 cases (29.2%) that showed biopsy Gleason score 4+3=7. There was no difference in age, preoperative serum PSA level, maximum tumor percentage per core, or the number of positive cores between Gleason score 3+4=7 and Gleason score 4+3=7 on biopsy. Gleason score 4+3=7 on biopsy showed an overall correlation with increasing pathological stage (organ confined, focal extraprostatic extension (EPE), non focal EPE, seminal vesicle invasion/lymph node metastases) ($p=0.005$). In multivariate analysis, biopsy Gleason score 4+3=7 ($p=0.03$), number of positive cores ($p=0.002$), maximum percent of cancer per core ($p=0.006$) and preoperative serum PSA ($p=0.03$) all correlated with pathological stage. There was also a higher risk of positive margins at radical prostatectomy with biopsy Gleason score 4+3=7 [120/524 (22.9%)] compared to biopsy 3+4=7 [231/1263 (18.3%)], $p=0.03$. Biopsy Gleason score 4+3=7 was also associated with an increased risk of biochemical progression after radical prostatectomy ($p=0.0001$). In multivariate analysis, biopsy Gleason score 4+3=7 ($p=0.001$), maximum percent of cancer per core ($p<0.0001$) and preoperative serum PSA ($p<0.0001$), yet not the number of positive cores correlated with risk of biochemical progression after radical prostatectomy.

Conclusions: Our study further demonstrates that Gleason score 7 should not be considered as a homogeneous group for the purpose of patient management and prognosis, and the dominant Gleason pattern 3 or 4 should be taken into account in reporting Gleason score 7 in biopsy material.

786 Non-Invasive Micropapillary Urothelial Carcinoma: A Report of 18 Cases

A Amin, JI Epstein. The Johns Hopkins Hospital, Baltimore.

Background: Invasive micropapillary urothelial carcinoma is a variant of urothelial carcinoma that is considered more aggressive since it often presents at higher stage. Although typically not specified, micropapillary urothelial carcinoma usually refers to invasive tumor although non-invasive micropapillary urothelial carcinoma also exists. The current study analyzes the morphology and outcome of non-invasive micropapillary urothelial carcinoma unaccompanied by invasive carcinoma.

Design: 18 non-invasive micropapillary urothelial carcinomas (w/o a history of prior urothelial carcinoma) were identified in our archives (2000-2011). Progression was defined as recurrent urothelial carcinoma of higher stage.

Results: 88% were male, with a mean age 71.9yrs. Non-invasive micropapillary urothelial carcinoma was seen in 2 patterns: 1) as a variant of non-invasive high grade papillary urothelial carcinoma (HGPAP) ($n=14$ cases); and 2) as a variant of CIS ($n=4$ cases, 1 also with HGPAP). All were identified on biopsy specimens. Data on the initial treatments were available in 12 patients and included: Surveillance ($n=5$); BCG ($n=5$); intravesicle chemotherapy ($n=1$); and radical cystectomy ($n=1$). Of the 11 cases with follow-up, 4 patients experienced recurrence treated with BCG in 2 cases and cystoprostatectomy in 2 cases. All patients were disease free at last follow-up (Mean 33.9 months; Median 24 months; Range 5-96 months).

Conclusions: The current study is the first to systematically analyze the morphology and outcome of non-invasive micropapillary urothelial carcinoma unaccompanied by invasive carcinoma. Our results demonstrate that recurrence, progression, and survival rates in non-invasive micropapillary urothelial carcinoma are favorable. It follows more or less a similar clinical course as HGPAP and CIS. Often the term "micropapillary urothelial carcinoma" is used without specifying whether invasive or non-invasive. Invasive micropapillary urothelial carcinoma is considered very aggressive where some authorities have recommended radical cystectomy if found on TUR even in the absence of documented muscularis propria invasion. It is therefore critical to differentiate and clearly specify whether micropapillary urothelial carcinoma is invasive or non-invasive in Pathology reports. Furthermore, recognition and reporting non-invasive micropapillary urothelial carcinoma will hopefully lead to larger studies adding to our understanding of its biology.

787 Microvessel Density Is Not Increased in Prostate Cancer: Digital Imaging of Tissue Microarray and Routine Sections

T Antic, D Binder, M Kocherginsky, C Liao, J Taxy, A Oto, M Tretiakova. University of Chicago, Chicago.

Background: Angiogenesis is considered a therapy target in many tumor systems including prostate cancer (PC). It is reported that there is increased vascularity in PC compared to normal prostate; however, this is not universally accepted. This study compares the microvessel density (MVD) of PC and normal prostate tissue using an automated approach to determine if MVD is a useful prognostic indicator and possible treatment target in PC.

Design: Tumor and normal prostatic tissue from 136 radical prostatectomy specimens was used to create tissue microarrays (TMA); an additional 60 radical prostatectomies were examined by routine histological sections. MVD was calculated by using CD31 immunohistochemical stain in ten 100X representative fields from tumor and normal tissue on routine sections, and in three to six 1.5 mm TMA cores. ACIS and Aperio automated systems were used to digitally analyze MVD in routine sections and TMA cores respectively. Wilcoxon signed rank test was used to compare MVD values in routine sections. In TMAs, a mixed effects model was used to account for multiple cores per patient.

Results: MVD was not significantly increased in tumors vs. normal prostate tissue in routine sections ($p=0.269$), and was lower in tumors in the TMAs ($p=0.024$). Both the vessel count and vessel area were higher in normal than in tumor in routine sections by ACIS analysis ($p<0.001$). Aperio analysis additionally showed significantly higher values in normal tissue for vessel area ($p=0.009$) and lumen ($p<0.001$), whereas vessel

perimeter and wall thickness were not significantly different ($p=0.06$ and $p=0.25$, respectively). Comparison of low grade ($n=168$ cores) vs. high grade PC ($n=30$ cores) on TMA showed no significant difference between MVD ($p=0.05$), vessel area ($p=0.88$), perimeter ($p=0.91$), lumen ($p=0.21$) or wall thickness ($p=0.93$).

Conclusions: The results, using two different approaches, show that MVD is not increased in PC compared to normal prostate. By calculating MVD from representative fields instead of vascular "hotspots" and using automated quantitation, we attempted to eliminate sources of bias possibly contributing to previous contradictory results. Similar MVD of low and high grade tumors indicate that MVD is neither an important nor reliable prognostic indicator for PC, and that antiangiogenesis drugs might not be of value.

788 Development of a *TFEB* Break-Apart Fluorescence In Situ Hybridization (FISH) Assay for Diagnosis of the t(6;11)(p21;q12) Renal Cell Carcinomas Harboring the *Alpha-TFEB* Gene Fusion in Archival Material

P Argani, R Yonescu, GJ Netto, PB Illei, CA Griffin. Johns Hopkins Medical Institutions, Baltimore, MD.

Background: Renal cell carcinomas (RCC) harboring the t(6;11)(p21;q12) chromosome translocation were first described in 2001, and subsequently have been shown to harbor a specific *Alpha-TFEB* gene fusion resulting in upregulation of native TFEB protein. Fewer than 20 genetically confirmed cases have been reported. Immunohistochemistry for TFEB protein is a highly sensitive and specific marker for the presence of the *Alpha-TFEB* gene fusion in optimally processed archival material; however, it is highly sensitive to variable fixation and thus often yields nondiagnostic results in consultation material. Break-apart fluorescence in situ hybridization (FISH) assays, such as those reported for the related *TFE3* gene used for the diagnosis of Xp11 translocation RCC, are typically less sensitive to fixation than immunohistochemical assays, and may resolve immunohistochemically-ambiguous cases. A break-apart FISH assay for *TFEB* gene fusions has not been reported.

Design: Using a cytogenetically confirmed t(6;11)(p21;q12) RCC, we developed a break-apart *TFEB* FISH assay. We used bacterial artificial chromosome (BAC) probes, 3 centromeric to and 2 telomeric to *TFEB*. The assay was validated on 6 additional confirmed cases of t(6;11)(p21;q12) RCC consisting of 2 additional genetically confirmed cases, and 4 morphologically typical cases which showed robust TFEB immunoreactivity. We also studied as negative controls 11 unrelated RCCs and normal tissues. For each case, 6 different observers counted signals derived from the BAC probes centromeric and telomeric to *TFEB* in 100 cells. The mean percentage of split signals per case among the observers was recorded.

Results: All 7 confirmed t(6;11)(p21;q12) RCC (patient ages 3-37 years; mean age 19) demonstrated a high percentage of cells with split signals (mean= 45%, range among cases, 30-60%). Of note, one of the cases had been resected 46 years before the *TFEB* FISH assay was performed, demonstrating the stability of the FISH assay in archival material. None of 11 unrelated RCC demonstrated a high percentage of cells with split signals (mean=5%; range among cases, 2-11%).

Conclusions: We report the development of a *TFEB* break-apart FISH assay for diagnosis of the t(6;11)(p21;q12) RCC which harbor the *Alpha-TFEB* gene fusion. This assay should allow more definitive identification of the t(6;11)(p21;q12) RCC in archival material, and permit further clinicopathologic studies to be performed on this distinctive neoplasm.

789 Expression of a-Methylacyl-CoA Racemase (AMACR) in Urothelial Carcinoma In Situ (CIS): Comparative Utility with More Traditional Markers (CK20, CD44s, p53) in the Distinction of Urothelial CIS and Reactive Urothelial Atypia

M Aron, DJ Luthringer, JK McKenney, DE Hansel, DE Westfall, R Parkh, M Vankalakanti, SK Mohanty, BL Balzer, MB Amin. Cedars-Sinai Medical Center, Los Angeles; Stanford School of Medicine, Stanford; Cleveland Clinic, Cleveland.

Background: The distinction of nonpleomorphic and subtle forms of CIS from reactive atypia can be challenging based on morphology. Various markers including CK20, CD44s and p53 may be used in making this distinction. AMACR is expressed in several carcinomas including breast, colon and prostate and their precursor lesions. It is known to be over expressed in a subset of high grade urothelial carcinomas, however not much is known about its expression in CIS. This study was undertaken to evaluate AMACR staining in CIS and to compare its utility with CK20, CD44s and p53 stained as an antibody cocktail (CIS-3).

Design: Forty five specimens including 7 benign ureters, and 38 bladder biopsies (17 reactive, 13 CIS, 8 CIS post therapy) were included in the study. The bladder biopsies were evaluated using the WHO/ISUP 2004 criteria. Immunohistochemistry was performed with AMACR and CIS-3 cocktail on all the 45 cases. Cytoplasmic staining for AMACR was graded as negative (absent to weak staining) and positive [moderate (diffuse granular) and strong (diffuse intense)]. p53 (brown, nuclear), CD44s (brown, membranous) and CK20 (red, cytoplasmic and membranous) was interpreted as positive. CIS-3 cocktail staining pattern was classified as: malignant (full thickness CK20+/-, full thickness p53+/- and CD44s-), reactive/benign (full thickness CK20 and p53- and CD44s+ basal to full thickness), and indeterminate (CK20 and p53+/- not full thickness and/or CD44s+).

Results: The staining pattern of AMACR and CIS-3 cocktail stain is outlined in the table.

Histopathology diagnosis	AMACR positivity (percent positive)	CIS-3 cocktail malignant pattern (percent positive)
Benign (n=7)	0	0
Reactive (n=17)	0	0
CIS (n=13)	70	92
CIS post therapy (n=8)	50	83

Of the 13 cases of CIS, AMACR showed moderate to strong staining in 9 (70%), weak staining in 2 and absent staining in 2 cases. In comparison, the CIS-3 cocktail showed a malignant pattern in 12 cases (92%) and an indeterminate pattern in the remaining case. The CIS-3 cocktail stained 7 of the 8 post therapy CIS while AMACR stained only 4 cases.

Conclusions: AMACR has potential utility as a marker for CIS. Compared to CIS-3 cocktail, its utility is limited especially in the diagnosis of CIS in a post treatment setting. CK20, p53, CD44s in the appropriate morphologic context remain reliable companion markers for the diagnosis of CIS.

790 Expression of Novel Markers Human Kidney Injury Molecule-1 (hKIM-1), S100A1 and Napsin A in the Differential Diagnosis of Renal Cell Carcinomas (RCC) with Clear and Papillary Features

M Aron, M Amin, P Zhang, M DePeralta-Venturina, SK Mohanty, S Wang, MB Amin. Cedars-Sinai Medical Center, Los Angeles, CA; William Beaumont Hospital, Detroit.

Background: The differential diagnosis of RCC with clear and papillary features includes the well established subtypes such as clear cell RCC, papillary (pap) RCC and recently recognized rarer subtypes including clear cell-papillary RCC (CC-PRCC) and translocation associated RCC. Expression of newer markers of RCC including hKIM-1, Napsin A, and S100A1 have not been reported in CC-PRCC and translocation associated RCC. hKIM-1 is a type I transmembrane glycoprotein expressed in injured renal proximal tubules but not in the normal nephron. S100A1 is a calcium-binding protein of the EF-hand family which is expressed in the entire nephron except the glomerulus. Napsin A is an aspartic proteinase that is expressed in type II pneumocytes, and the proximal and distal convoluted tubules of the kidney. This study was conducted to evaluate the utility of these markers in the differential diagnosis of RCC with clear and papillary features.

Design: 33 RCCs [translocation associated RCC (n=7), CC-PRCC (n=12), clear cell RCC (n=7) and pap RCC (n=7)] were included in the study. Representative sections were studied to confirm the histological diagnosis and sections from the tumor were stained with hKIM-1, S100A1 and Napsin A. The Kim-1 staining was graded as: 0=absent, 1+=<10%, 2+=11%- 50%, 3+=>50%. Napsin A and S100A1 stains were semiquantitatively graded as: 0 =absent; 1=weak, <25%; 2= moderate, 25-50%; 3=strong, > 50%.

Results: The results of the study are outlined in the table with immunoreactivity reported as percent positive.

Diagnosis	hKIM-1	S100A1	Napsin A
Translocation RCC	86	86	71
CC-PRCC	9	100	25*
Clear cell RCC	100	100	86*
Pap RCC	86	100	86

* weak staining seen in a majority of cases

Of note only 9% of CC-PRCC stained with hKIM-1 while all the clear cell RCC and 86% of the pap RCC and translocation RCC stained with this antibody. In addition, cases of clear cell RCC and CC-PRCC showed weak and focal staining with Napsin A.

Conclusions: 1) hKIM-1 has potential diagnostic utility in the distinction of CC-PRCC from clear cell RCC and pap RCC. 2) S100A1 is expressed in the entire range of analyzed RCCs with clear and papillary features. 3) Napsin A has distinct but limited expression in the subtypes of RCCs. Awareness of this data is critical while evaluating metastatic tumors in which pulmonary adenocarcinomas and RCC are in the differential diagnosis.

791 Comparative Utility of Novel Nuclear Markers Steroidogenic Factor (SF-1) and Forkhead Box L2 (FOXL2) in the Diagnosis of Sex Cord Stromal Tumors (SCST) of the Testis

M Aron, AM Gown, BL Balzer, M Amin, S Shen, DE Hansel, P Tamboli, G Paner, DJ Luthringer, SK Mohanty, LP Herrera, MB Amin. Cedars-Sinai Medical Center, Los Angeles; Phenopath Laboratories, Seattle; William Beaumont Hospital, Detroit; The Methodist Hospital, Houston; Cleveland Clinic, Cleveland; M.D. Anderson Cancer Center, Houston; University of Chicago, Chicago.

Background: SCSTs of the testis may demonstrate a range of cytoarchitectural patterns that can overlap with other tumors including germ cell tumors, metastatic tumors and paratesticular neoplasms. Immunohistochemistry plays an important part in the diagnosis of SCST of the testis, and although several markers have been identified, many available markers have overlap in staining reaction with differential diagnostic considerations. SF-1 (adrenal 4-binding protein; Ad4BP) is a nuclear transcription factor involved in gonadal and adrenal development. FOXL2 is a transcription factor required for ovarian differentiation in mammals. Both SF-1 and FOXL2 have been recently shown to be of value in ovarian tumors, however the expression of these markers and their potential utility in SCST of the testis is largely unknown.

Design: A total of 24 cases of SCST of the testes comprising of Leydig cell tumor (n=9), Sertoli cell tumor (n=3), large cell calcifying Sertoli cell tumor (LCCSCT) (n=3), unclassified and mixed SCST (n=6), and 1 case each of testicular tumor of androgenital syndrome (TTAG), signet ring stromal tumor and granulosa cell tumor were included in the study. All the cases were stained by SF-1 and FOXL2. The extent and intensity of nuclear staining was graded both qualitatively and semiquantitatively.

Results: The results of the study are outlined in the table.

Diagnosis	SF-1 percentage positivity	FOXL2 percentage positivity
Leydig cell tumor	78	11
Sertoli cell tumor	33	67
LCCSCT	33	0
Signet ring stromal tumor	100	100
Granulosa cell tumor	0	100
TTAG	100	0
Unclassified/mixed SCST	83	33
Total	66	29

Conclusions: 1) SF1 (66%) is a more sensitive marker for SCST of the testis, compared to FOXL2 (29%), however, its sensitivity is lower than that reported for ovarian tumors (100%). 2) FOXL2 is more sensitive for Sertoli cell tumors (67%) compared to Leydig cell tumors (11%), however its staining is lower than ovarian SCST (80%). 3) In 58% of SCST, either SF1 or FOXL2, but not both markers, were positive. 4) Depending on the differential diagnostic consideration and complexity of the case, SF1 or FOXL2, calretinin, melan-A and inhibin should constitute a comprehensive panel for SCST of the testis.

792 Primary Neuroendocrine Tumors of the Kidney. Morphological and Molecular Alterations of an Uncommon Malignancy

PP Aung, WM Linehan, CO Poropatich, MJ Merino. NCI/NIH, Bethesda, MD; Virginia Hospital Center, Arlington, VA.

Background: Primary neuroendocrine tumors of the kidney (PNRT) are rare and frequently mistaken with other kidney and urothelial cancers. The cellular origin of these tumors remains unclear. Tumor cells might originate from the entrapped neural crest cells in the metanephros during embryogenesis, neuroendocrine (NE) differentiation of a primitive totipotential stem cells, preexisting NE cell hyperplasia from metaplastic/tetratomatous epithelium, or association with other congenital renal abnormalities (Horseshoe kidney). In this study, we evaluated morphological and molecular findings of 11 PNRT cases.

Design: Tumors were classified following the WHO definition of PNRTs: well (typical or atypical carcinoid) and poorly differentiated (small cell carcinoma). IHC studies for CD56, synaptophysin, chromogranin, inhibin, glucagon, somatostatin, insulin, pancreatic polypeptide, gastrin, NSE, P53, CK7, RCC markers, CD10, CD99, MIB1, P53, WT1, EMA, vimentin, myogenin, pankeratin, LCA, CK20 and TTF1 were performed. Molecular analysis by CGH and LOH on locus of chromosome 3p21 were performed in some cases.

Results: Patients ranged in age from 35-65 years. Male-female ratio was 5:6. Five tumors occurred in left kidney, 3 in right and 1 in a horseshoe kidney. Laterality was unknown in 2 cases. Clinical symptoms included: incidental (80%), flank pain, chronic anemia and weight loss. Tumor size ranged from 3.2-11 cm. Morphologically, tumors showed solid, trabecular and pseudoglandular patterns. Lymphovascular invasion was found in 3 cases. Tumors were 2 atypical carcinoids (>2 mitosis/10HPF) and 9 typical carcinoids. High proliferative index by MIB-1 was observed in 2 cases that metastasized. The remaining cases showed <1% proliferative rate. IHC for synaptophysin, chromogranin, CD56, CD99 and NSE were positive. The remaining immunostains performed were negative. Two patients developed metastasis and the remaining cases are alive with no evidence of disease. LOH on chr 3p21 was found in some tumors, however, CGH study did not demonstrate chromosomal imbalances.

Conclusions: We conclude that PNRT tumors are uncommon and frequently misdiagnosed as Papillary type I, mesonephroma, Wilm's tumor or undifferentiated carcinoma. The tumors are positive for NE markers and may have LOH on chr 3p21 similar to a clear cell renal carcinoma. The classification as other NE tumors is useful and a high proliferative rate is an indicator of aggressive behavior/metastasis of tumors.

793 Sall4 and SF-1 Are Sensitive and Specific Markers for Distinguishing Granulosa Cell Tumors from Yolk Sac Tumors

S Bai, S Wei, A Ziober, Y Yao, Z Bing. Hospital of the University of Pennsylvania, Philadelphia, PA; University of Alabama at Birmingham, Birmingham, AL.

Background: Granulosa cell tumors could be misinterpreted as yolk sac tumors when they exhibit "reticular" growth patterns and contain prominent mitotic activities. Even though immunostains of alpha-fetoprotein and inhibin can be used to distinguish these two tumors, the reliability of antibodies targeting alpha-fetoprotein in tissues is often questioned. Since the approach to treating these two tumors is very different, alternative markers need to be explored. Sall4 is a relatively specific marker for germ cell tumors including yolk sac tumor. Steroidogenic factor-1 (SF-1) is a nuclear receptor and has been shown to be expressed in various sex cord stromal tumors. Whether Sall4 and SF-1 can be used as markers to distinguish yolk sac tumors from granulosa cell tumors has not been elucidated.

Design: 24 cases of granulosa cell tumors and 27 cases of yolk sac tumors, retrieved from the pathology archives of the Hospital of the University of Pennsylvania and University of Alabama at Birmingham Hospital, were immunohistochemically stained with SF-1 and Sall4 antibodies by following manufacturers' instruction. Nuclear stains for both antibodies were considered as positive and the intensity of staining was graded as negative, weak, moderate, and strong. Statistical significance was derived utilizing the student's t test.

Results: There were 24 female patients and 27 male patients. All the cases were reviewed to confirm the diagnoses. 23 out of 24 granulosa cell tumors (96%) were from ovaries, one (4%) was from a testis. Most of the yolk sac tumors were from testis (18 cases, 67%), 1 case from ovary (4%) and rest cases are from anterior mediastinal area or other sites with metastatic tumors (8 cases, 29%) of male patients. All yolk sac tumors were positive for Sall4 (100%) with moderate to strong grade staining intensity and negative for SF-1 (100%). In contrast, all granulosa cell tumors were positive for SF-1 (85% moderate to strong grade staining intensity and 15% mild grade staining intensity) and negative for Sall4 (100%). The difference was statistically significant (p<0.01).

Conclusions: This study showed that all granulosa cell tumors were positive for SF-1 and negative for Sall4. In contrast, yolk sac tumors were positive for Sall4 and negative for SF-1. This result indicated that these two markers could be used to distinguish these two tumors in a difficult situation.

794 Assessment of *TMPRSS2: ERG (T:E) Gene Fusion in Prostatic Adenocarcinoma (CaP) by Fluorescence In Situ Hybridization (FISH) and Immunohistochemistry (IHC): Correlation of *ERG* Break-Apart and *T:E* Fusion Probes with *ERG* and *TMPRSS2* Protein Expression*

M Bastacky, M Gogniat, C Sherer, K Cieply, A Gedansky, S Kavala, A Parwani, R Dhir, M Acquafondata, F Francis, S Bastacky. University of Pittsburgh, Pittsburgh, PA.

Background: *T:E* gene fusion leading to transcription factor *ERG* protein overexpression occurs in many CaPs. *T:E* gene fusion can be assessed using *ERG* break-apart and *T:E* fusion probes. The aim of this study is to compare both probe methods, correlating results with *ERG* and *TMPRSS2* protein expression.

Design: Formalin-fixed, paraffin-embedded tissue sections from 21 CaP pt samples (tissue microarray (n=10), needle bx (n=3), radical prostatectomy (n=8)) and control organ donor prostates (ODP; n=10) were obtained from the University of Pittsburgh tissue bank. Dual-color FISH (break-apart probe for *ERG* disruption, separate *ERG* and *TMPRSS2* probes for *T:E* fusion) and immunohistochemistry (*ERG* (Biocare Medical) and *TMPRSS2* (Epitomics)) were performed. FISH was positive if ≥ 20% of cells had *ERG* disruption or *T:E* fusion, with thresholds based on ODPs. IHC intensity (0-3) and distribution (0-100%) were scored. FISH and IHC results were correlated.

Results:

Comparison of FISH (*ERG* Disruption and *T:E* Fusion) and IHC (*ERG* and *TMPRSS2*) with Gleason Score

Gleason score	* <i>ERG</i> (FISH)	* <i>T:E</i> (FISH)	* <i>ERG</i> (IHC)	** <i>TMPRSS2</i> (IHC)
3+3=6	3/4 (75%)	3/4 (75%)	4/4 (100%)	4/4 (100%)
3+4=7	4/7 (57%)	5/7 (71%)	4/7 (51%)	7/7 (100%)
4+3=7	3/5 (60%)	3/5 (60%)	2/5 (40%)	5/5 (100%)
4+4=8	2/5 (40%)	3/5 (60%)	2/5 (40%)	5/5 (100%)

*stains CaP only, **stains benign prostate glands and CaP

Correlation of FISH (*ERG* Break-Apart vs *T:E* fusion) with *ERG* - IHC

	FISH+/Total	<i>ERG</i> -IHC+/FISH+	<i>ERG</i> (mean intensity score of + cases)
<i>ERG</i> - break-apart (total)	15/21 (71%)	12/15 (80%)	2.1/3
- <i>ERG</i> -BT	9/21 (43%)	9/9 (100%)	3/3
- <i>ERG</i> -UBT	4/21 (19%)	2/4 (50%)	1/3
- <i>ERG</i> -BT+UBT	2/21 (9%)	1/2 (50%)	3/3
<i>T:E</i> fusion	15/21 (71%)	12/15 (80%)	2.1/3

ERG-BT (One normal chromosome and one *ERG* balanced translocation); *ERG*-UBT (*ERG* unbalanced translocation)

Conclusions: 1) *ERG* disruption and *T:E* fusion probes had similar concordance rates (80%) with *ERG* protein expression. 2) False positive *ERG* disruption occurred with unbalanced but not with balanced *ERG* translocation, suggesting that a BT preserves *ERG* gene function while an UBT may disrupt the gene. 3) False positive *T:E* fusion FISH may be due to a positional effect of chr 21 in the tissue section, causing an apparent juxtaposition of *TMPRSS2* and *ERG*. 3) There was no correlation of CaP Gleason score with *ERG* gene disruption, *T:E* gene fusion, or *ERG* or *TMPRSS2* protein expression. 4) *ERG* gene disruption, *T:E* gene fusion, and *ERG* (but not *TMPRSS2*) protein expression correlated with CaP.

795 Finding of Prostate Carcinoma at the Capsular End of a Prostate Needle Biopsy Does Not Predict Positive Capsular Margin on Radical Prostatectomy Specimen

P Bernaczyc, R Milewski, L Chyczewski, J Kowalewska. Medical University of Bialystok, Bialystok, Poland.

Background: The status of surgical margin on radical prostatectomy specimen is considered to be an important prognostic factor in the prediction of postoperative progression of prostate cancer. Needle biopsy of the prostate provides important information that helps to predict pathological stage and margins. Many studies have demonstrated that the percent of cancer on the biopsy, number of positive cores, and fraction of positive cores may predict the status of margins on the subsequent resection. It is not established if the presence of carcinoma at the capsular (proximal) end of the needle biopsy has any prognostic value in prediction of margin involvement on the radical prostatectomy specimen.

Design: A search was conducted through the Department of Pathomorphology database for patients who had diagnostic prostate needle biopsy and subsequently underwent radical prostatectomy for prostate cancer. The results of the biopsy and prostatectomy specimens were reviewed, and the status of the capsular ends (marked with ink) of the needle biopsies was compared to the capsular margin involvement on matched prostatectomy specimen. The statistical software package Statistica 8.0 (StatSoft, Inc., Tulsa, OK) was used to carry out statistical test Chi-square and Fisher exact test; p<0.05 was considered significant.

Results: One hundred eight (108) patients, mean age 64.4 years (range 51-76), were identified who met the search criteria. Prostate carcinoma was found at the capsular end of 20 (18.5%) needle biopsies, and positive capsular margin was identified on 49 (45.4%) of the radical prostatectomy specimens. There was no statistically significant correlation between these two findings (Chi-Square test: p=0.65, Fisher exact test p=0.41). The sensitivity of finding positive capsular end of the biopsy was 20%, and its positive predictive value was 50%. The negative predictive value was 55.7%.

Conclusions: Our data shows that positive margin on the radical prostatectomy specimen is not related to the finding of prostate carcinoma at the capsular end of the prostate needle biopsy. Therefore, finding of prostate cancer at the capsular end of prostate needle biopsy should not be used as a predictive factor in the assessment of the pathological stage and margins for prostate cancer.

796 Molecular Factors Showing Multivariate Significance for Outcome in a Conservatively Treated Prostate Cancer Biopsy Cohort

D Berney, G Fisher, ZH Yang, H Moller, S Kudahetti, C Foster, V Reuter, P Scardino, J Cuzick. Barts and the London School of Medicine, London, United Kingdom; Memorial Sloan-Kettering Cancer Center, New York; Kings College London, London, United Kingdom; University of Liverpool, Liverpool, United Kingdom.

Background: Using standard clinical parameters it is still not possible to differentiate indolent from aggressive prostate cancer (PC). We have previously reported on a cohort of 808 clinically localised PCs diagnosed by TURP and treated conservatively with long term follow up, and shown in the TURP cohort that ki-67 and P53 predict outcome in a multivariate model independently of Gleason score (GS) and Serum PSA. A 31 gene cell cycle progression (CCP) RNA signature outperformed all immunochemical markers. We here present the results of translation of this work into the more clinically relevant biopsy cohort.

Design: Biopsy specimens from 1991-6 were collected from patients with conservatively treated PC. PSA and GS were available with an endpoint of death from PC. A biopsy tissue micro-array (TMA) was constructed, and immunohistochemically (IHC) stained for Ki-67 and P53. Immunochemical positivity was measured in each core in a semi-quantitative manner examining strength of signal from 0-3 and percentage positivity to give a composite score. Also, RNA levels of 46 cell cycle progression (CCP) genes were determined in this cohort and a mean CCP score calculated for each patient.

Results: Ki-67 (n=295) correlated with GS ($p < 0.001$). Assessed in 3 categories ($\leq 5\%$, $>5 \leq 10\%$, $>10\%$), it is significant in univariate (χ^2 trend=10.08, $p < 0.002$) and multivariate models including GS and PSA (χ^2 trend=5.66, $p < 0.017$). P53 was not significant in univariate or multivariate models. However, CCP score outperformed all IHC markers. In a multivariate analysis which included Gleason and PSA, CCP dominated (HR for change from 25th to 75th percentile = 2.07, 95% CI(1.50, 2.85) $\chi^2 = 20.8$, $P = 5 \times 10^{-6}$) with only GS providing a significant additional contribution ($\chi^2 = 15$, 1df, $P = 0.0001$).

Conclusions: IHC scoring on TMA prostate biopsies is practicable and yields significant results for Ki-67, but is currently considerably outperformed by CCP score. Ki67 results are less impressive than those on the TURP cohort; this may be due to the smaller samples analysed, where inadequate sampling may be an issue.

We suggest that despite the wealth of IHC data in radical prostatectomy and TURP cohorts, translating this into useful assays on small amounts of biopsy tissue may not be as informative as other techniques such as RNA expression data which showed its clear superiority in this set of material.

797 Value of Reflex ImmunoCyt Testing for the Diagnosis of Bladder Cancer

AB Berry, AY Odisho, AE Ahmad, MR Cooperberg, PR Carroll, BR Konety. University of California San Francisco, San Francisco, CA; University of Minnesota, Minneapolis, MN.

Background: An atypical diagnosis in voided urine cytology poses a dilemma for the clinical team, and frequently leads to cystoscopy, or other additional testing, to rule out the presence of tumor. ImmunoCyt, a triple immunofluorescent antibody assay, is an FDA cleared voided urine test for antigens associated with urothelial carcinoma (UC). While the test is designed to be used as a reflex test for atypical voided urine cytology, and can be employed by any fully functional cytology laboratory, few practices are currently using it in this way. We reviewed the initial outcomes for patients undergoing ImmunoCyt reflex testing at our institution to determine the usefulness of the test in determining the need for cystoscopic examination, the need for cystoscopy.

Design: The ImmunoCyt (uCyt) assay is performed at our institution reflexively on all voided urine cytology tests read as atypical. Subsequent patient workup, such as cystoscopy, biopsy, and follow up is currently at the discretion of the treating urologist. We retrospectively reviewed patients tested between January 2007 and June 2010. We examined medical records to determine patient history and the outcomes of subsequent cystoscopy, which was considered pertinent if performed within 90 days of the uCyt assay.

Results: Reflex uCyt testing was performed on 595 atypical voided urine samples from 324 patients, 506 of which were followed by cystoscopy within 90 days. Of the 595 samples, 441 (74%) were from patients with a history of UC. 142 samples (24%) were from patients with hematuria and no history of UC. Using cystoscopy within 90 days as a reference, reflex uCyt testing of samples with a history of UC showed a sensitivity and specificity of 73% and 49%, respectively, a negative predictive value (NPV) of 80% and positive predictive value (PPV) of 37%. In 159 samples with a history of low grade UC, reflex uCyt had a sensitivity of 75%, specificity of 50%, NPV of 82% and PPV of 39%, while in 221 assays in those with a history of high grade UC, it had a sensitivity of 74%, specificity of 44%, NPV of 79%, and PPV of 37%. With no prior history of UC, reflex uCyt had a sensitivity of 85%, specificity of 59%, NPV of 94% and PPV of 33%.

Conclusions: When used as a reflex test on atypical urine cytology a negative uCyt result can effectively be used to predict a negative cystoscopy. In those with a history of low grade UC, negative reflex uCyt can be used to obviate.

798 Novel Dual Color Immunohistochemical Method for Detecting ERG and PTEN Status in Prostate Carcinoma

R Bhalla, LP Kunju, SA Tomlins, K Christopherson, C Cortez, JM Mosquera, G Pestano, A Chinnaiyan, N Palanisamy. University of Michigan, Ann Arbor, MI; Ventana Medical System, Tucson, AZ; Weill Cornell Medical College, New York, NY; Michigan Center for Translational Pathology, Ann Arbor, MI; Howard Hughes Medical Institute, Ann Arbor, MI.

Background: *TMPRSS2-ERG* gene fusions occur in 50% of prostate cancers (PCA) and result in the overexpression of a chimeric fusion transcript that encodes a truncated ERG

product, which can be detected by immunohistochemistry (IHC). *PTEN* is a key tumor suppressor gene, implicated in many cancers, including PCA. Loss of *PTEN*, detected by fluorescent in situ hybridization (FISH) has been associated with poor prognosis. Concurrent *PTEN* deletion (del) and *TMPRSS2-ERG* fusions have been reported to be associated with an unfavorable outcome. We developed a novel automated dual color ERG and PTEN IHC assay to evaluate ERG and PTEN status as a single procedure.

Design: A dual immunostain, utilizing rabbit antibodies against ERG and PTEN, was performed on PCA tissue micro-arrays using automated protocols on the Discovery XT system (Ventana). A total of 120 cases from 101 localized (loc) and 19 metastatic (met) PCA were evaluated. Nuclear ERG expression was scored as present or absent (endothelial staining was used as positive control). Cytoplasmic PTEN staining was scored as normal (increased or equal staining compared to adjacent benign acini), and negative (decreased or absent staining). IHC results were compared with FISH results for *PTEN* del status.

Results: Out of 120 cases evaluated, 55 (46%) ERG positive (50 loc and 5 met PCA) and 33 (28%) *PTEN* deleted cases (20 loc and 13 met) were identified by IHC. Of the 55 ERG positive cases, *PTEN* loss was observed in 17(31%) cases (12 loc and 5 met) by IHC. *PTEN* status was concordant in 101 cases (84% sensitivity) by both IHC and FISH. Among 33 *PTEN* deleted cases as identified by IHC, 27 were confirmed (81% specificity) by FISH. IHC could not distinguish heterozygous and homozygous deletion status of *PTEN*.

Conclusions: Automated dual ERG-*PTEN* IHC is simple, reliable and easy to perform for the simultaneous assessment of ERG and *PTEN* protein expression in PCA. Antibody based detection of *PTEN* shows a high concordance with FISH, which may be an alternative for evaluation of *PTEN* status in PCA. We confirm the previously described association between *PTEN* loss and ERG fusion in our cohort. This assay may potentially be useful for screening patients to select them for therapeutic targeting of these pathways in high risk PCA.

799 Novel Dual Color Immunohistochemical Analysis for Detecting ERG and SPINK1 Status in Prostate Carcinoma

R Bhalla, LP Kunju, SA Tomlins, K Christopherson, C Cortez, JM Mosquera, G Pestano, A Chinnaiyan, N Palanisamy. University of Michigan, Ann Arbor, MI; Ventana Medical System, Tucson, AZ; Weill Cornell Medical College, New York, NY; Michigan Center for Translational Pathology, Ann Arbor, MI; Howard Hughes Medical Institute, Ann Arbor, MI.

Background: ETS gene fusions occur in around 50% of prostate cancers (PCA) and result in over-expression of a truncated ERG protein. Overexpression of SPINK1 defines an aggressive molecular subtype of ETS fusion-negative PCA (SPINK1+/ETS-, 10% of all PCA). Previously, we characterized an antibody against ERG as showing diagnostic utility for the detection of ERG rearranged PCA. The aim of our study was to develop a dual color immunohistochemistry based assay for reliable simultaneous assessment of ERG and SPINK1 proteins in PCA.

Design: ERG and SPINK1 protein expression was evaluated utilizing an automated dual color immunohistochemistry protocol (Ventana-Roche, Discovery XT) using monoclonal antibodies against ERG and SPINK1 proteins on 8 tissue microarrays (TMAs) including a spectrum of localized PCAs (including variant histology) and castrate resistant metastatic PCA. A total of 218 PCA cases -150 localized (loc) and 68 metastatic (met) PCA were examined. The percentage of SPINK1 positive tumor cells in each core was estimated and assigned values of 0%, 5% or multiples of 10%. Any positivity was considered as expression of SPINK1 protein. Nuclear ERG staining was considered positive.

Results: Of the 218 cases evaluated 77 (35%) cases (58 loc and 19 met) were positive for ERG. In the remaining 141 ERG negative cases, SPINK1 was positive in 20 (9%) cases (4 loc and 16 met). SPINK1 expression was found to be mutually exclusive with ERG expression, however, we identified one case, which demonstrated ERG as well as SPINK1 positivity in two independent foci. Unlike the homogenous staining of ERG in cancer tissues, heterogeneous SPINK1 staining was observed in the majority of the cases. Further studies are required to understand the molecular heterogeneity of PCA in SPINK1 positive cases.

Conclusions: This study confirms the mutual exclusivity of ERG and SPINK1, suggesting that ERG+/SPINK1- and ERG-/SPINK1+ PCA may represent different molecular subtypes of PCA. We have shown that the dual ERG/SPINK1 staining is easily implemented, reproducible and easy to interpret. Also, as it can be done on a single unstained level, it enables the routine subtyping of PCA. This may have utility in retrospective or prospective stratification for therapy, prognosis or risk stratification of precursor/atypical lesions.

800 Validation of the Contemporary Epstein Criteria for Insignificant Prostate Cancer in South-American Men

A Billis, L Meirelles, LLLL Freitas, AA Tavares, FF Carvalho, JPU Fontenele, LGF Cortes. University of Campinas (Unicamp) School of Medicine, Campinas, SP, Brazil.

Background: Due to widespread of PSA screening an increasing number of T1c prostate carcinomas are diagnosed as well as the so-called clinically insignificant tumors. The latter, in turn, may increase potentially unnecessary treatment. Epstein's criteria for prediction of clinically insignificant cancer on needle biopsies are widely used, however, there are discrepancies in the validation according to the country. In the United States (Johns Hopkins), Europe (Germany), Asia (South Korea), and Middle West (Egypt), the prediction rate is 84%, 76%, 69%, and 54%, respectively. This is the first validation from a South-American country (Brazil).

Design: The study was based on patients submitted to radical retropubic prostatectomy which needle prostatic biopsies met Epstein's criteria: stage T1c, PSA density < 0.15 , Gleason score ≤ 6 , fewer than 3 biopsies with prostate cancer, and no more than 50% of cancer involvement in any core. The mean, median, minimum and maximum number

of cores on biopsy was 11, 12, 6 and 20 cores, respectively. Each core was embedded separately and submitted in multiple containers. PSA density was calculated by dividing the absolute PSA value by the prostatic weight, which was defined as the weight of the surgical specimen minus the weight of the seminal vesicles. All biopsies and radical prostatectomies were checked by a senior uropathologist. Tumor extent in surgical specimen was evaluated by a semiquantitative point-count method.

Results: From a total of 400 patients submitted to radical retropubic prostatectomy, 169/400 (42.3%) had T1c prostate cancer. From 169 biopsies in stage T1c, 18/169 (10.7%) met Epstein's criteria for insignificant cancer. On radical prostatectomy, from these 18 cases, 17/18 (94.4%) were confined to the prostate; 13/18 (72.2%) were confined to the prostate with Gleason score ≤ 6 , and with any tumor extent; and, 11/18 (61.1%) were confined to the prostate with Gleason score ≤ 6 , and with limited extent.

Conclusions: The rate of prediction of clinically insignificant cancer on needle biopsies in our study was between that from Europe (Germany) and Asia (South Korea) and much higher than from Middle East (Egypt). The rate of prediction was lower when considering insignificant cancer confined to the prostate, with Gleason score ≤ 6 , and with limited extent. The wide differences among countries may be related to innate differences associated with racial, alimentary, environmental, and particularly to the sample of the needle prostate biopsy.

801 The Morphology and Immunohistochemical Phenotypic Expression of Focal Prostatic Atrophy

A Billis, L Meirelles, LLLL Freitas, BD Lins, JFL Bonfido, LBE Costa, PH Poletto. University of Campinas (Unicamp) School of Medicine, Campinas, SP, Brazil.

Background: Prostatic atrophy is one of the most frequent histologic mimics of prostate carcinoma. Inactive or active inflammation and ischemia are involved in its etiopathogenesis. Proliferative inflammatory atrophy (PIA) was proposed to designate focal simple or postatrophic hyperplasia occurring in association with inflammation and may represent a precursor lesion to high-grade prostatic intraepithelial neoplasia and, therefore, prostatic carcinoma. The atrophic luminal cells in PIA show aberrant phenotypic expression consistent with intermediate cells. We performed a detailed analysis of the morphology of focal atrophy and extended the study of immunohistochemical phenotypic expression to partial atrophy and to all subtypes of complete atrophy.

Design: We studied 120 needle prostatic biopsies showing only focal atrophy. The lesion was classified into partial and complete. The latter subtyped into simple, hyperplastic (or postatrophic hyperplasia) and sclerotic. Immunohistochemistry was performed for PSA, PAP, CK8, CK18, Cam 5.2, 34 β E12, p63, CK5, CK14, AR, CD44, c-met, GSTP, CD133, α 2 β 1 integrin, and c-myc.

Results: Partial atrophy was present in 69/120 (58.1%) biopsies; complete atrophy in 118/120 (98.3%) biopsies; and, in 67/120 (55.8%) biopsies both lesions were found. In 32/120 (26.6%) biopsies partial atrophy merged with complete atrophy in the same focus as well as in the same gland. Chronic inespecific inflammation was seen only in complete atrophy. The immunohistochemical phenotypic expression of partial atrophy was similar to normal acini. The luminal cells of complete atrophy (simple, hyperplastic, or sclerotic subtypes) were PSA-/PAP-/34 β E12+ consistent of an intermediate-type cell. In complete atrophy foci with or without inflammation there was overexpression of GSTP, c-met, and CD44.

Conclusions: Partial atrophy and complete atrophy are frequently found in the same biopsy. The mergence of these two lesions and the transitions in the same gland seems to favor that partial atrophy precedes complete atrophy. The absence of inflammation in partial atrophy as well as in areas of mergence between the lesions favors that chronic inespecific inflammation may be a secondary phenomenon. Aberrant phenotypic expression of luminal cells was seen in all subtypes of complete atrophy but not in partial atrophy as well as overexpression of GSTP, c-met, and CD44 was seen only in complete atrophy.

802 Prostate Total Tumor Extent vs. Index Tumor Extent: Which Is Predictive of Biochemical Recurrence Following Radical Prostatectomy?

A Billis, L Meirelles, LLLL Freitas, AS Polidoro, HA Fernandes, MM Padilha, LA Magna, LO Reis, U Ferreira. University of Campinas (Unicamp) School of Medicine, Campinas, SP, Brazil.

Background: It is controversial whether tumor extent or volume in radical prostatectomies is predictive of biochemical recurrence following surgery. We compared the predictive value of total tumor extent vs. predominant nodule extent (index tumor).

Design: A mean of 32 paraffin blocks were processed from prostate surgical specimens step-sectioned at 3 to 5mm intervals from 300 patients submitted to radical retropubic prostatectomy (RP). Each transversal section of the prostate was subdivided into 2 anterolateral and 2 posterolateral quadrants. Tumor extent at RP was evaluated by a semiquantitative point-count method previously described. Time to biochemical recurrence following RP was analyzed with the Kaplan-Meier product-limit analysis using the log-rank test for comparison between the groups and prediction of time to biochemical recurrence using univariate and multivariate Cox proportional hazards model.

Results: Considering the total tumor extent, more extensive tumors showed higher preoperative PSA ($p < 0.01$), higher clinical stage ($p = 0.02$), higher pathological stage ($p < 0.01$), higher positive margins ($p < 0.01$), and higher Gleason score in RP ($p < 0.01$). More extensive tumors showed significantly shorter time to biochemical recurrence (log-rank, $p = 0.04$). Using Cox proportional hazards model, total tumor extent was predictive of time to biochemical recurrence in univariate analysis ($p < 0.01$) but not in multivariate analysis including preoperative PSA and all pathological parameters. Considering the index tumor extent, more extensive tumors showed higher preoperative PSA ($p < 0.01$), higher clinical stage ($p = 0.01$), higher pathological stage ($p < 0.01$),

higher positive margins ($p < 0.01$), and higher Gleason score in RP ($p < 0.01$). More extensive index tumors showed significantly shorter time to biochemical recurrence (log-rank, $p < 0.01$). Using Cox proportional hazards model, index tumor extent was significantly predictive of time to biochemical recurrence in univariate ($p < 0.01$) as well as multivariate analysis with the forward selection and including preoperative PSA and all pathological parameters.

Conclusions: Based on our study, total tumor extent is significantly predictive of time to biochemical recurrence following RP but only index tumor extent is predictive on both univariate and multivariate analyses including preoperative PSA and all pathological parameters.

803 P53 in Epithelioid Angiomyolipoma: An Immunohistochemistry Study and Gene Mutation Analysis

Z Bing, Y Yao, T Pasha, JE Tomaszewski, PJ Zhang. Hospital of the University of Pennsylvania, Philadelphia; University of Buffalo, Buffalo.

Background: Epithelioid AML (EAML) is a rare variant of AML and is more often associated with aggressive behaviors. The pathogenesis of EAML has been poorly understood. The expression and mutation analysis of p53 in EAML has only been described in case reports with conflicting results.

Design: We studied p53 expression and gene mutation in EAMLs by immunohistochemistry, single-strand conformation polymorphism (SSCP) and direct sequencing in paraffin materials from 8 EAMLs. The score for p53 nuclear staining was calculated by using the Allred score system. A group of typical AMLs was also analyzed for comparison.

Results: Of the 8 patients, 5 were from men, 3 from women, with an average age of 41.9 \pm 17.7 years. 5 tumors arose from kidneys, one each from heart, liver and uterus. 2 patients had history of tuberous sclerosis, 4 had metastasis and 1 had local recurrence. All EAMLs and 5 of 12 typical AMLs were positive for p53 immunorexpression. EAMLs showed much stronger p53 nuclear staining (Allred score 6.4 \pm 2.5) than the typical AML (2.3 \pm 2.9) ($p < 0.01$). There was no p53 SSCP identified in either EAMLs or 8 typical AMLs. P53 mutation analysis by direct sequencing of exons 5-9 showed 4 mutations in 3 of 8 EAMLs but none of 8 typical AMLs. The mutations included two missense mutations in one case and two silent mutations in another two cases. For the two cases with silent mutations, both of them were renal tumors. For one case (case 1), in exon 5 codon 154 was changed from GGC to GGG, which was a silent mutation coding for amino acid glycine. For the other case, the silent mutation involved exon 6 codon 218 which was changed from GTG to GTT (both of the codons coding same amino acid valine). The case with two missense mutation was a hepatic PeComa. Both mutations involved the exon 5, one involving codon 165 with change from CAG to CAC (coding amino acid changed from glutamine to histidine), and the other involving codon 182 with change from TGC to TAC (coding amino acid changed from cysteine to tyrosine).

Conclusions: EAMLs had more frequent and stronger p53 expression than the typical AMLs. Four new p53 mutations were identified in 3 of 8 EAMLs, two of which were missense mutations found in a hepatic PeComa, two were silent mutations involving two renal EAMLs. The finding of abnormal p53 expression and mutations might be contributed to its less predictable behavior. However, the abnormal p53 expression cannot be entirely explained by p53 mutations in the exons examined in EAML.

804 MicroRNA Expression Analysis Suggests Genetic Similarity among Urachal Adenocarcinoma Morphologic Variants

ML Bissonnette, T Stricker, M Tretiakova, R Jimenez, GA Barkan, V Mehta, S Sirintrapun, G Steinberg, K White, G Paner. University of Chicago, Chicago, IL; Mayo Clinic, Rochester, MN; Loyola University Medical Center, Maywood, IL; Wake Forest University, Winston-Salem, NC.

Background: The vast majority of urachal carcinomas are adenocarcinomas, and several morphological variants of urachal adenocarcinoma have been described that include: mucinous, enteric, signet ring cell, not otherwise specified (NOS), and mixed subtypes. The clinical significance of these morphologic variants is not known. Recent immunohistochemical (IHC) studies on these subtypes have shown overlapping immunoprofiles. In this study, we analyzed the miRNA expression of these subtypes to determine if there is genetic distinction between these entities.

Design: Archival formalin-fixed paraffin embedded material of 12 urachal adenocarcinomas were selected from multiple institutions: 3 mucinous, 3 enteric, 2 signet ring, 2 mixed (enteric and mucinous) and 2 NOS subtypes. Each single subtype contained $>50\%$ of that particular subtype. The cases included 2 pure mucinous, 2 pure enteric, and 1 pure signet ring subtype. RNA was extracted, and the level of miRNA expression was determined for each sample using a 598 human miRNA code set with the nCounter miRNA Expression Assay (NanoString, Seattle, WA).

Results: Total RNA was extracted for all 12 cases. Of the 598 unique human miRNAs in the assay expression code set, 111 were highly expressed in all 12 samples. The remaining miRNAs were not well expressed in any of the samples. There were no significant differences in miRNA expression levels among any of the urachal adenocarcinoma morphological variants. Additionally, there were no significant differences in miRNA expression levels among the pure mucinous, pure enteric, and pure signet ring cases. The mixed subtypes did not show any significant miRNA expression level differences compared to the single or the pure subtypes.

Conclusions: Our study suggests that the morphological variants of urachal adenocarcinoma are genetically similar. These findings corroborate previous reports that showed immunophenotypic overlap of these tumor subtypes. The overlap in miRNA expression profiles among these morphological variants suggests a varied phenotypic manifestation of a single neoplastic process and suggests similarity in tumor biology.

805 Urothelial Carcinoma with Prominent Squamous Differentiation in the Setting of Neurogenic Bladder – Role of HPV Infection

EB Blochin, KJ Park, SK Tickoo, VE Reuter, H Al-Ahmadie. Memorial Sloan-Kettering Cancer Center, New York, NY; Ackerman Academy of Dermatopathology, New York, NY.

Background: Squamous cell carcinoma (SCC) of the urinary bladder (UB) is rare; even more rare is its association with human papillomavirus (HPV). We report on two cases of HPV-positive urothelial carcinoma (UC) of the UB with predominant squamous differentiation (SQ) arising in patients with neurogenic bladder (NB) and long standing history of self catheterization (CATH).

Design: Two cases of apparent SCC of UB with basaloid appearance occurring in patients with neurogenic bladders were identified prospectively. p16 immunohistochemistry and HPV in situ hybridization (ISH) were performed. A retrospective institutional database review of SCC arising in NB was also performed and slides assessed for morphologic features.

Results: Patient 1 was a 44 year old female with h/o lipomeningomyelocele and laminectomy at age 5, using clean intermittent (CI) CATH 20x/day from a young age. Patient 2 was a 48 year old who was paraplegic at T8 from a motor vehicle accident (MVA) at 23. In 2000 she underwent bladder-intestinal augmentation cystoplasty and was using CICATH. Neither had significant gynecologic histories. Tumors from both patients had a basaloid appearance with diffuse, strong p16 and punctate nuclear staining by HPV-ISH. One was almost entirely composed of SCC with in situ SCC in the surface urothelium resembling high grade dysplasia of the uterine cervix. The other showed a combination of SQ and glandular features as well as SCC in situ arising at the junction of native bladder and small intestine. Retrospective analysis of 250 cases of UC with SQ or pure SCC of the UB revealed 4 patients with a history of NB. Two used CICATH (one since 1985 after MVA; one since 1986 for multiple sclerosis). One patient used self CATH 2-3x a day since 1998 after surgery for endometriosis, and one had NB of uncertain etiology not requiring CATH. Microscopically, the tumors were either pure SCC or exhibited prominent SCC component in an otherwise usual UC. All 4 cases showed prominent keratinization. p16 was patchy in 1 case where it focally labeled UC in situ and invasive SCC. HPV ISH in this case was negative.

Conclusions: This is the first report of HPV-associated UC of the bladder with prominent squamous differentiation arising in patients with neurogenic bladder and self CATH. These 2 cases demonstrate that HPV-induced urothelial carcinoma may develop from physical trauma, SQ metaplasia, viral inoculation and stepwise carcinogenesis similar to that seen in uterine cervical cancers.

806 Gleason Grading Reproducibility Highlights Problematic Patterns for Differentiating Gleason Grade 3 Versus Gleason Grade 4: Implications for Active Surveillance Patients

M Bonham, S Hawley, LP Kunju, D Troyer, L Fazili, E Jones, M Nicholas, J McKenney, L True, J Simko. University of California, San Francisco, San Francisco, CA; Stanford University Medical Center, Palo Alto, CA; University of Michigan, Ann Arbor, MI; Eastern Virginia Medical School, Norfolk, VA; University of British Columbia, Vancouver; University of Texas Health Science Center at San Antonio, San Antonio, TX; University of Washington, Seattle.

Background: Active Surveillance (AS) is becoming a more accepted management strategy for patients with prostate cancers that have low risk of progression. Most of the AS management protocols rely heavily on the Gleason score obtained from serial biopsies; scores of 7 or higher trigger a recommendation for primary treatment with curative intent. This places heavy emphasis on discriminating between Gleason patterns 3 and 4. We have instituted a rapid biopsy review program within a multi-institutional clinical trial to evaluate variability & to guide standardization among participating pathologists for cases that are borderline between patterns 3 and 4.

Design: Digital images from 27 cases were reviewed by 7 participating prostate pathologists. For each case, at least two images (100X and 200X magnification) were circulated.

Results: Agreement was unanimous (7/7 pathologists) in 2 of 27 cases. Five pathologists agreed on the score in 16 cases. Of these 16 cases, 2 were scored as 6, 13 as 7, and one as tertiary pattern 5. In 11 cases pathologists assigned ≥ 3 Gleason scores; in 3 cases 4 or more Gleason scores were assigned. Fewer than 5 pathologists agreed on the score of Gleason 6 vs. 7 in 33% of cases. The percentage of cases for which a Gleason score 6 was assigned by an individual pathologist ranged from 11% to 60%. Of cases with marked grading variance, 6 consisted of small, tightly packed glands, making identification of a cribriform architecture difficult; 3 consisted of small, angulated, poorly formed glands, which is a morphology poorly defined by the ISUP 2005 Gleason grading criteria.

Conclusions: The presence of Gleason grade 4 is a threshold event for more aggressive treatment in active surveillance patients. In the present study the prostate pathologists did not reach a consensus as to whether pattern 4 was present in 33% of the cases. The difficulties in delineating this important treatment threshold include the definition of cribriform growth among crowded glands and classification of poorly-formed single glands.

807 ERG Protein Expression and Genomic Rearrangement Status in Primary and Metastatic Prostate Cancer – A Comparative Study of Two Monoclonal Antibodies

M Braun, D Goltz, Z Shaikibrahim, W Vogel, D Boehm, V Scheble, A Dobi, F Fend, N Wernert, G Kristiansen, S Perner. University Hospital of Bonn, Bonn, Germany; University Hospital of Tuebingen, Tuebingen, Germany; Uniformed Services University of the Health Sciences, Rockville.

Background: Overexpression of the ERG protein is highly prevalent in prostate cancer (PCa) and most commonly results from gene fusions involving the *ERG* gene.

Recently, an N-terminal epitope targeted mouse and a C-terminal epitope targeted rabbit monoclonal anti-ERG antibody have been introduced for the detection of the ERG protein. Independent studies reported that immunohistochemical (IHC) stains with both monoclonal anti-ERG antibodies (ERG-MAbs) highly correlate with the underlying *ERG* gene rearrangement status. However, a comparative study of both antibodies has not been provided so far. Here, we are the first to compare the mouse ERG-MAb to the rabbit ERG-MAB for their concordance on the same PCa cohort. Furthermore, we assessed if the ERG protein expression is conserved in lymph node and distant PCa metastases, of which a subset underwent decalcification.

Design: We evaluated tissue microarrays of 278 specimens containing 265 localized PCa, 29 lymph node, 30 distant metastases, and 13 normal prostatic tissues. We correlated the ERG protein expression with the *ERG* rearrangement status using an ERG break-apart fluorescence in-situ hybridization (FISH) assay and IHC of both ERG antibodies.

Results: ERG protein expression and *ERG* rearrangement status were highly concordant regardless of whether the mouse or rabbit ERG-MAB was used (97.8% versus 98.6%, respectively). Of interest, both ERG antibodies reliably detected the ERG expression in lymph node and distant PCa metastases, of which a subset underwent decalcification. If an ERG protein expression was present in localized PCa, we observed the same pattern in the corresponding lymph node metastases.

Conclusions: This is the first study to comprehensively compare the two available ERG-MAbs. By demonstrating a broad applicability of IHC to study ERG protein expression using either antibody, this study adds an important step towards a facilitated routine clinical application. Further, we demonstrate that the clonal nature of the *ERG* rearrangement is not restricted the genomic level, but proceeds in the proteom. Together, our results simplify future efforts to further elucidate the biological role of ERG in PCa.

808 Improved Method of Detecting the ERG Gene Rearrangement in Prostate Cancer Using Combined Dual-Color Chromogenic and Silver In-Situ Hybridization

M Braun, J Stomper, D Boehm, W Vogel, V Scheble, N Wernert, Z Shaikibrahim, F Fend, G Kristiansen, S Perner. University Hospital of Bonn, Bonn, Germany; University Hospital of Tuebingen, Tuebingen, Germany.

Background: The recently detected *TMPRSS2-ERG* fusion revealed as a recurrent and prevalent prostate cancer (PCa) specific event, which potentially qualifies it for clinical utilizations. To detect this alteration, fluorescence *in-situ* hybridization (FISH) is the method of choice. However, FISH harbors some disadvantages for widespread adoption in clinical practice. Subsequently, the chromogenic *in-situ* hybridization (CISH), that uses organic chromogens, and the enzymatic metallography silver *in-situ* hybridization (SISH) emerged as promising bright-field alternatives. Compared to CISH, SISH signals are very distinct and superior with regard to signal clarity and resolution, but rule out a multi-color protocol. However, the precise localization of genomic targets using a dual-color approach is indispensable for gene break-apart and fusion assays. In order to bridge this gap, we aimed to develop a dual-colour combined CISH and SISH (CS-ISH) gene break-apart assay on the example of the *ERG* gene commonly rearranged in PCa.

Design: On the basis of the *ERG* break-apart FISH assay, we established a dual-colour ERG break-apart CS-ISH assay and compared these results with those obtained by FISH. We assessed 178 PCa and 10 benign specimens for their *ERG* rearrangement status applying a dual-colour FISH and CS-ISH ERG break-apart assay on consecutive sections.

Results: We observed a highly significant concordance (97.7%) between FISH-based and CS-ISH-based results (Pearson's correlation coefficient 0.955, $P < 0.001$).

Conclusions: Our findings demonstrate that the *ERG* rearrangement status can reliably be assessed by CS-ISH. Further, we confirm that the CS-ISH technique combines the accuracy and precision of FISH with the ease of bright field microscopy. We developed a tool which allows a much broader spectrum of applicants to study the biological role and clinical utilization of *ERG* rearrangements in PCa. Moreover, our study is the first proof-of-principle for bright-field CS-ISH gene fusion or break-apart assays.

809 Rearrangement of the ETS Genes *ETV-1*, *ETV-4*, *ETV-5* and *LK-1* Is a Clonal Event during Prostate Cancer Progression

M Braun, Z Shaikibrahim, P Nikolov, D Boehm, W Vogel, R Menon, V Scheble, F Fend, G Kristiansen, N Wernert, S Perner. University Hospital of Bonn, Bonn, Germany; University Hospital of Tuebingen, Tuebingen, Germany.

Background: ETS gene rearrangements are frequently found in prostate cancer (PCa). Several studies have assessed the rearrangement status of the most commonly found ETS gene, *ERG*, and the less frequent genes, *ETV-1*, *ETV-4*, *ETV-5* and *ELK-4* in primary PCa. However, the frequency in metastatic disease is still not well investigated. Recently, we have assessed the *ERG* rearrangement status in both primary PCa and the corresponding lymph node metastases, and observed that *ERG* rearrangement in primary PCa transfers into lymph node metastases, suggesting it to be a clonal expansion event during PCa progression. As a continuation, we investigated in this study whether this observation is valid also for the less frequent ETS rearranged genes *ETV-1*, *ETV-4*, *ETV-5* and *ELK-4*.

Design: Using dual color break-apart FISH assays, we evaluated the status of all the less frequent ETS gene rearrangements for the first time on tissue microarrays (TMAs) constructed from a large cohort comprised of primary PCa and the corresponding lymph node metastases. Additionally, we evaluated the rearrangement status of all these ETS genes in a second cohort comprised of distant metastases.

Results: *ETV-1*, *ETV-4*, *ETV-5* and *ELK-4* rearrangements were found in 8/81 (10%), 5/85 (6%), 1/85 (1%) and 2/86 (2%) of the primary PCa, respectively, and in 6/73 (8%), 5/85 (6%), 4/72 (6%), 1/75 (1%) of the corresponding lymph node metastases, respectively. Rearrangements of *ETV-1* and *ETV-5* were not found in any of the distant metastases cases, whereas *ETV-4* and *ELK-4* rearrangements were found in 1/25 (4%) and 1/24 (4%) of the distant metastases, respectively.

Conclusions: Our results suggest that rearrangement of the less frequent ETS genes is a clonal event during prostate cancer progression. Our findings provide insights into potential clonal expansion events during PCa progression and may have significant implications in understanding the molecular basis of the metastatic cascade of PCa.

810 Worrisome Histologic Features in Benign Renal Oncocytoma: Immunohistochemical and Cytogenetic Analysis

M Brunelli, M Ficial, D Segala, E Munari, S Pedron, S Gobbo, M Chilosi, A Yilmaz, K Trpkov, B Delahunt, JN Eble, L Cheng, G Martignoni. University of Verona, Verona, Italy; University of Calgary, Calgary, AB, Canada; University of Otago, Wellington, New Zealand; Indiana University, Indianapolis, IN.

Background: Renal oncocytoma is a benign renal cell neoplasm that accounts for about 7% of kidney tumors. It sometimes shows atypical histological features (macroscopic central scar including worrisome cells with either clear cell changes or basophilic type 1 papillary renal cell carcinoma-like appearance, cytological atypia, oncoclasts, necrosis, perirenal fat infiltration, vascular invasion) which can represent a potential source of misdiagnosis of malignancies. The aim of the study is to characterize the immunophenotypic and cytogenetic profile of renal oncocytomas with atypical features.

Design: Seventy-six renal oncocytomas were retrieved from the Pathology database, University of Verona. Revision of the whole histological slides was performed, with morphological identification of atypical features. Ten cases representative of the group of worrisome histologic features were selected for immunophenotypic and cytogenetic analyses. Immunohistochemistry was performed using antibodies against Parvalbumin, CD10, CD13, Vimentin, Cytocheratin 7 (CK7), Racemase and S100A1. Fluorescence In Situ Hybridization (FISH) was used to detect chromosome 1, 2, 6, 7, 10, 17, Y and 11q13 abnormalities in "classical" and worrisome patterns.

Results: Tumors with at least one atypical morphological pattern were 48,7%. Central fibrous scar including epithelial cell proliferations was the most common atypical feature and was present in the 26,3%, cytological atypia in 15,8%, oncoclasts in 10,5%, vascular invasion in 9,2% and perinephric fat extension 2,6% of the cases. Mitosis were present in 1,3% of cases whereas no necrosis was found. Cell proliferations in the context of central fibrous scar had an immunophenotype similar to that observed in papillary renal cell carcinoma (CK7, CD10, CD13 and Racemase expression), but the entire chromosomal profile tested showed numerical normal pattern. All other atypical morphological features had a disomic chromosomal profile, with the exception of the areas of cytological atypia, that demonstrated frequent trisomies (67% of cases). **Conclusions:** Immunohistochemistry and cytogenetic investigations could be a useful tool in differential diagnosis between benign renal oncocytoma with atypical features and malignant epithelial tumors of the kidney, especially when the diagnosis should be done on limited material.

811 Clinicopathologic Characteristics of Renal Cell Carcinoma in Patients 45 Years of Age and Younger

R Carr, A Van Dyke, G Cai, K Haines, AJ Adeniran. Yale University School of Medicine, New Haven, CT.

Background: Renal cell carcinoma (RCC) occurs mainly in older people and is infrequently diagnosed in children and young adults. Limited studies have been conducted on RCC in the younger age group, hence the clinical and morphologic spectrum remain incompletely defined, and the behavior is poorly understood. The aim of this study was to analyse the clinicopathologic characteristics of RCC in patients 45 years old and younger.

Design: Based on the retrospective review of our files, cases diagnosed as renal cell carcinoma in patients 45 years old and younger in our institution between 1985 and 2011 were identified. Slides in our files were reviewed on all cases. Gross findings were obtained from pathology reports. Follow-up data was obtained from the clinical database. **Results:** We identified a total of 102 cases of RCC in patients aged 45 years and younger (63 males and 39 females). Age range: 3-45 years, median age: 40 years. Median tumor size: 3.7cm (range, 0.5-27cm). Laterality of tumor was evenly split between right and left but tumor most commonly located in the lower pole. Histological types: 58 clear cell, 24 papillary, 11 chromophobe, 5 translocation-associated, 2 multilocular cystic, 1 medullary and 1 mixed. Sixty-six patients underwent radical resections, 33 had partial resections while three had percutaneous needle biopsies. Tumor was unifocal in 94 cases while 8 had multifocal tumors. Approximately 50% of the tumors had Fuhrman nuclear grade 2. Pathologic stage at diagnosis: 53 pT1a, 17 pT1b, 14 pT2a, 5 pT2b, 9 pT3a and 1 pT3b. At the time of diagnosis, lymph node involvement, renal sinus fat invasion, main renal vein invasion, perinephric fat invasion and microvascular angiolymphatic invasion were identified in 5, 5, 5, 9 and 11 cases, respectively. Microscopic coagulative necrosis was identified in 33 cases, while sarcomatoid differentiation was present in 7 cases. Distant metastasis was present in 8 cases. Clinical outcome data: 4 alive with disease, 57 alive no disease, 25 alive NOS, 7 dead of disease (10 months average survival; 7 months median survival; 5 male; 3 female).

Conclusions: Although uncommon in children and young adults, RCC is predominantly clear cell type, occurs more commonly in males and mostly has an indolent course. Clear cell and translocation-associated subtypes account for the clinically aggressive cases.

812 Immunohistochemical Profile of Renal Cell Carcinoma in Patients Younger than 45 Years of Age: Analysis of 87 Cases of Different Tumor Subtypes

R Carr, G Cai, Y Bao, ML Prasad, SK Tickoo, AJ Adeniran. Yale University School of Medicine, New Haven, CT.

Background: Renal Cell Carcinoma (RCC) is distinctly rare in children and young adults. Because of the rarity of the tumor in this age group, the immunohistochemical

profile has not been fully described. The goal of this study is to define the immunohistochemical profile of the various subtypes of RCC in patients aged 45 and younger.

Design: A tissue microarray block with 87 cases of RCC (49 clear cell [CRCC], 23 papillary (PRCC), 10 Chromophobe [ChRCC] and 5 translocation-associated [TxRCC]) was constructed. The tumors were stained with the following diagnostic antibodies: cytokeratin (CK) AE1/AE3, CK7, CK903, TFE3, TFEB, CD10, AMACR, C-KIT, Vimentin, EMA, CA-IX; and with the following prognostic antibodies: PAX-8, survivin and VHL. The slides were reviewed and a stain was deemed to be positive if it demonstrated moderate to strong intensity in more than 5% of the tumor cells.

Results: Results of the immunohistochemical stains are listed in Table 1.

Table 1: Results of Immunohistochemical stains

	CRCC	PRCC	ChRCC	TxRCC
AE1/AE3	45/49	23/23	6/10	1/5
TFE3	0/49	0/23	0/10	5/5
TFEB	0/49	0/23	0/10	0/5
CD10	38/49	10/23	7/10	4/5
AMACR	17/49	23/23	1/10	2/5
C-KIT	1/49	1/23	8/10	0/5
CK903	4/49	9/23	0/10	0/5
Vimentin	49/49	23/23	2/10	5/5
CK7	16/49	18/23	9/10	0/5
EMA	31/49	18/23	10/10	1/5
CA-IX	34/49	4/23	0/10	0/5
PAX-8	21/49	17/23	2/10	2/5
Survivin	39/49	18/23	9/10	2/5
VHL	17/49	4/23	10/10	2/5

The overall profiles of the different tumor types are listed in Table 2.

Table2: Immunohistochemical Profile

Tumor type	Immunohistochemical profile
CRCC	AE1/AE3, Vimentin, CD10, EMA, CA-IX positive; PAX-8 variable; C-KIT, CK903 negative
PRCC	AE1/AE3, AMACR, Vimentin, CK7, EMA, PAX-8 positive; C-KIT, CA-IX, negative
ChRCC	AE1/AE3, CD10, C-KIT, CK7, EMA positive; AMACR, Vimentin, CK903, CA-IX, PAX-8 negative
TxRCC	TFE3, CD10, Vimentin positive; AE1/AE3, C-KIT, CK903, CK7, CA-IX negative

Conclusions: There is a significant overlap between the immunoprofile of RCC subtypes in patients aged 45 and younger and that in RCC subtypes in older patients. PAX-8 is expressed by a significant proportion of PRCC and variable proportions of the other subtypes, with a distinctive nuclear staining pattern. Survivin is expressed in a significant proportion of all RCC subtypes while VHL is highly expressed in ChRCC and variably in all other subtypes. The significance of this finding is uncertain, as further work needs to be done to determine the prognostic significance of these markers on the various subtypes of RCC.

813 Should Fuhrman Grading in Clear Cell Renal Cell Carcinomas Be Based on Nucleoli Only?

SS Chan, L Lee, J Chin, JA Gomez, M Moussa, GM Yousef, MY Gabriel. LHSC, London, ON, Canada; St. Michael's Hospital, Toronto, ON, Canada.

Background: Fuhrman grading has been shown to be second only to stage in prognostic significance for clear cell renal cell carcinomas (ccRCC). One major limitation of this system, however, is the variability in applying the grading criteria (including nuclear size, nuclear shape and nucleolar prominence) amongst pathologists. The use of nucleolar prominence as the only criteria for Fuhrman grading is under debate. In this multi-institutional study, we compare the interobserver variability and prognostic significance of using nucleolar prominence only vs. using all criteria for Fuhrman grading.

Design: 77 radical nephrectomies with a diagnosis of organ-confined ccRCC (1990-1998) were included in this study. All slides from all cases were re-reviewed and independently graded by three pathologists at different institutions. Each pathologist graded every ccRCC twice, once using all Fuhrman grading criteria (nuclear size, nuclear shape, nucleolar prominence) and then again based on nucleolar prominence only. Clinical data from 50 cases including length of follow-up, local recurrence, distant metastasis and death due to RCC was also collected. Data from three pathologists was used to determine the interobserver variability scores, and to determine the prognostic significance of each grading system.

Results: Interobserver Variability: The mean kappa values ranged from 0.42 to 0.66 using all Fuhrman grading criteria vs. 0.46 to 0.92 using nucleolar grade only between pathologists.

The mean kappa value when the two Fuhrman grading methods were applied by the same pathologist ranged from 0.24 to 0.39.

Prognostic Significance:

14 out of 50 cases of ccRCC developed metastasis.

Table 1: The Distribution of Metastasis Using All Fuhrman Criteria vs. Nucleoli Only

	All Criteria (n=50)	Nucleoli Only (n=50)	p-Value
Grade 1&2	1/15 (7%)	1/5 (20%)	(p>0.999)
Grade 3&4	13/35 (37%)	13/45 (29%)	(p>0.999)

*The overall mean follow up time for all cases was 91 months.

Conclusions: Interobserver agreement on Fuhrman grade was considerably improved by using nucleolar prominence compared with using all Fuhrman grading features. Importantly, using nucleolar grading only was comparable to using all features for Fuhrman grading in predicting prognosis. Hence, we consider nucleolar grading to be a reliable system to grade ccRCC that can improve consistency amongst pathologists without compromising on prognostic utility.

814 Xp11.2 Translocations in Adult Renal Cell Carcinomas with Clear Cell and Papillary Features

SM Chan, MY Gabriel, IJ Zbieranowski, LM Sugar, GM Yousef, GA Bjarnason, CG Sherman. Univ. of Toronto, Toronto, Canada; Univ. of Western Ontario, London, Canada.

Background: Xp11.2 translocation renal cell carcinoma (RCC) is a rare tumor with unpredictable clinical course and prognosis. Recognition of these tumors depends on the identification of a RCC with unique histology, particularly clear cell and papillary (CCP) features, in a child or young adult. Less is known about Xp11.2 RCCs in adults with regards to identification and prognosis. Our objectives were to determine the incidence of Xp11.2 translocations in adult RCCs with clear cell and papillary features, and to characterize the clinicopathological features and prognosis of adult Xp11.2 RCCs. **Design:** Slides from 1047 nephrectomies for RCC in adults from 1999-2009 were retrieved from multiple institutions. Cases were reviewed histologically in order to detect any degree of clear cell and papillary change. Tissue microarrays were constructed from the clear cell and papillary RCCs as well as 40 non-papillary clear cell, 5 papillary, 3 chromophobe and 2 unclassified RCCs. Immunohistochemistry using TFE3, a marker highly sensitive (97.5%) and specific (99.6%) for Xp11.2 translocations and TFEB, another marker of translocation carcinomas was performed. Four pathologists independently reviewed the TFE3 and TFEB and only cases in which there was consensus agreement for moderate or strong staining were considered positive. Clinical and pathologic data were also retrieved.

Results: Out of 1047 RCCs, 140 (13%) exhibited clear cell and papillary features. Four out of these 140 (3%) were positive for TFE3 and all were negative for TFEB. All of the non-papillary clear cell, papillary, chromophobe and unclassified RCCs were negative for TFE3 and TFEB.

Comparison of the Clinicopathological Features & Prognosis of TFE3+ CCRCC, TFE3- CCRCC & Non-Papillary Clear Cell RCCs

	TFE3+ CCRCC (n=4)	TFE3- CCRCC (n=136)	Non-Papillary Clear Cell RCC (n=40)
Mean Age (Years)	54	62	60
Mean Size (cm)	4.1	6.0	5.2
pT1	4(100%)	80(60%)	28(70%)
pT2	0(0%)	17(13%)	2(5%)
pT3	0(0%)	35(26%)	10(25%)
pT4	0(0%)	1(1%)	0(0%)
Local Recurrence	0(0%)	13(10%)	9(23%)
Distant Metastasis	0(0%)	31(23%)	5(13%)
Death due to RCC	0(0%)	11(8%)	4(10%)

*Mean follow up for TFE3+ RCCs was 55 months

Conclusions: Xp11.2 translocation RCCs diagnosed by TFE3 immunohistochemistry were identified in 3% of adult RCCs that had clear cell and papillary changes. These tumors appear to present with smaller tumour size, lower stage and better prognosis in comparison to non-Xp11.2 CCRCC and clear cell RCCs. In addition to Xp11.2 translocation carcinoma, coexistence of clear cell and papillary features may be present in other subsets of tumors that have yet to be characterized.

815 Utility of Gata3 in the Diagnosis of Urothelial Carcinoma

A Chang, A Amin, P Illei, E Gabrielson, JI Epstein. The Johns Hopkins Hospital, Baltimore.

Background: Distinguishing invasive high-grade urothelial carcinoma (UC) from other carcinomas occurring in the genitourinary tract may be difficult. In men, UC must be differentiated from high-grade prostatic adenocarcinoma and spread from an anal squamous cell carcinoma (SCC).

Design: Immunohistochemistry for GATA3, thrombomodulin, and uroplakin III was performed on a tissue microarray (TMA) containing cores from 35 radical cystectomy specimens with invasive high-grade UC. A TMA with 38 high-grade (Gleason score ≥ 8) prostatic adenocarcinomas and tissue sections from 15 cases of invasive anal SCC were stained with GATA3. Additionally, tissue sections from 15 cases of pulmonary metastases of UC and a TMA with 25 cases of pulmonary SCC and 5 cases of non-small cell carcinomas of the lung with squamous features were stained with GATA3.

Results: Of the 28 GATA3 positive UCs, 25 (89%) cases showed moderate or strong staining, while 3 (11%) cases had weak staining. All positive GATA3 staining was non-focal with at least 20% of the tumor cells being positive. Of the 7 cases that failed to express GATA3, 5 were positive for thrombomodulin and/or Uroplakin III, while 2 cases were negative for all 3 markers. None of the 38 high grade prostatic adenocarcinomas were positive for GATA3. Weak GATA3 staining was present in occasional basal cells of benign prostate glands, in a few benign atrophic glands, and in urothelial metaplasia. Of the 15 cases of anal SCCs, 2 cases showed focal weak staining and 1 case showed focal moderate staining. Weak staining was also rarely observed in the benign anal squamous epithelium. Twelve (80%) of the metastatic UC to the lung were positive for GATA3 with 11 cases showing diffuse moderate or strong staining and 1 case showing focal moderate staining. None of the pulmonary SCC or non-small cell carcinomas with squamous features were GATA3 positive.

	Positive Cases	Negative Cases
GATA3	28 (80%)	7 (20%)
Thrombomodulin	22 (63%)	13 (37%)
Uroplakin III	21 (60%)	14 (40%)

Conclusions: GATA3 is a sensitive immunohistochemical marker for UC and positive staining in UC is typically non-focal and moderate or strong in intensity. In male patients, when excluding high-grade prostatic adenocarcinoma, GATA3 is a specific marker. Caution must be taken as rare cases of anal SCC can be GATA3 positive, however this staining, unlike staining in UC, tends to be focal and weak. GATA3 is also a useful marker when diagnosing metastatic UC. Studies assessing GATA3 expression in invasive cervical SCC will be performed.

816 Utility of Gata3 and Pax8 Immunohistochemistry in Diagnosing Sarcomatoid Urothelial Carcinoma (UC) and Sarcomatoid Renal Cell Carcinoma (RCC)

A Chang, F Brimo, EA Montgomery, JI Epstein. The Johns Hopkins Hospital, Baltimore.

Background: PAX8 is a sensitive marker for RCC. GATA3 is a newly described marker for UC. Both have not been studied in their ability to distinguish sarcomatoid RCC from sarcomatoid UC from other spindle cell lesions seen in the GU tract.

Design: TMAs were constructed from 45 cases of sarcomatoid RCC, 46 cases of sarcomatoid UC, and compared to an existing TMA of 161 primary sarcomas. In addition, sections from 10 sarcomatoid UCs involving the upper urinary tract, 13 atypical epithelial angiomyolipomas (AMLs) of the kidney, 12 inflammatory myofibroblastic tumors (IMTs) and 4 leiomyosarcomas (LMSs) involving the bladder were studied. Only moderate or strong staining was considered positive.

Results:

	PAX8 (+)	GATA3 (+)	PAX2 (+)	RCC (+)	CD10 (+)
Sarcomatoid RCC	31/45 (69%)	0/45 (0%)	3/45 (7%)	2/45 (4%)	23/45 (51%)

	PAX8 (+)	GATA3 (+)	Thrombomodulin (+)
Bladder Sarcomatoid UC	3/46 (7%)	14/46 (30%)	9/46 (20%)

Of 10 cases of sarcomatoid UC of the upper urinary tract, 1 (10%) was positive for PAX8 and 2/10 (20%) were positive for GATA3. Of the 161 primary sarcomas, none of the cases that would be considered in the differential diagnosis of sarcomatoid RCC or UC were positive for either PAX8 or GATA3 (only 1 positive EWINGS/PNET for PAX8).

None of the renal 13 atypical epithelioid AMLs were PAX8 positive, and all of the IMTs and LMSs of the bladder were GATA3 negative. Of the 17 cases of sarcomatoid RCC with an epithelial component present for examination (10 clear cell, 2 chromophobe, 2 papillary, and 2 unclassified), 15 (88%) were PAX8 positive, and of those 15, 10 (67%) retained PAX8 staining in the sarcomatoid areas. Of the 19 sarcomatoid UC with an epithelial component available for examination (7 invasive high grade UC, 11 high grade papillary non-invasive carcinomas, and 1 CIS), 14 (74%) were GATA3 positive, and of those cases, 6 (43%) retained GATA3 staining in the sarcomatoid areas.

Conclusions: PAX8 is the most sensitive marker for sarcomatoid RCC. While PAX8 can be utilized to exclude atypical epithelioid AMLs and sarcomas with high grade and spindle cell morphology, sarcomatoid UC may also be PAX8 positive limiting its utility. GATA3 is a specific marker for sarcomatoid UC and can be used to exclude sarcomatoid RCC and other spindle cell lesions, although its sensitivity in sarcomatoid UC is not high. Focal weak nonspecific nuclear staining was seen in a few cases with both PAX8 and GATA3, such that only moderate-strong nuclear staining should be considered positive.

817 High Risk Human Papilloma Virus DNA Detected in Primary Squamous Cell Carcinoma of Urinary Bladder

J Chapman-Fredericks, M Cioffi-Lavina, M Accola, W Rehrauer, M Garcia-Buitrago, C Gomez-Fernandez, P Ganjei-Azar, R Cote, M Jorda. University of Miami, Jackson Memorial Hospital, Sylvester Cancer Center, Miami, FL; University of Wisconsin School of Medicine, Madison, WI.

Background: The oncogenic role of Human Papillomavirus (HPV) in many epithelial neoplasms has been well documented, however its role in bladder carcinogenesis is controversial. We previously reported that 37% of primary urinary bladder squamous cell carcinomas (SCC) demonstrate diffuse p16 immunoreactivity. p16 has been used as a surrogate marker for HPV infection, but p16 expression may be due to non HPV-related mechanisms. We attempted to detect HPV DNA in the tumor cells of p16 positive primary bladder SCC using in situ hybridization (ISH) and a signal amplification Invader assay followed by genome sequencing.

Design: Fourteen cases of p16 positive primary SCC of the bladder (8 male, 6 female) were reviewed. Analysis for High Risk (HR) HPV was performed in all cases using both 16/18 ISH and Invader assay. Screening for HR HPV and identification of HPV types 16/18 was accomplished using Cervista™ HPV HR and Hologic Cervista™ HPV 16/18 reagents, respectively. HR HPV positive samples were then amplified with type specific primers and products of amplification were DNA sequenced using Big Dye version 2.0 on an Applied Biosystems instrument.

Results: HPV 16/18 ISH was negative in all cases. However, 3 of 14 cases (21.4%) were positive for HR HPV using the Cervista™ detection method. HPV DNA was amplified and sequenced in all 3 positive cases using type specific primers. Two of the positive cases demonstrated HPV 16 genotype using Cervista™ HPV 16/18 reagents, and this finding was confirmed by amplification and sequencing. The genotype of the third positive case could not be determined using the Cervista™ HPV 16/18 method but by sequencing it was found to be HPV type 35. The 3 HPV DNA cases were all from female patients ages 52, 64 and 70 years.

Conclusions: HR HPV DNA was identified in a 21% of p16 positive bladder SCC by two independent methods (Invader signal amplification and HPV DNA sequencing). This study confirms that HR HPV is present in a subset of primary bladder SCC. Since ISH method failed to detect the presence of HR HPV in some cases, it appears that ISH can not be used as the sole method for detection of HPV. The fact that all cases used in this study were known to express p16 by IHC but only 21.4% contained HR HPV DNA, suggests that other non-HPV related mechanisms may contribute to p16 expression in bladder SCC. Thus, p16 should not be used as a surrogate marker for the presence of HPV in this setting.

818 E-Cadherin Expression in Prostatic Adenocarcinoma: Correlation with Gleason Score and Comparison with Invasive High Grade Urothelial Carcinoma

EC Chastain, S Ali, AO Osunkoya. Emory University School of Medicine, Atlanta.

Background: Alteration of expression of the cellular adhesion molecule E-cadherin has been linked to invasive phenotypes of a variety of neoplasms. Hitherto, there have been limited studies of E-cadherin expression in prostatic adenocarcinoma (PCa). The utility of E-cadherin in the distinction between PCa and urothelial carcinoma (UCa) has also not been well characterized. The goals of this study are; (a) to determine E-cadherin expression in PCa, with emphasis on correlation with Gleason score, and (b) to determine if it can be included in the panel of markers to distinguish between PCa and UCa.

Design: A search through the surgical pathology and consultation files of a large academic institution was made for cases of PCa with Gleason scores 6, 7, 8 and 9. 10 cases of usual type invasive high grade UCa were also included in the study. To exclude the possibility of variability of marker expression, TMA analysis was not utilized. All cases were obtained from representative slides of radical prostatectomy, cystectomy, transurethral resection, or needle core biopsy specimens. Slides were stained with antibodies to E-cadherin and examined for degree of expression (Negative: 0, weak: 1+, moderate: 2+ and strong: 3+).

Results: 81 cases of PCa were identified with Gleason scores as follows; 23 cases (Gleason score 3+3=6), 25 cases (Gleason score 3+4=7 or 4+3=7), 17 cases (Gleason score 4+4=8), and 16 cases (Gleason score 4+5=9). 65 cases (80%) of PCa had moderate to strong (2+ to 3+) E-cadherin expression and only 16 cases (20%) showed negative or weak (1+) E-cadherin expression. Moderate to strong (2+ to 3+) E-cadherin expression was observed in 20/23 cases (87%) of Gleason score 3+3=6, 22/25 cases (88%) of Gleason score 3+4=7 or 4+3=7, 11/17 cases (65%) of Gleason score 4+4=8 and 12/16 cases (75%) of Gleason score 4+5=9. Of the 16 cases with negative or weak (1+) E-cadherin expression, 3/23 cases (13%) were Gleason score 3+3=6, 3/25 (12%) were Gleason score 3+4=7 or 4+3=7, 6/17 cases (35%) were Gleason score 4+4=8, and 4/16 cases (25%) were Gleason score 4+5=9. 10/10 cases (100%) of usual type invasive high grade UCa had moderate to strong (2+ to 3+) E-cadherin expression.

Conclusions: E-cadherin expression in PCa is not consistently decreased with increased Gleason score, and thus may not be involved in differentiation of PCa. The expression of E-cadherin in PCa, Gleason scores 4+4=8 and 4+5=9, also precludes this marker from being used in a panel to distinguish between high grade PCa and usual type invasive high grade UCa.

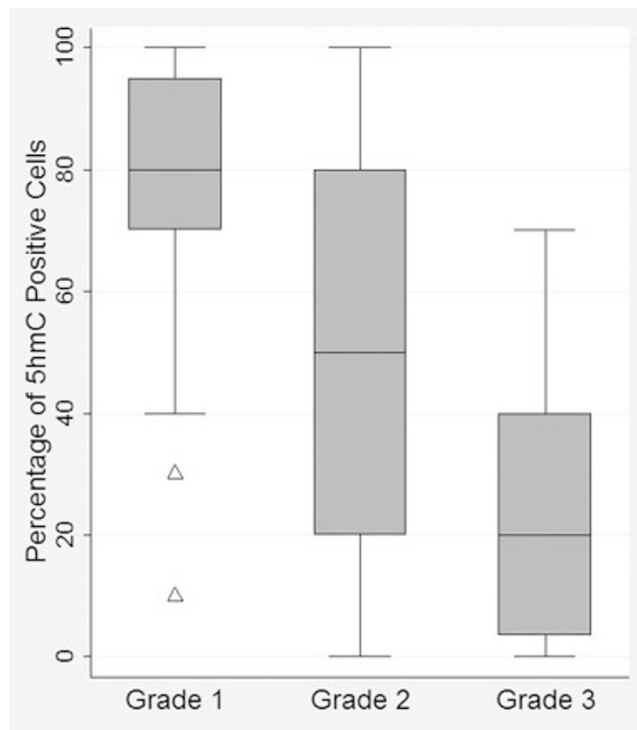
819 5-Hydroxy-Methyl-Cytosine Content Is Strongly Associated with Degree of Histologic Differentiation in Penile Squamous Cell Carcinomas

A Chauh, MC Haffner, WG Nelson, KL Lecksell, S Yegnasubramanian, AL Cubilla, GJ Netto. Johns Hopkins University, Baltimore, MD; Instituto de Patologia e Investigacion, Asuncion, Paraguay.

Background: Cytosine methylation represents an important epigenetic modification that plays a crucial role in normal differentiation as well as carcinogenesis. Recent evidence suggests that methylated cytosine (5mC) can become oxidized to 5-hydroxymethylcytosine (5hmC) in mammalian genome. We have recently shown that global 5hmC levels are greatly reduced in invasive adenocarcinoma. Here we evaluate the status of 5hmC in squamous cell carcinoma of the penis and explore the association of 5hmC with the degree of tumor differentiation.

Design: Thirty-eight formalin-fixed paraffin-embedded archival cases of penile squamous cell carcinoma were selected to build a tissue microarray (TMA). Each tumor was sampled 3–9 times. TMA spots were scanned using the APERIO system and uploaded to the TMAJ platform (<http://tmaj.pathology.jhmi.edu>). In total, 147 individual TMA spots were evaluated. Histological grade was assigned in each spot. Global 5hmC levels were assessed using a 5hmC specific antibody and standard immunohistochemical techniques. Extent of 5hmC expression was estimated in each spot as a percentage of positive cells. Association between 5hmC extent and grade was evaluated by the Kruskal-Wallis test and trends were confirmed using Cuzick's test.

Results: Normal squamous epithelium showed strong staining for 5hmC. In invasive tumors, extent of 5hmC expression showed a strong association with tumor differentiation. 5hmC extent decreased with increasing histologic grade (Figure 1). Differences were significant ($P = .0001$), as well as trend across ordered categories ($P < .0001$).



Conclusions: In penile squamous cell carcinomas, global 5hmC levels significantly decrease with increased histologic grade. Our finding suggests that alterations in 5hmC expression are associated with carcinogenesis and are inversely correlated with tumor differentiation in penile squamous cell carcinoma.

820 Loss of PTEN Immunoreexpression Is Associated with Increased Risk of Recurrence after Prostatectomy for Clinically-Localized Prostate Cancer

A Chauh, S Peskoe, N Gonzalez-Roibon, J Hicks, AM De Marzo, EA Platz, GJ Netto. Johns Hopkins University School of Medicine, Baltimore, MD; Bloomberg School of Public Health, Johns Hopkins University, Baltimore, MD.

Background: PTEN is one of the most frequently lost tumor suppressor genes in human cancers. Specifically, loss of PTEN has been described in more than two-thirds of patients with prostate cancer, and several studies have suggested that PTEN loss is associated with tumor progression. The current study evaluates the prognostic role of PTEN loss as a predictive of recurrence following prostatectomy for clinically-localized prostate cancer, independent of known clinicopathological factors.

Design: PTEN expression was evaluated in a nested case-control study that included 451 cases (recurrence) and 451 controls (nonrecurrence). Patients were matched on Gleason grade, pathological stage, race/ethnicity, and age at surgery. All radical prostatectomies were performed at our institution between 1993 and 2001. Recurrence was defined as biochemical recurrence, development of clinical evidence of metastasis, or death from prostate carcinoma. Triplicate tumor samples per patient were used to build 16 tissue microarrays (TMAs). PTEN expression was evaluated using immunohistochemistry. Any TMA spot showing loss of PTEN expression, either focal or diffuse, was classified as "PTEN markedly decreased". Additionally, an H-score was calculated as the sum of the products of stain intensity (0 to 3+) and extent (percentage) in each TMA spot and the mean H-score of all spots per case was used. Odds ratios (OR) of recurrence and 95% confidence intervals (95% CI) were estimated using conditional logistic regression to account for the matching factors, and to adjust for year of surgery, preoperative PSA concentrations, and status of surgical margins.

Results: Markedly decreased PTEN expression was observed in 62% percent of the recurrence cases and 53% of the nonrecurrence controls ($P = .01$). Men whose TMA spots all had markedly decreased PTEN expression had a 60% higher risk of recurrence (OR = 1.6; 95% CI 1, 2.5) when compared with all other men. The OR of recurrence was 2.2 (95% CI 1.3, 3.6; $P = .002$) comparing a mean H score < 10 to ≥ 10 .

Conclusions: In patients treated by prostatectomy for clinically-localized prostate cancer, decreased immunohistochemical expression of PTEN is associated with an increased risk of recurrence, independent of known clinicopathological factors.

821 Immunohistochemical Expression of Phosphorylated S6 Is Associated with Degree of Differentiation in Penile Squamous Cell Carcinoma

A Chauh, AL Cubilla, J Hicks, KL Lecksell, AL Burnett, GJ Netto. Johns Hopkins University, Baltimore, MD; Instituto de Patologia e Investigacion, Paraguay.

Background: Activation of the mTOR pathway is essential for normal cell growth, differentiation, and specialization. Additionally, dysregulation of this pathway has been implicated in the pathogenesis of several cancers, including tumors of the kidney, prostate, and bladder. However, studies on the status of the mTOR pathway in penile squamous cell carcinomas (SCC) are scant. Herein, we evaluate the immunoreexpression of members of the mTOR pathway in a large series of penile carcinomas.

Design: One-hundred and twelve cases of penile SCC were used to build 4 tissue microarrays (TMA). Each tumor was sampled 3–12 times. TMA spots were scanned using the APERIO system and uploaded to the TMAJ platform (<http://tma.pathology.jhmi.edu>). Immunohistochemical expression of phosphorylated AKT (phos-AKT), phosphorylated mTOR (phos-mTOR), and phosphorylated S6 (phos-S6) was assessed by immunohistochemistry, using a previously described protocol (Am J Surg Pathol 2011;35:1549). Percentages of positive cells were estimated in each TMA spot and average values per case were used for data analysis.

Results: Low extent of phos-AKT (mean 1.3%, SD 2%) and phos-mTOR (mean 0.5%, SD 2%) expression were observed. Higher phos-S6 expression was noted (mean 38%, SD 26%). No association was observed between expression levels of phos-AKT, phos-mTOR, or phos-S6 and histologic subtype ($P > .05$). However, low grade (grades 1 or 2) tumors had significantly higher levels of phos-S6 than high grade (grade 3) tumors (52% vs. 31%, $P = .0001$). The difference in phos-S6 expression by histologic grade was independent of histologic subtype. There was no significant association between phos-AKT or phos-mTOR and histologic grade.

Conclusions: Expression levels of phos-S6 were associated with histologic grade in penile SCC, independent of histologic subtype. Well to moderately differentiated tumors had higher levels of phos-S6 compared to high grade tumors. In light of the recently identified specific inhibitors of S6 kinases, these findings might be useful in the planning of future clinical trials for patients with penile cancer.

822 Unclassified Renal Cell Carcinoma: A Contemporary Study of 116 Cases with Emphasis on Tumors with Aggressive Behavior

Y Chen, H Al-Ahmadie, A Gopalan, SW Fine, VE Reuter, SK Tickoo. Memorial Sloan-Kettering Cancer Center, New York.

Background: Renal cell carcinoma, unclassified (URCC) is a diagnosis given to renal cell tumors that do not fit into one of established histologic subtypes in the current WHO classification. They constitute 3–5 % cases in several surgical series. The clinicopathologic spectrum and genetic alterations in URCC have not been well studied.

Design: Using current diagnostic criteria for URCC, we retrospectively identified a cohort of 116 patients who were diagnosed and surgically treated at our institution in 1989–2010. Low grade oncocytic tumors were excluded for the purpose of this study.

Results: 68 (59%) patients were men and 48 (41%) women. Mean age at nephrectomy was 58.1 years (11–86), mean tumor size was 6.7 cm (1.3–18.0), and 15 patients had multiple tumors bilaterally or ipsilaterally. Median follow-up is 26 months (6–202). Based on histologic features, we were able to divide the tumors into 3 main groups: I). Tumors with a mixture of clear and eosinophilic cells, variable architectural patterns including alveolar, papillary and solid, and without extensively infiltrative borders; many of these resembled translocation-associated RCC, but were TFE3/B negative. (n=31;27% II). Tumors lacking clear cells, with variable but often prominent papillary architecture and extensively infiltrative borders; some of these raised the possibility of collecting duct carcinoma or type 2 papillary RCC. (n=57;49% III). Tumors predominantly composed of high-grade oncocytic cells in variable architectural patterns other than papillary. (n=28;24%) There was no significant difference in age, gender or tumor size among the 3 groups. As summarized in table, there were significant differences among the groups for high tumor stage, lymph node and distant metastases at presentation, as well as death due to disease, with tumors in group II appearing to be the most aggressive.

Histologic Groups	N	≥ pT3 (%)*	N1/2 (%)*	M1 (%)*	Met. for M0 Pt in F/U (%)	DOD (%)
I	31	19 (61)	7 (23)	2 (6)	9 (29)	7 (23)
II	57	38 (67)	29 (51)	13 (23)	17 (30)	27 (47)
III	28	6 (21)	0	0	3 (11)	2 (7)
p value		<.001	<.001	<.001	.133	<.001

* Stage at nephrectomy

Conclusions: Sub-grouping high-grade URCC by morphology reveals groups with dissimilar clinical course and outcome. Tumors in group II (with usually prominent papillary architecture, infiltrative borders, and lacking clear cells) present with early metastasis and are associated with highest cancer-specific mortality. Further studies including mutation and expression analysis are ongoing to identify molecular alterations which may help better define subsets of tumors in the URCC category.

823 Chromophobe Renal Cell Carcinoma: Is Grading Necessary?

JC Chevillat, WR Sukov, CM Lohse, HR Thompson, BC Leibovich. Mayo Clinic, Rochester, MN.

Background: It has been demonstrated that Fuhrman grading is not appropriate for chromophobe renal cell carcinoma (ChRCC). The objective of this study was to determine if nucleolar grading and the recently described ChRCC grading system by Paner et al. (Am J Surg Pathol 2010;34:1233–1240) provide prognostic information.

Design: Pathologic features of 185 patients with ChRCC treated surgically between 1970–2006 were reviewed including nucleolar grade, ChRCC grade, the 2010 TNM groupings, sarcomatoid differentiation, and coagulative tumor necrosis. Cancer-specific (CS) survival was estimated using the Kaplan-Meier method and associations with CS survival were evaluated using Cox proportional hazards regression models.

Results: Twenty-three patients died from ChRCC at a mean 3.0 years (yrs) following surgery (median 1.3; range 0–16) with estimated CS rates (95% CI) at 5, 10 and 15 yrs following surgery of 89% (84–94), 86% (81–92) and 85% (78–91), respectively. Univariate associations with CS survival included the 2010 TNM stage groupings, sarcomatoid differentiation, coagulative tumor necrosis, ChRCC grade, and nucleolar grade (all $p < 0.001$). These last four features remained significantly associated with CS survival after adjusting for the 2010 TNM stage groupings. When the analysis was restricted to the 155 patients with non-sarcomatoid TNM stage groupings I and II ChRCC, only stage grouping (I vs II) was significantly associated with CS survival ($p = 0.03$).

Conclusions: Although the ChRCC grading system described by Paner et al and nucleolar grade are associated with CS survival in ChRCC, they add no additional prognostic information once TNM stage and sarcomatoid differentiation are assessed.

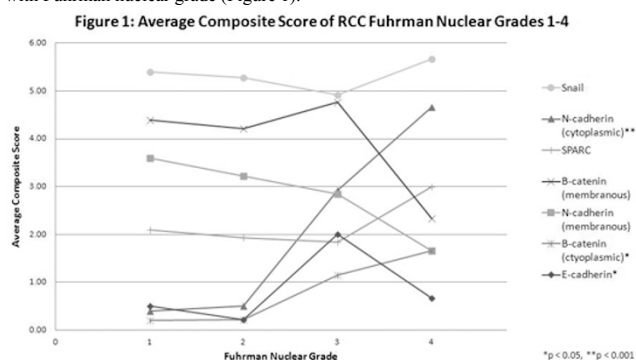
824 Does Increasing Fuhrman Nuclear Grade Reflect Evolving Epithelial-Mesenchymal Transition in Clear Cell Renal Cell Carcinoma?

JL Conant, Z Peng, MF Evans, S Naud, K Cooper. University of Vermont College of Medicine, Burlington, VT.

Background: We have previously demonstrated that sarcomatoid renal cell carcinoma (SRCC) is an example of epithelial-mesenchymal transition (EMT). E- to N-cadherin switching, dissociation of β -catenin from the membrane into the cytoplasm, and increased expression of Snail and SPARC confirmed that SRCC is an example of EMT. In general, all SRCC are considered Fuhrman nuclear grade 4. Nuclear grade is an important prognostic indicator in clear cell renal cell carcinoma (RCC). The goal of this study was to evaluate the expression of EMT markers in clear cell RCC, Fuhrman grades 1–4 (without a sarcomatoid component), to determine if there is a progression towards SRCC EMT with increasing nuclear grade.

Design: E-cadherin, N-cadherin, β -catenin, Snail, and SPARC expression was analyzed by immunohistochemistry on 40 formalin-fixed, paraffin-embedded clear cell RCC specimens, Fuhrman nuclear grades 1–4. Expression was scored as absent, mild, moderate, or strong according to intensity and extent (composite score 0–6).

Results: Expression of E-cadherin, cytoplasmic N-cadherin, and cytoplasmic β -catenin increased with increasing Fuhrman nuclear grade (Spearman 0.33, 0.59, and 0.40, respectively). The expression of all remaining EMT markers did not differ significantly with Fuhrman nuclear grade (Figure 1).



Conclusions: With increasing Fuhrman nuclear grade, there is a progressive increase in cytoplasmic expression of N-cadherin and β -catenin. While not statistically significant, there is a trend toward progressive decrease in membranous expression of these two markers, suggesting that N-cadherin and β -catenin dissociate from the membrane and into the cytoplasm as nuclear grade increases, representing potentially incipient EMT with increasing Fuhrman nuclear grade.

825 Urothelial CIS with Microinvasion: A Morphologic and Prognostic Study

R Cox, JI Epstein. The Johns Hopkins Hospital, Baltimore.

Background: CIS is rarely accompanied by early superficial invasive urothelial carcinoma (UC). There is no standard definition of microinvasion and some definitions have included cases with quite extensive invasion. As a result, the significance of small foci of invasion is unknown. One one hand limited invasion could be associated with a good prognosis, and on the other hand once CIS shows the ability to invade it is possible it is associated with a poor prognosis.

Design: 14 cases of CIS with microinvasion were reviewed from the consultation files of one of the authors. Cases with previous diagnoses of invasive UC were excluded. Microinvasion was defined as tumor invading less than a 40x high dry lens (i.e. <0.5mm) from the basement membrane. The inflammatory reaction was categorized from 0 for no reaction to 3+ for extensive reaction.

Results: Patients ranged in age from 57–89 (mean 73). 12/14 patients were male. 2 patients had a prior history of non-invasive high grade papillary UC, while 1 patient had a history of non-invasive low grade papillary UC of the kidney. 1 patient was diagnosed with concurrent non-invasive high grade papillary UC. Microscopically, 10 cases had a depth of invasion less than one-half of a 40x field with the remaining 4 cases deeper yet still less than a 40x field. 6 cases had invasive nests of cells, 4 had individual invasive cells, and 4 cases had both nests and individual cells. One case had invasive micropapillary features. The inflammatory response was 0 in 2 cases, 1+ in 2 cases, 2+ in 8 cases, and 3+ in 2 cases. Desmoplastic stromal reaction was noted in only 2 cases. 4 cases had focal (<50% surface area) and 2 cases had extensive denudation. Follow up information was available for 12/14 patients (mean: 40.2 mos., range: 4 mos. to 14 yrs.). 9 patients showed no evidence of disease at the last follow-up. 2 patients were alive with recurrent disease (one 15 mos. after the original diagnosis and one at 3 yrs.). 1 patient died of unknown causes at 7.5 yrs. The mode of treatment was known for 8 patients: 4 received BCG only; 3 had cystectomy (2 for BCG refractory disease, 1 for invasive UC into the muscularis propria); and 1 received no additional treatment.

Conclusions: CIS with microinvasion is relatively rare and foci of invasion can be very subtle, sometimes highlighted by keratin immunohistochemistry. Using the currently proposed definition, these patients have an overall favorable prognosis, although the presence of BCG refractory disease and progression of the disease into deeper invasion can lead to cystectomy.

826 Clear Cell Papillary Cystadenoma of the Epididymis and Mesosalpinx: Immunohistochemical Relationship to Clear Cell Papillary Renal Cell Carcinoma (RCC)

R Cox, JI Epstein. The Johns Hopkins Hospital, Baltimore, MD.

Background: Clear cell papillary cystadenoma of the epididymis and mesosalpinx is rare and may be associated with von Hippel Lindau disease. Although rare, metastases of clear cell RCC to the testis and paratesticular region have been documented. Prior studies on a few cases showed the efficacy of CK7 and RCC in differentiating between this entity and metastatic clear cell renal cell carcinoma. Due to the emergence of additional markers commonly used in evaluating a renal origin for metastatic RCC, we have evaluated the immunohistochemical staining patterns of clear cell papillary cystadenomas using both CK7 and RCC as well as PAX 8, carbonic anhydrase IX (CAIX), and AMACR.

Design: Six cases of clear cell papillary cystadenoma were retrieved from our consult files from 2003-2011. 5 cases involved the epididymis and 1 involved the mesosalpinx. Patients ranged in age from 20-65 years.

Results: The lesions were composed of cysts, tubules, and papillary cores, lined by cuboidal to columnar bland-appearing cells with clear cytoplasm. In 3 cases there was reverse polarity of nuclei. All cases had areas that resembled the newly described clear cell papillary RCC. All lesions were strongly positive for CK7, yet AMACR staining was negative in 4 of the 6 cases; the remaining 2 cases showed only focal, weak staining. CAIX was positive in all lesions (diffusely positive in 5, patchy in 1), yet all were negative for RCC. PAX 8 showed diffuse positivity in 5 of the 6 lesions, with 1 epididymal lesion negative.

Conclusions: Clear cell papillary cystadenoma of the epididymis and mesosalpinx are morphologically similar to, and can be confused with, metastatic clear cell RCC. Due to the prevalence of both entities in patients affected by von Hippel Lindau disease, and the propensity for clear cell RCC to metastasize to unusual sites, immunohistochemical markers are a useful adjunct in the diagnosis of the two lesions. Although a positive CK7/negative RCC staining profile can be used to differentiate clear cell papillary cystadenoma from metastatic clear cell RCC, care must be taken when using the newer markers for renal origin, as both carbonic anhydrase IX and PAX 8 are commonly positive in both lesions. An additional interesting finding is the similarity in the staining pattern of clear cell papillary cystadenoma to the recently described clear cell papillary RCC, along with the observation that they also share certain morphological features.

827 Expression of Parafibromin in Renal Tumors and Its Potential Correlation with Tumor Prognosis

C Cui, P Lal, Y Ma, JE Tomaszewski, Z Bing. Hospital of the University of Pennsylvania, Philadelphia, PA.

Background: Parafibromin, encoded by HRPT2 gene, is a recently identified tumor suppressor. Complete and partial loss of parafibromin expression has been found in the parathyroid carcinoma, the hyperparathyroidism-jaw tumor (HPT-JT), lung carcinoma and breast carcinoma. So far, little has been known about its role in renal tumors. Parafibromin expression has only been examined in a small series of chromophobe renal cell carcinomas and oncocytomas of kidney. In this study, we report the expression of parafibromin in a large series of renal tumors, including clear cell renal cell carcinoma (RCC), papillary RCC, chromophobe RCC and oncocytoma, using tissue microarrays (TMA).

Design: 19 cases of renal oncocytoma, 23 cases of chromophobe RCC, 37 cases of papillary RCC, and 61 cases of clear cell RCC, from 1991 to 2009, were retrieved from the pathology archives of the Hospital of the University of Pennsylvania and used for the construction of multiple renal tumor TMAs. The constructed renal tumor TMAs were sectioned, incubated with primary and secondary antibodies and visualized with the avidin-biotin-peroxidase complex method. The staining was classified into 3 patterns according to Gill et al. Diffuse staining in over 95% nuclei with strong intensity was considered "diffusely strong positive." No nuclear staining in all (>99%) of tumor tissue was defined as "Negative staining". All other staining patterns were "Weak staining".

Results: All of the 19 cases of oncocytoma showed strong nuclear staining (100%). 12 of the 23 chromophobe RCC showed positive nuclear staining (52%); 11 were negative. Among the 37 cases of papillary RCC, 15 are type 1 papillary RCC, 1 of them was positive for parafibromin stain; 22 are type 2 papillary RCC, 6 of them are positive for parafibromin stain; the overall positive cases are 7 (19%). Out of the 61 clear cell RCC cases, only 3 of them were positive for parafibromin stain (5%).

Conclusions: Parafibromin expression varies significantly among the different types of renal tumors. Parafibromin may be a helpful marker in the differential diagnosis of renal tumors. Similar to parathyroid carcinomas, parafibromin appears to have tumor suppressor functions in renal carcinomas. Preserved expression of parafibromin is associated with benign tumors in the spectrum- oncocytoma; whereas loss of its expression is associated with malignant tumors bearing more adverse prognosis. These findings may indicate a potential role of parafibromin as a prognostic marker in renal tumors.

828 Retrospective Analysis of Survival in Muscularis Propria-Invasive Bladder Cancer

AM D'Souza, KS Pohar, T Arif, S Geyer, DL Zynger. The Ohio State University Medical Center, Columbus, OH.

Background: Muscularis propria-invasive bladder cancer is associated with significant morbidity and mortality. Our aim was to analyze prognostic factors in a recent cohort of radical cystectomy (RC) patients at a single institution to evaluate outcomes based on current practice patterns.

Design: Between 2007-2010, 180 radical cystectomies (RC) were performed on patients with biopsy proven pT2 disease. A retrospective analysis of overall survival

(OS) was conducted upon these 180 patients utilizing Kaplan Meier survival curves and multivariable modeling.

Results: Pathologic stage at RC was pT0/a/is, n=35, 19%; pT1, n=12, 7%; pT2, n=41, 23%; pT3, n=61, 34%; pT4, n=31, 17%. At last follow-up 76 patients (42%) had died. 1.5 year OS was as follows pT0/pTis, 80%; pTa, 100%; pT1, 77%; pT2a, 80%; pT2b, 61%; pT3a, 58%; pT3b, 43%; pT4, 12%. Substaging of pT2 and pT3 showed a non-statistically significant improved survival in lower substages. Stages were collapsed into three stage groups with pT0/a/is/1/2a surviving longer than pT2b/3a/3b, and pT4 having the worst prognosis (p<0.00001). Patients with a stage based response (25%) had improved OS (p=0.00043), although in multivariable analyses collapsed RC stage group was a more significant prognostic factor than stage based response. 30% of patients were pN1+ at RC, with pN1+ as a negative predictor of survival (p<0.00001). The 1.5 year OS was 66% for pN0 and 30% for pN1+. Neoadjuvant chemotherapy (NAC), given to 45% of patients, was not associated with improved OS (p=0.746). However, in the NAC group there was more frequent downstaging comparing cT prior to RC versus pT at RC (48% vs 17%). There was a higher incidence of NAC patients with pT0 (24% vs 8%) and in the low stage group pT0/a/is/1/2a (46% vs 28%). Surprisingly, a higher incidence of pN1+ was seen with NAC (40% vs 22%). A small group of pN1+ patients were ≤pT2a at RC, and all had a history of NAC.

Conclusions: pT4 was the strongest negative predictor of survival, followed by pT2b/3a/3b and pN1+. Improved OS was seen with RC stage ≤pT2a. Positive lymph nodes were not limited to high stage disease. No survival benefit was demonstrated with NAC. NAC patients were noted to have a higher frequency of low pT stage, yet more frequent node positivity. For patients that receive NAC, pT stage may not accurately reflect tumor burden. Our findings represent treatment outcomes based on recommended guidelines outside the context of a clinical trial.

829 Prognostic Significance of Extraprostatic Extension of Prostate Cancer

D Danneman, F Wiklund, P Wiklund, L Egevad. Karolinska Institutet, Stockholm, Sweden.

Background: Extraprostatic extension (EPE) is a well-established risk factor for recurrence of prostate cancer after radical prostatectomy. The 2009 ISUP consensus conference on handling and staging of radical prostatectomy specimens recommended that the extent of EPE should be reported for stratification of patients in prognostic groups. However, it remains unclear how this should be done. The aim of this study was to stratify EPE based on extent and other characteristics to identify risk groups.

Design: A total of 1156 men underwent radical prostatectomy at the Karolinska Hospital from 1998 to 2005. Men with neoadjuvant treatment or TURP prior to surgery or unavailable histological slides or clinical follow-up were excluded and 1051 cases remained for review. All specimens had been completely embedded. The slides were reviewed. EPE was identified and classified according to extent, localization and presence of perineural invasion (PNI) at EPE. Cox regression models were used to explore association between histopathological features and biochemical recurrence.

Results: EPE was observed in 44.7% of cases (470/1051) and predicted a higher progression rate than that of organ-confined prostate cancer (hazard ratio [HR] 1.4, 95% confidence interval [CI] 1.1 to 1.8; p = 0.007). Focal vs. established EPE according to Epstein (HR 2.0 [1.1-3.5], p = 0.027) and Wheeler (HR 2.2 [1.2-3.9], p = 0.010) and radial distance of EPE (dichotomized by median invasion depth 1.1 mm, HR 1.5 [1.1-2.2], p = 0.015) were all predictive of recurrence (HR 2.0, 2.2 and 1.5, respectively and p = 0.027, 0.010 and 0.015, respectively). A limitation of the Epstein and Wheeler criteria was that they only identified 7.9% and 8.3% of EPE as focal, while dichotomized radial extent split the EPE cases into two equal groups of 50% each. PNI at EPE, circumferential length of EPE, number of sections and foci with EPE and bilateral vs. unilateral EPE showed no significant association with outcome.

Conclusions: Radial extent of EPE predicts recurrence after radical prostatectomy but not circumferential extent, PNI at EPE, number of sections or foci of EPE and laterality. Radial extent can be estimated either by subjective or semiquantitative methods or by measuring invasion depth. The results are useful for the stratification of prostate cancer patients in risk groups after radical prostatectomy.

830 Differential Gene Expression Profiling in Proliferative Inflammatory Atrophy: A Comparative Molecular Study between PIA, HGPIN and Prostate Cancer

I de Torres, MT Quiles, C Blazquez, M Arbos, A Navarro, S Ramon y Cajal, J Morote. Hospital Universitari Vall d' Hebron. Universitat Autònoma de Barcelona, Barcelona, Spain; Institut de Recerca Vall d' Hebron (VHIR), Barcelona, Spain; Hospital Universitari Vall d' Hebron., Barcelona, Spain.

Background: The relevance of proliferative inflammatory atrophy (PIA) as a premalignant lesion in prostate cancer remains uncertain. To elucidate the relationship between both kind of lesions we tried to characterize new signaling pathways in PIA and compared them to high grade prostatic intraepithelial neoplasia (HGPIN) and prostate cancer (PCa).

Design: Prostatectomy fresh specimens from 35 patients undergoing radical prostatectomy were selected. In a subset of 20 cases paired representative areas of benign prostatic tissue, HGPIN, PIA and PCa (Gleason grade 6 to 9), were obtained. The corresponding frozen blocks were serially cut and stained (Arcturus HistoGene kit). Representative areas of PIA, HGPIN and PCa were microdissected using LCM microscopy (Leica Microsystems) and total RNA was extracted (Qiagen). After RNA amplification (Nugen Technology) transcriptional profiling was performed with Affymetrix human U133 plus 2.0 arrays. Genes showing fold-change > 1.5 in expression level between lesions (CA, HGPIN and PIA) and benign tissues were identified as differentially expressed (FDR < 1%). Gene enrichment analysis was performed using DAVID Bioinformatics.

Results: Transcriptional profiling yielded a PIA-specific signature (379 genes) associated to inflammation, apoptosis, angiogenesis and cell adhesion. Similarly, HGPIN and CA gene signatures were established (68 and 426 transcripts, respectively). The transcriptional program shared by PIA and PCa was significantly enriched in biological processes linked to the positive regulation of apoptosis and to steroid biosynthesis. PIA, HGPIN and PCa shared the regulation of genes involved in extracellular matrix organization, including collagens and proteoglycan metabolism-related genes. Among them, AGR2 was one of the most highly upregulated genes. Thus AGR2 protein was overexpressed in PIA, HGPIN and PCa compared with benign samples (3-fold in HGPIN, $p < 0.01$; 6-fold in PIA and PCa $p < 0.001$).

Conclusions: The analysis of the genomic transcriptional profile in PIA-specific signature reveals biological processes that may be underlying carcinogenic programs. Our preliminary results suggest that AGR2 could be an early cancer biomarker in PIA lesions, which is consistent with the hypothesis that PIA is a premalignant lesion in PCa.

831 ERG Rearrangement Is Associated with an Earlier Age at Diagnosis in a PSA-Screening Clinical Trial Cohort from Tyrol (Austria)

F Demichelis, G Schaefer, K Park, B Stenzel, JM Mosquera, S Setlur, C Lee, H Klocker, M Rubin. Weill Medical College of Cornell University, New York, NY; Centre for Integrative Biology, University of Trento, Trento, Italy; Innsbruck Medical University, Innsbruck, Austria; Brigham and Women's Hospital and Harvard Medical School, Boston, MA.

Background: The Tyrol Prostate Specific Antigen (PSA) Screening Cohort, a population-based cohort of men tested with PSA for early detection and treatment of prostate cancer (PCa), started in 1993 and includes men aged 45 to 75. PSA serum levels measurements were used to detect men at risk for PCa. Urological examination and prostate biopsy (PB) was recommended with age-adjusted serum PSA level thresholds. About one third of the PCa cases were detected in men with PSA 2.0 to 4.0 ng/ml. Information on digital rectal examination (DRE), ultrasonography (US), transrectal ultrasound-guided PB, and radical prostatectomy (RP) specimens was also available. We investigated the prevalence of ERG rearrangement in cases of this PSA-screening clinical trial cohort, and sought to describe associations with Gleason score, tumor stage, and age at diagnosis, and to investigate a previously reported association between gene rearrangement and a SNP in *TM6SS2*.

Design: Archived RP specimens ($n=399$) and corresponding blood samples were obtained. ERG IHC was performed on RP slides using Ventana Discovery XT platform. Semiquantitative ERG expression was evaluated, with moderate (2+) and strong (3+) intensities considered as positive. Genotype data was determined by Affymetrix Human SNP Array 6.0 with DNA extracted from peripheral blood mononuclear cells. rs915823 was identified as tag SNP for the previously reported rs12329760 using HapMap genotypes ($R^2 > 0.8$).

Results: ERG rearrangement for 399 men from Tyrol cohort was 60.4%. ERG fusion status was associated with earlier age at diagnosis ($p=0.003$), but not with tumor grade or stage. The risk SNP (rs915823) was queried in 351 out of 399 subjects with known ERG fusion status. There was no overall association between the SNP alleles and ERG fusion. However, we observed an association between the C allele of the SNP and higher levels of pre-operative PSA ($p=0.02$).

Conclusions: ERG rearrangement PCa prevalence in the Tyrol cohort is higher than generally reported in other Caucasian (~50%), Japanese (~16%) and African American (~30%) cohorts. We did not detect association between the *TM6SS2* SNP and ERG rearrangement. However, the C allele was associated with higher levels of pre-operative PSA. ERG fusion status was strongly associated with earlier age at diagnosis of PCa, even after controlling for PSA levels.

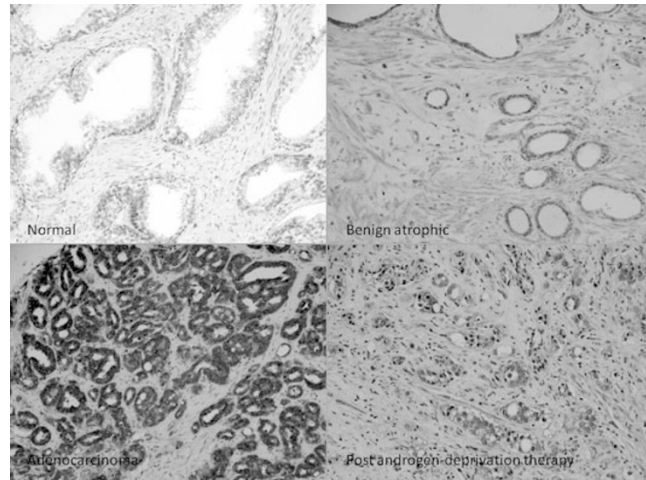
832 Overexpression of the Soluble Epoxide Hydrolase in Human Prostate Adenocarcinoma with a Downregulation Following Androgen Deprivation Therapy

X Ding, J Liao, H Li, J Huang, G-Y Yang. Northwestern University Feinberg School of Medicine, Chicago, IL; David Geffen School of Medicine at UCLA, Los Angeles, CA.

Background: Soluble epoxide hydrolase (sEH) is a bifunctional enzyme with C-terminal hydrolase and N-terminal phosphatase activities. The C-terminal hydrolase converts anti-inflammatory epoxyeicosatrienoic acids (EETs) to dihydroxyeicosatrienoic acids (DHETs). The phosphatase activity involves cholesterol and androgen metabolism. sEH gene deficient mice shows dysregulated circulating testosterone levels. However, little is known if this bifunctional enzyme involves in prostate carcinogenesis.

Design: Prostate specimens were collected from 75 patients with prostatectomy including benign and malignant tissues. Additional 26 prostate cancer specimens with androgen deprivation therapy were also selected. 95% (71/75) prostate cancer in this study has Gleason score 7. A high-throughput tissue microarray (TMA) was constructed for these specimens. Immunohistochemistry was carried out using Rabbit specific anti-sEH antibody and Avidin-biotin-peroxidase approaches. The proper positive and negative controls were also established. Based on the staining intensity, the staining of the prostate tissues was classified as no staining (0), low intensity (+), moderate intensity (++) or high intensity staining (+++).

Results: Distinct over-expression of sEH was identified in prostate adenocarcinoma compared to normal and benign atrophic prostate. 72% (49/69) prostatic adenocarcinoma showed diffuse moderate to strong positive staining for sEH. The positive staining was specifically identified in the cytoplasm. In contrast, 71% (52/73) normal and 94% (17/18) benign atrophic prostate epithelium were negative or weakly positive for sEH. In 26 cases of hormone-treated cancer, a significant decrease of staining intensity of sEH was observed with only 38% (10/26) cancers displaying moderate to strong positivity (38% versus 72% in non-treated cancer, $p < 0.05$).



Conclusions: This study has clearly demonstrated an over-expression of sEH in prostate adenocarcinoma. Its expression was markedly down-regulated following androgen deprivation therapy. This study warrants further exploring the role of sEH in prostate carcinogenesis.

833 The Role of Immunohistochemistry (IHC) in the Differential Diagnosis of Invasive Plasmacytoid Urothelial Carcinoma (PUC) and Its Mimics

KL Dishongh, JK McKenney, AR Sangoi, N Gokden. University of Arkansas for Medical Sciences, Little Rock, AR; Stanford University School of Medicine, Stanford, CA; El Camino Hospital, Mountain View, CA.

Background: PUC is a rare and aggressive variant of bladder cancer that is characterized by tumor cells closely resembling plasma cells. PUC may mimic plasmacytoma, lymphomas, and carcinomas such as lobular carcinoma of breast (LCB) and poorly differentiated carcinomas of gastrointestinal system (PDCGIS) secondarily involving the bladder. There is limited data regarding the comparative immunophenotypes of these morphologically similar tumors.

Design: The surgical pathology and consultation files at three institutions were searched for PUC, LCB and PDCGIS from 1998 to 2010. H&E slides of 31 cases were reviewed to confirm diagnoses. A focused IHC panel including E-Cadherin, P63, P53, CD138, MUM-1, estrogen receptor (ER), progesterone receptor (PR), GCDFFP-15, CEA 125, cytokeratin 7 (CK 7), and cytokeratin 20 (CK 20) was performed. Percent immunoreactivity in the neoplastic cells was graded as 1 to 4+.

Results: PUC ($n=11$) showed immunoreactivity for CD138 and P53, but were negative for MUM-1, ER, PR, and GCDFFP-15 in all cases. E-Cadherin expression was completely lost in 25% of cases, and nuclear P63 was not expressed in 55% of cases. 99% had CK7 expression while 73% expressed CK20. LCB ($n=10$) were immunoreactive for ER (100%), PR (60%), GCDFFP-15 (90%), CK 7 (100%), P53 (60%), CD 138 (100%), CEA 125 (20%), but negative for MUM-1, P63, E-cad, and CK 20 in all cases. PDCGIS ($n=10$) were immunoreactive for CD138 and E-cad, but negative for ER, PR and GCDFFP-15 in all cases. Other variably positive markers in PDCGIS included P53 (90%), P63 (30%), CEA 125 (10%), CK 7 (60%), and CK 20 (80%).

Conclusions: It is important to recognize PUC because it is an aggressive bladder cancer variant with poor prognosis that presents at an advanced clinical stage. Particularly in small samples, the distinction from morphologically similar plasmacytomas/lymphomas or carcinomas from other anatomic sites may be difficult. The typical immunoprofile of PUC is CD138 (+), CK7/20 (+), and MUM-1 (-), ER/PR/GCDFFP-15 (-). The absence of MUM-1 staining in PUC would be helpful in the distinction from plasma cells and lymphocytes. PDCGIS has a variable immunoprofile which overlaps significantly with PUC. P63 and E-cad expression in a subset of PUC and ER, PR and GCDFFP-15 negativity is useful in distinction from LCB.

834 The Impact of the 2005 Modified Gleason Grading System on the Clinical Outcome of Prostate Cancer

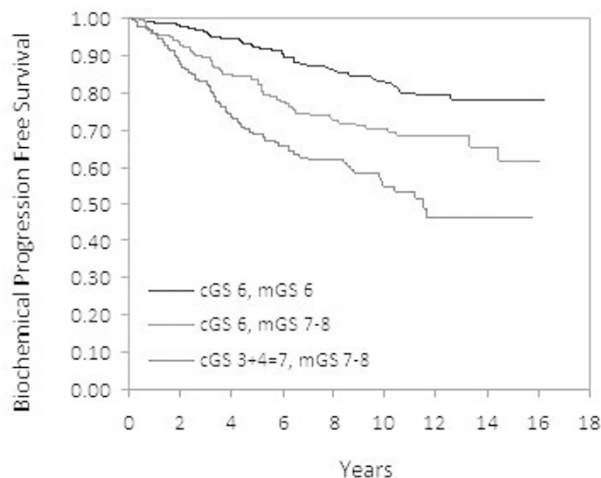
F Dong, C Wang, AB Farris, S Wu, H Lee, H Olumi, WS McDougal, RH Young, C-L Wu. Massachusetts General Hospital, Boston, MA.

Background: The 2005 International Society of Urological Pathology (ISUP) Consensus Conference modified the Gleason grading system for prostate cancer. In the modified criteria, certain architectural features of classical Gleason pattern 3 adenocarcinoma were reclassified as Gleason pattern 4. In this study, we evaluated the clinical outcomes of patients with prostate cancer upgraded by ISUP criteria.

Design: The histology of 1240 consecutive radical prostatectomy specimens at a single institution between 1993 and 1999 were reviewed, and each case of adenocarcinoma was graded based on the original and modified Gleason grading systems. The outcomes of 806 patients with classical Gleason score 3+3=6 or 3+4=7 and modified Gleason score 6 to 8 prostate cancer were analyzed, with a median clinical follow up of 11.9 years.

Results: Of 622 patients with classical Gleason score 3+3=6 prostate cancer, 210 (34%) had modified Gleason score 7 or 8 by the ISUP criteria. Compared with patients with modified Gleason score 3+3=6 and classical Gleason score 3+4=7 cancer, patients with classical Gleason score 3+3=6 and upgraded by ISUP criteria were at intermediate risk for biochemical progression, the development of metastatic disease, and overall mortality

following radical prostatectomy (log-rank $p < 0.0001$). The hazard ratio for upgrading was 1.60 (95% confidence interval 1.09 to 2.35, $p = 0.02$) for PSA failure and 5.02 (95% confidence interval 1.77 to 14.2, $p = 0.003$) for the development of metastasis.



Conclusions: Patients with classical Gleason score 3+3=6 prostate cancer and upgraded by the ISUP modified Gleason grading system are at intermediate risk for biochemical failure following radical prostatectomy compared to patients with modified Gleason score 3+3=6 cancer and patients with classical Gleason score 3+4=7 cancer. The recognition of this intermediate-risk histological pattern may be useful in guiding the prognosis and clinical management of patients with prostate cancer.

835 Renal Cell Carcinoma before and after Sunitinib Therapy. Morphological and Molecular Changes

R Doshi, M O'Donnell, A Bex, L Beltran, A Sahdev, J Peters, DJ Harrison, GD Stewart, T Powles, DM Berney. Barts Cancer Institute, London, United Kingdom; University of Edinburgh, Edinburgh, United Kingdom; Whipps Cross Hospital, London, United Kingdom; Netherlands Cancer Institute, Amsterdam, Netherlands.

Background: The use of tyrosine kinase inhibitors (TKI) has transformed the treatment of clear cell renal cell carcinoma (ccRCC). We have previously published 48 patients with metastatic ccRCC, treated with Sunitinib for 16 weeks and then given a nephrectomy, if feasible. Pretreatment biopsy material was taken for diagnostic purposes. Little translational work on this treated tissue is available. Changes in morphology after TKI therapy are not well documented and the possibility of a 'regression score' in treated cancers may aid further therapy.

Design: Pretreatment biopsies and nephrectomies were analysed for standard pathological parameters (grade, stage, type and necrosis). After initial review, a number of non-standard pathological parameters were scored semi-quantitatively: necrosis associated with acute inflammation (NAI), chronic lymphoplasmacytic infiltrate (CLI), fibrinoid eosinophilic debris (FED) and areas of small endothelial vessels (SEV). A tissue microarray was constructed from the biopsy material and nephrectomies. Ki-67 expression was scored in these specimens.

Results: 48 patients with ccRCC were diagnosed on renal biopsy. Of the 25 patients who had a nephrectomy after Sunitinib treatment, NAI was seen in 8(32%), CLI in 21 (84%), FED in 18(72%) and SEV in 23(92%). These changes were seen significantly less frequently in the pretreatment biopsies NAI, 2(8%), CLI 3(12%), FED 3(12%) and SEV 4(16%) though comparison is difficult due to the limited nature of the biopsies. A Wilcoxon matched paired test showed the Ki-67 expression to be significantly higher in the post treatment nephrectomies ($p=0.02$) than in the pre treatment samples.

Conclusions: There appear to be recognisable stigmata of Sunitinib therapy. Areas of small vessels are the most prominent feature and may be due to either endothelial proliferation or tumor regression creating packed vessel clusters. We speculate that the possible vessel proliferation as well as the inflammatory response and associated unusual necrosis and fibrinoid areas are due to chemokine induction by pathway alterations secondary to TKI therapy. The increase in Ki-67 after treatment suggests that in spite of the regressive changes induced by the TKI, there is an induction of resistant clones showing high levels of proliferation, ultimately resulting in drug failure. Creation of a regression score linked to outcome analysis may aid future drug development strategies.

836 Standardization of Gleason Grading among 337 Pathologists

L Egevad, F Algaba, DM Berney, L Boccon-Gibod, E Comperat, AJ Evans, R Grobholz, G Kristiansen, C Langner, A Lopez-Beltran, R Montironi, P Oliveira, B Vainer, M Varma, P Camparo. Karolinska Institutet, Stockholm, Sweden; Fundacio Puigvert-University Autonomus, Barcelona, Spain; St Bartholomew's Hospital, London, United Kingdom; Hopital Armand Trousseau, Paris, France; Hopital La Pitié-Salpêtrière, Paris, France; University of Toronto, Toronto, Canada; Kantonsspital Aarau, Aarau, Switzerland; University Hospital, Bonn, Germany; Medical University, Graz, Austria; Cordoba University Medical School, Cordoba, Spain; Polytechnic University of the Marche Region, Ancona, Italy; Hospital da Luz, Lisboa, Portugal; Rigshospitalet, Copenhagen, Denmark; University Hospital of Wales, Cardiff, United Kingdom; Hopital Foch, Paris, France.

Background: A key decision in the 2005 ISUP revision of the Gleason grading of prostate cancer was to always include the highest grade in the Gleason score (GS) of needle biopsies (NBX), even if only a minute focus. This may have caused a reporting

shift from GS 6 to 7 or higher. Our aim was to analyze contemporary reporting of GS 6 vs. 7 among a large group of pathologists.

Design: A panel of 15 experts in urological pathology reviewed 25 digitized NBX with GS 6-7 cancer and reached 2/3 consensus in 15 cases. The expert diagnosis was GS 3+3, 3+4 and 4+3 in 6, 7 and 2 cases, respectively. A total of 85 microphotographs of single cores from these 15 cases were published on a website and members of the European Network of Urology (ENUP) were invited to report GS.

Results: Among 618 ENUP members, 337 (54.5%) replies were received from 19 countries. There was agreement between experts and the majority member vote in 12 of 15 cases, while members upgraded from GS 3+4 to 4+3 in 2 cases and from 4+3 to 4+4 in 1 case. Mean GS of expert consensus and member grading was 6.60 and 6.74, respectively ($p < 0.001$). Mean member GS was higher than consensus GS in 9 of 15 cases. A Gleason pattern (GP) 5 was reported by at least one member in 10 of 15 cases with mean 2.0%, range 0.3% - 5.6% per case. The agreement between consensus and member GS was 58.2%-89.3% (mean 71.4%) in GS 6 cases and 46.3%-63.8% (mean 56.4%) in GS 7 cases ($p = 0.009$), overall 46.3% to 89.3% (mean 62.4%).

Conclusions: There is disagreement among pathologists on how to report GS 6-7 cases. While undergrading used to be prevalent in the pathology community, some pathologists now tend to assign a high GS even to cases diagnosed as GS 6 by experts. The detection threshold for minimal foci of GP 4 and 5 in NBX needs to be better defined. Image libraries reviewed by experts may be useful for standardization.

837 BCA2 Is Differentially Expressed in Renal Oncocytoma: An Analysis of 158 Renal Neoplasms

L Ehsani, A Seth, AO Osunkoya. Emory University School of Medicine, Atlanta; Sunnybrook Health Sciences Center, Toronto, Canada.

Background: The distinction between renal oncocytoma and renal cell carcinoma, especially chromophobe renal cell carcinoma and clear cell carcinoma with oncocytic features is important due to the different biologic potentials of these tumors. RING E3 ligases have now become the subject of intense studies for their roles in disease and as potential therapeutic targets. All RING E3 ligases, including BCA2, contain a consensus protein sequence that would complex two or more zinc ions in the expressed protein. Identification of which ubiquitin ligases specifically affect distinct cellular processes is essential to the development of targeted therapeutics in these tumors. The ubiquitin-proteasome system regulates the turnover of proteins that have essential roles in the cell cycle, apoptosis, DNA damage repair, and in protein trafficking, which makes this pathway a target for oncogenic events. In this study we investigated expression of BCA2 in renal oncocytoma and renal cell carcinoma.

Design: Tissue microarrays (TMAs) were constructed from 158 patients with clear cell renal cell carcinoma, chromophobe renal cell carcinoma, papillary renal cell carcinoma, oncocytoma and oncocytic neoplasm, favor oncocytoma. The latter tumors were cases provisionally signed out as such by consulting general pathologists, and were morphologically consistent with renal oncocytoma, but invaded perinephric adipose tissue. Immunohistochemical stains for BCA2 were performed on the TMAs.

Results: The tumors were composed of 114/158 (72%) cases renal cell carcinoma, in which 104/114 (91%) were clear cell renal cell carcinoma, 8/114 (7%) were chromophobe renal cell carcinoma and 2/114 (2%) were papillary renal cell carcinoma. 38/158 (24%) cases were renal oncocytoma and 6/158 (4%) were cases provisionally signed out by consult contributors as oncocytic neoplasm, favor oncocytoma. 114/158 (100%) cases of renal cell carcinoma were negative for BCA2. 38/38 (100%) cases of renal oncocytoma were positive for BCA2. 6/6 (100%) of cases designated as oncocytic neoplasm, favor oncocytoma were also positive for BCA2.

Conclusions: This is the first study to date evaluating the expression of BCA2 in renal neoplasms. BCA2 is differentially expressed in renal oncocytoma, including those with locally invasive potential. BCA2 is a marker that may be utilized in the distinction between renal oncocytoma and its mimickers, and may also be a potential therapeutic target in patients with large renal oncocytomas, who are not good surgical candidates.

838 A FISH Assay for Detection of Excess Chromosome 12p Material To Distinguish Germ Cell Tumors from Somatic Carcinoma

RM Elliott, MK Rao, K Wang, H Al-Ahmadie, Y Chen, SW Fine, A Gopalan, SK Tickoo, SC Jhanwar, VE Reuter. Memorial Sloan-Kettering Cancer Center, New York.

Background: The diagnosis of metastatic or primary extragonadal germ cell tumors (GCT) presents a unique challenge for the surgical pathologist since these tumors can mimic other tumor types. Because the treatments of GCTs vary drastically from those of the entities they mimic, there is a need for a laboratory test that can distinguish them. Excess chromosome 12p material, especially as i12p, is a recurrent abnormality in GCTs that would presumably not be detected in somatic tumors. In this study, we attempt to distinguish a set of GCTs from high grade somatic carcinoma (CA) using a new FISH assay.

Design: The set of GCTs consisted of 3 embryonal carcinomas (EC), 3 seminomas, 1 yolk sac tumor (YST), 2 immature teratomas, and 1 teratoma with secondary somatic malignancy in the form of carcinoma. The set of CAs consisted of 3 colonic adenoCAs, 3 urothelial CAs, 2 pulmonary adenoCAs, 1 pulmonary squamous cell CA, and 1 renal cell CA. FISH was performed on 5 μ sections prepared from formalin-fixed, paraffin-embedded tissue. Two cytogenetic technologists, blinded to the histologic diagnoses, performed the FISH analysis.

Four probes were used: ETV6 (12p13), CEP (12p11.1-12q11), CHOP(12q13) and MDM2(12q13). A sample was considered positive if:

>10% of cells had i12p, indicated by a doublet ETV6 signal with one CEP signal, 5-10% of cells had i12p and demonstrated an excess of ETV6 relative to 12q signals (CHOP and MDM2), >10% of cells had excess 12p material without i12p, indicated by excess ETV6 relative to 12q signals.

Results: Of the 10 GCTs, FISH analysis detected excess 12p material in 7 cases. The positive cases included 3 ECs, 2 seminomas, the YST, and the teratoma with secondary somatic malignancy in the form of carcinoma. The 3 GCTs negative for excess 12p were a seminoma and two immature teratomas. Of the 10 CAs, FISH detected excess 12p material in 3 cases: two colonic adenoCAs and the pulmonary squamous cell CA.

Conclusions: 1. The sensitivity of this FISH assay for the detection of GCT is 70%, which is comparable to prior studies.

2. False negatives consisted of teratoma and seminoma, both of which have been shown to have a lower frequency of 12p excess than other GCT types.

3. Even when FISH probes specific for 12p and 12q loci are used, there is a high false positive rate (30%).

4. Specific types of high grade CA with a known propensity for genomic instability, such as colonic adenoCA, may have a higher frequency of 12p excess than has been previously appreciated. If these entities can be excluded, the false positive rate may be reduced.

839 Prognostic Gleason Grade Grouping: Data Based on the Modified Gleason Scoring System

JJ Epstein, PC Walsh, AW Partin. The Johns Hopkins Hospital, Baltimore.

Background: There are some problems with reporting Gleason score (GS): 1) GS6 is typically the lowest grade assigned on biopsy (bx). However, GS ranges from 2-10, so men are concerned when told they have GS6 cancer on bx, logically but incorrectly assuming that their tumor is in the mid-range of aggressiveness. 2) Within the literature, GS3+4=7 & GS4+3=7 are often combined as GS7. 3) GS8-10 are also typically lumped together.

Design: We have previously shown that tertiary Gleason patterns in RP influence biochemical free survival rates (BFS), acting as an intermediary between grades. We identified 8,039 men who underwent RP at our institution since 2004 without tertiary patterns to study the sole effect of grade derived from the two predominant patterns.

Results: Of 4,510 GS2-6 tumor on bx, 1 had GS2-4 and 7 had GS5. Of 3,548 GS2-6 tumor at RP, 1 had GS2-4, and 44 had GS5. Therefore, 99.8% and 98.7% of biopsy & RP GS2-6 tumors were GS6, respectively, so cases were combined as GS2-6. Prognostic Grade Group (2-6; 3+4; 4+3; 8; 9-10) was among the strongest predictors of biochemical free survival (BFS) in multivariable models. At a median follow-up of two years (range 1-7), 2-year BFS rates for men with 3+3, 3+4, 4+3, 8, and 9-10 at bx were 97.4%, 90.0%, 84.7%, 73.1%, and 46.0% respectively ($p<0.001$); and 98.8%, 93.6%, 85.6%, 73.7%, and 48.9% ($p<0.001$), respectively, based on RP pathology.

Conclusions: GS 3+4=7 has a very favorable prognosis with an estimated 2-year BFS of 90.0% and 93.6% for bx and RP, respectively; these results warrant the designation of "moderately differentiated". GS4+3=7 had a significantly worse prognosis than GS3+4=7. The current study shows GS9-10 has almost twice the risk of progression compared to GS8. We propose reporting Gleason grades, along with descriptive terminology, and including Prognostic Grade Groups which accurately reflect prognosis: GS2-6 (*well-differentiated*), *Prognostic Grade Group I/V*; GS3+4=7 (*moderately differentiated*), *Prognostic Grade Group II/V*; GS4+3=7 (*moderately-poorly differentiated*), *Prognostic Grade Group III/V*; GS8 (*poorly differentiated*), *Prognostic Grade Group IV/V*; and GS9-10 (*undifferentiated*), *Prognostic Grade Group V/V*. One would still report a case as "Gleason Score 5" or "Gleason score 6", (rather than "Gleason Score 2-6") along with Prognostic Grade Group I. The descriptive terms (i.e. well, moderately, etc.) would only be used along with GS in Pathology reports so that men could better understand their grade. Men will, for example, be reassured with a GS6 that their Prognostic Grade Group is I/V along with a description of the tumor as well-differentiated.

840 Upgrading/Downgrading of Prostate Cancer from Biopsy to Radical Prostatectomy: Incidence and Predictive Factors

JJ Epstein, B Trock, A Chang. The Johns Hopkins Hospital, Baltimore.

Background: There is the potential for both under and overtreatment if the biopsy (Bx) Gleason Score (GS) does not accurately reflect the radical prostatectomy (RP) GS. The needle biopsy and corresponding RP GS may not be the same for several reasons including: 1) pathology error; 2) borderline cases; and 3) and sampling error.

Design: We analyzed 6,308 totally embedded RP and corresponding Bx (2004-2010), accounting for the updated Gleason system. We excluded cases with RP tertiary higher grade patterns, and only included cases with at least 10 biopsy core sampling.

Results: 26.2% of cases were upgraded from a Bx GS6 to higher grade at RP. Almost 2/3rds of the cases had matching GS 3+4=7 at BX and RP with an approximately equal number of cases downgraded to GS6 or upgraded to GS4+3=7 at RP. When the Bx was 4+3=7, there was an almost equal split between 3+4=7 and 4+3=7 at RP. A Bx of GS8 led to an almost equal distribution between RP GS 4+3=7, 8, and 9-10. Over three-quarters of the cases had matching GS 9-10 at BX and RP. In univariate analysis, clinical stage, serum PSA, RP weight, number of positive cores, and maximum percent of cancer per core all correlated with upgrading and downgrading. Age was predictive only in upgrading. In multivariable analysis, age ($p<0.0001$), serum PSA level ($p<0.0001$), RP weight ($p<0.0001$), and maximum % cancer/core ($p<0.0001$) predicted upgrade from BX GS6 to higher at RP. Nomograms for predicting upgrading and downgrading were developed to aid clinicians in assessing the likelihood of the accuracy of a biopsy Gleason score.

Biopsy GS	RP GS 3+3=6	RP GS 3+4=7	RP GS 4+3=7	RP GS 8	RP GS 9-10	Total Cases
3+3=6	73.8%	21.6%	3.5%	0.6%	0.5%	4,376
3+4=7	15.6%	64.3%	16.5%	2.0%	1.6%	1,219
4+3=7	7.6%	39.4%	39.8%	5.7%	7.5%	437
8	1.6%	17.1%	26.2%	30.0%	25.1%	187
9-10	4.5%	4.5%	6.7%	6.7%	77.6%	87

Conclusions: Higher clinical stage, serum PSA, and extent of cancer on cores correlates with more extensive cancer which correlates to higher grade at RP. It is logical that these variables correlate with a higher risk of upgrading due to sampling error on biopsy. Although not intuitive, our findings are consistent with the literature in showing that smaller prostates are associated with an increased risk of upgrading from biopsy to RP. GS upgrading and downgrading remains an important issue using the updated Gleason system, even when accounting for tertiary Gleason patterns in the RP in entirely submitted RP specimens. More accurate Gleason grading can reduce upgrading, yet in the best of circumstances, approximately one-quarter of GS6 tumors on biopsy will be GS7 or higher at RP.

841 Accuracy of Risk Assessment Tools To Predict EPE in Patients 45 Years Old or Younger with Prostate Cancer Treated by Radical Prostatectomy

SM Falzarano, E Walker, K Streater Smith, EA Klein, M Zhou, C Magi-Galluzzi. Cleveland Clinic, Cleveland; Cleveland Clinic, Cleveland, OH.

Background: Controversy exists regarding the outcome associated with a prostate cancer (PCA) diagnosis in young patients. We aimed to evaluate existing calculators for prediction of extraprostatic extension (EPE) in men 45 years old or younger who underwent radical prostatectomy (RP) at our institution.

Design: We queried our RP database for all men diagnosed with PCA from 2000 to 2011 and selected patients 45 years old or younger. Preoperative and postoperative characteristics of the patients were collected in an IRB approved database. The association between D'Amico risk group stratification and presence of EPE was explored; the Memorial Sloan-Kettering Cancer Center (MSKCC) Pre-treatment Prostate Cancer Nomogram (<http://nomograms.mskcc.org/Prostate/PreTreatment.aspx>) and the CaP Calculator (<http://www.capcalculator.org/>) that includes Roach formula, Gancarczyk prediction model, and 2007 Partin tables, were used to predict the risk of EPE based on the preoperative features. Predicted values were compared to the real incidence of EPE.

Results: One hundred and twenty-two patients aged 45 years or younger were included. Patients' median age and preoperative PSA were 44 years (range 36-45), and 4.18 ng/ml (range 0.70-90.80), respectively. Eighty-nine (74%) men met D'Amico criteria for low-risk, 26 (22%) for intermediate-risk and 5 (4%) for high-risk disease. Ten (11%) low-risk patients, 8 (31%) intermediate-risk, and 4 (80%) high-risk had EPE at RP. D'Amico criteria showed a strong association with the presence of EPE at RP ($p=0.0006$). The areas under the curve (AUC) for the CaP calculator tools and the MSKCC nomogram were 0.82, 0.80, 0.86, and 0.82 for the Roach formula, Gancarczyk prediction model, 2007 Partin tables and the MSKCC nomogram, respectively. The cutoffs at which the sensitivity and specificity were optimized were 39% for the Roach formula, 30% for Gancarczyk prediction model, 23% for the 2007 Partin tables and 11% for the MSKCC nomogram.

Conclusions: All the risk assessment tools examined had high discrimination power. However, the predicted risks were, in general, low with optimized cutoffs for detection ranging from 11% to 39%. The lack of calibration could limit their use in younger populations.

842 Neoadjuvant Docetaxel Treatment for Locally Advanced Prostate Cancer Affects miRNA Expression: A Pilot Study

SM Falzarano, M Zhou, P Carver, EA Klein, R Dreicer, C Magi-Galluzzi. Cleveland Clinic, Cleveland, OH.

Background: Taxanes are microtubule-stabilizing drugs used investigational in adjuvant and neoadjuvant settings of prostate cancer (PCA) treatment in attempt to improve systemic control of high risk disease. Understanding mechanism of response to taxanes is essential to develop novel combination therapies. MicroRNAs (miRNAs) are small noncoding RNA molecules that negatively regulate gene expression by binding target messenger RNAs and inhibiting their stability and/or translation. In cancer, miRNAs can act as oncogenes and/or tumor suppressor genes. Our objective was to identify miRNAs that are affected by neoadjuvant docetaxel in high-risk PCA.

Design: Whole cell RNA was extracted from formalin-fixed paraffin-embedded radical prostatectomy specimens from 8 patients with high grade PCA treated with neoadjuvant docetaxel, 8 high grade untreated PCA and their corresponding untreated non-neoplastic tissue. Tumors were matched by Gleason score, patient age and year of surgery. Expression of 88 cancer-associated miRNAs was quantified using a PCR-based miRNA microarray assay.

Results: Thirty-eight (43%) miRNAs (including miR-205, miR-222, and miR-1) were significantly downregulated in untreated PCA compared to untreated non-neoplastic tissue, and one (miR-183) was upregulated ($p<0.05$). In 25 of the downregulated miRNAs, fold regulation was less than 2 (range -2.1 to -8.0). Twenty (23%) miRNAs (including miR-218, miR-124, and let-7b) were significantly upregulated in treated compared to untreated PCA ($p<0.05$). Four of them (miR-125a-5p, miR-222, miR-1 and miR-133b) showed fold regulation greater than 2 (range 2.4 to 5.1). Sixteen of 38 miRNAs downregulated in untreated tumors (including miR-125a-5p, miR-222, miR-1 and miR-133b) were upregulated in treated PCA. Expression levels of 7 of them (miR-133b, miR-27b, miR-29b, miR-34a, miR-140-5p, miR-9 and miR-15b) were reverted to values similar to untreated non-neoplastic tissue as a result of docetaxel treatment.

Conclusions: MicroRNAs may play a potential role in PCA response to taxanes. A subset of miRNAs are downregulated in untreated tumors but upregulated in treated PCA to levels comparable to non-neoplastic tissue, suggesting a miRNA modulation towards a non-neoplastic expression profile with neoadjuvant docetaxel treatment. miR-133b has been reported to be involved in the regulation of apoptosis, by functionally targeting members of the BCL-2. Further studies are underway to evaluate the miRNA-mediated effects of taxanes in PCA.

843 Concordance of *TMPRSS2-ERG* Fusion Status by Quantitative PCR with ERG Protein Expression by Immunohistochemistry Using Anti-ERG Monoclonal Antibody EPR3864

SM Falzarano, C Milward, T Maddala, DB Cherbavaz, M Lee, EA Klein, C Magi-Galluzzi. Cleveland Clinic, Cleveland, OH; Genomic Health, Inc, Redwood City, CA. **Background:** *TMPRSS2-ERG*, the most common gene fusion in prostate cancer (PCA), is associated with expression of a truncated protein product of the oncogene *ERG*. We recently demonstrated that ERG detection by immunohistochemistry (IHC) in PCA was highly predictive of *ERG* rearrangement as assessed by FISH. The objective of the current study was to compare ERG IHC with *TMPRSS2-ERG* fusion mRNA expression by quantitative PCR in a large cohort of patients treated with radical prostatectomy (RP) for clinically localized PCA.

Design: 187 RP specimens from patients with clinical stage T1/T2 PCA treated with RP between 1987-2004 were included in the study. RNA was extracted from manually dissected formalin-fixed paraffin-embedded sections obtained from selected RP blocks and expression of *TMPRSS2-ERGA* and *TMPRSS2-ERGB* was quantified using RT-PCR. A prespecified endpoint was used to classify samples as fusion positive or negative. The same RP blocks were used to build 10 Tissue Microarrays (TMA) composed of three representative 1.5 mm tissue cores from each tumor using the antibody EPR3864. Any nuclear staining was considered indicative of ERG expression. Endothelial cells were used as a positive control because they are strongly positive for ERG. To compare the accuracy of IHC ERG protein detection in determining the *TMPRSS2-ERG* fusion status with assessments by RT-PCR (standard reference), sensitivity, specificity, positive (PPV) and negative (NPV) predictive values, with corresponding 95% confidence intervals (CI) were calculated.

Results: *TMPRSS2-ERGA* and/or *TMPRSS2-ERGB* fusions were present in 110 (59%) analyzed tumors by RT-PCR. ERG IHC was detected in 112 (60%) tumors, 106 (95%) of which were positive for fusion by RT-PCR. We identified 6/112 (5%) tumors demonstrating ERG protein expression without any of the *TMPRSS2-ERG* fusions as assessed by RT-PCR. Conversely, 4/110 (4%) cases with *TMPRSS2-ERG* fusions by RT-PCR had no detectable ERG protein expression in any of the informative cores. ERG IHC was highly concordant with the *TMPRSS2-ERG* RT-PCR, with a sensitivity of 96% (95% CI: 91%-99%), specificity 92% (84%-99%), PPV 95% (89%-98%), and NPV 95% (87%-99%).

Conclusions: ERG detection by IHC showed a high concordance with *TMPRSS2-ERG* mRNA overexpression measured by RT-PCR in a large cohort of RP patients. The consistency of these results supports the utility of both methods for assessing *TMPRSS2-ERG* fusion status. IHC may be a useful adjunctive tool since it is easier to perform and less costly.

844 Neoplastic Retraction Cleaving on Prostate Needle Biopsies: Is It a Prognostic Factor?

WJ Favaro, A Billis, VHA Cagnon, L Meirelles, LLLL Freitas, BD Lins, JFL Bonfido, LBE Costa, PH Poletto. University of Campinas (Unicamp) School of Medicine, Campinas, SP, Brazil; Biology Institute, University of Campinas (Unicamp), Campinas, SP, Brazil. **Background:** Neoplastic periacinar retraction cleaving (NPRC) is an additional criterion for the diagnosis of prostate adenocarcinoma, especially when prominent. A recent study showed that NPRC on surgical specimens from patients submitted to radical prostatectomy (RP) predicts time to biochemical recurrence (TBR) following surgery. We studied on prostate needle biopsies a possible prognostic value of NPRC.

Design: The study was based on 358 biopsies from patients submitted to RP. NPRC was considered as absent (grade 0), slight (grade 1), evident (grade 2), and intense (grade 3) according to the distance of the epithelium to the stroma. In cases with several grades present in the same biopsy it was considered the higher grade. Grading of NPRC was related to several clinicopathological variables: age, race, clinical stage, preoperative PSA, RP tumor extent using a semiquantitative point-count method, biopsy and surgical specimen Gleason score, pathologic stage, and surgical margin status. For statistics, we used the Kaplan-Meier product-limit analysis, and the Cox stepwise logistic regression model and the binary logistic regression for univariate and multivariate analyses.

Results: From the total of 358 biopsies, 49 (13.7%), 176 (49.2%), 127 (35.5%) e 6 (1.7%) biopsies showed grades 0, 1, 2 e 3, respectively. For statistical analysis we considered group 1 (grades 0 and 1) vs. group 2 (grades 2 and 3). There was no statistically significant difference comparing the 2 groups according to age ($p=0.05$), race ($p=0.49$), preoperative PSA ($p=0.74$), clinical ($p=1.00$) or pathologic stage ($p=0.12$), biopsy ($p=0.72$) or surgical specimen Gleason score ($p=0.58$), positive surgical margins ($p=0.59$) and TBR following surgery (log-rank, $p=0.95$). Tumor extent in the surgical specimen was significantly higher in group 2 ($p=0.03$). Group 2 was not significantly predictive of biochemical recurrence or TBR in univariate or multivariate analyses. Group 2 was significantly predictive of tumor extent in the surgical specimen in univariate ($p=0.01$) and multivariate analyses ($p=0.04$).

Conclusions: In our study, evident or intense neoplastic retraction cleaving on prostate needle biopsies was associated with and significantly predictive of more extensive tumors in the surgical specimen of patients submitted to radical prostatectomy. It seems that retraction cleaving is associated and more intense with tumor growth.

845 Characterization of Reactive Stroma in Human Prostate Cancer and Role of Prostate Cancer Stem Cells (PCSCs), Growth Factors, Matrix Metalloproteinases (MMPs) and Steroid Hormone Receptors (SHRs) in Its Pathogenesis

WJ Favaro, A Billis, L Meirelles, LLLL Freitas, LO Reis, U Ferreira. School of Medicine, University of Campinas (Unicamp), Campinas, SP, Brazil; School of Medicine (UNESP), Botucatu, SP, Brazil.

Background: Reactive stroma occurs in many human cancers and it is likely to promote tumorigenesis. The aim of this study was to characterize the reactive stroma environment and to find any association of PCSCs, MMPs, SHRs and growth factors in its pathogenesis.

Design: Reactive stroma was evaluated in 20 needle prostatic biopsies, and divided into 2 groups: cancer without reactive stroma (Group 1); and cancer with intense reactive stroma (Group 2). The samples were submitted to morphological and immunohistochemical analyses for smooth muscle (SM) α -actin, vimentin, androgen receptor (AR), estrogen receptor α and β (ER α , ER β), fibroblast growth factor 2 (FGF-2), insulin like growth factor 1 (IGF-1), MMP-2, CD44, CD133, p63, Prostate Stem Cell Antigen (PSCA), ATP-binding cassette membrane transporter (ABCG2) and *C-Myc*.

Results: There was increased collagen fibers and decreased smooth muscle cells in Group 2. In Group 2 vimentin and SM α -actin were positive, indicating a myofibroblast phenotype. PCSCs of the epithelial compartment were ABCG2/PSCA/*C-Myc*/CD44/CD133/p63/ER α and in the stroma were ABCG2/*C-Myc*/CD133/Vimentin/ER α . These cells had intense immunoreactivity in Group 2 comparing to Group 1. IGF-1, FGF-2 and MMP-2 were significantly higher in Group 2. Intensified AR was verified in the epithelial compartment from all groups. However, this receptor was only intense in the stromal compartment in Group 2. ER α immunoreactivity was more intense in the stromal compartment from Group 2 in relation to Group 1. ER β was present mainly in the epithelial compartment and only in the stromal compartment of Group 2.

Conclusions: Reactive stroma was composed of myofibroblasts and fibroblasts stimulated to express extracellular matrix components. Intensified FGF, IGF and MMP immunoreactivities certainly compromised the glandular epithelial-stromal interaction and could be considered as regulators of reactive stroma. PCSCs were intensely associated with reactive stroma. The dynamic paracrine signaling of the SHRs discloses the role of these hormones in the activation mechanisms of reactive stroma and occurrence of PCSCs. Thus, it can be concluded that reactive stroma may be considered an important biological component of prostatic cancer.

846 An Evaluation of the Pathologic Reporting of Prostate Biopsy and Prostate Transurethral Resections with Urothelial Carcinoma

EJ Fichtenbaum, DL Zynger. The Ohio State University Medical Center, Columbus, OH.

Background: Urothelial carcinoma (UC) involving the prostate is almost always via secondary spread from a primary bladder tumor. In situ UC within the prostate occurs in the prostatic urethra or prostatic ducts. Invasive tumor extends into the prostatic subepithelial tissue or fibromuscular stroma. Invasion into the fibromuscular stroma (pT4a) of the prostate forecasts a far more ominous prognosis. Moreover, treatment options differ depending on the extent of prostatic involvement. We aim to understand problematic areas in the reporting of UC within prostate biopsy/TURP (transurethral resection of the prostate) specimens.

Design: We conducted a retrospective review between 2007 and 2010 of prostate biopsy/TURP (n=60) containing UC at our institution. All reports and available slides (30/60) were re-reviewed to assess reporting terminology and determine stage concordance.

Results: Upon re-review, definitive prostate tissue was present in 87% (26/30) of cases. Of the 4 cases that had no prostate tissue present, 2 included a statement that no prostate was present and 2 did not. 13% (8/60) of reports had a diagnosis of invasive urothelial carcinoma with no depth of invasion stated (ambiguous with respect to prostatic subepithelial invasion vs pT4a). 3 of the 8 cases were available for re-review with 2 determined to be pT4a, while 1 was in situ within the ducts. Terminology used for bladder anatomy (muscularis propria and lamina propria) was found in 37% (22/60) of reports. 13 of 22 (59%) reported muscularis propria and/or lamina propria without explicit reference to the bladder or prostate. 5 of these 13 (38%) were available for review with 2 containing bladder tissue while the remaining 3 did not. Discordant stage between the pathology report and re-review was identified in 10% (3/30) of cases. 2 cases were reported as pT4a but only had in-situ tumor within the ducts. 1 case stated that the tumor extended into the muscularis propria but was found in prostatic fibromuscular stroma (pT4a).

Conclusions: In this study we reveal reporting ambiguities of UC within prostate biopsies/TURP. We provide the following recommendations for these specimens: 1. Depth of tumor involvement within the prostate should be clearly stated as non-invasive/in-situ, invasive into the subepithelial tissue, or invasive into the fibromuscular stroma, 2. Absence of prostatic tissue should be documented, 3. Presence of bladder tissue should be noted, 4. Tumor involving bladder tissue should be reported with specific reference to the bladder.

847 Identification and Validation of Immunohistochemical Markers To Discriminate Urothelial Carcinoma Invading the Prostatic Fibromuscular Stroma vs In-Situ Tumor of the Prostatic Ducts

EJ Fichtenbaum, WL Marsh, DL Zynger. The Ohio State University, Columbus.

Background: Within the prostate, discrimination between urothelial carcinoma (UC) invading the fibromuscular stroma (pT4a) versus in-situ tumor of the prostatic ducts can be difficult. The goal of this study was to assess immunohistochemical (IHC) markers for their use in determining depth of tumor invasion within the prostate.

Design: 9 cases with UC involving the prostate were used to screen candidate markers for utility in differentiating tumor depth (CK5/6, CK7, CK20, p53, p63, HMWK, androgen

receptor (AR), PSA, PSAP, laminin, CD44, CD141). IHC was semi-quantitatively evaluated (0, <5%; 1+, 5-10%; 2+, 11-50%; or 3+, >50%). CK5/6 (Dako, D5/16B4) was identified as a promising marker. A retrospective review of cystoprostatectomies (CP) was performed to identify cases with UC involving the prostate upon which CK5/6 was assessed. CK5 (Novocastro, XM26), a recently available antibody requiring more moderate fixation conditions and a lower concentration compared to CK5/6 and thus ideal to use in double stains, was validated on the CP cases. Subsequently, the following double stain combinations were performed: CK5 (red)/p53 (brown), CK5 (brown)/p53 (red), CK5 (brown)/CK7 (red), CK5 (red)/CK7 (brown) and AR (brown)/CK7 (red). **Results:** 41 CP with UC in the prostate were identified (in-situ tumor only, n=4; fibromuscular stroma invasion only, n=21; in-situ tumor and fibromuscular stroma invasion, n=16). Both CK5/6 and CK5 were able to clearly differentiate basal cells (CK5/6: 20/20; 3+, 100% and CK5: 20/20; 3+, 100%) surrounding in-situ tumor from UC within ducts (CK5/6: 12/20; 0, 40.0%; 1+, 20.0%; 2+ 25.0%; 3+, 15.0% and CK5: 5/20; 0, 75.0%; 1+, 5.0%; 2+, 5.0%; 3+, 15.0%). The remaining markers were not effective in determining depth of tumor invasion when used as a single stain. CK5 (brown)/CK7 (red) and CK5 (red)/p53 (brown) robustly color contrasted in-situ tumor from surrounding basal cells and were further validated in 19 cases. Basal cells were not visible using CK5 (red)/CK7 (brown) or AR (brown)/CK7 (red). CK5 (brown)/p53 (red) did allow in-situ and basal cell discrimination; however, the nuclei were more easily visible using CK5 (red)/p53 (brown).

Conclusions: In this study we recommend the use of either CK5 or CK5/6 as an IHC marker to assist in determining depth of UC invasion within the prostate. Additionally, we propose the double stain combinations of CK5 (brown)/CK7 (red) and CK5 (red)/p53 (brown) to simultaneously highlight the in-situ tumor within prostatic ducts and the surrounding prostatic basal cells.

848 Incidental Prostate Pathology in Cystoprostatectomy Specimens: Is Partial Prostate Sampling Adequate?

E Filter, MY Gabril, JA Gomez, P Wang, J Izawa, J Chin, M Moussa. London Health Sciences Centre, London, ON, Canada.

Background: The standard treatment for muscle-invasive bladder cancer is radical cystoprostatectomy (RCP). The reported rate of incidentally detected prostate adenocarcinoma (Pca) in RCP varies from 14% to 54%. Overall, 25% of patients undergoing RCP harbour "clinically significant" disease despite a normal preoperative prostate exam. The wide variability in incidental Pca detection may be explained by different institutional grossing protocols. The aim of our study is to evaluate the incidence, pathologic features and clinical significance of incidental Pca in RCP specimens with partial versus complete prostate submission.

Design: 158 RCP performed for invasive bladder cancer between 1990 and 2006 in our institution were reviewed. No cases had previous history of Pca. Pathological features of Pca (Gleason score, margin status, extraprostatic extension, seminal vesicle invasion, lymphovascular invasion, and tumor focality) were assessed and correlated with clinical data (PSA, distant metastasis and survival). Two approaches of sampling were compared in our institution: partial versus complete prostate submission.

Results: 158 RCP cases were reviewed. 59 (37.3%) and 99 (62.7%) cases represented partial and complete prostate sampling respectively. Incidental Pca was detected in 72/158 (45.5%) in which Gleason score was ≥ 7 in 31.9% of cases. 17/72 (23.6%) and 55/72 (76.4%) with incidental Pca were cases with partial and complete sampling of the gland respectively.

Table 1: Focality of Pca in Partial vs. Complete Prostate Submission

Pca Incidence	Partial (n=17/72) (23.6%)	Complete (n=55/72)(76.4%)
Unifocal (33/72) (45.8%)	8/33 (24.2%)	25/33 (75.8%)
Multifocal (39/72)(54.1%)	9/39 (23.1%)	30/39 (76.9%)

The overall rate of concomitant Pca and invasive and/or in situ urothelial carcinoma (CIS) of the prostate was 29.1% (21/72). Both types of cancers were identified in 13/21 (61.9%) of RCP cases with microscopic examination of the entire prostate compared to 8/21 (38.1%) of cases with partial submission. 6/21 cases (28.6%) contained both Pca and CIS involving prostatic urethra. Of these 6 cases, 4 (66.7%) were detected with complete prostate evaluation.

Conclusions: Our findings suggest that complete evaluation of the prostate in RCP specimens yields higher detection rates of both incidental Pca and involvement by invasive and/or in situ urothelial carcinoma. Although there is currently no internationally accepted protocol for prostate sampling in cases of RCP, our data support consideration of this approach.

849 ERG Immunohistochemical Expression in Dominant Prostate Cancers and Paired Lymph Node Metastases

SW Fine, HA Al-Ahmadie, Y Chen, M Dudas, SK Tickoo, VE Reuter, A Gopalan. Memorial Sloan-Kettering Cancer Center, New York, NY.

Background: TMPRSS2-ERG gene fusions occur in about 50% of prostate cancers with resultant overexpression of a protooncogene, ERG. ERG overexpression by immunohistochemistry is a good surrogate for ERG gene rearrangement. Prior studies have revealed that ERG expression can vary both within and between tumor nodules in a given prostate. In cases with lymph node metastasis, positive lymph nodes contralateral to the dominant primary tumor may be seen in 30-40% of cases, suggesting significant "crossover" of lymphatic channels. The relationship of ERG status in dominant (largest) primary prostate cancers and matched lymph node metastases has not been well studied.

Design: 15 cases of primary prostate cancer and paired lymph node metastases were selected for study. Group 1 (n=9 cases) had bilateral positive lymph nodes with unilateral dominant primary tumors, while Group 2 (n=6 cases) had unilateral positive lymph nodes with unilateral dominant primary tumors contralateral to the side of lymph node metastasis. Multiple areas from the primary cancer, including high and low grade foci, were arrayed in triplicate in a single TMA. ERG immunohistochemistry was performed

on sections from the TMA and whole sections from positive lymph nodes.

Results: ERG status of primary tumors:

12 of 15 cases had both high and low grade foci available for sampling and in 11 of these cases ERG status was concordant for all grades. Group 1: 9/9 cases had matching ERG status for all grades. Group 2: 2/6 cases had matching ERG status for all grades; 1/6 had discordant ERG status in different grades (low grade - negative, high grade - positive); 3/6 had only high grade areas which were concordant for ERG status.

Comparison of ERG status between positive lymph nodes and primary tumors:

Group 1: 9/9 cases – ERG status matched that of the dominant tumor; Group 2: 6/6 cases – ERG status matched that of dominant tumor. In the single case with discordant ERG status between low and high grade areas, the ERG status in the positive lymph node matched that of the high grade component.

Conclusions: ERG status of positive lymph nodes is concordant with ERG status of the dominant primary tumor. This is true even when the dominant tumor is contralateral to the metastasis, supporting the existence of lymphatic crossover. Within a given tumor, ERG status of low and high grade foci is usually concordant. Further studies are ongoing to investigate ERG status in cases with positive lymph nodes and more than one dominant/high grade primary tumor nodule to better assess the clonality of these metastatic lesions.

850 Immunohistochemical Profile of Clear Cell and Related Renal Cell Cancers, with Emphasis on CK7 and Carbonic Anhydrase-IX (CA-IX) Staining

SW Fine, Y Chen, HA Al-Ahmadie, A Gopalan, VE Reuter, SK Tickoo. Memorial Sloan-Kettering Cancer Center, New York, NY.

Background: Immunohistochemical (IHC) staining is often used as an important differential diagnostic adjunct for renal tumors, both in metastatic and primary settings. In this differential, clear cell renal cell carcinoma (CC-RCC) is usually considered as CA-IX and CD10 diffusely positive and CK7 negative. We have occasionally observed unusual staining patterns among typical CC-RCCs mimicking those in other RCCs that may be considered in their differential diagnosis. Using a small panel of commonly used stains, we analyzed the IHC patterns in CC-RCC and some of its closely related entities.

Design: IHC was performed for CK7, CA-IX, CD10, and 34BE12 on 10 cases of clear cell papillary RCC (CCP), 7 multilocular cystic RCC (MLC), 7 clear cell RCC with prominent (>35%) cystic component (CC-RCC-C), and 15 clear cell RCCs without cystic change (CC-RCC-NC). Immunoreactivity was analyzed for percent cells positive, location of positive staining, and patterns of staining.

Results: CK7 positivity was present in all cases of CCP, MLC and CC-RCC-C, with 100% cells staining positive in 10/10 CCP and 2/7 MLC. 2 (13%) CC-RCC-NC showed very focal CK7 reactivity, but only in small cystic areas present in these 2. CK7 positivity was also more concentrated in and around cystic areas in CC-RCC-C. CA-IX was positive in all cases in all 4 tumor groups, but only CCP showed a predominantly "cup-like" reactivity with absence of staining on luminal aspect of the cells. CD10 was either completely negative, or was only very focally positive in CCP (2/7, 20% cases) and MLC (3/7, 43%), mostly in a luminal pattern. Whereas, CD10 positivity was seen in 71% of CC-RCC-C (mixed luminal and box patterns) and 87% of CC-RCC-NC (predominantly box-pattern), respectively. 34BE12 was mainly positive in CCP and MLC (60 and 43% cases), with only 1 case each of CC-RCC-C and CC-RCC-NC showing focal reactivity.

Conclusions: 1) CK7 immunoreactivity should not exclude the possible diagnosis of clear cell RCC, particularly in cystic lesions; however, diffuse positive staining in 100% or close to 100% cells in a tumor is not a characteristic of clear cell RCC.

2) CK7 positivity appears to be mostly related to cystic features in the tumors, except in clear cell papillary RCC, where it stains all the cells irrespective of relationship to cystic areas.

3) Diffuse membranous CA-IX reactivity is seen in a variety of clear cell tumors, but "cup-shaped" reactivity is a characteristic of only clear cell papillary RCC.

851 Gene Expression Profiling of Clear Cell Papillary Renal Cell Carcinoma

KE Fisher, Q Yin-Goen, D Alexis, JS Sirintrapun, W Harrison, BR Isett, MR Rossi, CS Moreno, AN Young, AO Osunkoya. Emory University School of Medicine, Atlanta; Wake Forest University School of Medicine, Winston-Salem.

Background: Clear cell papillary renal cell carcinoma (CCPRCC) is a recently described distinct variant of renal cell carcinoma (RCC) that shares some overlapping histologic and immunohistochemical features of clear cell RCC (CCRCC) and papillary RCC (PRCC). Our previous work elucidated differential molecular expression biomarkers that distinguish CCRCC (carbonic anhydrase IX [CA9]) from PRCC (schwannomin-interacting protein 1 [SCHIP1]) and α -methylacyl coenzyme-A racemase [AMACR]). Although the immunohistochemical profile of CCPRCC is well described, the mRNA expression profile of CCPRCC has not been well characterized in multiple series. Using a select subset of previously identified candidate genes, we investigated the gene expression profile of CCPRCC.

Design: 12 cases of CCPRCC with classic histologic and immunohistochemical profile were selected for molecular analysis after histologic review by the senior author. RNA was extracted from formalin-fixed paraffin-embedded tissue and cDNA was prepared. Quantitative PCR was performed in triplicate, targeting CA9 (Hs00154208_m1), AMACR (Hs01091292_m1), and SCHIP1 (Hs00205829_m1). 28S ribosomal RNA was used as an amplification control (RNA28S1, Hs03654441_s1).

Results: Successful cDNA amplification occurred in the 12 cases of CCPRCC. SCHIP1 was successfully amplified in 1/12 cases (8.3%), CA9 in 9/12 cases (75%), and AMACR in 6/12 cases (50%). Three cases of CCPRCC coexpressed both CA9 and AMACR mRNA, and one case coexpressed CA9, AMACR, and SCHIP1 mRNA. CCPRCCs expressed approximately 60 to 1000-fold more CA9 mRNA compared to AMACR

mRNA (Comparative $\Delta\Delta C_t$ values ranging between -5.979 and -9.896).

Conclusions: Variable expression of CA9, AMACR, and SCHIP1 mRNA in CCRCC confirms that these tumors are distinct from CCRCC and PRCC, they share some molecular expression profiles of both CCRCC and PRCC. The increased expression of CA9 mRNA relative to AMACR mRNA, suggests that the clear cell molecular phenotype is likely more dominant in a subset of patients with CCRCC. SCHIP1 mRNA which is typically increased in PRCC was also not amplified in the vast majority of cases. Amplification optimization and investigation of additional candidate genes is ongoing. Understanding the molecular basis of CCRCC will assist in future sub-classifications and molecular-targeted treatment of patients with this unique tumor.

852 Tumor Regression after Neoadjuvant Chemotherapy Independently Predicts Survival in Bladder Cancer Patients

A Fleischmann, A Perren, GN Thalmann, R Seiler. University of Bern, Bern, Switzerland.

Background: Tumor regression after chemotherapy predicts survival in different cancers. In bladder cancer these studies are still missing.

Design: A cohort of 59 patients with histopathologically proven urothelial bladder cancer received neoadjuvant chemotherapy (median 4 cycles) before cystectomy and lymphadenectomy. Indications were clinically positive lymph nodes (n=41), advanced primary tumour stage cT4 (n=15) and other reasons (n=3). A tumor regression grade (TRG) was defined similar to the method proposed by Mandard et al. (Cancer 1994;71:2680-6) for esophageal cancer. TRG 1: complete regression without residual cancer and with extensive fibrosis of the tumor bed; TRG 2: presence of residual cancer cells scattered through the predominating fibrosis; TRG 3: residual cancer outgrowing fibrosis or absence of regression. Histopathological characteristics of the untreated tumors (growth patterns, histological subtypes, nuclear size, peri- and intratumoural inflammation, mitotic rate) were correlated with TRG and different parameters of the treated tumors were tested for overall survival (OS) stratification.

Results: Seventeen patients each (28%) had TRG 1 and TRG 2, 25 patients (44%) TRG 3. In the untreated cancers, the only parameter with significant ($p<0.05$) predictive value for therapy response was a high mitotic rate. Higher TRG grades were significantly ($p<0.05$) associated with unfavorable characteristics in surgical specimens (higher ypT and ypN stage, number of positive blocks and diameter of residual tumor). In univariate analysis, TRG, ypT, number of blocks with residual tumor tissue, largest diameter of primary tumor and ypN stratified OS significantly. In multivariate analysis, only TRG predicted OS independently ($p<0.05$).

Conclusions: The suggested tumor regression grade in bladder cancer is an independent predictor of survival. A favorable chemotherapy response is associated with a high mitotic rate in the untreated tumor. This parameter might help to identify patients which benefit from neoadjuvant chemotherapy.

853 Re-Visiting the Use of Common Biomarkers in Cytogenetically Confirmed Subtypes of Renal Epithelial Neoplasia

T Flood, P Dal Cin, MS Hirsch. Brigham & Women's Hospital, Boston, MA.

Background: There is great variability in the reported protein expression patterns in renal epithelial neoplasms (RENs). One explanation is that newer REN subtypes, such as clear cell tubulopapillary renal cell carcinoma (CCTPRCC) and mucinous tubular and spindle cell carcinoma (MTSCC), were misclassified as clear cell renal cell carcinoma (CCRCC) and/or papillary renal cell carcinoma (PRCC), affecting the data. The goal of this study was to revisit the diagnostic utility of common antibodies in cytogenetically confirmed RENs to determine more accurate specificity, sensitivity, and clinical use of these markers.

Design: IHC with CK7, AMACR, and CD117 (cKIT) was performed on 100 RENs with classic confirmatory karyotypes, including 53 CCRCC with loss of chromosome 3p, 22 PRCC with trisomies 7 and 17, 9 chromophobe carcinomas (ChRCCs) with multiple monosomies, 5 oncocytomas (RO) with loss of chromosome 1, and 5 MTSCCs with specific monosomies. Additionally, 6 CCTPRCCs with classic morphologic features were evaluated. IHC staining of tumors were assessed independently and semi-quantitatively by 2 pathologists: 0 no reactivity; 1+ <10%; 2+ 11–25%; 3+ 26–50%; and 4+ >50%; a score of $\geq 2+$ was considered a positive result.

Results: Rare cases of CCRCCs were positive for CK7 (6/53, two 3+, four 4+) and CD117 (1/53); whereas AMACR staining was present in 64% (34/53) of cases. Of the 6 CK7+ CCRCCs, 3 were AMACR positive and 3 were negative. Most PRCCs showed strong staining for CK7 (18/22) and AMACR (21/22) with few cases expressing CD117 (2/22). All CK7 negative PRCCs were of the 'type II' variant, were positive for AMACR, and negative for CD117. Approximately half of the ChRCCs were positive for CK7 (5/9) and CD117 (4/9) with AMACR usually absent (1/9 positive). All 5 ROs were negative for both CK7 and AMACR, but positive for CD117. CK7 and AMACR were positive in 2/5 and 4/5 MTSCCs, respectively; none were positive for CD117. All 6 CCTPRCCs were diffusely positive for CK7 and completely negative for AMACR.

Conclusions: To our knowledge this is the first study that has determined the diagnostic value of certain IHC markers on cytogenetically confirmed subtypes of RENs. Overall the data shows that when morphologic findings in RENs overlap, variable expression patterns of CK7, AMACR, and CD117 can be useful adjuncts. A CK7+/AMACR- finding is sensitive and specific for CCTPRCC (6/6, 100%) and argues against CCRCC (3/53, 6%) and PRCC (1/22). Additionally, the presence of CD117 can reliably help distinguish RO from PRCC and MTSCC, both of which can demonstrate oncolytic features, but not from ChRCC.

854 A New microRNA-Based Diagnostic Test for Classification of Kidney Tumors

E Fridman, S Rosenwald, E Meiri, E Goren, S Zilber, Y Huang, I Barshack, I Burnstein, I Krivitsky, M Zepeniuk, N Dromi, Y Goren, Y Spector. Sheba Medical Center, Tel-Hashomer, Israel; Sackler School of Medicine, Tel Aviv University, Tel Aviv, Israel; Rosetta Genomics Ltd., Rehovot, Israel; Rabin Medical Center, Petah Tikva, Israel; Temple University Hospital, Philadelphia, PA.

Background: Renal cancers account for more than 3% of adult malignancies and cause more than 13,000 deaths per year in the US alone. The four most common types of kidney tumors include the malignant renal cell carcinomas clear cell, papillary and chromophobe as well as the benign oncocytoma. These histological subtypes vary in their clinical courses and their prognosis, and different clinical strategies have been developed for their management. In some of the kidney tumor cases it is difficult for the pathologist to distinguish between tumor types on the basis of morphology and immunohistochemistry (IHC). In this work we present the development and validation of a microRNA-based test for classifying primary kidney tumors.

Design: Over 180 Formalin Fixed Paraffin Embedded (FFPE) samples of primary kidney tumors were collected and reviewed by pathologists from different institutes according to morphology and available IHC labeling data. High-quality total RNA, including the well-preserved microRNA fraction, was extracted from the FFPE samples using a proprietary protocol. Expression levels of hundreds of microRNAs were profiled using a custom microarray platform. Technical validation of the array results was performed using qRT-PCR. An assay which classifies the kidney tumors was developed based on the expression of differential microRNAs in these four tumor types. A validation set of 201 independent samples was classified using the assay and analyzed blindly.

Results: A set of 24 differential microRNAs was identified that allows accurate classification of kidney tumors. A diagnostic assay based on the microarray technology was developed and clinical validation performed using an independent, blinded sample set. The test was able to produce results for 92% of the validation set of 201 samples with accuracy of 95%.

Conclusions: Expression levels of certain microRNAs are highly specific to subtypes of renal cell tumors. These findings were the basis for the development and validation of a standardized diagnostic assay for the classification of renal cell tumors in FFPE samples from resections or biopsies. The validation results showed 95% accuracy and demonstrated again the diagnostic power of microRNAs.

855 Microsatellite Instability in Prostatic Adenocarcinoma: Association with a Mucinous Phenotype

CS Friedman, DJ Pisapia, P Ghosh, MM Shevchuk. NYP-Weill Cornell Medical College, New York, NY; NYP-Columbia University Medical Center, New York, NY; Maimonides Medical Center, Brooklyn, NY.

Background: The loss of DNA mismatch repair genes and subsequent microsatellite instability (MSI) plays a key role in carcinogenesis of approximately 15% of colonic carcinomas, including patients with Lynch syndrome, as well sporadic cases. A characteristic histologic feature of MSI-associated colonic carcinomas is mucinous change. Several studies have also shown loss of mismatch repair genes in prostatic adenocarcinomas. However no specific histologic phenotype of this tumor has been described in relation to MSI. We examined prostatic adenocarcinomas with mucinous change for their possible association with MSI.

Design: Index cases consisted of 22 prostatic adenocarcinomas with mucinous extravasation involving at least 5% of the tumor. Control cases consisted of 22 prostatic adenocarcinomas (without mucinous change), matched for primary and secondary Gleason patterns, and for pathologic stage. MSI was studied by immunohistochemical staining for MLH1, MSH2, MSH6, and PMS2 by our Translational Research Laboratory.

Results: The Gleason scores of the set of mucinous tumors and of the matching controls were as follows: 16 cases were Gleason score 7; including 4 cases of 3+4, 7 cases of 4+3, and 5 cases of 4+3 with tertiary pattern 5. Two cases were Gleason score 8(3+5) with tertiary pattern 4, and 4 cases were Gleason score 9(4+5). In each set there was 1 case of stage pT2a, 11 cases of pT2c, 7 cases of pT3a, and 3 cases of pT3b. The mean age of the patients with mucinous adenocarcinoma was 64 (range 46-78), and of the control patients the mean age was 62 (range 54-75). MSH6 was absent in 6 (26%) of the mucinous carcinomas, and in 1 (4.5%) of the control cases. MLH1, MSH2 and PMS2 were retained in all cases. This difference is statistically significant ($p=.039$).

Conclusions: Mucinous prostatic adenocarcinomas, characterized by the presence of extravasated mucus, are more likely to be associated with MSI, specifically with the loss of MSH6. This suggests that a subset of patients with loss of MSH6 might be at increased risk for prostatic carcinoma; and that the mucinous phenotype may be a histologic indicator. This association is interesting in light of a recent study which reported that MSH6-associated colonic carcinomas appear to be a distinctive subset of MSI-related tumors. If supported by future studies of larger numbers of cases, these observations may help to identify patients with MSI-related prostate cancer.

856 Detection of ERG in Japanese Transition Zone Prostate Cancer

B Furusato, H Takahashi, T Kimura, J Miki, S Mizukami, M Okayasu, T Yamamoto, H Kuruma, S Egawa, H Hano. The Jikei University School of Medicine, Tokyo, Japan.

Background: Incidence of transition zone-prostate cancer (TZ-PCa) is relatively common in Japan. Gene fusion involving the ERG oncogene is a frequent alteration in prostate cancer (PCa) and studies from the Western countries have suggested that ERG expression is less common in TZ-PCa than in peripheral zone-prostate cancer (PZ-PCa). Here, we assessed the ERG expression in Japanese PCa by zonal origin and compared with clinicopathological parameters to see whether any differences exist between Japan and the Western countries.

Design: We evaluated 92 index tumors from Japanese patients who had undergone radical prostatectomy for PCa, using an antibody-based detection method to determine ERG expression. Expression status was compared with clinicopathological findings including zonal origin of index tumor (TZ, PZ, or both), tumor size, Gleason score, pathological stage and Body mass index (BMI).

Results: In 92 cases, the index tumor distribution was 42.4% (39/92), 32.6% (30/92) and 25% (23/92) in PZ, TZ, and both zones, respectively. Overall, ERG expression was detected in 16.3% (15/92) of the cases. Among the ERG positive cases, 73.3% (11/15) were detected in PZ-PCa, 20% (3/15) were detected in TZ-PCa and 6.7% (1/15) were detected in tumor located in both zones. ERG expression was associated with Gleason score in PZ-PCa ($p=0.01$) and TZ-PCa (marginally, $p=0.046$). There was no association between ERG expression and rest of the parameters including tumor size, pathological stage and BMI in both TZ- and PZ-PCa's.

Conclusions: Although there are significant differences in the rate of overall ERG expression between Japan (16.3%) and Western PCa's (50%), there is a similar trend of ERG expression in TZ-PCa from both countries. The lower frequency of ERG expression in TZ-PCa may be a common trend among Western and Aisan (Japan) countries, which may suggest distinct molecular alterations from PZ-PCa. Therefore, further studies are required to determine whether this finding is reproducible in multi-institutional analysis to better understand differences in molecular profiles between PZ- and TZ-PCa's.

857 Tissue Microarray Analysis of Prostate Cancer Specimens Supports a Positive Feedback Loop among Molecules Involved in Hyaluronan Synthesis, Degradation, and Signaling

V Ganta, A Rizzardi, L Marston, J Tiffany, R Vogel, N Rosener, G Metzger, J McCarthy, E Turley, S Schmechel. University of Minnesota, Minneapolis, MN.

Background: Hyaluronan (HA) has been implicated in the biology of prostate cancer (PCa). Hyaluronan synthase 2 (HAS2), Hyaluronidase 1 (Hyal1), and HA receptors including RHAMM and CD44 comprise the hyaluronome, which regulates HA metabolism and function. HA signaling is implicated in regulation of tumor cell proliferation, angiogenesis, inflammation, and metastasis. We sought to investigate the role of these factors in PCa aggressiveness by analyzing their expression in patients with PSA failure.

Design: We built tissue microarrays (TMAs) from tumor present in prostatectomy specimens from a cohort of 161 patients for which PSA follow-up data was available. We used IHC stains directed against HAS2, Hyal1, RHAMM and CD44, and a biotinylated HA binding protein directed against HA, on TMA sections. From whole slide images of stained TMA sections, we used a software algorithm (Genie Histology Pattern Recognition, Aperio, Vista, CA) to automate tissue annotation into several image classes (tumor, stroma, and empty glass). We performed stain intensity analysis separately in tumor and stromal channels (Color Deconvolution, Aperio).

Results: Established pathologic parameters (tumor stage, nodal status, margin status and preoperative PSA) were each separately associated with time to PSA failure. In tumor areas, HAS2, Hyal1 and RHAMM were significantly and positively correlated with each other. Stromal HA levels were significantly associated with time to PSA failure, with patients having higher HA levels being more likely to fail. This relationship held in both univariate and multivariate models (adjusting for established pathologic parameters) ($p=0.02$ and 0.03 respectively).

Conclusions: There is substantial evidence indicating that malignant progression of prostate tumors is related to increases in the synthesis and degradation of HA and to alterations in RHAMM expression and function. Our data are consistent with this evidence and suggest a model of prostate tumor progression in which increased synthesis and degradation of HA could activate RHAMM function and increase tumor cell proliferation, angiogenesis, inflammation, and metastasis. These data further emphasize the importance of the tumor microenvironment in tumor progression and they suggest it may be possible to better manage PCa patients by using therapeutics that inhibit the interaction of tumor associated RHAMM with fragmented HA.

858 Nuclear and Membranous Smo Expression Is Associated with Low Tumor Grade and Stage in Renal Cell Carcinomas (RCC)

J Garbaini, K-A Kim, RN Al-Rohil, CE Sheehan, RP Kaufman, JS Ross, A Hayner-Buchan. Albany Medical College, Albany, NY.

Background: The hedgehog signaling pathway has been reported to be aberrantly activated in many solid tumors, including renal cell carcinoma (RCC). Smoothed (Smo) is a G protein-coupled receptor which can act as an oncogene, causing unregulated activation of the Hedgehog (Hh) pathway. The current study examines the expression of Smo in RCC.

Design: Tissue sections from 146 formalin-fixed, paraffin-embedded RCC, 119 clear cell type (CC) and 27 other types, were immunostained by an automated method (Ventana Medical Systems Inc., Tucson, AZ) using goat polyclonal Smo antibody (Santa Cruz Biotech, Santa Cruz, CA). Nuclear (nSmo), membranous (mSmo), and cytoplasmic (cSmo) immunoreactivity based on intensity and distribution was semiquantitatively scored and the results were correlated with clinical and morphologic variables.

Results: nSmo overexpression was noted in 64 (44%) tumors and correlated with low grade (54% LG vs 30% HG, $p=0.005$ overall; 56% LG vs 31% HG, $p=0.008$ CCs) and early stage (50% early vs 29% advanced, $p=0.038$ overall; 51% early vs 32% advanced, $p=0.057$ trend for CCs; 43% early vs 0% advanced, $p=0.097$ trend for others). mSmo overexpression was noted in 86 (59%) tumors and correlated with tumor type (69% CCs vs 15% others, $p<0.0001$) and low grade (60% G1 vs 70% G2 vs 63% G3 vs 30% G4, $p=0.013$ overall; 60% G1 vs 78% G2 vs 69% G3 vs 33% G4, $p=0.01$ CCs) and showed a trend toward correlation with early stage (74% I vs 56% II vs 73% III vs 29% IV, $p=0.054$ CCs). cSmo overexpression was noted in 123 (84%) tumors and correlated with tumor type (81% CCs vs 100% others, $p=0.013$). On multivariate analysis, high tumor grade ($p=0.003$) and advanced stage ($p=0.018$) independently predicted overall survival.

Conclusions: Nuclear and membranous Smo overexpression correlate with low tumor grade and early pathologic stage in RCC indicating that Smo expression may exert a favorable prognostic impact for the disease. Based on these findings, further study of Smo expression in RCC appears warranted.

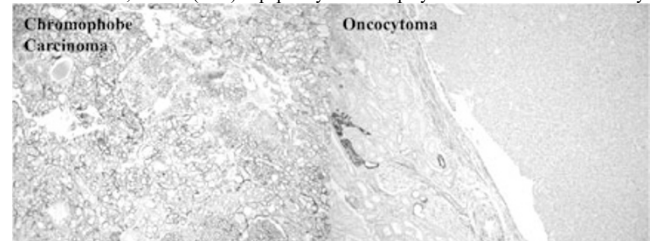
859 Expression of the Na⁺/K⁺-Transporting ATPase Gamma Subunit FXYD2 in Chromophobe Renal Cell Carcinoma and Renal Oncocytoma

JP Gaut, DL Crimmins, CM Lockwood, JJ McQuillan, JH Ladenson. Washington University School of Medicine, St. Louis, MO.

Background: Chromophobe renal cell carcinoma (RCC) is a deadly form of renal cancer that is histologically similar to the benign renal oncocytoma. There are no robust markers available to distinguish these neoplasms. Chromophobe RCC and renal oncocytoma are presumably derived from the distal nephron. FXYD2 is a distal tubule protein that is highly expressed in normal kidney. It is the aim of the current study to evaluate FXYD2 expression in RCC.

Design: Case records of Barnes Hospital were searched and identified 41 chromophobe RCCs, 38 oncocytomas, 15 clear cell RCCs, and 11 papillary RCCs. Immunohistochemistry for FXYD2, cytokeratin 7 (CK7), and kidney-specific cadherin (KspCdh) was performed along with histochemical analysis for colloidal iron. Fluorescence in situ hybridization (FISH) analysis for chromosomes 1, 2, 6, 10, and 17 was performed on a subset of tumors.

Results: Immunohistochemical staining for FXYD2 showed diffuse, strong immunoreactivity in the basolateral membrane of distal tubules of normal human kidney. 83% (34/41) of chromophobe RCCs were immunoreactive for FXYD2 in a membranous pattern (figure). In contrast, only 8% (3/38) of renal oncocytomas (figure), 11% (2/15) of clear cell RCCs, and 0% (0/11) of papillary RCCs displayed FXYD2 immunoreactivity.



CK7 was immunoreactive in 79% (15/19) of chromophobe RCCs and 39% (7/18) of oncocytomas. KspCdh showed positive staining in 95% (18/19) of chromophobe RCCs and 44% (8/18) of oncocytomas. Colloidal iron stained 79% (15/19) of chromophobe RCCs, and 11% (2/18) of oncocytomas. FISH demonstrated monosomy 1, 2, 6, 10, and 17 in 69% (9/13) of chromophobe RCCs and 11% (2/18) of oncocytomas.

Conclusions: FXYD2, a distal tubule protein, is preferentially expressed in chromophobe RCC. Although both chromophobe RCC and oncocytoma are believed to derive from the distal nephron, they show differential expression of FXYD2, a distal tubule specific protein. This unexpected result highlights subtle differences between these two tumor types. Importantly, FXYD2 may be a diagnostically useful marker to distinguish benign oncocytoma from chromophobe RCC.

860 Interstitial Cystitis, Another IgG4 Related Disease?

Y Ge, H Zhou, SS Shen, JY Ro. The Methodist Hospital, Weill Medical College of Cornell University, Houston, TX.

Background: Interstitial cystitis (IC) is a chronic inflammation and/or injury to the bladder wall. Primary symptoms are urinary frequency, urgency and severe lower abdominal or perineal pain, which often resulting in serious impairment of quality of life. The cause of IC is largely unknown, though several theories including autoimmune, infection, toxic substance and genetic factor have been proposed. The histologic hallmark of IC is the presence of abundant mast cells infiltrating the muscle bundles. In addition, we recently noticed that plasma cells are notably increased in some of the cases, raising the possibility of an IgG4-related disease. We therefore evaluated the number of IgG4 positive plasma cells and the ratio of IgG4/IgG plasma cells in cases with IC.

Design: A total of 45 cases of clinically and histologically confirmed IC from 1/2006 to 9/2011 were retrieved from The Methodist Hospital. The female to male ratio was 41 to 4. The average age was 48.6 years (range 18-92 years). The specimens included 43 bladder biopsies and 2 cystectomies. Immunostains for IgG4 and IgG were performed on sections of paraffin blocks. The plasma cells positive (+) for IgG4 and IgG were counted and the IgG4/IgG ratio was calculated. Cases with more than 30 IgG4 + plasma cells per one high power field (HPF) with IgG4/IgG ratio greater than 50% were considered significant.

Results: There were 9 out of 45 patients had IgG + plasma cells greater than 30/HPF in bladder specimens. In four of the 9 cases, IgG4 + plasma cells were predominant with increased IgG4/IgG ratio. The number of IgG4 + plasma cells ranged from 31 to 82 per HPF (average 56/HPF). The IgG4/IgG ratios were from 51 to 56 with an average of 52.5. The four patients with increased IgG4 + plasma cells included one male (48 years) and three females (21, 77 and 84 years) with an average age of 57.5 years. Histologically, the four cases had similar features as other cases of IC in addition to increased plasma cells.

Conclusions: Due to lack of knowledge on etiology and pathogenesis, there is currently no effective treatment available for IC. Because IC varies so much in symptoms and severity, most researchers believe it is not one, but several diseases. Our findings suggest that a fraction of the patients with IC may be part of IgG4-related systemic disease. Further investigation of the mechanism is crucial to understand the pathogenesis and provide effective treatment for patients with IC.

861 The Diagnostic Accuracy and Clinical Role of Percutaneous Renal Needle Core Biopsy in Renal Cortical Neoplasms

LL Gellert, R Mehra, Y Chen, A Gopalan, S Fine, H Al-Ahmadie, VE Reuter, S Tickoo. Memorial Sloan-Kettering Cancer Center, New York, NY.

Background: The role of renal needle core biopsy in the management of renal cortical neoplasm remains controversial. In a prior ex vivo study, in combination with immunohistochemistry (IHC), we determined the diagnostic accuracy of this procedure. In the present study, we report our experience with in vivo renal needle core biopsies (NCB), and its impact on clinical management.

Design: We identified 217 consecutive cases of percutaneous NCB for renal masses performed at our institution between 2006 and 2011. All pathology reports, H&E and IHC slides were reviewed. Clinical data were collected from patient charts.

Results: Of the 217 cases, 178 showed neoplastic and 39 benign tissue. Of these 39 cases, 11 were performed for evaluation of the cryoablation bed, 3 were proven to be inflammation/infection, and 25 were neoplasms. In the 178 cases in which a neoplasm was identified, the diagnosis was: 80 clear cell renal cell carcinoma (CCRCC), 27 low grade (LG) oncocytic neoplasms (9 oncocytoma, 9 chromophobe (CHR-RCC) and 9 NOS), 7 papillary RCC (PRCC), 4 clear cell papillary RCC (CCPAP), 5 angiomyolipoma (AML), 1 medullary RCC (MRCC), 1 mucinous tubular and spindle cell carcinoma (MTSCC), 1 RCC unclassified (RCC-U), 1 PRCC/MTSCC, 15 urothelial carcinoma and 35 others (including metastasis, and lymphoma etc). Overall, 88% of in vivo NCB cases yielded adequate material. 30 patients underwent subsequent nephrectomy. The biopsy diagnosis was confirmed on nephrectomy in 29 of 30 cases, with a concordance rate of 96% (24/25) in CCRCC, 100% (2/2) in CHR-RCC, 100% (2/2) in oncocytoma and 100% (1/1) in MTSCC. There was a significant difference in clinical management (ablation, surgery, chemotherapy, vs active surveillance [AS]) between each diagnostic group (table 1). Of the 80 CCRCC cases, 84% were treated and 16% went on AS. Of the 44 benign or LG cases, 35% were treated and 65% went on AS.

Table 1. Clinical management following biopsy diagnosis.

Diagnosis on biopsy	Total	Cryoablation	Nephrectomy	Chemotherapy	Active Surveillance
Clear cell RCC	80	12	24	31	13
Papillary RCC	7	3	0	2	2
Chromophobe RCC	9	2	2	1	4
Oncocytoma	9	1	2	0	6
Low grade oncocytic renal neoplasm, NOS	9	0	0	0	9
Clear cell papillary RCC	4	1	0	0	3
AML	5	0	0	0	5
Misc*	5	0	2	3	0
Total	128	19	30	37	42

*Includes 1 MRCC, 1 RCC-U, 1 sarcomatoid carcinoma, 1 MTSCC, 1 PRCC/MTSCC

Conclusions: In vivo percutaneous NCB of renal masses yields diagnostic material in 88% of cases with high diagnostic accuracy. This information is useful in deciding subsequent management of these patients.

862 DNA Mismatch Repair Deficiency in Urothelial Carcinoma: An Immunohistochemical Study in Upper Versus Lower Genitourinary Tract Tumors

LL Gellert, R Mehra, J Shia, Y Chen, A Gopalan, S Fine, S Tickoo, VE Reuter, H Al-Ahmadie. MSKCC, New York, NY.

Background: The loss of mismatch repair proteins (MMR) has been reported in Lynch syndrome (LS)-associated as well as sporadic urothelial carcinoma (UC). Few studies have focused on the expression of MMR proteins in UC with different histological grade and/or location.

Design: We retrospectively identified 88 UC cases, including 41 bladder tumors and 47 upper tract (ureter and renal pelvis) tumors. MMR proteins (MLH1, MSH2, MSH6, and PMS2) were evaluated by immunohistochemistry (IHC) on whole sections. Abnormal staining was defined as total loss of protein in the tumor with appropriate internal control. The IHC findings were correlated with clinical and pathological characteristics.

Results: In upper tract tumors, loss of MMR proteins was detected in 4 of 47 cases (8.5%). Two of these 4 cases lost both MSH2 and MSH6 proteins. The other 2 cases lost MSH2 and less than 1% of the tumors cells showed weak nuclear staining for MSH6. In bladder urothelial carcinoma, loss of MMR proteins were detected in 2 of 41 cases (5%); one tumor lost both MSH2 and MSH6 proteins, and the other tumor lost both PMS2 and MLH1 proteins.

The loss of MMR protein expression was present in both non-invasive and invasive components. In the normal urothelium adjacent to the tumor, all MMR proteins were retained. Tumors of both low grade and high grade morphology showed loss of MMR protein expression. Detailed results are summarized in table 1.

Table 1. MMR proteins in upper and lower tract urothelial carcinoma.

Tumor	Grade	N	Loss of MSH2/MSH6	Loss of MLH1/PMS2
Renal pelvis UC	High grade	33	1	0
	Low grade	4	2	0
Ureter UC	High grade	8	1	0
	Low grade	2	0	0
Bladder UC	High grade	39	1	1
	Low grade	2	0	0
Total		88	5	1

Conclusions: Overall, alterations in MMR protein expression are present in a minority of urothelial carcinoma of both upper and lower tracts. MSH2 and/or MSH6 protein was lost in 8.5% (4/47) of the upper tract UC but only 2% (1/41) of bladder UC. As loss of MSH2/MSH6 is highly suggestive of hereditary MMR deficiency, our findings support the inclusion of upper tract UC in the LS tumor spectrum, and suggest that the urinary bladder may be affected as well in LS patients, albeit at a lower frequency. The finding that none of the 47 upper GU tract tumors had loss of MLH1/PMS2 suggests that sporadic epigenetic inactivation of the *MLH1* gene is likely a rare event. Loss of

MMR proteins in both non-invasive and invasive components of urothelial carcinoma suggests that these aberrations are early events in the tumorigenesis and it may have implications in testing urothelial tissues for detecting LS patients.

863 Primary Clear Cell Renal Cell Carcinoma and Its Metastasis: A Comparative Analysis of Histologic and Immunophenotypic Features

EM Genega, VE Brown, B Bahamon, A Ward, L Quintana, S Signoretti. Beth Israel Deaconess Medical Center, Boston, MA; Brigham & Women's Hospital, Boston, MA.

Background: Clear cell renal cell carcinoma (CCRCC), the most common type of RCC and the type that most frequently metastasizes, is a heterogeneous neoplasm with significant variability in its histologic features within a given tumor and amongst tumors. The study of predictive and/or prognostic tissue biomarkers for metastatic CCRCC is usually conducted by analyzing the primary tumor, which is more readily available, rather than the metastases (METS) that are targeted by systemic therapy. However, it is not known to what extent the primary tumor is representative of its metastatic lesions. In this study, we evaluated and compared histological and immunophenotypic features in a series of primary CCRCCs and their METS.

Design: Slides and tissue blocks from primary CCRCCs and their METS were retrieved. Histologic features, including predominant and highest Fuhrman grade (1-2 = low FG; 3-4 = high FG) and growth pattern (GP), were compared in the primary tumor (PT) and the corresponding METS. Carbonic anhydrase IX (CAIX) immunostaining was performed on one or more representative sections of the primary and metastatic tumors using the M75 antibody. Additional biomarkers are currently under evaluation.

Results: Twenty patients were identified, 3 had metachronous METS, 16 had synchronous METS and one had both. Twenty-nine METS were found: 4 adrenal METS, 5 lymph node METS, and 20 distant METS. All PT were high FG; 12 had a highest FG (HFG) = 3 and 8 had a HFG = 4. The predominant FG (PFG) of the PT was 2 in 9 cases, 3 in 10 cases and 4 in one case. Twenty-five METS were also high FG (12 with HFG = 3 and 13 with HFG = 4). The remaining 4 METS had HFG = 2. In 19 METS, the HFG matched the HFG of the corresponding PT, while in 5 METS the HFG matched the PFG of the corresponding PT. The HFG of the remaining 5 METS was higher than the HFG of the PT. Assessment of the GP revealed that in 25 METS the GP matched that of the PT and in 2 cases it did not; the GP of two METS was not evaluable. Immunohistochemical analysis of the METS (n=24) and corresponding PT (n=20) revealed CAIX expression was concordant (ie +/- 10% positive cells) in 21 of 24 METS.

Conclusions: 1. For CCRCC that metastasize, the PFG and HFG of the PT is more often high grade. 2. The majority of CCRCC METS (83%) had a high FG component that matched the HFG of the corresponding PT or was higher. 3. The vast majority of CCRCC METS (88%) showed CAIX levels similar to those observed in the corresponding PT.

864 Smaller Prostate Size Is Independently Associated with Biochemical Recurrence in Gleason 7 Prostate Cancer

B Gershman, F Dong, FJ McGovern, NM Heney, WS McDougal, C-L Wu. Massachusetts General Hospital, Boston, MA.

Background: Prostate size is associated with a number of negative prognostic indicators. We evaluated the effect of prostate size on biochemical recurrence following radical prostatectomy.

Design: A retrospective review was conducted to identify patients with Gleason 6-10 prostate cancer who underwent radical retropubic prostatectomy at a single institution from 1993 - 1999. Patients were excluded if they received neoadjuvant therapy, had less than 8 weeks of follow-up, or had serum PSA that did not fall below 0.2 ng/ml post-operatively. Biochemical recurrence was defined as a PSA rise to 0.2 ng/ml or greater with a confirmatory value if available. Cox proportional hazards models were used to evaluate for association between variables and biochemical recurrence.

Results: A total of 877 patients underwent surgery with a mean follow-up of 7.5 ± 4.5 years (range 0.2 - 16.3). Mean age, PSA, and prostate weight were 61.0 ± 6.9 years, 7.3 ± 5.5 ng/ml, and 46.7 ± 19.1 grams, respectively. Gleason score was distributed as follows: 6 in 422 patients (48.1%), 7 in 372 patients (42.4%), and 8-10 in 83 patients (9.5%). Using univariate Cox proportional hazards models, older age, higher PSA, higher Gleason score, presence of pT3 or pT4 disease, positive margins, and smaller prostate weight were associated with biochemical recurrence (p < 0.05 for each). After stepwise addition of each variable in a multivariate Cox model, prostate weight lost significance only when Gleason score was included in the model. To assess for effect modification, multivariate Cox models were stratified by Gleason score (Table 1). In this analysis, prostate weight was associated with biochemical recurrence only for Gleason 7 disease, but margin status was associated with recurrence for Gleason 6 disease.

Cox proportional hazards model stratified by Gleason score

	Gleason 6		Gleason 7		Gleason 8-10	
	HR	p-value	HR	p-value	HR	p-value
Age (years)	1.01	0.657	1.02	0.091	0.993	0.778
PSA (ng/mL)	1.04	0.312	1.05	<0.001	1.02	0.485
Prostate weight (grams)	0.985	0.147	0.986	0.023	1.01	0.355
pT3+ vs pT2	0.675	0.410	1.42	0.076	1.39	0.302
Positive Margin	3.98	<0.001	1.43	0.054	0.779	0.406

Conclusions: Smaller prostate size is independently associated with biochemical recurrence for Gleason 7 disease while a positive surgical margin is associated with biochemical recurrence for Gleason 6 disease. These results have implications in the management of patients with small prostate glands.

865 Smaller Prostate Size Is Associated with Greater Volume of Disease at Prostatectomy

B Gershman, F Dong, DM Dahl, FJ McGovern, NM Heney, WS McDougal, C-L Wu. Massachusetts General Hospital, Boston, MA.

Background: Smaller prostate size is associated with a number of negative prognostic indicators including higher Gleason score and positive surgical margins. We hypothesized that this may be related to longer time to diagnosis for patients with smaller glands and investigated whether gland size is related to volume of disease at prostatectomy.

Design: A retrospective review was performed of patients with Gleason 6-10 prostate cancer who underwent radical prostatectomy from 2001 through 2010. Patients were identified from a prostatectomy tumor bank database. Univariate and multiple logistic regression were performed to determine association between prostate weight and volume of disease at prostatectomy. Number of quadrants with prostate cancer on surgical pathology was used as a surrogate for volume of disease.

Results: A total of 2054 patients underwent radical prostatectomy. Mean age, PSA, and prostate weight were 59.6 ± 6.6 years, 6.0 ± 4.7 ng/ml, and 45.5 ± 17.5 grams, respectively. Gleason score was 6 in 1055 patients (51.4%), 7 in 858 patients (41.8%), and 8-10 in 141 patients (6.9%). Number of quadrants with prostate cancer was distributed as follows: 1 quadrant in 274 patients (13.3%), 2 quadrants in 557 patients (27.1%), 3 quadrants in 464 patients (22.6%), and 4 quadrants in 759 (37.0%). On one-way analysis of variance, increasing number of quadrants with cancer was associated with decreasing prostate weight ($p < 0.001$). On univariate and multiple logistic regression (Table 1), smaller prostate weight, higher PSA, and higher Gleason score were associated with increasing volume of disease.

Multiple logistic regression of number of quadrants with prostate cancer. One quadrant with cancer is reference category for pairwise comparisons.

	OR for 2 vs 1 Quadrants	p-value	OR for 3 vs 1 Quadrants	p-value	OR for 4 vs 1 Quadrants	p-value
Age (years)	1.02	0.220	1.03	0.066	1.02	0.199
PSA (ng/ml)	1.08	0.001	1.09	0.003	1.16	< 0.001
Prostate weight (grams)	0.988	0.003	0.975	< 0.001	0.967	< 0.001
Gleason score						
6	ref		ref		ref	
7	1.27	0.184	1.93	< 0.001	2.64	< 0.001
8-10	1.77	0.150	2.53	0.019	3.87	< 0.001

Conclusions: Smaller prostate gland size is independently associated with increased volume of disease at prostatectomy. This supports the idea of a delay in diagnosis of prostate cancer for patients with smaller glands.

866 Can Quantitation and Sub-Categorization of Extraprostatic Extension (EPE) Predict Biochemical Recurrence (BCR)

JC Gomez-Gelvez, M Diaz-Insua, M Menon, N Gupta. Henry Ford Hospital, Detroit.

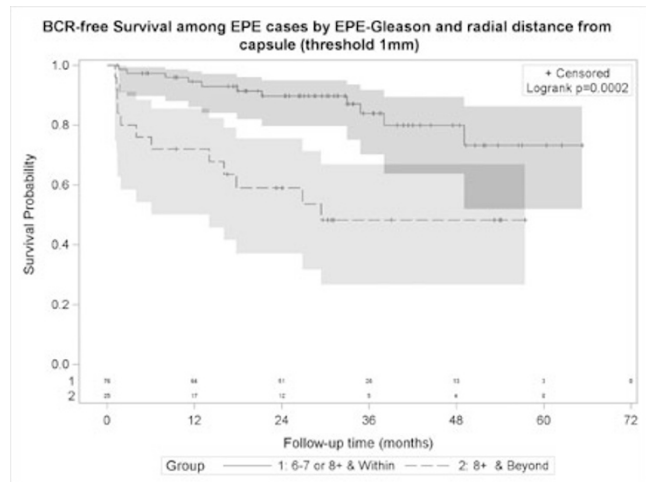
Background: EPE is defined as extension of tumor in to the periprostatic soft tissue. Prostatic capsular morphology is complex and varies from region to region. Pathologists use several different histologic criteria to diagnose EPE, but not all cases of EPE show progression of the disease. We aimed to quantify and assess the association of various EPE histologic features and BCR.

Design: Specimens from a matched cohort of 101 robotic-assisted radical prostatectomies with pT3aN0M0 performed between 2005-2008 at our institution were reviewed. EPE location, number of EPE foci, GS of EPE focus, radial extension (RE) and circumferential extension (CE) of EPE were noted. EPE was classified into three broad histologic categories (HC): 1. Tumor within adipose tissue (AT) or in fibroconnective tissue (FCT) at the level of AT (FAT) 2. Tumor in FCT beyond the prostatic muscular stroma but still not at the level of AT (FC) 3. Tumor beyond the normal contours of the prostate gland (BOC) in anterior region, base and bladder neck but not FAT or FC. Statistical significance of associations with BCR was assessed with conditional logistic regression.

Results: BCR was seen in 23 cases with 78 corresponding controls without BCR after a median follow up of 29 months. In univariate analysis, GS of EPE and RE with 1mm cutoff, were significantly (p -value<0.05) associated with BCR while CE classified into tertiles (4 and 10mm cutoff), and HC of EPE were marginally associated. Majority of BCR cases belonged to FAT (21 cases) and only 1 case of BCR was seen in FC.

EPE category	BCR	No BCR
FAT	21/79 (26.6)	58/79 (73.4)
BOC	1/4 (25.0)	3/4 (75.0)
FC	1/18 (5.6)	17/18 (94.4)

In a multivariable model, only RE remained an independent predictor of BCR (OR=8.37, 1.74-40.12). An interaction between GS of EPE and RE was also found predictive with low or high GS of EPE and RE within 1mm (group 1, BCR 11/76=14.5%) and high GS of EPE and RE beyond 1mm (group 2, BCR 12/25=48%; OR=5.46, 1.98-15.00). Corresponding Kaplan-Meier graph is shown below.



Conclusions: Combination of GS of EPE focus and RE may identify risk of BCR among patients with EPE. More samples are required to define more clearly the role of CE and HC of EPE on BCR.

867 Zonal Distribution of Neuroendocrine Cells (NECs) within Prostates (PR) with Prostatic Carcinoma (PCA)

Y Gong, SM Cavone, FU Garcia. Drexel University College of Medicine, Philadelphia, PA.

Background: NECs within the Pr gland have been well studied using normal Pr. However, NECs in patients with PCA have not been fully characterized. We studied the zonal distribution of NECs in Pr with carcinoma (Ca), within the Ca and in a cohort of metastatic cases. In addition, we determined if age, pre-operative PSA (pPSA) and proliferative index (PI) correlated with NECs.

Design: 42 cases treated with radical robotic prostatectomy were identified in the IRB approved database. Tissue microarrays (TMAs) were prepared using 1.5 mm needles. Two tissue cores from seminal vesicle (SV), central zone (CZ), transitional zone (TZ), peripheral zone (PZ) and the index Ca from whole mount paraffin blocks of each patient were used. These benign cores were obtained from at least two 10x fields away from Ca. The presence of NECs was identified with immunohistochemistry (IHC) for chromogranin A (CrgA), and synaptophysin (Syn). NECs were quantified per 100 epithelial cells. Co-expression of p63 with CrgA and Syn was also studied to assess stem cell phenotype. PI of Ca was studied with Ki-67 IHC and quantified with image analysis. Student t-test was used compare zonal distribution of NECs. In addition, fifteen cases with metastatic PCA were studied for CrgA and Syn IHC expression.

Results: Patient age ranged from 38 to 68 years old (<60, 28 cases and ≥60, 14 cases). PSA ranged from 0.8 to 37.9 ng/ml (<4, 6 cases, ≥4, 31 cases, and unknown 5 cases). CrgA revealed that NECs were highest in PZ (1.29 ± 1.78), followed by CZ (0.98 ± 1.24) and lowest in TZ (0.42 ± 0.67) ($p < 0.05$ between all zones). Similar values were obtained for Syn (Data not shown). NECs were similar in all zones regardless of age or pPSA. Co-IHC showed NECs did not express stem cell marker p63 in all three zones. Interestingly, NECs were not present in SV epithelium. In PCA, NECs were present in 17.9% of primary PCA, no difference was observed in different Gleason grades (G6 $0.49 \pm 1.2\%$, G7 $2.5 \pm 0.8\%$, and G8-9 $0.64 \pm 1.9\%$). The PI of PCA with NECs was $2.6 \pm 1.6\%$, PI of PCA without NECs was $3.5 \pm 4.6\%$ and there was no significant difference ($p=0.62$). Significantly higher NECs (33.3%) were present in metastatic PCA.

Conclusions: PZ of Pr with PCA had the highest NECs, followed by CZ and TZ. This is different from previous studies in which the TZ has the highest. Increasing age and pPSA did not affect zonal distribution of NECs. Primary PCA with NECs seems to have lower PI suggesting an inhibitory role of NECs. NECs did not exhibit stem cell phenotype. Metastatic PCA had higher NECs compared to primary PCA.

868 Dysregulation of mTOR Pathway in Plasmacytoid Variant of Urothelial Carcinoma of the Urinary Bladder

ND Gonzalez-Roibon, A Chaux, AO Osunkoya, T Al-Hussain, J Hicks, JI Epstein, GJ Netto. The Johns Hopkins University SOM, Baltimore, MD; Emory University SOM, Atlanta, GA.

Background: Mammalian target of rapamycin (mTOR) pathway plays an important role in cell growth, migration, and proliferation. mTOR pathway dysregulation has been linked to oncogenesis in several malignancies, including conventional urothelial carcinoma of bladder. Several antineoplastic agents targeting mTOR pathway are currently available. Plasmacytoid variant of urothelial carcinoma (UC) is a rare but aggressive variant of bladder cancer. The current study assesses mTOR pathway status as well as c-myc and p27 expression, two markers known to interact with this pathway.

Design: Nineteen cases of plasmacytoid UC were retrieved from the surgical pathology files of our 2 institutions, including 12 cases from the consultation service of 2 of the authors. Whole sections were evaluated for immunopositivity of PTEN, phosphorylated mTOR (phos-mTOR), phosphorylated AKT (phos-AKT), phosphorylated S6 (phos-S6), c-myc, and p27. Antibody sources and IHC parameters were as previously described (Cancer 2010;116:5517). Cases with >10% loss of cytoplasmic PTEN expression were considered to show loss of PTEN. For the remaining markers, expression intensity (0

to 3+) and extent (0%–100%) was evaluated in each tumor. An H-Score (Σ intensity X percentage) was calculated. Pairwise correlation coefficients (CC) were estimated to assess relationship among markers expression.

Results: PTEN loss was encountered in 5 cases (28%) of plasmacytoid UC. In contrast, high levels of phos-mTOR (mean 218, range 97–285), phos-AKT (mean 211, range 67–295) and phos-S6 (mean 248, range 164–298) were found. Low expression of c-myc (mean 51, range 0–223) and of p27 (mean 61, range 0–225) were noted. phos-AKT expression positively correlated with phos-mTOR (CC = 0.54, P = .02), phos-S6 expression negatively correlated with c-myc expression (CC = -0.67, P < .005).

Conclusions: We found dysregulation of the mTOR pathway in plasmacytoid urothelial carcinoma of the urinary bladder. These results suggest that the use of mTOR inhibitors might be beneficial for patients with this aggressive variant of urothelial carcinoma.

869 ERG Immunorexpression Does Not Predict Risk of Recurrence after Prostatectomy for Clinically-Localized Prostate Cancer

ND Gonzalez-Roibon, S Peskoe, A Chau, R Albadine, J Hicks, A De Marzo, EA Platz, GJ Netto. The Johns Hopkins University SOM, Baltimore, MD; The Johns Hopkins Bloomberg School of Public Health, Baltimore, MD.

Background: We previously demonstrated that *TMPRSS2-ERG* fusion detected by FISH does not predict recurrence of localized prostate cancer after prostatectomy. We also demonstrated that ERG immunorexpression is a suitable surrogate for *ERG* fusion. Herein we evaluate the role of ERG protein immunorexpression as a predictor of recurrence in clinically-localized prostate cancer, independent of known clinicopathological factors.

Design: A nested case-control study was conducted in patients who underwent radical prostatectomy for clinically-localized prostate cancer at our institution between 1993 and 2004. The study included tumors from 444 cases (recurrence) and 444 controls (nonrecurrence). Patients were matched for age, race, Gleason sum, and pathologic stage. Cases were defined by the presence of biochemical recurrence, metastasis, or prostate cancer death. Triplicate tissue cores were used to construct the 16 tissue microarrays (TMAs) set. ERG protein nuclear expression was evaluated using immunohistochemistry as previously described (Am J Surg Pathol 2011; 35:1014). In each tumor spot, an H-score was calculated as the sum of the product of nuclear staining intensity (0 to 3+) and the extent (percentage). ERG expression for each patient was classified based on 1) the patient having any positive TMA spot, and 2) the mean H score across a patient's TMA spots. The odds ratio (OR) of recurrence was estimated using conditional logistic regression to take into account the matching factors and to adjust for year of surgery, preoperative serum PSA level, and status of surgical margins.

Results: After multivariable adjustment, 48.5% of the recurrence cases and 48.3% of the nonrecurrence controls had ERG expression in any TMA spot (P = 0.97). Further, no association was found between ERG positivity (OR 0.87; 95% CI 0.60, 1.25; P = 0.45) or the extent of ERG staining (versus no staining; 0 < H score < 165: OR 0.70, 95% CI 0.44, 1.12; H score \geq 165: OR 1.04, 95% CI 0.67, 1.62) and risk of recurrence.

Conclusions: Prostate tumor immunohistochemical expression of ERG protein did not predict recurrence in patients treated by radical prostatectomy for clinically-localized disease.

870 Histologic Findings on Prostate Needle Core Biopsies Following Cryotherapy as Monotherapy for Prostatic Adenocarcinoma

CE Gooden, CK Kovach, PT Nieh, AO Osunkoya. Emory University School of Medicine, Atlanta.

Background: The histologic features seen in the prostate following cryotherapy can be highly variable. However, most previous studies were performed on specimens following salvage cryotherapy which introduces additional confounding variables of the histologic changes after other treatment modalities. We examined prostate needle core biopsies from a cohort of patients following cryotherapy as monotherapy for prostatic adenocarcinoma (Pca), to evaluate the true spectrum of morphologic changes in the prostate.

Design: A search was made through the surgical pathology and expert consultation files of the senior author for prostate needle core biopsies following cryotherapy. Cases that had prior radiation therapy or androgen deprivation therapy were excluded from the study. The Gleason scores from the original needle core biopsies were documented. All histologic findings from the post-cryotherapy needle core biopsies including time interval from therapy to repeat biopsy were also documented.

Results: 30 cases were identified. Average patient age was 69 years (range: 51–81 years), and the average time interval between cryotherapy and repeat biopsy was 19.2 months (range: 2–60 months). The original Gleason scores were as follows: 3+3=6 in 14/30 cases (46%), 3+4=7 in 8/30 cases (27%), 4+3=7 in 2/30 cases (7%), 4+4=8 in 3/30 cases (10%), 4+5=9 in 2/30 cases (7%), and 5+4=9 in 1/30 cases (3%). Post cryotherapy, 11/30 cases had recurrent/residual Pca which showed no therapy related changes, similar to the residual benign glands. Gleason scores were higher in 5/11 cases (46%), same in 4/11 cases (36%) and lower in 2/11 cases (18%). Additional histologic findings were as follows: chronic inflammation 24/30 cases (80%), myxoid stromal change 24/30 cases (80%), hemosiderin pigment in the stroma 21/30 cases (70%), stromal fibrosis 9/30 cases (30%), necrosis 8/30 cases (27%), calcifications 6/30 cases (20%), acute inflammation 5/30 cases (17%), granulomas 4/30 cases (13%), hemorrhage 4/30 cases (13%), vessel wall thickening and prominent endothelial cells 3/30 cases (10%), squamous metaplasia 3/30 cases (10%).

Conclusions: This is one of the first studies to review the histologic findings following cryotherapy as monotherapy for Pca. Unlike other non-surgical therapeutic modalities, cases with recurrent/residual Pca and benign glands showed therapy related changes predominantly involving the stroma. It is therefore conceivable that benign or malignant prostatic glands are either completely destroyed during cryotherapy, or left unaltered if not in the direct field of cryoablation.

871 Correlation between ERG Immunohistochemical Expression and Radiation Response in Prostate Cancer

A Gopalan, Y Chen, H Al-Ahmadie, S Fine, J Eastham, S Tickoo, V Reuter. Memorial Sloan-Kettering Cancer Center, New York, NY.

Background: *TMPRSS2-ERG* gene fusions occur in about 50% of prostate cancers with resultant overexpression of a protooncogene, ERG. It is now known that ERG overexpression, concomitantly with other genetic alterations, leads to accelerated prostate carcinogenesis. The prognostic significance of this overexpression, however, is still controversial, and targeting the gene therapeutically has proved difficult. A recent report has suggested that overexpression of the *TMPRSS2-ERG* fusion product induces DNA damage in PC3 cell lines, which implies increased radiosensitivity. Another recent study has shown that expression of *TMPRSS2-ERG* fusion in PC3 cells caused persistent unrepaired DNA breaks and thus increased radiosensitivity. Further, they showed that in DU145 cells the response differed based on fusion type: type 3 fusions did not alter radiosensitivity while type 6 fusions increased radioresistance. There is no published data on ERG expression in irradiated human prostate cancer. Our aim was to investigate the utility of the ERG antibody as a biomarker in residual/recurrent prostate cancer after radiation therapy.

Design: ERG IHC (rabbit mAb; clone EPR3864; Epitomics; 1:250 dilution) was performed on a TMA consisting of gradable tumors from 38 patients with prostate cancer who had failed radiation treatment and subsequently undergone salvage radical prostatectomy. The control group was a cohort of 521 patients who underwent radical prostatectomy for clinically localized disease without prior radiation therapy, where we had previously determined *TMPRSS2-ERG* fusion status by a FISH assay.

Results: Of the 38 cases represented in the TMA, 36 were evaluable. ERG antibody was positive in 17 (47%) and negative in 19 (53%). In the control non-irradiated group, 42% of the population had *TMPRSS2-ERG* fusion. There was no difference in pathologic stage between ERG positive and negative cancers in the post radiation cohort.

Conclusions: 1. The incidence of *TMPRSS2-ERG* fusion is similar in prostate cancers without prior radiation therapy and cancers which failed radiation therapy, thereby suggesting that ERG negative tumors were not preferentially selected among radiation-resistant tumors in this cohort.

2. ERG positive and negative irradiated prostate cancers had a similar distribution of pathologic stage.

3. Further studies, including interaction of the fusion with other functional cofactors, are necessary to validate the assessment of the fusion as a potential biomarker of treatment response.

872 ERG vs. Alpha-Methylacyl-CoA Racemase Expression in Histologic Variants of Adenocarcinoma of the Prostate

S Gottipati, J Hudson, P Humphrey. Washington University, Saint Louis, MO.

Background: The utility of the widely used p63/34 β E12/alpha-methylacyl-CoA racemase (AMACR) triple stain immunohistochemistry (IHC) can be limited in some variants of prostate adenocarcinoma (PC) including atrophic, foamy gland and pseudohyperplastic PC, where almost a third of these variants do not express AMACR. The recent discovery of *TMPRSS2: ERG* gene rearrangement in PC and the subsequent development of a highly specific antibody to ERG have generated considerable interest in ERG IHC as an aid in detecting prostate cancers. However, added diagnostic value of ERG expression beyond AMACR expression has not been addressed. The aim of the study was to investigate whether ERG IHC can provide an advantage in diagnosis of these deceptively benign-appearing variants.

Design: 97 radical prostatectomy cases of variant PC, including atrophic, foamy gland, and pseudohyperplastic (PH) adenocarcinomas were selected from our files. All cases had both variant adenocarcinoma and usual acinar adenocarcinoma components. H&E, triple stain with AMACR, and ERG IHC stains were obtained. Both the intensity (0-3) and the percentage of glands stained (1-4) were scored, generating an IHC score ranging from 0-12 for both ERG and AMACR expression. We searched for areas that were either completely negative or stained weakly for AMACR and compared these foci with ERG IHC to assess for difference in comparative staining.

Results: 50 of the 97 cases were positive in ERG IHC. Both ERG and AMACR antibodies marked usual acinar adenocarcinoma with greater intensity as compared to the variants. 15 cases had foci which were completely negative for AMACR including 12 foamy glands, 6 atrophic, 3 pseudohyperplastic, and 4 usual acinar adenocarcinoma foci; these foci were strongly positive with ERG. 16 cases showed significantly weaker staining with AMACR as compared to ERG in foci of variants and usual acinar adenocarcinoma of which there were 10 foci each of usual acinar and foamy glands and 5 foci of atrophic glands. The IHC scores of ERG/AMACR in these 31 cases was 11.6/8.3 for usual acinar, 11.2/6.2 for atrophic, 10.8/6.8 for microcystic, and 9.9/5.2 for foamy gland foci. In 2 cases AMACR was positive in ERG negative foci, which included one focus each of usual acinar and foamy gland PC.

Conclusions: ERG immunostains provide added value beyond AMACR immunostains in a substantial number of cases of prostatic adenocarcinoma with atrophic, foamy gland, and pseudohyperplastic variant histological appearance, that can be deceptively benign appearing.

873 Immunohistochemical Evaluation of *TMPRSS2-ERG* Gene Fusion in Adenosis of the Prostate

WM Green, JL Hicks, A DeMarzo, JJ Epstein. The Johns Hopkins Hospital, Baltimore.

Background: Adenosis (atypical adenomatous hyperplasia) is a benign lesion that morphologically mimics prostate adenocarcinoma. To date, there is no convincing evidence that adenosis is a precursor lesion to prostate adenocarcinoma, although the relationship between these two lesions is still debated. The *TMPRSS2-ERG* fusion has recently been identified as a common chromosomal rearrangement which occurs early

in the development of invasive adenocarcinoma of the prostate. This fusion is present in 50% of adenocarcinoma and 20% of high-grade prostatic intraepithelial lesions. Until recently, FISH was the only method available to detect these rearrangements. There is near perfect association between the ERG gene rearrangements and expression of truncated ERG protein. A specific anti-ERG antibody is now available that has 95.7% sensitivity and 96.5% specificity for detecting ERG protein expression, thus serving as a useful marker for ERG rearrangements. Here, we utilized this antibody to further evaluate the relationship between adenocarcinoma and adenosis of the prostate.

Design: We performed a search of the JHH pathology database to identify cases of prostate biopsies, transurethral resections of the prostate (TURP), and radical prostatectomies which included adenosis in the final diagnosis. Slides were immunostained for ERG. Quality control was assessed by examining endogenous endothelial cells as an internal positive control. The pattern of ERG staining was then assessed in adenosis.

Results: In this preliminary study, 26 cases including 15 (58%) biopsies, 7 (27%) TURPs, and 4 (15%) radical prostatectomies were evaluated by IHC for ERG expression. The quality of the stain was adequate in 100% of the cases as evidenced by staining of the positive internal controls. Although we confirmed the presence of adenosis in all cases, no foci of adenosis were positive for ERG protein expression.

Conclusions: In this preliminary study, 26 cases of adenosis were indirectly evaluated for TMPRSS2-ERG rearrangement by ERG immunostaining and none of these cases showed ERG protein expression. We are in the process of gathering additional consult cases of adenosis for IHC analysis of ERG expression. If our initial findings corroborate that ERG expression is not observed in adenosis, it supports the notion that adenosis is not a precursor lesion of adenocarcinoma. Moreover, these results suggest that positive IHC for ERG could be a useful marker to exclude a diagnosis of adenosis.

874 Utilization of a TFE3 Break-Apart FISH Assay in a Renal Tumor Consultation Service

WM Green, GJ Netto, C Griffin, L Morsberger, PB Illei, X Zhou, P Argani. The Johns Hopkins Hospital, Baltimore, MD.

Background: Xp11 translocation Renal Cell Carcinomas (RCC) are characterized by chromosome translocations involving the Xp11.2 breakpoint, resulting in gene fusions involving the *TFE3* transcription factor. In archival material, the diagnosis can often be confirmed by TFE3 immunohistochemistry (IHC), but variable fixation (especially prevalent in consultation material) can lead to equivocal results. A *TFE3* break-apart FISH assay has been developed to detect *TFE3* gene rearrangements; however, the utility of this assay in a renal tumor consultation practice has not been examined.

Design: We reviewed our renal tumor consultation cases which were sent to rule in or rule out Xp11 translocation RCC. *TFE3* FISH results were evaluated in the context of other clinical, morphologic, and IHC features of the cases, including TFE3 IHC.

Results: 62 cases were submitted to rule in or rule out Xp11 translocation RCC. 22 were positive for *TFE3* rearrangements by FISH, including 21 Xp11 translocation RCC and 1 melanotic Xp11 translocation renal cancer. Patients ranged from 6 to 67 years of age (mean=28.9; median=27). Novel or distinctive morphologic features of these cases included extensive cystic change simulating multilocular cystic RCC (2 cases), sarcomatoid transformation (2 cases), trabecular architecture mimicking a carcinoid tumor (1 case), and focal desmin and diffuse racemase immunoreactivity (1 case each). 16 of the 21 FISH-positive cases were unequivocally (3+) positive for TFE3 by IHC, but 4 were equivocal and 1 was negative. Of the 40 other cases, which were negative by both FISH and IHC, 10 could be classified as clear cell RCC, 3 as clear cell papillary RCC, 3 as papillary RCC, 2 as RCC in the setting of tuberous sclerosis, and 1 as chromophobe RCC, while 21 remained unclassified. Of these 21 cases, 6 were morphologically indistinguishable from Xp11 translocation RCC. All 6 of the latter cases were TFE3 negative by IHC, and 4 of 6 were diffusely immunoreactive for Cathepsin K (an otherwise specific marker of translocation RCC).

Conclusions: Utilizing a *TFE3* break-apart FISH assay, we identify 21 novel genetically confirmed Xp11 translocation RCC. These results expand the morphologic and immunohistochemical spectrum of these neoplasms. *TFE3* FISH resolves cases with equivocal TFE3 IHC results. While many cases in the differential diagnosis of Xp11 translocation RCC can be confidently reclassified into other existing RCC categories, a subset of cases overlaps greatly with Xp11 translocation RCC, and may represent a novel translocation RCC subtype in which not *TFE3* but a related gene is implicated.

875 Determination of Intratumoral Heterogeneity for PTEN Loss in Prostate Cancer by IHC for PTEN and ERG

B Gumuskaya Ocal, B Gurel, JL Hicks, T Lotan, AM De Marzo. Johns Hopkins, Baltimore, MD.

Background: The determination of tumor heterogeneity for key oncogenic factors is important for understanding multi-step tumor progression. ERG rearrangements and PTEN loss are two of the most common genetic alterations in prostate cancer. Heterogeneity of PTEN loss has been shown to be common (~46%) in primary prostate cancer, even within tumor foci with homogeneous ERG rearrangements as assessed by FISH (BJUI 107:477, 2011), suggesting that PTEN loss generally occurs after ETS family member rearrangements. Yet, the determination of ERG and PTEN status using interphase FISH assays is cumbersome. ERG protein overexpression, as assessed by IHC, is highly associated with ERG gene rearrangement in prostate cancer. We have recently validated an IHC assay to detect PTEN protein loss in tissue samples that is highly sensitive for detecting either heterozygous and homozygous PTEN deletions as assessed by genomic means (Lotan et al., Clin Cancer Res. 2011 Aug 30). We used IHC to determine ERG and PTEN status to calculate the fraction of cases with homogeneous/heterogeneous ERG and PTEN staining in a given tumor.

Design: Using a single standard tissue section from the index tumor from radical prostatectomies (N= 68), enriched for relatively high grade (53% Gleason 7, 21%

Gleason 8-9) and stage tumors, we examined ERG (Biocare Medical) and PTEN (Cell signaling) status by IHC. IHC for ERG was categorized as positive or negative in a given tumor focus. PTEN loss was assessed as a dichotomous variable as either present or markedly decreased/absent. We determined whether ERG or PTEN staining was homogeneous or heterogeneous in a given tumor.

Results: 59% (N=40) of cases showed ERG positivity, with 7% of these (N=3/40) cases showing intratumoral ERG heterogeneity. 63% (N=43/68) of cases showed PTEN loss, and of these, 67% (N=29/43) showed heterogeneous loss. In ERG homogeneously positive cases, any PTEN loss occurred in 70% (N=26/37) of cases, and of these, 65% (N=17/26) showed heterogeneous loss. In ERG negative tumors, 58% (N=16/28) showed PTEN loss, and of these, 69% (N=11/16) showed heterogeneous PTEN loss. ERG expression did not correlate with Gleason score or stage, while any PTEN loss correlated with increased Gleason score (P=0.017) and pathological stage (P<0.001).

Conclusions: These results support the concept that in most cases of PTEN loss, the loss commences as a subclonal event within an established prostatic carcinoma clone. The combination of ERG and PTEN IHC staining can be used as a simple test to ascertain PTEN status within a given prostate cancer in either a research or clinical setting.

876 ERG Protein Expression and ERG Gene Rearrangement in Prostate Cancers of Different Zonal Origin

CC Guo, MP Mikulasovich, MT Deavers, P Troncoso, BA Czerniak. University of Texas MD Anderson Cancer Center, Houston, TX.

Background: Recent studies have demonstrated that most prostate cancers carry the *TMPRSS2-ERG* fusion gene. To evaluate the utility of ERG immunohistochemistry in the analysis of this gene fusion, we compared ERG protein expression with ERG gene rearrangement in prostate cancers of different zonal origin.

Design: We selected 22 radical prostatectomy specimens with multifocal prostatic adenocarcinoma from our pathology files. The ERG protein expression was evaluated by immunohistochemistry (IHC) using the ERG (9 FY) antibody (Biocare Medical, Concord, CA), and the ERG gene rearrangement was evaluated by fluorescence in situ hybridization (FISH) using ERG break-apart probes.

Results: The mean age of patients was 58.5 years (range 46-71 years). Two separate tumor foci in each RP specimen, one in the peripheral zone (PZ) and one in the transition zone (TZ), were analyzed. The Gleason scores of the PZ tumor foci ranged from 6(3+3) to 7 (4+3) and the tumor volume ranged from 0.3 to 3.0 cm³ (mean, 1.4 cm³). The Gleason scores of the TZ tumor foci ranged from 5(3+2) to 7 (4+3) and the tumor volume ranged from 0.5 to 12.8 cm³ (mean, 4.1 cm³). On FISH analysis, 11 of the 22 PZ tumor foci showed rearrangement of the ERG gene, including deletion (n=8) and translocation (n=3), but none of the TZ foci had rearrangement. On IHC analysis, all 11 PZ tumor foci with the ERG rearrangement showed positive immunoreactivity for ERG in nuclei, while all tumor foci without the ERG rearrangement (n=33) showed negative immunoreactivity.

Conclusions: Our study demonstrates an excellent correlation between ERG protein expression and ERG gene rearrangement in prostatic adenocarcinoma, suggesting that the ERG IHC may be an effective tool to evaluate the *TMPRSS2-ERG* gene fusion in prostate cancer. Although we did not find ERG protein expression in the TZ tumor foci, the number of cases in our study was small. Other studies have reported that prostate cancers of TZ origin may also carry the ERG gene rearrangement but the frequency is lower than that in prostate cancers of PZ origin.

877 Argininosuccinate Synthetase Deficiency as a Possible Therapeutic Indicator for Pegylated Arginine Deiminase (ADI-PEG20) Therapy in Bladder Cancer

S Gupta, JS Bomalaski, PD Carver, DE Hansel. Cleveland Clinic, Cleveland; Polaris Group, San Diego.

Background: Deletions of chromosome 9 have been commonly identified in urothelial cancer (UCC). A previous study had identified microsatellite instability in the argininosuccinate synthetase (ASS1) gene locus (on chromosome 9), although the significance of this finding was unclear. ASS1 plays a critical role in the biosynthesis of arginine from citrulline and a deficiency of ASS1 leads to arginine auxotrophy. This can be further exacerbated by administration of the pegylated form of arginine deiminase (ADI-PEG20), which has been shown to carry low toxicity in phase I/II clinical trials. Thus, reduced levels of ASS1 can serve as an indicator for ADI-PEG20-responsive tumors. We therefore evaluated the expression of ASS1 in bladder cancer variants to explore the possibility of expanding therapeutic avenues for this population.

Design: Formalin fixed, paraffin embedded samples of normal urothelium (n=19), conventional UCC (n=148), and other variants including the micropapillary variant of UCC (n=17), small cell carcinoma (n=19), squamous cell carcinoma (n=39) and adenocarcinoma (n=19), were used in the construction of tissue microarrays (TMAs). TMAs were immunostained for ASS1 and scored based on the intensity of stain (0-3+; high staining was considered 2-3+). The results were then correlated with various parameters such as age at diagnosis, sex, race and pathologic staging.

Results: Compared to normal urothelium where 68.4% of the cases showed high expression of ASS, conventional UCCs demonstrated lower levels of staining (41% of the non-metastatic subset; n=61 and 52.8% of the metastatic subset; n=87). Surprisingly, the paired lymph node metastases from the latter group showed high staining in only 31.5% (n=38) of the patients. High levels of ASS1 immunoreactivity were maintained in the micropapillary variant of UCC (76.4% of cases) and pure bladder adenocarcinoma (84.2%). In contrast, both pure small cell and squamous cell carcinoma of the bladder demonstrated marked reduction in ASS1 expression: only 26.3% of small cell carcinoma specimens and 10.2% of the squamous cell carcinoma specimens had high expression of ASS1, suggesting these two subtypes of bladder cancer could potentially respond to ADI-PEG20 therapy.

Conclusions: ADI-PEG20 represents a potentially exciting new therapeutic agent for metastatic conventional UCC, small cell carcinoma and squamous cell carcinoma. This is especially relevant as limited therapies are currently available for these less common forms of bladder cancer.

878 Decreased Stromal Androgen Receptor Expression in African-Americans with Prostate Cancer

CS Hale, MX Kong, Q Ren, Y Li, S Krauter, L Chiriboga, I Osman, V Reuter, R Wiczorek, J Melamed, P Lee. NYU Langone Medical Center, New York; Memorial-Sloan Kettering Cancer Center, New York.

Background: African-Americans (AA) have prostate cancer (PCa) mortality 2-3 times that of Caucasians (CA). The basis for this disparity is not fully understood; however, data suggest molecular changes in different ethnicities are responsible. Expression of regulatory molecules, such as epithelial growth factor receptor, has been found to vary significantly between racial groups. Androgen receptor (AR) expression is critical for PCa tumorigenesis and progression. The relationship between race and stromal androgen receptor expression has not previously been analyzed.

Design: Immunohistochemical double staining for AR and smooth muscle actin was performed on a tissue microarray containing 148 cases of prostate cancer (known race n=31 for AA and n=63 for CA). AR positivity in fibroblasts was quantified as a percentage. The histologic pattern of smooth muscle and fibroblasts surrounding benign and cancerous areas was evaluated semiquantitatively.

Results: Earlier *in vitro* co-culture experiments with cancer epithelial (PC3 and LNCaP) and stromal (either AR positive or AR negative) cells have indicated that stromal AR inhibits PCa growth. Moreover, stromal AR has been found to be decreased in PCa. In the present study we find stromal AR expression to be 75% lower in cancer, irrespective of race (16.4±11.5%, n=107, versus 4.7±0.8%, n=148, P < 0.0001). Among AA men with PCa, the percent of AR-positive stromal cells is 83% lower (1.5±0.5%, n=31) than in CA men with PCa (8.5±1.7%, n=63, P < 0.0002). As additional evidence of stromal-epithelial interaction, we observe immediate juxtaposition of continuous smooth muscle fibers around a high percentage of benign prostate glands (64±3.0%, n=103). Continuous smooth muscle is less prevalent around cancerous glands (46±2.4%, n=141, P < 0.0001), with smooth muscle admixed with an intervening fibroblastic component. Lack of continuous and immediate juxtaposition of smooth muscle fibers is more pronounced in AA men with PCa (39±4.4%, n=47) relative to CA men with PCa (54±5%, n=39, P < 0.0229).

Conclusions: Stromal-epithelial interaction is an important factor in progression of PCa. Decreased stromal AR expression may contribute to African-Americans' poorer clinical outcomes. This is supported by evidence that stromal AR inhibits prostate cancer growth. In the era of personalized medicine, understanding differences in PCa biology will aid selection of more targeted therapies.

879 Hemangioma in Kidney with End-Stage Renal Disease: A Novel Association

SL Haley, ON Kryvenko, M Aron, SS Shen, JI Epstein, NS Gupta, M Amin, LD Trung. The Methodist Hospital, Houston, TX; Cornell University, New York, NY; Cedars Sinai Medical Center, Los Angeles, CA; Henry Ford Medical Center, Detroit, MI; The Johns Hopkins University, Baltimore, MD.

Background: Tumors often develop in kidneys with end-stage renal disease (ESRD), almost all of which are epithelial neoplasms. Renal hemangioma associated with ESRD has been recently described, but this condition remains largely unknown.

Design: Hemangiomas in 10 nephrectomy specimens from 8 patients from three institutions were studied.

Results: All 8 patients had ESRD due to lupus nephritis (3), hypertension (2), diabetes (1), focal segmental glomerulosclerosis (1), or unknown cause (1). Seven patients were on dialysis, from 1.1 to 31 years. Hemangiomas were detected on surveillance renal imaging (8 kidneys) or incidentally (in 1 kidney with a mass on CT suspicious for renal cell carcinoma (RCC); and in 1 kidney with imaging features of acquired cystic kidney disease [ACK]). Symptoms directly related to hemangioma were not seen in any patient. Bilateral hemangiomas were noted in two patients. Tumors measured 0.1 to 2.8 cm, significantly smaller than their imaging sizes. Hemangiomas appeared as a single mass in 7 kidneys; two masses (one intrarenal and one in sinus fat) in 1; at least four intrarenal masses in 1; and multiple masses throughout the kidney, sinus fat, and hilar lymph node in 1. Almost all tumors were in the medulla and often abutted on sinus fat. All tumor masses demonstrated isolated or interconnected capillary-sized vascular channels lined by a single layer of benign cuboidal CD34+, CD31+, D2-40 - endothelial cells, separated by a cellular stroma that molded to the contour of the vascular channels and contained smooth muscle actin positive cells. Most had no capsule, and none demonstrated necrosis or increased mitoses. Extramedullary hematopoiesis was noted in each tumor. The background tissue showed changes of ESRD in all 10 kidneys, ACK in 5, ACK-related inflammatory/hemorrhagic masses in 2, RCCs in 2, and incidental papillary adenomas in 1. There was no recurrence at 1-36 months of follow-up.

Conclusions: Renal hemangioma may represent a novel type of neoplasm that develops against the background of ESRD, with or without ACK. It has a uniform and distinctive morphology amenable to diagnostic accuracy. Its pathogenesis and the basis for its recent emergence remain unknown, but its characteristic clinicopathologic profile points to ESRD-related angiogenic factors affecting a localized vascular bed in the kidney with ESRD.

880 Predictors of Insignificant Prostate Cancer on Radical Prostatectomy (RP) Following Disease Progression during Active Surveillance (AS)

JS Han, AD Toll, A Amin, B Carter, JI Epstein. The Johns Hopkins Hospital, Baltimore.

Background: Since 1996, >800 men have enrolled in our AS program. Criteria for AS are: 1) biopsy (bx) with no Gleason pattern 4 or 5; 2) no core >50% involvement; 3) <3 positive cores on >12 core sampling; and 4) PSA density <0.15. Men who show worse bx findings regardless of PSA measurements on annual repeat bx are considered to have failed AS. However, some men on follow-up who fail bx criteria have "insignificant prostate cancer" on RP defined as: 1) Organ confined; 2) Dominant nodule <0.5 cm³; and 3) no Gleason pattern 4 or 5.

Design: 67 men who on annual follow-up bx failed bx criteria and subsequently underwent RP were identified. Variables evaluated included at the time of initial and failed bx: PSA, PSA density, free/total PSA, maximum % of cancer per core, extent ASAP & HGPIN, and no. of positive cores along with any interval negative biopsies.

Results: Median age at RP was 66.4 (43.4-75.0). Mean time between first bx and RP was 30.3 mos., with an average of 3 bx (2-9). Findings at RP were: non-organ confined [15 (22.4%)]; margins + [2 (3%)]; SV + [1 (1.5%)]; Gleason score 6 [30 (44.8%)]; GS 3+4=7 [(22 (32.8%))]; GS 4+3=7 [13 (19.4%)]; GS 9 [2 (3%)]. Mean and median dominant tumor nodule volume (DTV) at RP was 0.56 cc and 0.32 cc, respectively (0.01 cc-2.93 cc). 19 (28.4%) had clinically insignificant cancer at RP. DTV correlated with with PSA & maximum % cancer per core at time of failed criteria. With PSA <4 and maximum core involvement <50%, 7/8 patients (87.5%) had clinically insignificant cancer at RP vs. 5/19 (26.3%) men with PSA ≥4 ng/ml & maximum core involvement ≥50%. A subgroup analysis was done of patients (n=37) who failed AS criteria without Gleason pattern 4/5 on failed bx, as men with Gleason pattern 4/5 all have significant cancer by definition. 16/37 (43.2%) showed insignificant cancer at RP. PSA at diagnosis was lower in men with insignificant cancer (3.68 ng/ml) vs. significant cancer (5.37 ng/ml) (p=0.0003). With PSA at diagnosis <4 ng/ml, 10/11 (90.9%) men showed insignificant cancer at RP vs. 6/26 (23.1%) men with PSA at diagnosis ≥4 ng/ml (p=0.0002).

Conclusions: Most men who fail bx criteria while on AS have significant disease at RP justifying their treatment. However, about 1/4 of these men are overtreated with insignificant cancer in their RP. Biopsy and PSA data both at the time of initial bx and at time of failed bx criteria can help stratify men who are more likely to have insignificant cancer despite failing AS biopsy criteria. These men may be candidates to stay on AS without definitive treatment.

881 Potential Utility of GATA3 Immunorexpression and HPV Status in the Differential Diagnosis of Urothelial vs Squamous Cell Carcinomas of Distal Penile Urethra

JS Han, GJ Netto, S Lee, N Gonzalez-Roibon, H Ross, R Sharma, AL Cubilla, A Chaux.

Johns Hopkins University, Baltimore, MD; Instituto de Patologia e Investigacion, Asuncion, Paraguay.

Background: Squamous cell carcinoma (SCC) and urothelial carcinoma (UC) occur as primary tumors of the distal penile urethra, possibly reflecting histogenesis from the native squamous or urothelial mucosa at this site. As there may be a considerable morphologic overlap between the two tumor types, the utility of GATA3, a transcription factor that has been recently used as a marker of urothelial differentiation, and human papillomavirus (HPV) status was evaluated in the differential diagnosis of the two entities.

Design: We retrieved 6 cases originally classified as primary urothelial carcinoma of distal urethra from our surgical pathology archives. All H&E sections were retrieved and reviewed by 2 urologic pathologists on the study. Medical records were also reviewed. Extension from other urologic sites was clinically excluded in all cases. Whole routine representative sections were stained for GATA3 (BioCare, GATA3 clone L50-823) using standard immunohistochemistry techniques. In situ hybridization for high-risk HPV (HR-HPV) was also performed in all cases. In addition, GATA3 immunorexpression was evaluated in a tissue microarray (TMA) containing 38 cases of SCC of the penile glans.

Results: In the TMA section, all 38 cases of penile glans SCC were negative for GATA3. Based on the morphologic review, GATA3 immunohistochemistry, and HR-HPV in situ hybridization, the 6 distal urethral tumors were reclassified as shown in Table 1.

GATA3 and HR-HPV in 6 distal urethral carcinomas originally diagnosed as UC

Case No.	Age	Reclassified Diagnosis	GATA3	HR-HPV
1	48	Basaloid SCC	Negative	Positive
2	69	Invasive UC	Positive	Negative
3	70	Invasive UC	Positive	Negative
4	73	Invasive UC	Positive	Negative
5	60	Warty-Basaloid SCC	Negative	Negative
6	73	Warty-Basaloid SCC*	Negative	Positive

* A noninvasive UC component was positive for GATA3 and negative for HR-HPV

The original diagnosis of invasive urothelial carcinoma was confirmed in 3 cases. The 3 additional cases that were reclassified as SCCs were of basaloid or warty-basaloid subtype. One of the latter revealed a noninvasive component that displayed urothelial differentiation, as suggested by its GATA3 positivity and lack of HR-HPV.

Conclusions: We found no expression of GATA3 in bona fide penile glans SCC. In difficult distal urethral carcinoma tumors displaying ambiguous urothelial/squamous features, GATA3 and HR-HPV detection may aid in differentiating SCC from UC.

882 Distinctive Immunohistochemical Profile of the Penile Distal Urethra

JS Han, GJ Netto, AL Cubilla, S Lee, N Gonzalez-Roibon, R Sharma, A Chauh. Johns Hopkins University, Baltimore, MD; Instituto de Patologia e Investigacion, Asuncion, Paraguay.

Background: The true nature of the epithelium covering the penile distal urethra remains undefined. Some authors argue that, given its purported embryogenesis and pathology, the epithelium of the distal urethra would be more closely related to a squamous epithelium than to urothelium. Herein, we evaluate a panel of stains routinely used as markers of urothelial differentiation.

Design: Eleven total penectomies performed for squamous cell carcinoma of the glans were selected based on the presence of intact distal urethra in the tissue blocks. In all cases, the distal urethral mucosa was histologically unremarkable and uninvolved by tumor. Standard immunohistochemistry for CK7, CK20, thrombomodulin, p63, and GATA3 (BioCare, GATA3 clone L50-823) was performed.

Results: In all cases, 2 distinctive cell layers were observed in the epithelial lining of the distal urethra. The superficial layer was composed of a single file of tall columnar cells with clear cytoplasm and conspicuous cell borders. Stratified cubical cells with scant cytoplasm and undefined cell borders were observed underlying the superficial columnar layer. All distal urethral sections were negative for CK20 and thrombomodulin. Staining for CK7 was strong and diffuse in the superficial columnar cells, and negative to weak in the underlying layers in all cases. p63 displayed an inverse pattern of expression, with absence of staining in the superficial columnar cells, and strong and diffuse positivity in the underlying layers. With the exception of 1 case, GATA3 staining was observed transmucosally in all distal urethral sections.

Conclusions: The epithelium of the distal urethral mucosa is distinctive, morphologically and immunohistochemically. It is composed of 2 cell layers, a superficial columnar simple epithelium (CK7+/p63-/GATA3+), and an underlying stratified epithelium composed of cubical cells (CK7-/p63+/GATA3+).

883 Can Positive Surgical Margins (PSM) and Extraprostatic Extension (EPE) in Robot-Assisted Laparoscopic Radical Prostatectomies (RALP) Be Predicted?

JM Hawkins, RC Heintzelman, J Jaffe, FU Garcia. Drexel University College of Medicine, Philadelphia, PA.

Background: Since the advent of RALP, the PSM rate has not changed, remaining at 15%. PSM and EPE are independent predictive factors for biochemical recurrence and prostate cancer specific mortality. Despite the importance of PSM and EPE in predicting outcomes, few studies to date have explored the predictive pathologic factors associated with PSM and EPE in RALP. Our objective is to identify clinical and pathologic features to help identify those patients to improve RALP outcomes.

Design: We reviewed retrospectively 285 RALPs performed by 2 surgeons from 2007 to 2011. Prostates were whole mounted, entirely submitted and reviewed by one pathologist. Patient demographics, pre-operative data and pathology report information were reviewed from a Departmental database. This information included: tumor volume, prostate volume, pathologic stage, PSM and EPE and location (apex, base, anterior and posterolateral).

Results: PSM+EPE were present in 13.7% of cases. Average values of clinical and pathological characteristics were analyzed using a t-test. PSM+EPE were seen in the apex 7.7%, base 5.1%, anterior 23.1% and posterolateral 28.3%. Multifocality was present in 17.9%, with discordance in 17.9%. Gleason scores (GS) of ≤ 6 , 7, 8/9 within this subset were 12.8%, 74.4%, 12.8%. Percent core involvement on biopsy correlates with average percent tumor on biopsy, prostatic specific antigen (PSA), GS, prostate volume and tumor volume ($p < 0.01$). Tumor volume, prostate volume and GS were predictive of PSM+EPE using linear regression ($p < 0.05$).

Table 1. Average Clinical and Pathology Characteristics

	Total Cohort (n=285)	PSM+EPE (n=39)	PSM/EPE Negative (n=196)	P Value
Age	58.26	57.46	58.58	p=0.36
PSA (ng/mL)	6.61	11.54	5.23	p=0.005
% Core Involved	28.67	40.70	23.03	p=0.0001
Avg % Tumor on Biopsy	25.31	35.60	19.49	p=0.0004
Prostate Vol (cc)	35.88	34.45	37.07	p=0.36
Tumor Vol (cc)	2.95	7.28	1.72	p=0.001

Conclusions: 1) 13.7% of post-RALP patients have PSM+EPE, highlighting the need to categorize this population preoperatively. 2) Posterolateral and anterior were the most common and should be evaluated during surgery. 3) Tumor volume, prostate volume and GS are predictive of PSM+EPE in RALP. 4) Percent core involvement on biopsy correlates with the average percent tumor, PSA, GS, prostate and tumor volume and might be a useful feature to identify this population. 5) Additional biopsy information will be studied in a larger cohort to further identify this population.

884 Expression of ERG Protein, a Prostate Cancer Specific Marker, in High Grade Prostatic Intraepithelial Neoplasia (HGPIN) Detected in Prostate Biopsy: Lack of Utility To Stratify HGPIN Cancer Risks

H He, AO Osunkoya, P Carver, S Falzarano, C Magi-Galluzzi, M Zhou. Cleveland Clinic, Cleveland, OH; Emory University, Atlanta, GA; Beijing University, Beijing, China; New York University, New York, NY.

Background: HGPIN is a premalignant lesion to prostate cancer (PCa). A diagnosis of HGPIN in prostate biopsy (PBx) is associated with a 20-25% of risk of PCa in subsequent PBx. No clinicopathological parameters and biomarkers can reliably identify patients who actually harbor PCa. ERG gene fusion is highly specific for and is identified in 40-50% of PCa and 20% HGPIN which is always associated with ERG-positive PCa. Positive immunostains for ERG highly correlate with ERG gene fusion. We studied

whether a positive ERG immunostain in HGPIN could identify patients with PCa on repeat biopsy.

Design: Ninety-four patients with initial HGPIN diagnosis in PBx and at least one follow-up PBx were included. Immunostain for ERG (clone ID: EPR3864) was performed on the initial PBx with HGPIN.

Results: Patients mean age was 63 years (range 48-78). A mean of 1.8 (range 1-5) repeat biopsies were obtained at a mean interval of 27.4 months (range 1.5-140). Repeat PBx showed PCa, benign, HGPIN, atypical glands suspicious for cancer in 36 (38%), 26 (%), 27 (%) and 5 (%) patients. ERG immunostain was positive in 5/94 (5%) PBx with HGPIN, in which PCa was found in 2 (40%) in subsequent PBx. Of 89 initial PBx with negative ERG staining, PCa was found in 34 (38%) repeat biopsies. The cancer detection rate was not different between ERG positive and negative cases ($p=0.299$).

Conclusions: ERG protein expression is uncommon in HGPIN (5%). PCa was detected at a similar rate on follow-up PBx in ERG-positive HGPIN cases and ERG-negative cases. Our study confirms that ERG expression is of no clinical utility in stratifying HGPIN cancer risks.

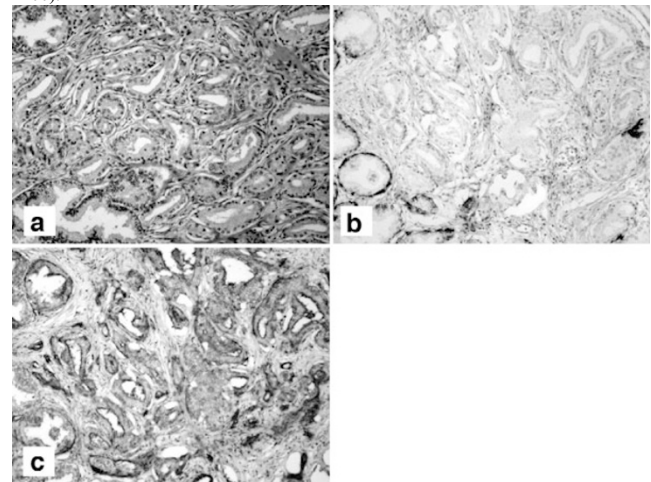
885 Monoclonal Antibody 6C4 Distinguishes Prostatic Carcinoma from Benign Mimics in Which PIN4 Immunostaining Is Non-Diagnostic

JF Hechtman, GQ Xiao, Y Kinoshita, PD Unger, DE Burstein. Mount Sinai School of Medicine, New York, NY.

Background: 6C4 is a monoclonal antibody to glutamate receptor 2 (GluR2), an excitatory amino acid receptor subunit in the central nervous system. 6C4 reactivity in prostatic tissue has not been previously investigated. Recently, our data have shown that benign prostatic epithelium is strongly reactive for 6C4 while low-grade prostatic carcinoma is negative. Post-atrophic hyperplastic and adenosis-like prostatic glands are common mimics of low-grade prostate carcinoma (PCa). Due to the frequent absence of basal cells on p63 and high molecular-weight cytokeratin (HMCK) immunostain in these mimics, it is not uncommon for them to pose a diagnostic challenge to urologic pathologists, particularly in biopsy specimens. The goal of this study is to assess the utility of 6C4 in the discernment of post-atrophic or adenosis-like prostatic epithelia from low-grade PCa.

Design: 10 prostate sections with post-atrophic or adenosis-like areas were chosen from separate prostatectomy specimens. Each was stained with monoclonal antibody to GluR2 (6C4, gift of J. Morrison, 0.8 microgram/ml) in parallel with PIN4, a triple antibody cocktail against alpha methyl acyl coA racemase (AMACR), Ker903 and p63 (Biocare Medical, CT, USA). Membranous and cytoplasmic staining patterns of 6C4 were considered positive.

Results: Post-atrophic glands were remarkable for architectural and cytologic atypia (Figure 1a; hematoxylin and eosin; original magnification x100). Basal cell markers were negative in all ten cases, and weak or strong positivity for AMACR was seen in the secretory epithelium in 4 of 10 cases (Figure 1b; PIN4 immunostaining; original magnification x100). Uniform and strong positive staining with 6C4 was demonstrated in these glands in all ten cases (Figure 1c; 6C4 immunostaining; original magnification x100).



Conclusions: As seen in other benign prostate glands, the uniform positivity of 6C4 in post-atrophic and adenosis-type glands readily separated them from prostate cancer with low Gleason's score, which are 6C4 negative. Therefore, 6C4 has a potential diagnostic advantage over PIN4 in distinguishing low-grade PCa from the aforementioned mimics.

886 Insignificant Prostate Cancer: Analysis of Pathobiological Criteria and Predictive Factors

I Hierro, JE Perez-Enriquez, M Alvarez, C Marchal, L Vicioso, E Gallego, MV Ortega, L Perez-Villa, FJ Machuca, A Matilla. Virgen de la Victoria Hospital, Málaga, Spain.

Background: Prostate specific antigen (PSA) screening and needle biopsy (NB) has been associated with a sharp increase in prostate cancer (PCa) detection as with decreased incidence of high-grade or high-risk PCa with a stage migration toward organ confined disease. Many of these patients will probably not require treatment because of the indolent course of the disease. The aim of this study is to evaluate in NB the predictive value of criteria of Epstein for insignificant PCa, as well as other clinical and immunohistochemical parameters, to identify patients that might benefit from active surveillance.

Design: We retrospectively studied 300 cases who subsequently underwent both early (8-12 cores) NB and radical prostatectomy from 2004 to 2010. Forty eight cases met predictive criteria of Epstein for insignificant PCA. Several clinical, histological and immunohistochemical parameters (table 1) as well as tumor length (mm) and unilateral affectation were correlated with the findings of prostatectomy. We considered insignificant a tumor when it met the "classical" criteria of Epstein (PSAD < 0.15 ng/ml, volume ≤ 0.5cc of the entire gland, with a Gleason score ≤ 6, with no grades 4 or 5) and also when it met the "liberal" criteria (organ-confined disease).

Clinical, histological and immunohistochemical parameters in NB

Parameters	Value	Range
No. of patients	48 (16%)	
Mean age (years)	61.4	46-71
Mean preoperative PSA (ng/ml)	6.7	3-15
Mean PSA density (ng/ml ²)	0.10	0.03-0.15
Tumour volume (cc)	65.2	27-308
		No. cases (%)
No. of positive biopsy core	1	34 (70.8%)
	2	14 (29.2%)
% core involvement	0-15%	07 (14.6%)
	16-30%	12 (30.8%)
	31-45%	05 (12.6%)
Proliferation index (ki-67)	3.06%	
p53 expression	Positive	-
	Negative	48 (100%)
Bcl2 expression	Positive	17 (14.6%)
	Negative	31 (85.4%)

Results: The prevalence of potentially insignificant PCA in NB in our experience was 16%. Only 10 cases (20.8%) met the "classical" criteria and 37 cases (77%) met the "liberal" criteria of insignificant tumor in prostatectomy specimen. None of the histological and immunohistochemical factors in the biopsy predicted the existence of insignificant tumor in radical prostatectomy considering both "classical" and "liberal" criteria.

Conclusions: We have not identified any factors: clinical, histological or immunohistochemical, that can predict with certainty the insignificant nature of a tumor and, therefore, useful to propose more conservative treatment options.

887 Prognostic Value of Tumor Volume in Prostate Cancer

C Hilliges, F Wiklund, P Wiklund, L Egevad. Karolinska Institutet, Stockholm, Sweden.

Background: Tumor volume of prostate cancer has been shown to correlate with recurrence rate after radical prostatectomy. However, it remains controversial whether it is an independent prognostic factor and if total tumor volume (Vtot) or the volume of the main tumor (V1) is the best predictor of outcome.

Design: Tumor volume was measured on radical prostatectomy specimens from the Karolinska Hospital 1998 - 2002. Men with neoadjuvant treatment or TURP prior to surgery, unavailable clinical follow-up data or histological slides were excluded and 282 cases remained for analysis. All specimens were completely embedded, cancer was outlined with Indian ink and the volumes of the main tumor (V1), secondary tumor foci (V2) and other tumor foci (V3) were measured by computerized planimetry. Vtot was calculated by adding V1, V2 and V3. Cox regression models were used to assess the correlation between clinical and histopathological features and biochemical recurrence.

Results: Mean follow-up time was 60.8 months (range 1-144). Gleason scores (GS) were 5-6 (47.2%), 7 (40.8%) and 8-10 (12.1%). Extraprostatic extension (EPE), positive surgical margins (PSM) and seminal vesicle invasion (SVI) were seen in 47.5%, 46.8% and 12.8%, respectively. Mean Vtot was 2.9 ml (range 0.04-15.3) and mean V1 was 2.4 ml (range 0.02-15.3). Both Vtot (hazard ratio [HR] 1.13, 95% confidence interval [95% CI] 1.07-1.19) and V1 (HR 1.12, 95% CI 1.06-1.18) predicted recurrence free survival in univariate analysis. Recurrence rate in men with Vtot <1, 1-1.9, 2-2.9, 3-3.9 and ≥4 ml was 27.3%, 28.8%, 37.5%, 48.5% and 63.9%, respectively. In multivariate analysis adjusting for preoperative serum PSA, GS, EPE, PSM and SVI only GS (p<0.001) and PSM (p<0.001) remained independent predictors of recurrence.

Conclusions: Total tumor volume of prostate cancer and volume of the main tumor both predict biochemical recurrence rate in univariate analysis but not in multivariate analysis including preoperative serum PSA and other histopathological prognostic factors. Postoperative measurement of tumor volume is a time-consuming procedure that is unnecessary in routine practice.

888 Current Immunomarkers Are Inadequate for Accurate Classification of Renal Epithelial Tumors

C Himmetoglu Ussakli, L True. University of Washington, Seattle, WA.

Background: There are 7 distinct variants of renal epithelial tumors in adults (WHO 2004): Clear cell(CC), papillary(PAP), chromophobe(CHR), collecting duct(CD), translocation(TC), mucinous tubular and spindle cell(MTSC) carcinomas; oncocytoma(ONC), and urothelial carcinoma(UC). Although these have unique molecular phenotypes, the histological features overlap. The immunophenotypes of these variants have been extensively studied to resolve the challenge of distinguishing them. We hypothesize that the immunophenotype, based on currently used antibodies(Ab), is not sufficiently specific to resolve the differential diagnosis of these variants.

Design: 57 articles reporting immunohistochemical profiles of primary adult renal epithelial tumors were reviewed, supplemented by our institutional experience. Only the 7 histological variants were included in the study. TCs were excluded due to presumed specificity of anti-TFE3 Ab. The most commonly used and/or investigated markers were selected for review. Expression percentages and cut-off values for positivity were based on the authors' criteria. The range of expression (as percentages) of each marker per tumor type was noted.

Results: Based on the literature expression of the 16 most frequently reported markers varies widely.

	AMACR	CAIX	CD10	CD117	CK5/6	CK7	HMWCK	p63
CC	20-81%	50-100%	80-94%	0-7%	0%	0-26%	0-13%	0%
CD	0%	0%	40%	0%	17%	33-100%	0-67%	14%
CHR	0-19%	0-30%	19-72%	9-100%	0%	62-100%	0%	0%
MTSC	93-100%	0-40%	11-17%	n/a	0%	92-100%	0%	n/a
ONC	11-29%	0-14%	0-100%	40-100%	0%	0-100%	0-10%	n/a
PAP	85-100%	0-57%	0-93%	0-18%	0-0%	45-100%	0-33%	0%
UC	0%	90%	55%	4-20%	75%	90-92%	100%	93-97%

	RCC	VIMENTIN	CD15	EGFR	S100A1	PAX8	EMA	PAX2
CC	44-75%	70-100%	50-75%	84-100%	81%	91-93%	65-84%	50-93%
CD	0%	40-100%	0%	100%	n/a	50-100%	87%	0-100%
CHR	0%	0-33%	5-25%	75-95%	6-30%	57-80%	75-100%	0-9%
MTSC	7-92%	100%	67%	n/a	95-100%	100%	95%	75%
ONC	0%	0-10%	57-100%	5-50%	n/a	81%	85%	17-86%
PAP	25-100%	50-100%	41-100%	68-100%	85%	76-100%	40-88%	53-75%
UC	n/a	n/a	n/a	n/a	n/a	9-18%	n/a	0%

Expression of AMACR rules out CD and UC. CK5/6, p63 and/or HMWCK immunoreactivity supports a diagnosis of UC or CD. Expression of CAIX, CD117, CD15 and/or RCC marker rules out CD. The only marker unique to a tumor type is p63 (for UC). No other single marker is sufficiently specific for a tumor type to unequivocally categorize a histologically problematic case.

Conclusions: Since the distinction of renal epithelial tumors is important for clinical management and since clinical decisions are often based on needle biopsies, accurate distinction of these histological variants is of importance. Explanations for why the range of marker expression is so wide include different specificities of the antibodies, different sizes of specimens (TMAs vs whole tissue sections), different criteria for what is interpreted as positive, and the intrinsic heterogeneity of differentiation within each case. More specific tissue-based assays usable in formalin fixed tissue are needed for accurate classification of small samples of renal epithelial neoplasms.

889 Digital Imaging Tools for Differentiating between Type 1 and Type 2 Papillary Renal Cell Carcinoma

JA Hipp, JD Hipp, KP Lakshmi, UJ Balis. University of Michigan Health Systems, Ann Arbor, MI.

Background: The recent availability of digital whole slide data sets has created new opportunities for pathologists to perform numerical and quantitative assessment of histologic features. One promising pattern matching algorithm, Spatially-Invariant Vector Quantization (SIVQ), has already exhibited broad utility in the detection of subtle architectural and nuclear features, making a compelling case for the exploration of its utility to differentiate between type 1 and type 2 Papillary Renal Cell Carcinoma (PRCC). Successful automated distinction of these two diagnostic entities would have immediate utility for the diagnosing pathologist.

Design: Digital whole slide images were obtained from PRCC type I and II cases. Use of a region-of-interest extraction tool, dCore, followed by use of an image aggregation tool, ImageMicroArray Maker, allowed for generation of a montage of diverse examples of each sub-type, as a combined monolithic image. Type 1 and type 2 image arrays served as a vehicle for expedited analysis of candidate features. Ring vectors were chosen for their ability to exhibit high affinity for: 1) the interface between dark blue nuclei and small nucleoli (vector 1, type 1 PRCC) and 2) areas containing nucleoli with white clearing and a blue nuclear rim (vector 2, type 2 PRCC). SIVQ analysis with these vectors was then performed on the representative region for each case, for confirmation of each ring vector's discriminant efficacy.

Results: From the initial validation region, vector 1 (type 1 PRCC) identified 47/54 nuclei (sensitivity 87%) as well as 3/35 (specificity 91%) of type 2 PRCC nuclei. Similarly, vector 2 (type 2 PRCC) identified 25/35 nuclei (sensitivity 87%) and 2/54 type 1 PRCC nuclei (specificity 96%). Confirming the above chosen vectors in the representative regions, the sensitivity and specificity was found to be 95% & 95% and 87% & 84% for vector 1 and 2, respectively.

Conclusions: SIVQ allows for efficient identification of both type 1 and type 2 PRCC nuclei, with high sensitivity and specificity. We attribute this slight differential performance of the two vectors to the observation that type 1 PRCC has increased homogeneity, leading to increased pattern matching performance (higher sensitivity) as compared to type 2 PRCC type, which exhibited large irregular nuclei with prominent nucleoli (decreasing homogeneity). We anticipate that such feature detection tools will facilitate the creation of turnkey decision support systems for the pathologist pitted with the distinction between these two diagnostically important morphological variants.

890 Integration of Architectural and Cytologic Driven Image Algorithms for Prostate Adenocarcinoma Identification

JD Hipp, J Monaco, PL Kunju, J Cheng, Y Yagi, J Rodriguez-Canales, MR Emmert-Buck, S Hewitt, MD Feldman, JE Tomaszewski, M Toner, RG Tompkins, T Flotte, D Lucas, JR Gilbertson, A Madabhushi, UJ Balis. University of Michigan, Ann Arbor; Rutgers The State University of New Jersey, Piscataway, NJ; Harvard, Boston; National Cancer Institute, NIH, Bethesda; Perlman School of Medicine at the University of Pennsylvania, Philadelphia; Mayo Clinic, Rochester, MN; Massachusetts General Hospital, Boston, MA.

Background: The advent of digital slides offers new opportunities including the use of image analysis techniques to facilitate computer aided diagnosis (CAD) solutions. However, the development and testing of prostate cancer CAD solutions requires a ground truth map of the cancer which in turn requires a pathologist to annotate, or paint, each of the malignant glands in prostate cancer with an image editor software - a time consuming and exhaustive process.

Recently, two CAD algorithms have been described: probabilistic pairwise Markov models (PPMM) and spatially-invariant vector quantization (SIVQ). Briefly, SIVQ

operates as a highly sensitive and specific pattern matching algorithm, making it optimal for the identification of epithelial morphology, whereas PPMM operates as a highly sensitive detector of malignant perturbations in glandular architecture.

Design: By recapitulating algorithmically how a pathologist reviews prostate tissue sections, we created an algorithmic cascade of PPMM and SIVQ as previously described by Doyle *et al.* (2011) where PPMM identifies the glands with abnormal luminal architecture, and this area is then screened by SIVQ to identify the epithelium.

Results: The performance of this algorithm cascade was assessed qualitatively (using heatmaps) and quantitatively (using ROC curves). The PPMM-SIVQ analysis had approximately 90% sensitivity, 90% specificity (Sample #1), 85% sensitivity, 94% specificity (Sample #2), and 90% sensitivity, 88% specificity (Sample #3). This data demonstrates greater performance in the identification of only the prostatic adenocarcinoma than PPMM or SIVQ alone.

Conclusions: This ability to semi-autonomously paint nearly all the malignant epithelium of prostate cancer has immediate applications to future prostate cancer CAD development as a validated ground truth generator. In addition, such an approach has potential applications as a pre-screening/quality assurance tool.

891 Functional Distinction between the Full-Length Human Androgen Receptor and Its Splicing Variants in Castration-Resistant Prostate Cancer

R Hu, C Lu, AM De Marzo, WB Isaacs, J Luo. University of Wisconsin, Madison, WI; The Johns Hopkins University, Baltimore, MD.

Background: Multiple androgen receptor splicing variants (AR-Vs) arising in castration-resistant prostate cancer (CRPC) have recently been decoded and characterized. AR-Vs lack the AR ligand-binding domain, the intended target of all endocrine therapies for prostate cancer, suggesting a key mechanism underlying development of CRPC. However, the abundance of individual AR-V levels relative to the canonical full-length AR (AR-FL) is low, and both AR-FL and AR-Vs are overexpressed in CRPC. Due to sustained supply of tissue androgens under castrate conditions, AR signaling in CRPC may continue to rely on the canonical AR-FL. The goal of this study is to determine the relative importance of AR-FL and AR-Vs in CRPC.

Design: A set of detection and targeting tools were first developed to differentiate the AR-FL and AR-Vs. Genome-wide expression changes mediated by AR-FL and AR-Vs were investigated in various treatment settings using cell line models of CRPC that recapitulate the relative expression levels of AR-FL and AR-Vs. A variant-specific antibody was developed and used to detect AR-V7 expression in CRPC specimens from patients who developed obstructive urinary symptoms following hormone therapies.

Results: An acute adaptive shift toward AR-V-mediated signaling was observed after suppression of AR-FL signaling. AR-V7, one of the most abundant AR-Vs with a validated protein product, is dramatically induced (up to 100 fold) following treatment mimicking endocrine therapies. Both the endogenously induced AR-V7 and exogenously transfected AR-V7 activate an expression signature enriched for cell cycle genes, whereas activation of AR-FL is associated with a signature enriched for genes related to cellular synthesis, metabolism, and differentiation. In clinical CRPC specimens, AR-V7, but not the AR-FL, is positively correlated with UBE2C, a validated cell cycle gene involved in castration-resistant prostate cancer cell growth.

Conclusions: The cumulative *in vitro* and *in vivo* evidence supports a functional dichotomy between AR-FL and AR-Vs in CRPC. The emergence of AR-V mediated signaling may be an indicator of castration-resistant prostate cancer progression. Future therapies for CRPC patients should be designed to overcome this adaptive mechanism of drug resistance that may be manifested in at least a subset of CRPC patients.

892 A Subset of Invasive Urothelial Carcinomas of the Renal Pelvis Show Immunoreactivity with the Monoclonal Anti-PAX8 Antibody

J Hughes, AR Sangoi, JK McKenney. Stanford University, Stanford, CA; El Camino Hospital, Mountain View, CA.

Background: Positive staining with the polyclonal anti-PAX8 antibody has been shown in a subset of invasive urothelial carcinomas of renal pelvis origin. The expected immunoreactivity with polyclonal PAX8 in some tissues and neoplasms has now been shown to be due to cross reactivity. Immunoreactivity with the new monoclonal anti-PAX8 antibody has not been evaluated in upper tract urothelial carcinoma. Knowledge of the PAX8 immunoreactivity pattern in upper tract urothelial carcinomas is important in the diagnostic distinction from renal cell carcinoma, especially since small image guided biopsies are now commonly used to guide definitive clinical management.

Design: We identified invasive urothelial carcinomas of the renal pelvis with available H&E glass slides and paraffin blocks from our surgical pathology archives. All slides were reviewed to confirm diagnoses and a representative slide was stained with polyclonal anti-PAX8 (1:20 dilution, Proteintech, Chicago, IL) and monoclonal anti-PAX8 (1:50 dilution, clone BC12, BioCare, Concord, CA) antibodies using standard citrate retrieval techniques. Immunoreactivity was scored as positive if any nuclear staining was present in the invasive component and the total percentage of neoplastic cells with positive staining was recorded.

Results: Four of 20 invasive urothelial carcinomas of the renal pelvis (20%) had nuclear staining with a polyclonal anti-PAX8 antibody [80%, 80%, 50%, and 20% of neoplastic cells]. The same four renal pelvis tumors also demonstrated immunoreactivity with a monoclonal anti-PAX8 antibody; however, there was both a lower percentage and intensity of staining [$<5\%$, 10%, 20%, and $<5\%$ respectively of neoplastic cells]. Both antibodies displayed a heterogeneous patchy immunoreactivity pattern throughout the sections.

Conclusions: In this study, polyclonal and monoclonal anti-PAX8 immunoreactivity was seen in the same 20% of invasive urothelial carcinomas of renal pelvis origin. While the monoclonal anti-PAX8 antibody reacted with fewer neoplastic cells and demonstrated less intense staining, both antibodies displayed a heterogeneous pattern

of immunoreactivity with areas of stronger staining present. Knowledge of this potential immunoreactivity pattern is important when faced with the diagnostic distinction of renal cell carcinoma from invasive urothelial carcinoma on needle biopsy.

893 KRAS Is Mutated in a Subset of Mucinous Type Urachal Adenocarcinomas (UAC)

L Hutchinson, GP Paner, K Tomaszewicz, V Mehta, SJ Sirintrapun, GA Barkan, EF Cosar. University of Massachusetts, Worcester, MA; Loyola University Medical Center, Maywood, IL; Wake Forest University, Winston Salem, NC; University of Chicago, Chicago, IL.

Background: Activating mutations in *KRAS* and *BRAF* are frequently found in sporadic colorectal adenocarcinoma (CAC), and are established therapeutic markers. Mutations in *KRAS* can also occur in other organ adenocarcinomas such as lung and pancreas, particularly in mucinous type. The rare UAC has several morphological types that include intestinal, mucinous, signet ring cell, and other types. The intestinal UAC has striking morphologic and immunohistochemical overlap with CAC. To date, the mutational status of *KRAS* and *BRAF* in UAC has not been investigated.

Design: Twelve UACs (8 mucinous, 2 enteric, 1 signet ring cell, and 1 not otherwise specified [NOS] types) were included in the study. *KRAS* mutation analysis for codons 12 and 13 of the *KRAS* oncogene and *BRAF* mutation analysis for known mutations between codons 598 and 602 including the V600E mutation of the *BRAF* oncogene were performed.

Results: *KRAS* mutations were detected in 4/8 (50%) of mucinous type UAC (table). Mutations were all in codon 12 and included 2 glycine to aspartate (p.G12D), 1 glycine to thymine (p.G12C) and 1 glycine to aspartate (p.G12S). No *KRAS* mutation was detected in other morphologic types. No *BRAF* mutation was detected in all UAC analyzed.

AUC types	KRAS	BRAF
Mucinous	Positive (p.G12D)	Negative
Mucinous	Positive (p.G12D)	Negative
Mucinous	Positive (p.G12C)	Negative
Mucinous	Positive (p.G12S)	Negative
Mucinous	Negative	Negative
Mucinous	Negative	Negative
Mucinous	Negative	Negative
Mucinous	Negative	Negative
Mucinous	Negative	Negative
Enteric	Negative	Negative
Enteric	Negative	Negative
Signet ring cell	Negative	Negative
NOS	Negative	Negative

Conclusions: Mutations in *KRAS* are present in a subset of mucinous type UAC and may play a role in the oncogenesis of urachal mucinous tumors. Currently, there is no standardized chemotherapeutic regimen for UAC, and in some instances UAC patients received CAC regimens. Future drug trials such as those that targets epidermal growth factor receptor (EGFR) similar to those in CAC may perhaps uncover the clinical relevance of *KRAS* mutation in UAC.

894 Renal Cell Carcinoma with Syncytial-Type Tumor Multinucleated Giant Cells, a Rare Variant of Clear Cell Renal Cell Carcinoma

MT Idrees, TW Kieffer, DJ Grignon, JB Kum. Indiana University, Indianapolis, IN.

Background: Renal cell carcinoma (RCC) with syncytial-type tumor multinucleated giant cells (SGC) is a recently reported rare variant with only 5 cases reported in the English literature. Clinicopathologic features need to be evaluated in additional cases as it appears from published data that it may be associated with an aggressive clinical course. We report morphologic, immunophenotypic, and ultrastructural features in 5 additional cases.

Design: Five cases of RCC with SGC are identified from our files. All H&E slides are reviewed and immunohistochemical (IHC) studies are performed on representative tumor sections using a standard methods. IHC studies using antibodies against CAM5.2, AE1/3, vimentin, S100 protein, HMB45, SMA, CD10, CD68, EMA, hCG, CK20, CK7, and TFE-3 are performed on 3 cases. Ultrastructural studies are performed on 4 cases.

Results: Clinicopathologic information is available for 5 cases (Table 1); average tumor size is 7.2 cm. Three of 5 patients are male and 4 of 5 tumors are right sided. Two of 5 cases have sarcomatoid areas and 2 have lymph node involvement. One case each showed direct invasion of either the adrenal gland or liver. The adrenal gland is not examined in 2 cases. Microscopically, each tumor displays areas of classic clear cell RCC (CCRCC) and areas of mixed clear cells and SGC. The nuclear grades of SGC correspond to the existing CCRCC. SGC also show prominent emperipolesis and eosinophilic-hyaline globules. Ultrastructurally, the hyaline globules correspond to degenerative debris likely secondary to phagocytic activity. The staining profile of the SGC component is similar to the associated CCRCC and are PAS, vimentin, CD10, EMA, and AE1/3 positive; negative for S100, SMA, HMB45, CD68, TFE-3, hCG, CK20, CK7, mucicarmine, and PAS with diastase treatment.

Table 1. Renal Cell Carcinoma with Syncytial-Type Multinucleated Giant Cells

Case	1	2	3	4	5
Laterality	R	R	R	L	R
Sex	M	M	M	F	F
Age	43	62	57	60	60
Associated Tumor	CCRCC	CCRCC	CCRCC	CCRCC	CCRCC
Size	9.9	5.2	11.2	6	3.5
Stage	T4	T1b	T4	T3a	T1a
Fuhrman Grade	4	3	4	4	3
Sarcomatous Areas	Y	N	Y	N	N
Lymph Node Involvement	Y	Y	N	N	N
Direct Extension	Adrenal Gland	N	Liver	N	N

Conclusions: SGC in CCRCC is a rare but distinctive finding. The syncytial cells have the same immunoprofile as adjacent CCRCC. Additionally, they often show prominent emperipolesis and eosinophilic cytoplasmic globules. These tumors appear to present

at higher stage and most likely represent an aggressive variant of RCC. Further studies are needed to document the prognostic differences.

895 The Spectrum of Histopathological Findings in Vesical Diverticulum: Implications for Pathogenesis and Staging

M Idrees, J Kum, A Riley, L Cheng. Indiana University, Indianapolis, IN.

Background: Diverticula are saccular evaginations of urinary bladder mucosa that are encountered in all age groups with a prevalence of 1-10%. Intradiverticular neoplasms pose diagnostic and treatment challenges. The aim of this study was to document the common morphologic changes and neoplasms found in a large series of adult and pediatric vesical diverticula.

Design: Total of 176 diverticula from 137 cases of urinary bladder diverticula were identified including adult and pediatric cases. H&E stained slides were reviewed to evaluate the spectrum of neoplastic and nonneoplastic changes.

Results: A total of 176 diverticula from 137 patients were reviewed including 47 pediatric (mean age, 7.8 y) and 90 adult (mean age, 64.6 y); 92% were male. All cases had varying degrees of fibrosis and attenuation of the muscularis propria. Of the 96 nonneoplastic cases, the prominent morphologic findings included significant chronic inflammation-35, granulomatous inflammation including foreign body giant cell reaction-4, acute inflammation-7, squamous metaplasia-9, cystitis glandularis-9, and nephrogenic adenoma-1. The pediatric cases showed no malignancy. Of the 41 neoplastic cases, 29 had high-grade urothelial carcinoma (HGUC), 3 carcinoma in situ, 5 low-grade papillary urothelial carcinoma, 2 primary squamous cell carcinoma, 1 secondary melanoma, and 1 urothelial dysplasia. Two of the HGUC had neuroendocrine differentiation. Diverticulae from 19 cases were involved by primary tumors, of which 9 had coexisting intravesical neoplasia. In 14 of 29 HGUC, infiltration into adjacent fat was noted. Six of these cases arose within diverticula. Ten cystoprostatectomy cases had associated incidental prostatic carcinoma. The commonest presenting symptoms in neoplastic cases were hematuria followed by urinary retention.

Conclusions: Diverticulum of the urinary bladder is a relatively common clinical disorder in children and adults. Fibrosis, inflammation, and urothelial metaplastic changes are frequently encountered. In addition, specimens may harbor neoplasms, most commonly urothelial carcinoma. Hypothetically, attenuation of the muscle layer associated with diverticulum formation may facilitate tumor invasion into peridiverticular soft tissues. However, we could not clearly establish that muscle attenuation in bladder diverticula has statistically significant relationship with higher tumor stage.

896 Seminal Plasma Proteins in Prostate Cancer: Increased Semenogelin I Expression Is a Predictor of Biochemical Recurrence after Radical Prostatectomy

K Izumi, Y Li, Y Zheng, Q Yang, LA McMahon, J Gordetsky, JL Yao, H Miyamoto. University of Rochester, Rochester, NY.

Background: Semenogelins, predominantly expressed and secreted by the seminal vesicle, are the main structural proteins in human semen coagulum. Eppin (epidermal protease inhibitor), specifically expressed and secreted by the epididymis and testis, has been known to bind to semenogelin, resulting in inhibition of sperm motility. However, the role of these seminal plasma proteins in prostate cancer is poorly understood.

Design: We immunohistochemically stained for semenogelins I (SgI) and II (SgII) and eppin in 291 radical prostatectomy specimens. We then evaluated the association between their expressions in nuclei (n-), cytoplasm (c-), or intraluminal secretions (s-) of benign (BN)/high-grade prostatic intraepithelial neoplasia (PIN)/carcinoma (CA) cells and clinicopathologic profiles available for our patient cohort.

Results: Stains were positive in 32%/77%/84% (n-SgI), 87%/94%/84% (n-SgII), 56%/64%/37% (n-eppin), 7%/15%/11% (c-SgI), 6%/11%/9% (c-SgII), 68%/74%/95% (c-eppin), 97%/98%/13% (s-SgI), 98%/97%/11% (s-SgII), and 97%/98%/48% (s-eppin) of BN/PIN/CA, respectively. The levels of n-SgI and c-eppin were significantly higher in CA than in BN ($P < 0.001$ and $P < 0.001$) or PIN ($P = 0.065$ and $P = 0.001$) and in PIN than in BN ($P < 0.001$ and $P = 0.145$). Significantly higher n-SgII expression was found in PIN than in BN ($P = 0.028$) or CA ($P = 0.002$). Significantly lower n-eppin expression was seen in CA than in BN ($P < 0.001$) or PIN ($P < 0.001$). s-SgI, s-SgII, and s-eppin were all significantly lower in CA than in BN ($P < 0.001$) or PIN ($P < 0.001$). There were no statistically significant correlations between each stain and clinicopathologic features, such as Gleason score, pathologic stage (pT/pN), and preoperative prostate-specific antigen (PSA) levels, except higher PSA in patients with n-SgI(+) tumor than in those with n-SgI(-) tumor ($P = 0.017$). Kaplan-Meier and log-rank tests further revealed that patients with n-SgI(+) tumor had a higher risk for biochemical (PSA) recurrence ($P = 0.046$). Multivariate Cox model showed a trend toward significance ($P = 0.091$) in n-SgI positivity as an independent predictor for recurrence.

Conclusions: Compared to non-neoplastic prostate and PIN tissues, significantly increased (n-SgI and c-eppin) or decreased (n-eppin) expression was seen in prostate cancer. Our results suggest the involvement of semenogelins and eppin in prostate cancer development and progression. Moreover, SgI expression could be a reliable prognosticator in men who undergo radical prostatectomy.

897 Matrix Metalloproteinase-14: A Novel Marker of Tumor Progression and Invasion in Prostate Cancer

G Javid, R Aljumaily, R Kaimal, S Sharifi, A Agarwal. Tufts Medical Center, Boston, MA.

Background: Emerging evidence has shown that matrix metalloproteinase-14 (MMP14) plays a pivotal role in prostate cancer bone metastases, the leading cause of morbidity/mortality in affected patients. MMP14 is known as one of the critical proteases involved in cell migration which degrades extracellular matrix to furnish a path for cells to migrate, sheds cell surface molecules, and activates extracellular signal-regulated

protein kinase. We hypothesized that prostate cancer cells with higher expression of MMP14 have a more aggressive phenotype and tendency to migrate to the bone. The goal of this study is to evaluate the role of MMP14 monoclonal antibody in blocking migration and invasion of prostate cancer cell lines (PC-3 and DU-145) *in vitro*, and to further evaluate MMP14 expression pattern *in vivo* to assess if higher expression of MMP14 is associated with an invasive phenotype in human prostatic tissue.

Design: *In vitro:* Prostate cancer cell lines PC-3 and DU-145 were used. Chemotactic migration and chemoinvasion were evaluated using transwell apparatus following selective blockade of MMP14.

In vivo: Formalin Fixed Paraffin Embedded human tissues were retrieved, including 20 cases of prostate adenocarcinoma (PAC) with either perineural, lymphovascular or extraprostatic invasion, and 20 cases of benign prostatic hyperplasia (BPH; control). Immunohistochemistry was performed for MMP14. Intensity, using a 4-grade scale, and pattern (nuclear/cytoplasmic and diffuse/focal) of MMP14 staining were analyzed and compared in malignant epithelial cells, benign epithelial cells (BEC) adjacent to the tumor, and BEC in the BPH.

Results: *In vitro:* Monoclonal MMP14 antibody significantly decreased the invasion of prostate cancer cell lines through reconstituted basement membrane compared to controls.

In vivo: The PAC (mean age: 60 yrs) and the BPH groups (mean age: 64 yrs) each consisted of 20 patients. PAC cases showed diffuse 2+ to 3+ nuclear and cytoplasmic MMP14 staining (80%) in contrast to BEC in BPH that showed 0 to +1 focal cytoplasmic staining ($p < .0001$). The intensity of staining in the BEC adjacent to invasive tumor cells of PAC group was also focal, and significantly lower than the invasive cells ($p < .0001$).

Conclusions: Our *in vitro* and *in vivo* findings are significant and help understand the role of MMP14 as a potential biomarker of disease progression and invasion in prostate cancer. Moreover, the ability of the MMP14 monoclonal antibody in blocking tumor migration and invasion, suggests that MMP14 could serve both as a disease biomarker and also as a therapeutic target for PAC.

898 Androgen Receptor in Tumor and Stroma in Conservatively Treated Prostate Cancer

SS Jeetle, ZH Yang, E Stankiewicz, G Fisher, C Cooper, CS Foster, H Moller, P Scardino, VE Reuter, J Cuzick, D Berney. Barts Cancer Institute, London, United Kingdom; Memorial Sloan-Kettering Cancer Center, New York; Royal Marsden Hospital, Surrey, United Kingdom; Liverpool University Hospital, Liverpool, United Kingdom; Kings College London, London, United Kingdom.

Background: Androgen receptor (AR) is present in the epithelium and stroma of the prostate. Invasive malignancy may be due to down-regulation of stromal AR and maintenance or up-regulation of epithelial AR. Associations between stromal AR and prognosis have been suggested by others. We wished to determine if these changes were apparent in a cohort of 721 patients with conservatively treated prostate cancer (PC).

Design: 721 patients with clinically localized and conservatively treated prostate cancers, diagnosed on TURP from 1991-96 were investigated. Contemporary Gleason score and serum PSA were available with up to 10 years follow up. AR immunohistochemistry was performed on tissue microarrays of tumor and normal tissue and assessed semi-quantitatively in the stroma and epithelium. The end point was death from PC. Univariate and multivariate analysis including Gleason score and PSA was performed by proportional hazard (Cox) regression analysis.

Results: In the cancer cores, expression of epithelial AR was marginally but not quite significantly predictive of worse outcome on univariate analysis ($HR = 1.72$, 95%CI 0.96,3.09, $P = 0.07$) and it did not correlate with Gleason ($\chi^2 = 3.629$, $p = 0.163$) or PSA ($\chi^2 = 5.67$, $p = 0.225$). On Multivariate analysis with Gleason AR in tumor was also not significant ($HR = 1.64$, 95%CI 0.92,2.95, $P = 0.07$). There was no correlation of stromal AR expression with Gleason or PSA and univariate analysis was not significant. In 'normal' cores, epithelial and stromal AR was not associated with outcome on univariate analysis nor was there correlation with Gleason or PSA.

Conclusions: AR in cancer was only marginally and non-significantly predictive of outcome and we were unable to replicate the results of other studies showing the importance of stromal AR as a prognostic factor. Our study weakly supports the general consensus that AR may be important in the progression of prostate cancer but it is not the only mode of paracrine signalling. We suggest the relationship is complex and there may not be a simple two-way signalling between stromal and epithelial AR. Further large scale studies on translational material are needed to understand the specific role of AR in prostate cancer.

899 Mixed Epithelial and Stromal Tumor of Kidney. Molecular and IHC Findings of a Possible New Hereditary Syndrome

L Jin-Ping, BA Walter Rodriguez, PP Aung, M Linehan, MJ Merino. NCI/NIH, Bethesda; NCI, NIH, Bethesda.

Background: Mixed epithelial and stromal tumor (MEST) of the kidney is a rare renal tumor occurring predominantly in perimenopausal women. Recently it has been postulated that MEST and Cystic nephroma represent variants of the same process because their morphological and molecular characteristics. We report five new cases of kidney MEST and describe the occurrence of these tumors in a familial setting.

Design: Five cases of MEST including 2 familial tumors and 3 sporadic were studied. Tumors were immunohistochemically evaluated for ER, PR, SMA, Desmin, CA-125, Her2, calretinin, bcl-2, CD99, pax-8 and Ny-eso-1 antibodies. Protein expression of the DICER1 gene encoding an endoribonuclease was also performed. The presence of t(x;18)(p11.2;q11) translocation for human synovial sarcoma was investigated by RT-PCR. For loss of heterozygosity (LOH) analysis of the 3p12-3p21 region, tumor and normal kidney areas were microdissected and the DNA extracted. Comparative genomic hybridization (CGH) was also done to evaluate presence of genetic gain or losses in the MEST.

Results: The familial tumors occur in a 75-year old man with bilateral renal masses with similar morphologic features, and in his two daughters. One daughter is 47 years old and had a 3 cm renal mass, morphologically similar to the father's. The sister has a cystic renal mass and will undergo surgery. The three sporadic cases were all female aged 36, 40 and 52 years. Morphologically, the tumors were well circumscribed and varied in size, cystic component, and amount and cellularity of stroma. By IHC, ER, PR, SMA and Desmin were positive in the stromal cells for all five cases. Pax-8 was positive in the epithelial component. Calretinin showed focally positivity in both epithelial and stromal cells. CA-125 and Her2 were negative. One sporadic case, showed dense cellular spindle cell proliferation. Immunostain was positive for Bcl-2 and CD99. However, there was no evidence of the t(x;18) (p11.2;q11) translocation by RT-PCR. LOH for VHL markers (3p-3p21 loci) (D3S1038, D3S1110, D3S1597, D3S1317, D3S1560) was performed in all the cases but there were negative. CGH analysis also yield negative results for large areas of gain or losses. All patients have remained free of disease.

Conclusions: We conclude that Mixed Epithelial and Stromal Tumor of the kidney are neoplasms with excellent prognosis that can occur in a familial and hereditary setting. The histological and molecular profile for the hereditary and sporadic cases are similar.

900 ERG Expression in Mucinous Prostatic Adenocarcinoma and Prostatic Adenocarcinoma with Mucinous Features: Comparison with Conventional Prostatic Adenocarcinoma

H Johnson, M Zhou, AO Ouskoyia. Emory University School of Medicine, Atlanta; Cleveland Clinic Foundation, Cleveland.

Background: TMRSS2-ERG is the most common gene fusion in conventional prostatic adenocarcinoma, identified in about 40-70% of cases. ERG expression detected by rabbit anti-ERG monoclonal antibody has recently been utilized in predicting ERG rearrangement as assessed by FISH in needle core and radical prostatectomy specimens of patients with conventional prostatic adenocarcinoma. Mucinous prostatic adenocarcinomas and prostatic adenocarcinoma with mucinous features are rare subtypes of prostate cancer and ERG expression in these subtypes have not been well characterized in a large series.

Design: A search was made through the surgical pathology files of two major academic institutions for cases of mucinous prostatic adenocarcinoma and prostatic adenocarcinoma with mucinous features. The former were obtained from radical prostatectomy cases and the latter from radical prostatectomy cases, transurethral resection of the prostate and prostate needle core biopsies. A TMA composed of additional cases of mucinous prostatic adenocarcinoma was also included in the study. Immunohistochemical stains for ERG were performed on all the cases.

Results: 51 cases of mucinous prostatic adenocarcinoma and prostatic adenocarcinoma with mucinous features were identified. 25/51 (47%) cases were positive for ERG, including 10/24(42%) radical prostatectomy specimens, 7/14 (50%) biopsies, 2/4 (50%) transurethral resection of the prostate specimens, 6/9 (67%) from the TMA. In all cases of mucinous prostatic adenocarcinoma and prostatic adenocarcinoma with mucinous features that were positive for ERG, and had adjacent usual type adenocarcinoma on the same slide, there was identical expression of ERG in the latter component with the exception of one case.

Conclusions: This is the largest study to date specifically characterizing ERG expression in mucinous prostatic adenocarcinoma and prostatic adenocarcinoma with mucinous features. ERG was expressed in almost 50% of cases of mucinous prostatic adenocarcinoma and prostatic adenocarcinoma with mucinous features in our study, similar to known rates of ERG expression in conventional prostatic adenocarcinoma. In view of the identical expression of ERG in mucinous prostatic adenocarcinoma, prostatic adenocarcinoma with mucinous features, and adjacent conventional prostatic adenocarcinoma in the vast majority of cases, this study confirms that these rare subtypes of prostatic adenocarcinoma are clonally similar to conventional prostatic adenocarcinoma.

901 Molecular Prognostic Markers of Prostate Cancer: An Immunohistochemical Study on TMA Blocks from 428 Radical Prostatectomy Specimens

WY Jung, JY Ro, YM Cho. University of Ulsan College of Medicine, Asan Medical Center, Seoul, Korea; Cornell University, The Methodist Hospital, Houston, TX.

Background: Prostate cancer is a heterogeneous disease, ranging from clinically insignificant tumor to a rapidly fatal malignancy. Recent studies suggested molecular classification using zinc-alpha-2-glycoprotein (AZGP1), hCAP-D3, and mucin 1 (MUC1) and expressions of ERG gene fusion product and vimentin as prognostic markers of prostate cancer.

Design: A tissue microarray construct of prostate cancer tissues was generated from 428 cases that underwent radical prostatectomy from 1996 to 2006. Expressions of AZGP1, hCAP-D3, MUC1, ERG and vimentin as well as Ki-67 as a proliferation marker were assessed immunohistochemically and correlated with their clinical significance.

Results: Low expression of AZGP1 was associated with biochemical recurrence, clinical progression and increased risk of cancer-specific death. Whereas high expression of hCAP-D3, MUC1, and ERG was correlated with increased biochemical recurrence, and high expression of vimentin was correlated with clinical progression. Ki-67 expression was not informative due to low expression in most of cases. In multivariate analysis, only low expression of AZGP1 was a strong negative predictor of overall survival independent of Gleason score, pathologic tumor stage and resection margin involvement.

Conclusions: AZGP1, hCAP-D3, MUC1, ERG, and vimentin can be useful immunohistochemical prognostic markers. Validation of our results awaits further studies.

902 Role of Frozen Section Analysis during Radical Prostatectomy: A 1,993-Case Experience

Y Kakiuchi, J Gordetsky, H Miyamoto. University of Rochester, Rochester, NY.

Background: It remains unanswered whether intraoperative frozen section analysis (FSA) contributes to surgical margin (SM) status on radical prostatectomy (RP) specimens.

Design: We retrospectively studied a consecutive series of patients who underwent robotic-assisted laparoscopic RP performed at our institution between 2006 and 2001. From our surgical pathology electronic database, we identified 1993 cases coded as RP specimens, including 913 (45.8%) cases in which FSA was done for assessing the areas suspicious for positive SMs (+SMs).

Results: FSAs were reported as positive (n=49; 5.4%), negative (n=827; 90.6%), and atypical (n=37; 4.0%), respectively. Of the 49 cases with positive FSA, 25 (51.0%) were found to have +SMs on RP specimens while others showed either negative SMs (n=21; 42.9%) or indeterminate for margin status (n=3; 6.1%). On the other hand, among the cases with negative and atypical FSAs, 103 (12.5%) and 8 (21.6%) were +SMs on RP specimens, respectively. Thus, the rate of +SMs on RP was significantly higher in positive FSA cases than in negative (P<0.001) or atypical (P=0.005) FSA. Nonetheless, FSA failed to predict +SMs in 103 (12.5%) of 827 cases where negative FSAs were reported. Overall, 136 (14.9%) of 913 cases with FSA had +SMs, compared with 135 (12.5%) of 1080 cases with no FSA (P=0.068). The sensitivity, specificity, and positive and negative predictive values of FSA to identify +SMs on RP were 19.5%, 97.2%, 54.3%, and 87.5%, respectively.

Conclusions: Although the specificity and negative predictive value of FSA for isolating +SMs are high, the sensitivity and positive predictive value appear to be too low to anticipate that intraoperative FSA will reduce the incidence of +SMs substantially. Thus, our study suggests questionable utility of FSA during RP. However, further analyses, including those in clinicopathologic features of our cases, are required prior to concluding the importance of intraoperative FSA in RP.

903 The Immunohistochemical Profile of the Plasmacytoid Variant of Urothelial Carcinoma: A Study of 11 Cases

C-S Kao, M Idrees, L Cheng, DJ Grignon. Indiana University, Indianapolis, IN.

Background: Urothelial carcinomas (UC) exhibit many patterns, one of which is the plasmacytoid variant, characterized by discohesive tumor cells displaying a "plasmacytoid" appearance. Cells also frequently have a monocyte-like or signet ring cell-like morphology. The plasmacytoid variant is prone to misinterpretation as other neoplasms, especially in a limited sample, most commonly as plasmacytoma, metastatic lobular carcinoma of the breast or signet ring cell carcinoma of the gastrointestinal tract. Distinguishing plasmacytoid variant of urothelial carcinoma (PVUC) from other entities can be achieved using an appropriate panel of immunohistochemical stains. Furthermore, MUC protein expression has been the focus of studies on other aggressive variants of UC. The purpose of this study was to further define the IHC profile of PVUC including MUC protein expression.

Design: From our surgical pathology files, 11 cases of PVUC were identified and confirmed by reviewing hematoxylin and eosin stained sections. The plasmacytoid variant was defined by the presence of discohesive tumor cells with centrally or eccentrically located nuclei and moderate eosinophilic or amphiphilic cytoplasm, infiltrating as single cells, cords or solid aggregates. Immunohistochemical stains were performed on all cases and evaluated for proportion and intensity of positivity.

Results: PVUC expressed p53 protein (100%), MUC1 (90%), 34BE12 (80%), MUC4 (70%), CD138 (70%), CK20 (64%), CK7 (64%), p63 (55%), MUC5 (50%), MUC2 (40%), E-cadherin (30%), and uroplakin (27%). Progesterone receptor was positive in only one case (10%). MUM1, MUC6, CDX2, and estrogen receptor were uniformly negative.

Conclusions: PVUC can generally be recognized by careful morphologic evaluation. However, in a limited sample, the use of immunohistochemical stains may be necessary to make an accurate diagnosis. A panel including 34BE12, p53, MUC4/MUC5, MUM1, CDX2, and ER/PR can distinguish the tumor from mimics in most cases. MUC proteins, in particular MUC1 and MUC4, are frequently overexpressed. These transmembrane glycoproteins have been associated with aggressive tumor behavior in other sites, possibly through cell proliferation and apoptosis.

904 Divergent Morphology in Renal Pelvic Urothelial Carcinoma May Be Less Frequent Than Previously Reported

C-S Kao, M Idrees. Indiana University, Indianapolis, IN.

Background: Renal pelvic urothelial carcinomas exhibiting aberrant morphology, especially in higher grade tumors, is a well recognized phenomenon, and divergent morphology had been reported to be as high as 40% in the literature. However, we feel that the frequency of divergent morphology is far less than the percentage previously reported and may be secondary to practice bias. Our goal is to study the occurrence of divergent morphology within renal pelvic urothelial carcinomas in our patient population excluding consultation cases and report the most common variants.

Design: From our surgical pathology files, 119 cases of primary renal pelvic urothelial carcinomas from nephro-ureterectomy specimens within the past 10 years were identified and confirmed by reviewing hematoxylin and eosin stained sections. Histologic type, grade, invasion, stage, nodal status, metastasis, and the presence of divergent morphology were evaluated for all tumors. All the consultation cases where the surgery was performed elsewhere were excluded from the study.

Results: A total of 15 renal pelvic urothelial carcinomas out of a total of 119 cases show areas of divergent morphology, including squamous (27%), glandular/tubular (13%), sarcomatoid (13%), inverted (13%), mucinous (7%), plasmacytoid (7%), micropapillary (7%), lymphoepithelialoma-like (7%), and giant-cell (7%) differentiation. Two-thirds

of the cases with divergent morphology occurred in high grade flat-type urothelial carcinomas, while the remaining one-third occurred in high grade papillary urothelial carcinomas. Divergent morphology was not observed in any of the low grade papillary urothelial carcinomas nor was it observed in the majority of high grade urothelial carcinomas of the renal pelvis.

Conclusions: Our study shows that divergent morphology occurs in only 13% of renal pelvic urothelial carcinomas in our hospital based patient population, instead of the higher percentage that had been previously reported in the literature. The ones with divergent morphology are mostly high grade invasive urothelial carcinomas; however, the majority of the high grade renal pelvic urothelial carcinomas do not actually show aberrant differentiation. The most frequently observed ones are squamous, glandular/tubular, sarcomatoid, and inverted patterns. We recognize that the lower frequency than that reported in the literature may be secondary to the type of practice and possibly overrepresented in the literature.

905 Evaluation of LIN28 as a Pan-Germ Cell Tumor Marker Using Germ Cell Tumor Tissue Microarrays

A Karunamurthy, S Roy, S Rangathan, A Parwani. University of Pittsburgh Medical Center, Pittsburgh, PA.

Background: LIN28 a predominantly RNA-binding cytoplasmic protein, plays important role in gene expression regulation and maintenance of the pluripotency of embryonic stem cells. Recent studies have shown the role of LIN28 in malignant transformation of germ cells in animals. Our aim was to evaluate the diagnostic utility of LIN28 expression in testicular germ cell tumors (GCT).

Design: Two tissue microarrays constructed from various primary and metastatic testicular GCTs were stained with LIN28 antibody. The cytoplasmic staining was considered positive and scored as negative, weak, moderate, or strong staining.

Results: A total of 69 GCTs were obtained of which 52 (75%) were primary testicular GCTs (35 seminomas; 14 embryonal carcinomas; 3 yolk sac tumors; 6 teratomas and 20 intratubular germ cell neoplasias) and 17(25%) were metastatic testicular germ cell tumors containing (1 seminomas; 5 embryonal carcinomas; 3 yolk sac tumors; 8 teratomas and 1 choriocarcinoma) along with 19 normal testicular tissue cores adjacent to the above tumors. Strong LIN28 staining is observed in 30 (83%) seminomas, 25 (100%) embryonal and yolk sac tumors, 19 (95%) ITGCNs and 1 (100%) choriocarcinoma without any significant difference between primary and metastatic. Teratomas showed either negative (50%) or weak (50%) staining due to presence of mature epithelial or mesenchymal tissues. Normal testicular germ cells showed mostly (95%) weak staining.

Table 1 Immunohistochemical staining of LIN28 in 52 primary testicular GCTs and 17 metastatic testicular GCTs.

Specimen Category	Primary or Metastatic	Negative	Weak Staining	Moderate staining	Strong Staining
Seminoma (n=36)	Primary	0	0	6 (17%)	29 (83%)
	Metastatic	0	0	0	1 (0%)
Embryonal Carcinoma(n=19)	Primary	0	0	0	14 (74%)
	Metastatic	0	0	0	5 (26%)
Yolk sac tumor(n=6)	Primary	0	0	0	3 (50%)
	Metastatic	0	0	0	3 (50%)
Teratoma(n=14)	Primary	3 (25%)	1 (8%)	0	0
	Metastatic	3 (25%)	5 (42%)	0	0
Choriocarcinoma(n=1)	Primary	0	0	0	0
	Metastatic	0	0	0	1 (100%)
ITGCN(n=19)		0	0	1 (5%)	19 (95%)
Normal testicular tissue (n=19)		1 (5%)	18 (95%)	0	0

Conclusions: LIN28 cytoplasmic expression by immunohistochemistry increases from complete negativity in mature epithelial cells, weak staining in normal testicular germ cells to moderate to strong staining in neoplastic germ cells. LIN28 can be used as highly sensitive marker to diagnose both primary and metastatic testicular germ cell tumors, particularly intratubular germ cell neoplasias, classical seminomas, embryonal carcinomas, yolk sac tumors and choriocarcinomas. It could also be used in identifying the mixed germ cell components within teratomas.

906 Immunohistochemical Expression of SALL4 in Hepatocellular Carcinoma, a Potential Pitfall in the Differential Diagnosis of Yolk Sac Tumors

B Katz, ND Gonzalez-Roibon, A Chau, R Sharma, GJ Netto, M Torbenson. The Johns Hopkins University SOM, Baltimore, MD.

Background: SALL4 is a transcription factor that has been used as a marker for testicular germ cell tumors, including yolk salk tumor (YST). YST displays several histological patterns, including a hepatoid pattern that can resemble hepatocellular carcinoma (HCC). Given that both neoplasms share the expression of markers such as alpha-feto protein and glypican 3, SALL4 could prove to be of utility in resolving such a differential diagnosis. Previous studies have suggested that HCC is negative for SALL4. The current study evaluates SALL4 expression in a large series of HCC.

Design: Seventy-two formaline-fixed paraffin-embedded samples of HCC were retrieved from our surgical pathology archives and used to construct a set of nine tissue microarrays. Paired tumor and nonneoplastic liver parenchyma samples were spotted in 4-8 cores each. SALL4 expression was evaluated using standard immunohistochemistry (Sigma, SALL4 clone 6c3). Percentage and patterns of nuclear expression were assessed in each spot. Mean percent expression was calculated for each tumor. A cut off of 5% or more was used to indicate a positive SALL4 result.

Results: SALL4 expression was not identified in any of the nonneoplastic liver samples (0%). In contrast, 17/72 HCC (24%) were positive for SALL4. The pattern of nuclear expression in HCC was diffuse in 2 positive cases and punctuate/clumped in the remaining 15. Overall, positive cases of HCC showed strong (2+ or 3+) SALL4 expression.

Conclusions: This is the first report of positive expression of SALL4 in HCC (24%). This finding should be taken into consideration in the differential diagnosis of HCC vs YST. The unusual punctuate/clumped pattern seen in our HCC cases has not been previously described in YST and appears to be the most frequent pattern of nuclear expression in HCC. The significance of the latter pattern of staining requires further study.

907 Differential Expression of SPINK1 in Urothelial Neoplasia: Clinical and Pathological Implications

KR Kawaguchi, K Park, A Chinnaiyan, M Loda, BD Robinson, R Lis, DS Scherr, JE Rosenberg, MA Rubin, JM Mosquera. Weill Cornell Medical College, New York, NY; University of Michigan, Ann Arbor, MI; Dana Farber Cancer Institute; Harvard Medical School, Boston, MA.

Background: High serum level/tissue expression of SPINK1 (Serine protease inhibitor Kazal type I; Tumor associated trypsin inhibitor [TATI]) have been associated with poor outcome in epithelial malignancies. SPINK1 defines an aggressive *ETS*-negative prostate cancer (PCa) and transcripts can be detected in urine. Recent data suggest that loss of SPINK1 expression in urothelial carcinoma of bladder (UCB) may be associated with advanced stage. SPINK1 is also a potential therapeutic target, given structural similarities with EGF. We assessed the expression of SPINK1 in a wide selection of urothelial neoplasia and benign urothelium.

Design: Tissue microarrays (TMAs) of 390 tissue samples from bladder (n=373), kidney/ureter (n=9), prostatic urethra (n=6) and metastatic sites (n=2) were studied. These included biopsies and resections of high-grade urothelial carcinoma (HGUC) (n=134; 97 invasive) and lymph node metastases (n=2); low-grade urothelial carcinoma (LGUC) (n=77); papillary urothelial neoplasm of low malignant potential (PUNLMP) (n=1); inverted papilloma (IP) (n=4); urothelial carcinoma *in situ* (CIS) (n=83); neuroendocrine carcinoma of bladder (NECB) (n=4); bladder squamous cell carcinoma (n=3); urothelial dysplasia (UD) (n=13); urothelial atypia (UA) (n=18); papillary cystitis (n=1); radiation cystitis (n=1); and normal urothelium (n=49).

Semi-quantitative SPINK1 IHC evaluation was performed: >20% staining extent and 2-3 intensity (scale 0 to 3) was considered positive.

FISH was performed in 116 cases using SPINK1 locus/control and 5'/3' split probes.

Results: SPINK1 overexpression was present in 50% of HGUC with loss of expression in 55% of invasive tumors. SPINK1 overexpression was present in 53% of LGUC and in a PUNLMP, 82% of CIS, 31% of UD, 22% of UA, 50% of NECB, and 33% of SCC. The inverted papillomas were negative. SPINK1 expression was seen in umbrella cells of normal urothelium (76%) and papillary and radiation cystitis. SPINK1 overexpression was also noted in urothelial samples from kidney/ureter and prostatic urethra. SPINK1 amplification or gross rearrangements were not seen by FISH.

Conclusions: SPINK1 is expressed in a wide range of urothelial neoplasia and in umbrella cells of benign urothelium. This should be considered if urine-based tests for detection of SPINK1 in both urothelial and prostatic carcinomas are implemented. SPINK1 appears to be a very specific marker of CIS. Loss of SPINK1 expression, especially in invasive tumors, is noteworthy.

908 Individual Core Length, but Not Total Number of Cores or Total Core Length, Is Associated with Gleason Score Upgrading at Radical Prostatectomy in Patients Eligible for Active Surveillance

KR Kawaguchi, MP Herman, K Park, A Srivastava, AK Tewari, JM Mosquera, BD Robinson. Weill Cornell Medical College, New York.

Background: Active surveillance (AS) of prostate cancer is becoming an increasingly attractive option for men with potentially indolent disease who wish to avoid the risk of treatment side effects. While several studies have looked at the effect of biopsy number and quality on the detection of cancer and on Gleason score (GS) upgrading at radical prostatectomy, few have evaluated these parameters specifically in patients who are candidates for active surveillance. Moreover, none have examined the length of each needle core as a potential marker of biopsy quality in selecting patients for AS.

Design: This study included 79 patients who underwent radical prostatectomy (RP) at our institution but were candidates for active surveillance based upon Epstein criteria (≤ 2 cores involved, $\leq 50\%$ involvement of any core, $GS \leq 6$, and PSA density < 0.1 ng/ml). 55 of these men had GS 6 and organ confined (pT2) disease at RP ("control group"), while 24 had GS 7 and PT2 disease at RP ("upgraded group"). Number of cores taken, number of cores/core fragments received in pathology, and length of each core/core fragment was recorded for each case.

Results: Control and upgraded groups had an average of 19.4 (range: 6-43) and 17.2 (range: 4-49) cores taken per case, respectively (p=0.08). Core/core fragments received in pathology averaged 23.0 (range: 27-56) for the control and 21.3 (range: 5-70) for the upgraded groups (p=0.07). Mean (\pm SD) total length of tissue examined was 27.4 (± 13) mm and 23.1 (± 16) mm in the control and upgraded groups, respectively (p=0.2). However, average core length was 1.19 (± 0.55) mm in the control group versus 1.09 (± 0.58) mm in the upgraded group (p<0.0005). Other variables, including age, BMI, clinical stage, number cores positive, % core involvement, and pre-op PSA, did not differ between the two groups.

Conclusions: Although the number of cores taken, rate of core fragmentation, and total length of tissue examined did not differ between the control and upgraded groups, the length of individual cores did differ significantly between the two groups. These findings reaffirm the need for high quality biopsy technique in selecting patients for active surveillance, as suboptimal biopsy cores may be undersampling more central and anterior regions of the prostate and thus missing detection of higher GS cancer.

909 Utility of Minichromosome Maintenance Protein 2 (MCM 2) and Topoisomerase II-alpha (TOP2A) Immunohistochemical Staining in the Diagnosis of Neoplastic and Non-Neoplastic Urothelial Lesions

S Kerkoutian, JY Rao, SK Apple, D Lu, G Galliano, NA Moatamed. University of California Los Angeles, Los Angeles, CA.

Background: Occasionally, morphologic distinction of neoplasia or dysplasia from reactive changes in the bladder can be challenging. ProEx C is a novel biomarker cocktail containing antibodies against topoisomerase II alpha and minichromosome maintenance protein 2. These two proteins are overexpressed in the cell nucleus during aberrant S-phase induction of the neoplastic cells and in HPV infected cells. Studies have demonstrated the utility of ProEx C as an adjunct marker for assessing dysplasia in gynecologic specimens and cervical smears. The goal of this study is to evaluate the utility of ProEx C as an adjunct marker in distinguishing neoplastic and non-neoplastic urothelial lesions.

Design: Sixty-four bladder biopsy or cystectomy specimens were evaluated (29 high grade urothelial carcinoma (HGUC) including 4 carcinoma in situ (CIS), 13 low grade papillary urothelial carcinoma (LGPUC), and 22 benign/denuded). Four-micrometer thick serial sections of formalin-fixed, paraffin-embedded tissue were cut and mounted on positively charged glass slides. Immunohistochemical staining for ProEx C with appropriate positive and negative controls was performed. A nuclear staining pattern which extended above one-half of the thickness of urothelium or more than 10% of the cells was scored as positive. No staining, staining at the base of the urothelium, or less than 10% staining of the cells was scored as negative.

Results: All of the benign/denuded cases (0/22) stained negative for Pro Ex C. All of the HGUC and carcinoma in situ (CIS) cases (29/29) stained positive. Most of the LGPUC cases (11/13) stained positive for Pro Ex C. The sensitivity, specificity, positive predictive value (PPV), and negative predictive value (NPV) for ProEx C immunostaining were 95.2%, 100%, 100%, and 91.7%, respectively.

ProEx C Immunohistochemical Staining in Urothelial Lesions

	HGUC	LGPUC	Benign
Histology	29	13	22
ProEx C	29	11	0

Conclusions: ProEx C immunohistochemical staining has high sensitivity and high specificity for the diagnosis of HGUC and CIS. The sensitivity is slightly lower in LGUC. ProEx C appears to be a valuable marker in conjunction with morphology for distinguishing HGUC from reactive benign or denuded urothelium.

910 SPINK1 Expression in Bladder Urothelial Carcinoma *In Situ*: Important Clinical Implications

F Khani, K Park, Y-L Chiu, BD Robinson, MA Rubin, JM Mosquera. Weill Cornell Medical College, New York.

Background: Diagnosis of urothelial carcinoma *in situ* (CIS) can be challenging at times, particularly on small bladder biopsies. p53 overexpression, aberrant CK20 expression and reduced CD44 expression have been used as diagnostic aids in CIS with variable results. Based on our preliminary observations in tissue microarrays, we assessed the utility of SPINK1 immunohistochemistry (IHC) in the diagnosis of CIS and urothelial dysplasia in clinical specimens.

Design: 159 bladder specimens including 106 biopsies, 32 cystectomies, and 21 transurethral resections from 108 men and 51 women, age 39 to 94 years old were studied. IHC was performed using a monoclonal antibody for SPINK1 (Abnova). Two pathologists performed semi-quantitative IHC evaluation: more than 20% staining extent and 2-3 intensity (scale 0 to 3) was considered positive. Expression in CIS (n=82) was compared to urothelial dysplasia (n=13) and urothelial atypia (n=18). Benign urothelial samples (n=46) were used as controls, including cases of papillary cystitis, radiation cystitis, and cystitis cystica. SPINK1 results were compared with p53 expression in a subset of CIS (n=33), urothelial dysplasia (n=7), urothelial atypia (n=6) and benign controls (n=4).

Results: SPINK1 overexpression was seen in 74/82 CIS cases (90%), 7/13 dysplasia cases (54%), 3/18 urothelial atypia cases (17%), and 3/46 benign control cases (6.5%). In the subset group, p53 overexpression was seen in 23/33 CIS cases (70%), 5/7 dysplasia cases (71%), 5/6 urothelial atypia cases (83%), and 1/4 benign control cases (25%). SPINK1 staining was observed only in the umbrella cells in 40% of the benign controls, including in the cases of papillary cystitis, radiation cystitis, and cystitis cystica. For detection of CIS or urothelial dysplasia, SPINK1 IHC showed a sensitivity of 85% and specificity of 91%. In contrast, p53 IHC had a sensitivity of 70% and specificity of 40%. Used in combination, these two biomarkers have a sensitivity and specificity of 88% and 85%, respectively, for the detection of CIS and urothelial dysplasia.

Conclusions: We found SPINK1 to be a highly sensitive and specific marker for urothelial CIS and urothelial dysplasia. While it shows a similar sensitivity to p53, our study reveals that it is more specific. Positive SPINK1 expression may be helpful to distinguish CIS and urothelial dysplasia from atypical lesions, particularly in small bladder biopsies. We are currently planning validation studies incorporating either SPINK1 alone, or in combination with p53, as an additional diagnostic tool in routine practice.

911 MAGE-A Expression Is Associated with Features of Biologically Aggressive Urothelial Carcinoma of the Bladder

F Khani, EK Cha, B Volkmer, M Rink, YT Chen, DS Scherr, MA Rubin, JM Mosquera, RE Hautmann, K Kuefer, SF Shariat, BD Robinson. Weill Cornell Medical College, New York; Klinikum Kassel, Kassel, Germany; Hospital Ulm, Ulm, Germany.

Background: Cancer/Testis (CT) antigens comprise a group of immunogenic proteins that are normally expressed only in germ cells but are aberrantly activated in a variety of malignancies, including urothelial carcinoma of the bladder (UCB). MAGE-A, a member of the CT multigene family, is believed to encode a transcriptional regulator that

potently inhibits p53 function. Previous studies have shown that CT antigen expression, including MAGE-A, is more common in high-grade and advanced stage UCB. We sought to further elucidate the association of MAGE-A expression with pathologic features of UCB and clinical outcomes of patients treated with radical cystectomy (RC). **Design:** We evaluated a tissue microarray (TMA) containing samples from 361 consecutive UCB patients treated with RC between 1988 and 2003 at one academic center. In addition, 16 normal urothelium, 49 corresponding TUR specimens, and 92 corresponding lymph node (LN) metastases were analyzed. MAGE-A immunohistochemical staining was performed using a monoclonal antibody (6C1). Semi-quantitative MAGE-A expression was evaluated by two pathologists who were blinded to clinical outcome.

Results: MAGE-A was expressed in 152/361 (42.1%) RC-specimens, 20/49 (40.8%) TUR-specimens, and 38/92 (41.3%) LN metastases. No staining in benign urothelium was observed. MAGE-A expression was significantly associated with advanced clinical stage (p=0.01), pathological tumor stage (Ta/Tis=0%, T1=26%, T2=43%, T3=43%, T4=51%; p=0.02), and presence of lymph node metastasis (LN- 38% vs. LN+ 49%; p=0.04) but not tumor grade (p=0.25). After adjusting for the effects of established pathological features (stage, grade, LN metastasis), MAGE-A expression was not associated with disease recurrence (p=0.56) or cancer-specific mortality (p=0.56) at a median follow-up of 130 months. High concordance in MAGE-A expression between corresponding RC and TUR specimens (75%, p<0.001) and between corresponding RC and LN metastases (88%; p<0.001) was observed.

Conclusions: MAGE-A is expressed in >40% of high-risk UCB specimens at RC, and its expression is associated with advanced pathologic tumor stage and presence of LN metastases. Thus, MAGE-A expression, in combination with additional biomarkers, may identify patients with biologically aggressive disease and aid in selecting candidates for neoadjuvant chemotherapy. Incorporation of MAGE-A staining within a panel of other prognostic biomarkers is currently underway in this cohort.

912 Differences in *TMPRSS2-ERG* Gene Fusion, *PTEN* Deletion, and *SPINK1* Overexpression in Prostate Cancer in African-American and Caucasian Men

F Khani, JM Mosquera, K Park, A Srivastava, AK Tewari, MA Rubin, BD Robinson. Weill Cornell Medical College, New York.

Background: Prostate cancer (PCa) is known to exhibit differences among racial/ethnic groups, with African-Americans (AA) having a higher incidence and mortality from the disease than that observed in Caucasians (CAU). Although socioeconomic factors may contribute to these differences, underlying genetic differences are believed to play a role as well. In particular, *TMPRSS2-ERG* gene fusions, which are present in approximately 50% of PCa overall, have not been studied in large cohorts of AA patients. Similarly, while overexpression of *SPINK1* and deletion of *PTEN* have been associated with more aggressive PCa, differential expression in patients of different ethnicities has yet to be characterized.

Design: A tissue microarray (TMA) was constructed containing tumor samples from 105 AA men who underwent radical prostatectomy (RP) at our institution. The control group was derived from a cohort of 112 PCa from CAU men treated by RP at the same institution. Clinical and pathologic characteristics of the two groups were similar. *SPINK1* overexpression was evaluated by IHC using a monoclonal antibody. Any positive staining was considered overexpressed. *TMPRSS2-ERG* gene fusion and *PTEN* deletion were evaluated by FISH.

Results: *TMPRSS2-ERG* gene fusions were identified in 48/112 tumors (42.9%) in the control group of CAU men. In the AA cohort, however, *TMPRSS2-ERG* gene fusions were found in 28/105 tumors (26.7%; p<0.02). There was no significant difference in the mechanism of gene fusion between the two cohorts (translocation vs. translocation with deletion). Deletion of *PTEN* was seen in 16/95 tumors (16.8%) in CAU men while only 7/101 tumors (6.9%) in AA men (p<0.05). *SPINK1* overexpression was present in 24/105 tumors (22.9%) from AA patients in contrast to 11/106 tumors (10.4%) from CAU patients (p<0.02). *ERG* gene fusion and *SPINK1* overexpression were mutually exclusive in all cases. Furthermore, no deletion of *PTEN* was seen in the *SPINK1* positive tumors.

Conclusions: Although clinical and pathologic factors in these AA and CAU cohorts were similar, molecular abnormalities between the two groups differed significantly. Our findings suggest possible pathobiologic differences between prostate cancers from AA and CAU men, with *TMPRSS2-ERG* gene fusion and *PTEN* deletion playing a lesser role and *SPINK1* overexpression a larger role in AA as compared to CAU men. Further studies with clinical outcome data are needed in order to determine if these molecular differences explain, at least partially, the differences in incidence and mortality between these two racial groups.

913 Exploring the Role of miRNAs in Renal Cell Carcinoma Progression and Metastasis through Bioinformatic and Experimental Analyses

HWZ Khella, NMA White, H Faragalla, M Gabriel, M Boazak, D Dorian, B Khalil, TT Bao, MD Pasic, RJ Honey, R Stewart, KT Pace, GA Bjarnason, M Jewett, GM Yousef, Li Ka Shing Knowledge Institute of St. Michael's Hospital, Toronto, ON, Canada; University of Toronto, Toronto, ON, Canada; London Health Sciences Centre, London, ON, Canada; St. Michael's Hospital, Toronto, ON, Canada; Sunnybrook Odette Cancer Center, Toronto, ON, Canada.

Background: Metastasis results in most of the cancer deaths in RCC. miRNAs regulate many important cell functions and play an important roles in tumor development, metastasis and progression. In our previous study, we identified, through microarray analysis, a miRNA signature for metastatic RCC.

Design: We validated the top differentially expressed miRNAs on matched primary and metastatic ccRCC pairs by quantitative reverse transcription-polymerase chain reaction (qRT-PCR). We performed bioinformatics analyses including target prediction and

combinatorial analysis of previously reported miRNAs involved in tumour progression and metastasis. In addition, we examined the co-expression of the miRNAs clusters and compared the expression patterns of intronic miRNAs and their host genes.

Results: We observed significant dysregulation between primary and metastatic tumours from the same patient. This indicates that, at least in part, the metastatic signature develops gradually during tumour progression. We identified metastasis-dysregulated miRNAs that can target a number of genes previously found to be involved in metastasis of kidney cancer as well as other malignancies. In addition, we found a negative correlation of expression of miR-126 and its target VEGF-A. Cluster analysis showed that members of the same miRNA cluster follow the same expression pattern, suggesting the presence of a locus control regulation. We also observed a positive correlation of expression between intronic miRNAs and their host genes, thus revealing another potential control mechanism for miRNAs. Many of the significantly dysregulated miRNAs in metastatic ccRCC are highly conserved among species.

Conclusions: Our analysis suggests that miRNAs are involved in ccRCC metastasis and may represent potential biomarkers for kidney cancer metastasis.

914 Prognostic Relevance of mTORC1 Pathway Components in Papillary Renal Cell Carcinoma

M Kherad Pezhouh, D Rakheja, RF Yousser, Y Lotan, V Margulis, P Kapur. University of Texas Southwestern Medical Center, Dallas, TX.

Background: The mammalian target of rapamycin complex 1 (mTORC1) pathway is dysregulated in many human cancers and agents targeting the mTORC1 are being clinically used. mTORC1 pathway interacts with effectors of cell cycle progression and ultimately regulates protein translation and cell proliferation. We undertook this study to ascertain if Papillary Renal Cell Carcinoma (PRCC) demonstrates significant expression of mTORC1 pathway components and if the expression of activated mTORC1 has any prognostic significance.

Design: Standard immunohistochemical analysis was performed for p-S6, p-mTOR, p-4EBP1, HIF-1 α , p-AKT, PI3K, PTEN on sections of tissue microarrays constructed from 76 primary PRCC treated at our hospital with nephrectomy (1998-2008). Duplicate 1.0 mm cores of representative tumor were obtained from each case to construct the tissue microarrays. Cytoplasmic expression was assessed for each marker as the percentage of positive cells (0-3) and intensity of staining (0-3). A final Histo-score was calculated as the product of intensity and percentage and correlated with clinicopathologic parameters using T-test, Fisher's exact test, Pearson's correlation, or log-rank (Mantel-Cox) test.

Results: In our cohort, M:F ratio was 3.00 and mean age at diagnosis was 58.67 years. Mean tumor size was 5.08 cm. Fuhrman's nuclear grade was G1 in 7, G2 in 41, G3 in 25, and G4 in 3 cases. 9 (11.84%) patients had high pathologic stage (pT3-4), 10 (13.16%) developed subsequent metastases/ recurrence, and 5 (6.58%) died of the disease. Compared to normal proximal renal tubules, we found increased expression of p-S6 in 14 (18.4%) tumors, p-mTOR in 70 (92.1%), p-4EBP1 in 43 (56.6%), HIF-1 α in 34 (44.7%), PI3K in 40 (52.6%), and p-AKT in 41 (53.9%). PTEN expression was reduced in 40 (52.6%) tumors. Increased expression of p-S6 was significantly associated with higher tumor grade (P=0.03). Higher grade tumors also showed reduced expression of HIF-1 α (P=0.01) and increased expression of PTEN (P=0.00). There was a trend for tumors with metastases/ recurrence to show higher expression p-S6 (P=0.08). Increased expression of p-S6 also correlated with poor patient survival (P=0.01).

Conclusions: In this current work in clinically annotated PRCC where the patients had received no previous treatment, we found that increased expression of p-S6 correlates with higher grade, metastases, and poor patient outcome. Our results support consideration of therapeutically targeting mTORC1 pathway in PRCC.

915 Significance of Hormone Receptor and Ki-67 Labeling Index in Angiomyolipoma: A Clinicopathological and Immunohistochemical Study of 23 Cases

M Kim, H-J Lee, M-K Yeo, Y-s Lee, DY Kang. Chungnam National University School of Medicine, Daejeon, Korea.

Background: Angiomyolipoma (AML) is an uncommon renal tumor. Classically, it is composed of three distinct components; mature adipocytes, smooth muscle cells, and thick-walled blood vessels. It has recently been referred to as one of the perivascular epithelioid cell tumor (PEComa) family. We investigated hormonal receptor expression, other immunohistochemical (IHC) profiles (HMB-45, Bcl-2, and Ki-67 labeling index), and clinical information of 23 cases of AML.

Design: All the AML cases were retrieved from the archives of the CNUH from 2000 to 2010. 23 cases were found and among these, 3 cases underwent radiofrequency ablation were excluded for IHC study. Two tissue microarrays for each case consists of 2mm cores and IHC study for estrogen receptor alpha, progesterone receptor, HMB-45, Bcl-2, and Ki-67 was performed. Statistical analyses were done using the *t* test and ANOVA test with *p* values <0.05 considered statistically significant.

Results: Among 23 cases, none of them was related to the tuberous sclerosis complex. 17 of them discovered the renal mass incidentally while their routine examination; 5 of them had flank pain; 1 had gross hematuria. Other clinical features are remarked on the Table1. The results of IHC study revealed as follows: ER (6/20, 30%) PR (11/20, 55%) HMB-45 (19/20, 95%) Bcl-2 (17/20, 85%) ki-67 labeling index (13/20, 65%, range 1~20%). One case showed atypical histopathologic feature consistent with epithelioid AML. This case showed a large mass (9cm) and metastatic lesion to the mediastinum was diagnosed radiologically. No biopsy was done from the mediastinal mass. This case showed high Ki-67 labeling index (20%) and positive ER and PR expression as well as HMB-45 and Bcl-2.

Clinical and Pathologic Features of Angiomyolipoma of the Kidney.

Sex	Male	3
	Female	20
Mean age (vs) (range)	54.8 (36-75)	
Tumor location	Right kidney	15
	Left kidney	8
Size (cm) (range)	6.4 (1.5-22)	
Pathologic diagnosis	Classical AML	22
	Epithelioid AML	1

AML=Angiomyolipoma

Conclusions: Although, some previous reports have claimed that high Ki-67 index correlates with the epithelioid AML, we found no relationship between them. One epithelioid AML case from our study showed high Ki-67 labeling index, but some of classical AML also showed Ki-67 labeling index more than 10% of the cells. However, it was strongly associated with the ER and PR expression (*p*<0.05). This suggests the possibility of relationship between hormonal receptor expression and tumor growth.

916 Papillary Urothelial Neoplasm of Low Malignant Potential and Carcinoma with Extensive Urothelial "Eddy" Formation (pUNC-eUEF): A Distinct Morphologic Pattern with Low Risk for Progression

M-s Kim, JY Ro, YM Cho. University of Ulsan College of Medicine, Asan Medical Center, Seoul, Korea; The Methodist Hospital and Weill Medical College of Cornell University, Houston, TX.

Background: Urothelial carcinoma (UC) is the most common urinary bladder tumor with variable clinical outcome. We encountered papillary urothelial neoplasm of lower malignant potential (PUNLMP) and UC showing extensive urothelial "eddy" formation (pUNC-eUEF), superficially resemble to squamous eddy seen in inverted follicular keratosis of the skin, of which clinicopathologic features have not been reported yet.

Design: Among 756 patients that underwent transurethral resection of bladder tumor at Asan Medical Center, Seoul, Korea from 1996 to 2006, 10 cases demonstrated pUNC-eUEF, in which their clinicopathologic features and immunoprofile were analyzed. As control groups for comparison of immunohistochemical staining results, 22 cases of classic UC matched for stage and grade of pUNC-eUEF, 9 cases of UC with squamous differentiation (UC-Sq), and 9 cases of squamous cell carcinoma of urinary bladder (SqCC-UB) were included.

Results: All pUNC-eUEF were male with a mean age of 65.4 years (range, 52~79years). pUNC-eUEF consisted sheets or nests of large polygonal cells with prominent whirling pattern and intercellular bridges without evidence of keratinization. They were graded as PUNLMP (one case), low grade UC (eight) and high grade UC (one). All but one presented with non-invasive tumors (Ta) with only one case invaded subepithelial connective tissue (T1). pUNC-eUEF revealed immunoprofile of cytokeratin 7 and 20, p63, uroplakin-3, E2F1, D2-40, p53, and prostate acid phosphatase similar to UC rather than UC-Sq or SqCC-UB with the lowest Ki-67 labeling index (mean, 1.6%), compared to the control groups. During the mean follow-up of 73 months, three cases of pUNC-eUEF (3 cases of low grade UC) were recurrent. However, none progressed into muscle-invasive tumor or died of the disease.

Conclusions: This study suggests that pUNC-eUEF is a rare unique morphologic variant of UC with indolent clinical course. Further studies are required to better define the clinicopathologic parameters of this variant.

917 Subcellular Localization of DC-SCRIPT Correlates with Histologic Type, Grade and Stage of Renal Cell Carcinomas (RCC)

K-A Kim, JL Garbaini, RN Al-Rohil, CE Sheehan, RP Kaufman, JS Ross, A Hayner-Buchan. Albany Medical College, Albany, NY.

Background: Dendritic cell specific transcript (DC-SCRIPT) is a novel protein first discovered in dendritic cells encoded by an 8-kb mRNA transcription co-regulator which binds to multiple hormones and plays a key role in physiologic processes including cell growth and differentiation. Although previously linked to clinical outcome in breast cancer, DC-SCRIPT has not been previously studied as a prognostic factor for RCC.

Design: Tissue sections from 146 formalin-fixed, paraffin-embedded RCCs (119 clear cell type [CC] and 27 other types) were immunostained by an automated method (Ventana Medical Systems Inc., Tucson, AZ) using goat anti-human DC-SCRIPT/ZNF366 antibody (R&D Systems, Minneapolis, MN). Cytoplasmic and membranous immunoreactivity based on intensity and distribution was semiquantitatively scored and the results were correlated with clinical and morphologic variables.

Results: Cytoplasmic DC-SCRIPT overexpression was noted in 46 (32%) tumors and correlated with tumor type (87% papillary vs 24% CCs vs 38% others *p*<0.0001), high grade (60% G4 vs 42% G3 vs 14% G2 vs 0% G1, *p*<0.0001 overall; 53% G4 vs 39% G3 vs 10% G2 vs 0% G1, *p*<0.0001 CCs), and advanced stage (43% IV vs 26% III vs 60% II vs 26% I, *p*=0.022 overall; 43% IV vs 23% III vs 56% II vs 14% I, *p*=0.002 CCs). Membranous DC-SCRIPT overexpression was noted in 82 (56%) tumors and correlated with tumor type (61% CCs vs 33% others *p*=0.008) and low grade (60% G1 vs 63% G2 vs 65% G3 vs 25% G4, *p*=0.013 overall; 60% G1 vs 67% G2 vs 69% G3 vs 20% G4, *p*=0.006 CCs). There was no significant coexpression of cytoplasmic and membranous immunoreactivity. On multivariate analysis, high tumor grade (*p*=0.003) and advanced stage (*p*=0.018) independently predicted overall survival.

Conclusions: The association of cytoplasmic DC-SCRIPT immunostaining with non-clear cell histology and high tumor grade and stage, and membranous DC-SCRIPT with clear cell histology and low tumor grade supports recent studies that associate different biological functions of proteins with their subcellular localization. The associations of DC-SCRIPT expression in RCC with tumor type, grade and stage suggest that this biomarker has both potential diagnostic and prognostic significance in RCC and warrants further study.

918 Prognostic Relevance of mTORC1 Pathway Components in Chromophobe Renal Cell Carcinoma

T Kinard, D Rakheja, RF Youssef, Y Lotan, V Margulis, J Sugianto, P Kapur. University of Texas Southwestern, Dallas, TX.

Background: The mammalian target of rapamycin complex 1 (mTORC1) pathway is dysregulated in many human cancers and agents targeting the mTORC1 are being clinical used. mTORC1 pathway interacts with effectors of cell cycle progression and ultimately regulates protein translation and cell proliferation. We undertook this study to ascertain if chromophobe renal cell carcinoma (ChRCC) demonstrates significant expression of mTORC1 pathway components and if the expression of activated mTORC1 has any prognostic significance.

Design: Standard immunohistochemical analysis was performed for p-S6, p-mTOR, p-4EBP1, HIF-1 α , p-AKT, PI3K, PTEN on sections of tissue microarrays constructed from 43 primary ChRCC treated at our hospital with nephrectomy (1998-2008). Duplicate 1.0 mm cores of representative tumor were obtained from each case to construct the tissue microarrays. Cytoplasmic expression was assessed for each marker as the percentage of positive cells (0-3) and intensity of staining (0-3). A final Histo-score was calculated as the product of intensity and percentage and correlated with clinic-pathologic parameters.

Results: In our cohort, M:F ratio was 1.0 and mean age at diagnosis was 55.3 years. Mean tumor size was 7.0 cm. 8 (18.6%) had high pathologic stage (pT3-4), 3 (7.0%) developed metastases/recurrence, and 0 died of disease. Compared to normal proximal renal tubules, we found increased expression of p-S6 in 6 (14.0%) tumors, p-mTOR in 28 (65.1%), p-4EBP1 in 14 (32.6%), HIF-1 α in 41 (95.3%), PI3K in 12 (27.9%), and p-AKT in 13 (30.2%). PTEN expression was reduced in 29 (67.4%) tumors. Two tail t-test showed increased expression of p-S6 (P=0.04), p-4EBP1 (P=0.00), and p-AKT (P=0.04) to be significantly associated with higher stage. In addition, there was a trend for higher stage tumors to show higher expression of PI3K (P=0.06).

Conclusions: In this current work in clinically annotated ChRCC where the patients had received no previous treatment, we found that increased expression of pS6, p-4EBP1, p-AKT, and PI3K correlates with higher tumor stage. Our results support consideration of therapeutically targeting PI3K/AKT/mTORC1 pathway in ChRCC.

919 p63 Immunohistochemistry in Histologic Variants of Urothelial Cell Carcinoma

J Klapper, G-Q Xiao, PD Unger. The Mount Sinai Medical Center, New York, NY.

Background: Urothelial carcinoma (UC) occurs in a variety of histologic subtypes. p63, a member of the p53 family of transcription factors, is one of the most commonly used urothelial markers. There has been no prior systematic study regarding p63 immunohistochemical expression in histologic variants of UC.

Design: A total of 41 invasive UCs of different morphologic variants collected at our institution were stained with p63 monoclonal antibody (BioGenex, San Ramon, CA). Among the 41 UCs, 22 were of one morphologic variant and 19 contained more than one morphologic variant. For cases with more than one morphologic variant, each individual variant was counted as a separate event. In addition to p63, the two plasmacytoid UC cases were also stained with CD138 antibody (BioGenex, San Ramon, CA). Positive immunostaining was defined as uniform nuclear reactivity for p63 and cytoplasmic membrane staining for CD138.

Results: The results of p63 immunostaining are summarized in the table.

Histologic Variant	p63 positive cases/Total cases
Conventional	13/13
Clear cell	5/5
Microcystic	5/5
Sarcomatoid	4/4
Nested	4/4
Squamous	3/3
Small cell/neuroendocrine	2/2
Plasmacytoid	2/2
Rhabdoid	1/2
Micropapillary	0/7
Glandular/adenocarcinoma	0/6
Signet ring	0/2

Micropapillary, glandular and signet ring cell UCs were consistently negative for p63. Of the two rhabdoid variant cases, one was negative for p63. All other variants and conventional UC cases were consistently reactive with p63. The two cases of plasmacytoid UC were also positive for CD138; however, the coexisting conventional UC, carcinoma in-situ and normal urothelium in these same cases were also strongly positive for CD138.

Conclusions: The results of this study indicate that p63 is a sensitive marker for most UC variants, with the exception of the micropapillary, glandular, and signet ring cell variants, which were consistently negative for p63. Awareness of this exception is of importance, especially in the evaluation of metastatic disease possibly arising from urinary tract. Although CD138 has been reported as a marker for plasmacytoid UC, our preliminary study demonstrated strong staining for CD138 in conventional UC as well as benign urothelium, which has not been previously documented. This preliminary data indicates that CD138 may not be specific for plasmacytoid UC, and should not be used in isolation to determine or characterize this variant.

920 Prostate Cancer in Patients over Age 70 Treated by Radical Prostatectomy: Clinicopathologic Features and Outcome

J Ko, SM Falzarano, E Walker, K Streater Smith, EA Klein, M Zhou, C Magi-Galluzzi. Cleveland Clinic, Cleveland.

Background: Prostate cancer (PCA) is an increasingly important and controversial health care issue in aging populations. Consensus on screening recommendations in older men is lacking. We evaluated clinicopathologic features and outcome of patients (pts) >70 years who underwent radical prostatectomy (RP).

Design: Clinicopathologic features and follow-up (FU) data of RP pts diagnosed with PCA (2000-2011) were recorded. Pts given neoadjuvant therapy were excluded. Biochemical recurrence (PSAR) was defined as PSA >0.3 ng/ml after RP. Association between preoperative features (age, PSA, clinical stage [cT], biopsy [Bx] 1^o and 2^o Gleason pattern, Bx Gleason score [GS], highest percentage of core involvement [%hci]) and incidence of extraprostatic extension (EPE) was evaluated in univariate and multivariate analyses. Associations between postoperative features (RP GS, EPE, seminal vesicle involvement [SVI], margin of resection [MOR], pathologic stage [pT], tumor volume [TV]) and PSAR were evaluated in univariate analysis.

Results: 184 pts were >70 years old. Median age and preoperative PSA was 72 years and 6.00 ng/ml. Bx GS, cT (available in 183 pts), risk stratification by D'Amico criteria, RP GS, EPE, SVI, MOR, pT, and TV are displayed in Table 1. %hci was >50% in 70 (40%) and \leq 50% in 106 (60%). Median FU was 12.5 months (range 1-130). PSAR occurred in 14 (9%) pts. In univariate analysis, cT, Bx 1^o Gleason pattern, Bx GS, %hci >50, and D'Amico groups were significantly associated with EPE (p<0.05). In multivariate analysis Bx GS and %hci >50 retained significance. Univariately, RP GS, EPE, MOR status, and pT were significantly associated with presence of PSAR (p<0.05).

Conclusions: PCA in elderly population shows parameters of aggressive disease, such as RP GS \geq 7 in >90%, EPE in 39%, pT3 in 47%, and positive MOR in 36% of pts. Although these parameters are significantly associated with PSAR, the overall recurrence rate in our study was lower than previously reported. Longer FU is necessary to better estimate the impact of PCA biology on outcome.

Table 1. Clinicopathologic features

Clinical stage (cT)	# Patients (%)
T1a	3 (2%)
T1c	129 (70%)
T2a	41 (22%)
T2b	6 (3%)
T2c	1 (1%)
T3	3 (2%)
Bx GS	
GS6	57 (31%)
GS7	89 (48%)
GS8	29 (16%)
GS9-10	9 (5%)
D'Amico risk criteria	
Low	45 (25%)
Intermediate	97 (53%)
High	41 (22%)
RP GS	
GS6	14 (8%)
GS7	115 (62%)
GS7+5	19 (10%)
GS8	17 (9%)
GS9	19 (10%)
Pathologic stage (pT)	
pT2	98 (53%)
pT3a	71 (39%)
pT3b	15 (8%)
MOR status	
Positive	66 (36%)
Negative	118 (64%)
TV (mm³)	
Low (<0.5 cc)	22 (12%)
Medium (0.5-2.0 cc)	93 (50%)
Extensive (>2.0 cc)	69 (37%)
PSAR	
No	138 (91%)
Yes	14 (9%)

921 Histopathologic and Clinical Features of Vesical Diverticula

MX Kong, X Zhao, E Kheterpal, P Lee, S Taneja, J Melamed, F-M Deng. NYU Langone Medical Center, New York, NY; New York University School of Medicine, New York, NY.

Background: Urinary bladder diverticulum, an uncommon bladder disorder, only catches clinical attention when complicated with inflammation, calculi or malignancy. Limited information is known about the histopathologic and clinical features of bladder diverticulum.

Design: We retrieved 94 cases of bladder diverticula from the archives over the past 13.5 years (1998 to 2011). Slides were reviewed to identify pathologic findings. Retrospective clinical follow-up was obtained for all cases.

Results: Patients' ages ranged from 1 to 89 (66 \pm 18) years. The ratio of male to female was 90:4. Sixty-eight of 94 (72%) patients were Caucasian, which approximated 33% in local general population. The documented diverticular sizes ranged from 0.4 to 11.4 (4.4 \pm 2.8) cm. Diverticula most often involved the lateral wall (27%), followed by the posteriolateral (25%) and posterior (19%) walls of the bladder.

Sixty-six of 94 (70%) cases showed benign processes including: inflammation (48); squamous (5) or intestinal (1) metaplasia; nephrogenic adenoma (3); low to moderate grade dysplasia (2); reactive atypia (2); focal papillary hyperplasia (2); polypoid cystitis (2) and cystitis cystica (1). Twenty-eight cases (30%) showed primary carcinomas arising from the diverticula, of which 25 cases are of urothelial carcinoma and 3 cases of rare type carcinoma (table 1).

Table 1. Histologic findings in 28 neoplastic vesical diverticula

Histologic type	Urothelial Ca	25 (89%)
	Squamous cell Ca	2 (7%)
	Adenocarcinoma	1 (4%)
Grade	Low grade	6 (21%)
	High grade	22 (79%)
Pathologic stage	Ta	7 (25%)
	Tis	4 (15%)
	T1	11 (39%)
	T3	6 (21%)

Patient follow-up for neoplastic diverticula (1-108 months) showed none of the patients died from progression of vesical carcinoma. Fifteen (54%) cases had concurrent or subsequent urothelial carcinoma in non-diverticular bladder. Four cases with subsequent extra-diverticular urothelial carcinoma showed progression, with their pathology up-staging.

Conclusions: This study represents the largest case series up to date on surgically resected bladder diverticula. Inflammation, metaplasia and dysplasia are commonly seen in vesical diverticula. Patients with bladder diverticula appear to have significantly higher risk for development of urothelial carcinoma, which can occur synchronously or precede carcinoma of the non-diverticular bladder. Of note, in comparison to their non-diverticulum-associated counterparts, a significantly higher percentage of diverticulum-associated bladder carcinoma are high grade and invasive and may have a more adverse outcome.

922 Fluorescence In Situ Hybridization (FISH) as an Adjunct Tool in the Diagnosis of Primary and Metastatic Renal Cell Carcinoma in Core Biopsy and Fine Needle Aspiration Biopsy Specimens

Z Kos, S Amin, EC Belanger, C Marginean, KT Mai. The Ottawa Hospital and University of Ottawa, Ottawa, ON, Canada.

Background: We investigated the role of FISH in the diagnosis of primary renal neoplasms and extrarenal lesions suspicious for metastatic renal cell carcinoma.

Design: 32 consecutive renal biopsies (18 core needle biopsies and 14 fine needle aspiration biopsies (FNAB) with adequate cell blocks) and 9 biopsies of suspected metastatic tumours suspicious for renal cell origin were assessed. A standard immunohistochemical panel for CK7, RCC antigen, CD10, AMACR, PAX-2, vimentin and CD117 was performed on each specimen. In addition, FISH using probes for chromosomes 1, 3p, 7, 17, X and Y were performed.

Results: 24 renal lesions demonstrated typical histopathological and immunohistochemical features of subtypes of renal neoplasms: 11 papillary renal cell carcinoma (RCC), 7 clear cell RCC and 6 renal oncocytomas. FISH revealed chromosomal abnormalities consistent with the diagnosis in 20 (83%) of these cases. 8 renal lesions demonstrated atypical histopathological features and variable reactivity for CK7, AMACR and vimentin, and weak or negative reactivity for CD10, RCC antigen, PAX-2 and CD117. FISH was helpful in subtyping 5 of these lesions: with 1 case of oncocytic papillary RCC, 1 case of mixed clear cell and papillary RCC, 2 cases of clear cell RCC and 1 case of chromophobe RCC with papillary architecture. FISH was not contributory in the diagnosis of the remaining 3 cases.

Of 9 metastatic tumors suspicious of renal cell origin (positive staining for AMACR and vimentin and weak or negative reactivity for CK7, CD10, RCC antigen, PAX-2 and CD117), chromosomal changes suggestive of papillary RCC were seen in 3 cases, and changes of mixed clear cell and papillary RCC in 2 cases.

Conclusions: FISH study of core biopsies and FNAB, even with limited amounts of tissue, may be contributory for the positive diagnosis and subtyping of RCC.

923 Ureteral and Urethral Margin Status in Radical Cystectomy Specimens

Z Kos, F Siadat, EC Belanger, BN Nguyen, KT Mai. The Ottawa Hospital and University of Ottawa, Ottawa, ON, Canada.

Background: The status of ureteral and urethral resection margins in radical cystectomy specimens, performed for urothelial carcinoma, is a source of consternation for surgeons and pathologists alike. We correlated margin status with preoperative patient factors and postoperative outcome.

Design: Consecutive radical/total cystectomy specimens for urothelial carcinoma (UC) along with the associated clinical charts were reviewed.

Results: A total of 91 specimens (Male[M]/Female[F]:76/15) were reviewed. The ureters, urethra and their respective resection margins were assessed for both in situ and invasive UC. At least one ureter was involved by in situ UC (ISUC) in 23 cases, and invasive UC in 4 cases. At least one ureteral resection margin (not including subsequent ureteral resections) was involved by ISUC in 5 cases. No invasive UC was present at any of the ureteral margins. The urethra was involved by ISUC in 36 cases, and invasive UC in 21 cases. The urethral resection margin was positive for ISUC in 5 cases and invasive UC in 2 cases.

There were 41 (M/F:38/3) specimens with involvement of either the ureter, urethra or both by in situ or invasive UC, and 8 (M/F:7/1) specimens with either ureteral, urethral or both resection margin involvement.

Of the 41 patients with ureteral/urethral involvement: a) 25 had a history of low grade UC for at least 3 years (mean: 4.5 yrs), with multiple recurrences and resections, including BCG/radiation and chemotherapy in 18 patients. 10 patients subsequently developed high grade UC and 15 patients showed focal to extensive squamous differentiation; b) 9 patients had ISUC resistant to BCG treatment for at least 2 years (mean: 3.5 yrs); and c) 7 patients had no available history.

Of 8 patients with positive resection margins, the 5 patients with positive ureteral margins (all in situ disease), regardless of the status of the urethral margin, were associated with high-stage disease (lymph node metastases in 3 cases) and death due to disease in 0-2 years in 3 patients. The 3 patients with only a positive urethral resection margin, (2

invasive and 1 in situ) had no associated perivesicular tumour extension or lymph node metastasis, and were alive for 1-3 years of follow up.

Conclusions: Patients undergoing radical cystectomy for UC were more likely to have positive ureteral (+/-urethral) resection margins following a protracted history of recurrent low grade UC with multiple resections and presented with advanced stage at radical cystectomy. Cases with only positive urethral resection margins were associated with better clinical outcome.

924 Prostate Cancer Field Effect: Common Gene Expression Alterations in Prostate Cancer and Benign Prostatic Tissue

F Kosari, CM Ida, J Karnes, SJ Murphy, G Vasmatazis, JC Chevillet. Mayo Clinic, Rochester, MN.

Background: Prostate cancer field effect alterations provide important clues regarding cancer initiation, and may provide a role in chemoprevention and early detection. Field effect biomarkers are lacking due to small sample sets used for identification of candidate markers and limited independent validation. The objective of this study was to identify common gene alterations between prostate cancer and adjacent benign tissue in a large set of patient samples and to validate these markers with an independent group of patient samples.

Design: Microarray experiments were performed using Affymetrix U133Plus2 chips on benign prostate tissues from patients free of cancer (BP; n=28), prostate cancer from radical prostatectomy specimens (PCa; n=32) and benign posterior zone prostatic tissues from radical prostatectomy specimens (BPC; n=33). The candidate biomarkers that exhibited the greatest difference in expression in PCa and BPC relative to BP were validated in an independent set of BPC (n=33) and BP (n=18) using quantitative RT-PCR. Logistic regression modeling was performed separately on both the validation sample set and microarray data set to determine highest AUC for the association of BPC and PCa. Our results were also evaluated using an external public microarray dataset.

Results: Validated biomarkers included four up-regulated genes and three down-regulated non-exonic sequences not previously associated with PCa field effect. The logistic regression model based on *CCNB1* and non-exonic sequences of *NACA* locus discriminated between benign prostate tissue from men with and without PCa in the quantitative PCR validation set with an AUC of 0.84, and the external microarray dataset achieved an AUC of 0.90.

Conclusions: This study confirms the presence of prostate cancer field effect, and identifies validated biomarkers in benign prostate tissue associated with the presence of prostate cancer in radical prostatectomy specimens. Further work is needed to determine the significance of these changes in prostate needle biopsy specimens.

925 Prognostic Significance of Patterns of Seminal Vesicle Invasion of Prostate Cancer

A Kristiansen, F Wiklund, P Wiklund, L Egevad. Karolinska Institutet, Stockholm, Sweden.

Background: Seminal vesicle invasion (SVI) is an indicator of poor prognosis of prostate carcinoma, but the outcome varies and further stratification is needed. This study aimed to evaluate the prognostic significance of histopathological patterns of SVI after radical prostatectomy.

Design: A total of 1156 men underwent radical prostatectomy at the Karolinska Hospital from 1998 to 2005. Men with neoadjuvant treatment or TURP prior to surgery or unavailable histological slides or clinical follow-up were excluded and 1051 cases remained for review. SVI was found in 5.9% (62/1051) and intraprostatic SVI in another 2.2% (23/1051). Slides were reviewed for histopathological features including Gleason score (GS) of seminal vesicle (SV) component, bilateral vs. unilateral involvement, route of invasion (Type 1: via ejaculatory duct, Type 2: direct invasion excluding ejaculatory duct, Type 3: discontinuous invasion), tumor area, largest diameters, distribution in SV (perivesicular connective tissue, muscular wall, mucosa), surgical margin status in SV and invasion of vas deferens. The association with risk for biochemical recurrence was analyzed.

Results: SVI was associated with poor prognosis (HR 1.8 [95% CI 1.2-2.8], p=0.0047) with recurrence in 40.3% (25/62), while intraprostatic SVI was not (HR 1.1 [95% CI 0.5-2.4], p=0.75). The most common route of SVI was Type 1 (83.6%), while Type 3 was found in only 2 cases. The GS of the SV component was higher than that of the main tumor in 29.5% (16/61). A GS lower than 7 in the main tumor was only seen in 2 cases and never in the SV component. Invasion of SV mucosa was seen in 66.1% (41/62) and was always accompanied by muscle wall invasion. SV mucosal invasion was strongly associated with outcome (HR 3.3 [95% CI 1.1-9.8], p=0.029), while only 20% (4/20) of men with muscle wall invasion alone experienced recurrence. Other histopathological characteristics of SVI such as measures of extent, invasion route, local margin status and local GS of the SV component did not predict outcome.

Conclusions: The prognosis of patients with SVI is not uniformly poor. Invasion of the SV mucosa portends a higher risk of recurrence than invasion of the muscle wall alone. There is no evidence that other histopathological features of SVI need to be reported.

926 Morphologic Features of 184 Gleason Score (GS) 7 Prostate Cancers (PC) with Regional Lymph Node Metastases (LN+) at Radical Prostatectomy (RP)

ON Kryvenko, N Gupta, D Schultz, J Gomez, N Virani, Z Lane, JI Epstein. Henry Ford Hospital, Detroit; University of Michigan, Ann Arbor; The Johns Hopkins Hospital, Baltimore.

Background: Only a small percentage of GS7 PC at RP has LN+ and little is known about the pathological findings associated with LN+ in these cases.

Design: We analyzed 184 GS7 LN+ RPs from 2 institutions (2000-2011). A 1:1 Gleason and stage-matched control group without LN metastasis (LN-) was used. Remote tumor foci were defined as satellites with the same morphology as in dominant tumor; otherwise they were interpreted as multifocal.

Results: The LN+ group included GS347 (n=64), GS437 (n=66), GS347 with tertiary 5 (n=10), and GS437 with tertiary 5 (n=44). Pathologic stages were: pT2 (n=16), pT3a (n=77), pT3b (n=91). No difference in age was seen between LN+ and LN- cases. Mean preoperative PSA was higher in LN+ (12.2) vs LN- (8.1) cases, p=0.001. Mean percentage of positive biopsy cores was 59.1% in LN+ compared to 42.9% in LN-, p=0.0001. LN+ cases showed more non-focal extraprostatic extension (EPE) than LN- (89% vs. 68%, p=0.0001). LN+ cases showed more GS4 poorly formed and cribriform pattern; glomeruloid, fused, and mucinous GS4 was more typical for LN- cases (all p<0.05). pT3b LN+ cases showed extensive SV invasion with EPE and lymphovascular invasion (LVI) in SV, in LN- cases tumor invaded SV focally without LVI in SV. Graded subjectively as 1-3, nuclear size (2.03 vs 1.63, p=0.0001), nucleolar size (1.63 vs 1.45, p=0.002) and distribution (1.64 vs 1.45, p=0.005) varied in LN+ vs. LN-; no difference in nuclear pleomorphism was seen. Other morphologic findings are in table (IDC = intraductal spread).

	Prostate Weight (p=0.008)	Number of LNs (p<0.0001)	Tumor Volume (p<0.0001)	LVI (p<0.0001)	IDC (p<0.0001)	pT3a/pT3b (p<0.0001)	Satellites (p=0.002)
LN+	13.4 gms.	13.4	28.9%	79.3%	42.4%	77/91	12.5
LN-	9.4 gms.	9.4	14.8%	38.9%	21.2%	142/27	3.9

Conclusions: Within GS7, there are significant differences in cases with LN+ vs. LN- in preoperative PSA, percentage of positive cores, number of LN analyzed, tumor volume, morphology of pattern 4, stage, LVI, intraductal spread, satellite tumor foci, nuclear enlargement, and size and distribution of macronucleoli. These variables may be worthwhile to assess as prognostic markers in GS7 disease on biopsy (i.e. Gleason 4 morphology, IDC, cytology) or at RP (all variables) in men without LN dissection or LN-. This study also adds to the growing body of evidence on the adverse prognosis of IDC.

927 p16 Expression Is Not Associated with Human Papillomavirus (HPV) in Urinary Bladder Squamous Cell Carcinoma

JB Kum, Y Hu, R Montironi, A Lopez-Beltran, G Chen, GT MacLennan, MT Idrees, TM Ulbright, DG Grignon, JN Eble, L Cheng. Indiana University School of Medicine, Indianapolis, IN; Polytechnic University of Marche Region (Ancona) United Hospitals, Ancona, Italy; Cordoba University, Cordoba, Spain; First Affiliated Hospital of Wenzhou Medical College, Wenzhou, China; Case Western Reserve University, Cleveland, OH.

Background: Squamous cell carcinoma of the urinary bladder is an unusual histologic type of bladder neoplasm with unknown etiology. There is a well established association between human papillomavirus (HPV) infection and the development of uterine cervical and head/neck squamous cell carcinomas. However, the role of HPV in the pathogenesis of squamous cell carcinoma of the urinary bladder is uncertain. The purposes of this study are to investigate the potential role of HPV in the development of squamous cell carcinoma of the urinary bladder and to determine if p16 expression is a surrogate marker for HPV in this malignancy.

Design: Twenty-three cases of squamous cell carcinoma of the urinary bladder and 15 cases of urothelial carcinoma with squamous differentiation are included in this study. HPV infection is analyzed by both in situ hybridization at the DNA level and immunohistochemistry at the protein level. p16 protein expression is analyzed by immunohistochemistry.

Results: HPV DNA and protein are not detected in 23 cases of squamous cell carcinoma (0%, 0/23) and 15 cases of urothelial carcinoma with squamous differentiation (0%, 0/15). p16 expression is detected in 8 cases (35%, 8/23) of squamous cell carcinoma and 6 cases (40%, 6/15) of urothelial carcinoma with squamous differentiation. There is no correlation between p16 expression and the presence of HPV infection in bladder squamous cell carcinoma and urothelial carcinoma with squamous differentiation.

Conclusions: HPV does not play a role in the development of squamous cell carcinoma of the urinary bladder and urothelial carcinoma with squamous differentiation. p16 expression should not be used as a surrogate marker for evidence of HPV infection in either squamous cell carcinoma of the urinary bladder or urothelial carcinoma with squamous differentiation as neither HPV DNA nor protein is detectable in these neoplasms.

928 Sclerosing Sertoli Cell Tumor of the Testis: A Study of 20 Cases

JB Kum, MT Idrees, TM Ulbright. Indiana University, Indianapolis, IN.

Background: Sclerosing Sertoli cell tumor (SSCT) is rare, with only 19 previously reported cases. Most have been small, circumscribed masses and none has had a malignant course, but there is limited follow-up. We have examined 20 new SSCTs to better delineate their features and report long-term follow-up.

Design: We retrieved and reviewed H&E slides from 20 cases of SSCT (15 orchiectomies, 5 excisional biopsies) from in-house and consultation files. We required at least focal tubule formation by sex cord cells in a dense, hypocellular fibrous stroma that comprised at least 50% of the lesion. Morphologic and clinical data were collected.

Results: The patients ranged from 23-52 yrs old (mean, 37). Eleven SSCTs were left sided, 7 right, 2 unknown and none bilateral. The average size was 1.7 cm (range, 0.5 to 6 cm). In most the stroma represented 50-70% of the mass but in 2 it was at least 80%. The tumors formed cords, trabeculae, small nests, focal tubules (sometimes with a pseudovascular appearance) and rarely single cells. The cells had small, round, oval to polygonal nuclei with finely granular chromatin, small nucleoli and small amounts of pale, eosinophilic cytoplasm. No significant atypia or necrosis was seen and only 1 had identifiable mitotic figures (1-2/10 hpf). Clinical follow-up in 14 patients (8 months-16 years, mean 6.8 years) showed 8 alive and well, 5 alive with unknown

disease status and 1 patient, who presented with bone metastases, dead of disease at 27 months. The only features in the fatal case that differed from all others were the presence of lymphovascular invasion and lack of circumscription. Additionally it was 3.8 cm. Combining our cases with previously reported ones shows that SSCTs are unilateral, usually small (79% ≤ 2 cm) tumors that occur in a wide age range (18-80 yrs, mean 34), lack necrosis and rarely (<5%) have elevated mitotic rates or significant atypia. Only 1 of 26 with follow-up (mean, 10 years) was clinically malignant and it was 3.8 cm with invasive growth.

Conclusions: Sclerosing Sertoli cell tumors less than 2 cm with the typical features and lacking those associated with malignancy in Sertoli cell tumors NOS (Am J Surg Pathol 22(6): 709-721,1998) have a negligible risk of metastasis. This group (~80%) is adequately managed by orchiectomy alone.

929 Massive Localised Lymphedema of the Male External Genitalia: A Clinicopathologic Study of 7 Cases

S Lee, JJ Epstein. The Johns Hopkins Hospital, Baltimore.

Background: Massive localised lymphedema is a clinical and pathologic mimic of sarcoma strongly associated with morbid obesity. The tumor most commonly involves the lower limbs as large pendulous masses. Only 4 case of massive localised lymphedema involving external male genitalia have been reported. In this study we report an additional 6 cases localised to the external male genitalia and 1 involving the spermatic cord.

Design: 7 cases were retrospectively identified from our surgical pathology database, 4 of which were from the consult files of one of the authors.

Results: Of the 7 cases, 5 were in morbidly obese patients (4 presented with diffuse scrotal edema and 1 with a penile mass). A further case of diffuse scrotal edema was associated with penile Crohn's disease in a non-obese patient. The remaining case presented as an inguinal mass associated with an inguinal hernia and spermatic cord lipoma in a non-obese patient. In all cases the clinical impression was of a benign chronic process developing over 3 months to 1 year. Four cases from outside institutions were all referred with benign pathological diagnoses. Grossly, the lesions associated with obesity were large (range 10.5 – 55 cm) in comparison to the non-obese cases (4 – 4.2 cm).



Microscopically, all cases exhibited varying degrees of stromal fibrosis and edema, multinucleated stromal cells, perivascular chronic inflammation, lymphangiectasia and microvascular proliferation. In contrast to lesions in soft tissue locations, the presence of entrapped fat was a minor feature (and seen in only 4 cases including the case involving spermatic cord lipoma). Prominent dartos smooth muscle hyperplasia was noted in six lesions.

Conclusions: Massive localised lymphedema occurring in the male external genitalia may present as either diffuse massive enlargement or less commonly as localised smaller masses. Almost all cases are associated with obesity although localised lesions may be associated with local pathology. Lesions in the male external genitalia share many microscopic findings with massive localised lymphedema in other body regions although entrapped adipose tissue is not a prominent feature. A useful additional diagnostic feature is the presence of entrapped hyperplastic dartos muscle bundles within the fibrous areas.

930 CDX-2 Expression in Malignant Germ Cell Tumors of the Testes, Intratubular Germ Cell Neoplasia and Normal Seminiferous Tubules

MJ Lee, AP Vogt, AO Osunkoya. Emory University School of Medicine, Atlanta.

Background: CDX-2 is a caudal-type homeobox gene, encoding a transcription factor that plays an important role in proliferation and differentiation of intestinal epithelial cells. The utility of antibodies to CDX2 in the identification of adenocarcinomas of the gastrointestinal tract, particularly colorectal adenocarcinomas, in both primary and metastatic settings is well established. Patients with testicular tumors may occasionally lack an obvious palpable mass. However, the expression of CDX2 in malignant germ cell tumors of the testes which have metastatic potential has not been previously studied in a large series.

Design: A tissue microarray (TMA) was constructed from 56 malignant germ cell tumors of the testes including: 24 cases of classic seminoma, 8 cases of embryonal carcinoma, 8 cases of yolk sac tumor, 4 cases of malignant teratoma, 2 cases of choriocarcinoma, and 1 case of spermatocytic seminoma. 10 cases of intratubular germ cell neoplasia (IGCN) and 7 cases of benign testicles with normal seminiferous tubules were also included in TMA. Immunohistochemical stains for CDX2 was performed and analyzed. Only nuclear staining was considered positive.

Results: Positive expression of CDX2 was identified in 2/2 cases (100%) of choriocarcinoma, 4/8 cases (50%) of teratoma, 3/8 cases (38%) of embryonal carcinoma, 3/8 cases (38%) of yolk sac tumor and 1/29 cases (3%) of classic seminoma. CDX2 was negative in all cases of IGCN, normal seminiferous tubules and the only case of spermatocytic seminoma.

Conclusions: The role of CDX-2 in the differentiation of intestinal/enteric epithelial cells may contribute to the formation of trophoblastic, glandular, villous or cystic structures in germ cell tumors of the testes. This study suggests that the expression of CDX2 in a variety of malignant germ cell tumors of the testes may be a potential pitfall in metastatic tumors of unknown primary, which are thought to be of gastrointestinal/colorectal origin but are actually from a clinically occult testicular tumor.

931 High Grade Prostatic Intraepithelial Neoplasia (HGPIN) and Intraductal Carcinoma of the Prostate (IDC-P): "Small Cell" Variant

S Lee, JI Epstein. The Johns Hopkins Hospital, Baltimore.

Background: "Small-cell HGPIN" is an exceedingly rare variant of HGPIN. The single case in the literature was associated with invasive small cell carcinoma in the radical prostatectomy (RP).

Design: 3 cases were identified from the consult files of one of the authors.

Results: Prostatic biopsies from 3 patients showed foci of conventional and "small cell HGPIN" (including foci that would be regarded as IDC-P). 2 cases were associated with separate foci of acinar adenocarcinoma in other cores (Gleason scores 3+4 and 4+4 in 1 case; 3+3 in 1 case). Small and large-caliber ducts with small cell-like change typically showed cribriform proliferations of atypical cells with abrupt transition between centrally located small cells with large more typical HGPIN cells located at the duct periphery. "Small cell" areas showed crowded cells with uniformly bland vesicular nuclei and scant cytoplasm. Despite a "small cell appearance" at low magnification, no apoptotic bodies or mitotic figures were seen in the "small cell" areas. Immunostaining in 2 cases showed negative staining in the small cell population for NSE, chromogranin, and synaptophysin. Racemase was positive only in the large HGPIN cells in 1 case, although the other case showed positivity in both "small cell" and typical large HGPIN cell populations. The MIB-1 proliferation index varied from 0–10% with predominant labelling of larger HGPIN cells and minimal reactivity in the small cell population. One case with a subsequent RP showed extensive "small cell HGPIN" in addition to a small organ confined Gleason Score 3+4=7 adenocarcinoma. Another patient with "small cell HGPIN" on biopsy was alive at 10 years follow-up which would be unexpected if he had small cell carcinoma.

Conclusions: In contrast to the original report, our cases of "small cell HGPIN" were not associated with small cell carcinoma and showed no immunohistochemical evidence of neuroendocrine differentiation. Analogous to small cell urothelial CIS in the bladder, "small cell HGPIN" likely represents a morphologic mimic rather than true neuroendocrine differentiation. It may represent an extreme form of cellular maturation which is commonly seen toward the center of ducts involved by HGPIN. In order that it not be confused with small cell carcinoma, we propose that it be designated as "small cell-like HGPIN" or "small cell-like IDC-P", depending on the architecture of the neoplastic glands.

932 The Relationship between EZH2 Expression and Renal Cell Carcinoma

HW Lee, JY Park, I Hwang, HR Jung, SY Kwon, YN Kang, SP Kim, K Kwon, SS Lee, MS Choe. Keimyung University School of Medicine, Daegu, Korea.

Background: Enhancer of zeste 2 (EZH2) is a member of the Polycomb group proteins and part of Polycomb repressive complex 2. The EZH2 is important for transcriptional repression. Particularly, aberration of EZH2 has been implicated in oncogenesis and progression of various neoplasms. Renal cell carcinoma (RCC) remains a major cause of morbidity and mortality, and the incidence of RCC in the worldwide has continued to rise. Clear cell type make up the majority of the RCC. The objective of this study was to evaluate EZH2 expression in clear cell RCC and correlate the expression with prognostic factors.

Design: Tissue was obtained from surgically resected specimens of 176 patients who were diagnosed with clear cell RCC. EZH2 expression was determined by immunohistochemical staining. EZH2 expression with variable intensities was observed predominantly in nuclei and grouped into low and high expression. The association of EZH2 expression with clinicopathological characters and prognosis was determined by statistical analyses.

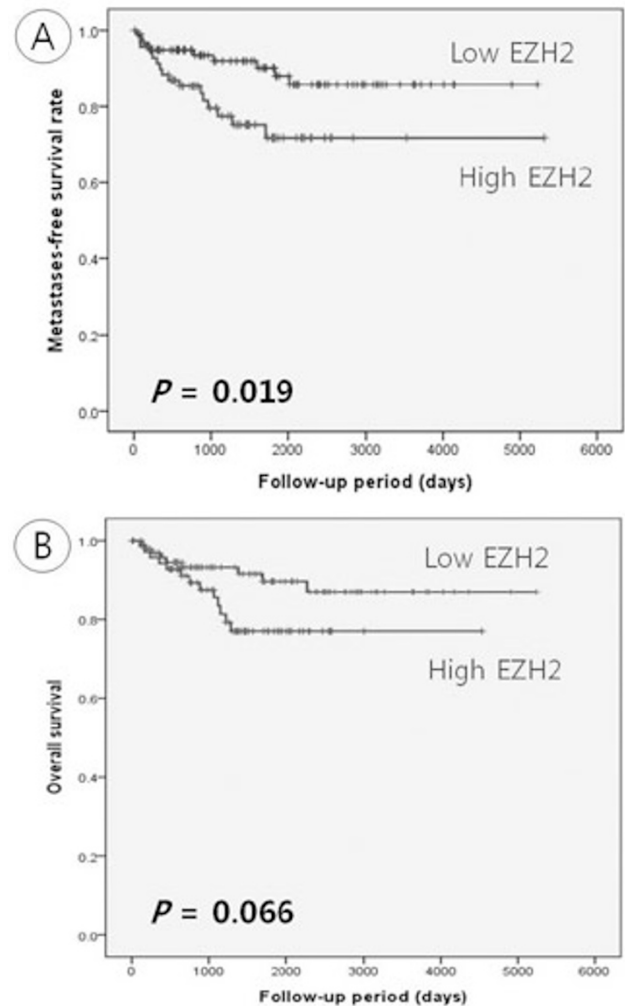
Results: High expression of EZH2 was significantly correlated with higher pT stage and histologic grade or more frequent distant metastases ($P = 0.001$, 0.025 and 0.024 , respectively). On the other hand, EZH2 had no significant association with age, gender or pN stage ($P > 0.05$).

Associations between clinicopathological parameters and patients' outcome

	Distant metastases (P-value)	DWD (P-value)
EZH2 Low vs. High	0.024**	0.073
Age (yr) ≤ 56 vs. > 56	0.02**	0.038**
Gender Male vs. Female	0.538	0.269
Histologic grade I-II vs. III-IV	0.011**	0.079
pT stage T1-2 vs. T3-4	0.0001**	0.007**
TNM stage I-II vs. III-IV	0.0001**	0.0001**

NOTE: P-values of χ^2 -tests are indicated; *, Fisher's exact tests are indicated; **, Statistically significant, $P < 0.05$; DWD, death with disease

Kaplan-Meier survival analyses with log-rank tests displayed that patients with high EZH2 expression had a significantly shorter disease-free survival ($P = 0.019$). EZH2 expression was associated with overall survival; however, differences did not reach statistical significance ($P = 0.066$).



Conclusions: From our results, we propose that EZH2 is a useful prognostic marker for aggressive behavior including distant metastases of clear cell RCC.

933 Florid Reactive Mesothelial Hyperplasia of the Tunica Vaginalis Mimicking Malignant Mesothelioma: A Study of 10 Cases

S Lee, JI Epstein, PB Illei. The Johns Hopkins Hospital, Baltimore.

Background: Florid reactive mesothelial proliferation of serosal surfaces can morphologically mimic malignant mesothelioma. Homozygous deletion of 9p21 as detected with fluorescence in-situ hybridisation (FISH) assays has been reported to be a specific finding in the majority (67%) of epithelioid mesotheliomas.

Design: Ten cases were identified from the archival material of our institution and the consult files of one of the authors were reviewed. FISH for 9p21 was performed in five cases, where blocks were available.

Results: All 10 cases were incidental findings on routine examination of hydrocele sacs (n=7), epididymal or paraepididymal cysts (n=2), or pyocele (n=1). Microscopically, all cases were characterized by linear arrays of simple tubular formations and cords of mesothelial cells orientated parallel to the surface, and embedded within fibrous and inflamed tunica. Irregular solid nests and cribriform glands were noted in two cases. The mesothelial proliferation typically showed a sharply demarcated linear deep border at the junction between more reactive fibrous tissue and subjacent fibroadipose soft tissue or dense fibrous tissue. In only one case was there was a significant associated surface papillary component. No confluent growth, spindle cell morphology, necrosis or atypical mitotic figures were identified. No homozygous deletion of 9p21 was detected by FISH in the five cases tested.

Conclusions: Reactive mesothelial proliferation of the tunica vaginalis is often an incidental finding on routine excision specimens of hydroceles. Microscopically there is a characteristic linear proliferation of mesothelial cells with a well defined deep border at the interface of more reactive fibrous tissue and either dense fibrous tissue or subjacent fibroadipose tissue. In contrast to malignant mesothelioma, the tubular proliferation is not present in more acellular dense fibrous tissue or adipose tissue and only involves more reactive appearing fibrous tissue. Negative FISH assays for 9p21 deletion may be a useful ancillary tool to aid distinction from mesothelioma.

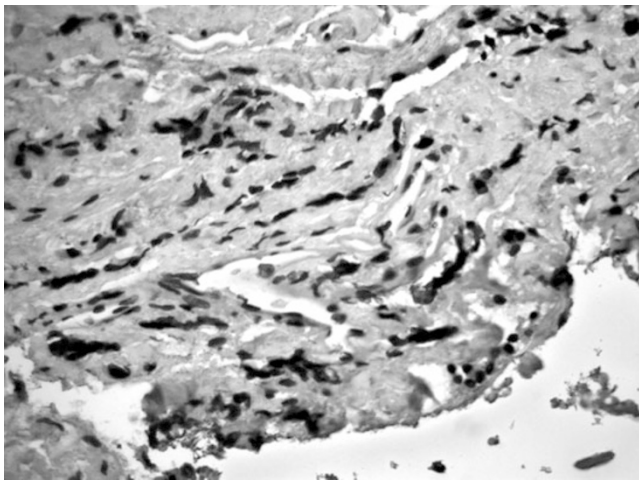
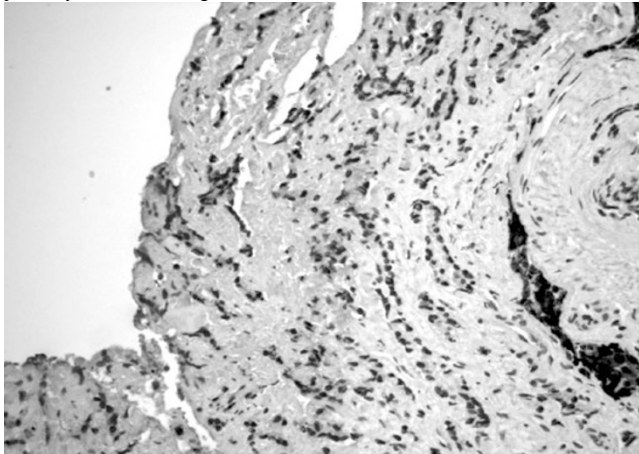
934 Utility of Triple Antibody Cocktail Stain in Radical Prostatectomy Specimens with Crushed Surgical Margins

G Li, N Al Daoud, AJ Evans, TH Van der Kwast. University Health Network, Toronto, Canada; Jordan University of Science and Technology, Irbid, Jordan.

Background: Triple antibody cocktail stain is in routine use to establish a diagnosis of prostate cancer in biopsies with a small suspect lesion. Due to crushing artefacts it may occasionally be difficult to diagnose a positive surgical margin in prostatectomy specimens. The potential utility of the cocktail stain as a decision aid in the distinction between carcinoma and benign glands at the crushed margin of a prostatectomy has not been investigated so far.

Design: Ten cases with crushed benign glands at the surgical margins of radical prostatectomies and 20 cases with crushed margins positive for carcinoma were retrieved from the pathology archives of Toronto General Hospital. Sixteen (80%) of the positive margins were apical margins, two (10%) were incised intra-prostatic margins, and one (5%) was a soft tissue margin. Two-colour triple antibody stain using a cocktail of antibodies against AMACR, HMWK and p63 was performed on the selected slides.

Results: In 10/10 specimens with crushed benign glands, basal cell staining continued to be detectable, while AMACR staining was completely negative in all cases (0/10). As for the positive margin cases, the crushed glands did not express basal cell marker staining (0/20), whereas 14/20 (70%) of the cases showed variable levels of racemase positivity at the inked margin.



Conclusions: In some instances, two-colour triple antibody cocktail stain may be of use in problematic radical prostatectomies with crushed glands at the surgical margins, helping to ascertain whether these glands are malignant or benign.

935 A Comparison of the Immunoreexpression of ERG Versus AMACR, PSA and PSAP in Prostatic Carcinomas

DGS Lim, M Teh, TP Thamboo. National University Health System, Singapore.

Background: ERG overexpression secondary to TMPRSS2-ERG gene re-arrangement occurs in 40-70% of prostate carcinomas (PCs) and immunoreexpression of ERG is reported to be a good surrogate for the detection of this fusion. We aimed to compare the immunoreexpression of ERG and other commonly used immunomarkers, in a series of PCs.

Design: Tissue microarrays were constructed from 33 radical prostatectomy and 54 TURP specimens. A corresponding core of benign prostatic tissue was included when available. Expression of ERG, α -methylacyl-CoA racemase (AMACR), prostate specific antigen (PSA) and prostate specific acid phosphatase (PSAP) was evaluated using commercially available monoclonal antibodies. Intensity of staining was scored as negative (no staining), weak (1+), moderate (2+) and strong (3+) and extent of staining was scored as: 1+ \geq 1% and $<$ 10%; 2+ \geq 10% and $<$ 50%; 3+ \geq 50% of cells showing immunoreactivity.

Results: 18/81 (22.2%), 78/83 (94.0%), 75/84 (89.3%) and 82/84 (97.6%) PCs showed immunoreactivity for ERG, AMACR, PSAP and PSA respectively. Seven tumors expressing ERG showed weak staining, 8 showed moderate staining and 3 demonstrated strong immunoreexpression. Seventeen tumors showed immunoreactivity for both ERG and AMACR (6 with Gleason score 6, 3 with Gleason score 7, 3 with Gleason score 8 and 5 with Gleason score 9). One tumor (Gleason score 9) showed strong and diffuse staining for ERG but only weak immunoreexpression of PSA and did not stain for AMACR or PSAP. None of the cores of benign prostatic tissue stained for ERG (0/62), whereas 1/68, 70/70 and 71/71 cores of benign prostatic tissue showed immunoreactivity for AMACR, PSAP and PSA respectively.

Conclusions: ERG is a significantly less sensitive but only slightly more specific marker for PCs compared to AMACR. Incorporating ERG into a panel of immunomarkers that includes AMACR, for the detection of PCs, is of limited diagnostic utility. PSA and PSAP are very sensitive markers for indicating prostatic origin regardless of ERG status.

936 Open and Robotic/Laparoscopic Partial Nephrectomy: A Large Single-Institutional Experience with Clinicopathologic Analysis and Follow-Up

L Liu, JG Pattaras, AO Osunkoya. Emory University School of Medicine, Atlanta.

Background: Interest in partial nephrectomy, or nephron-sparing surgery, for renal tumors has been stimulated by advances in renal imaging, improved surgical techniques, and increasing numbers of incidentally discovered low-stage renal tumors. There are however, only few large studies with emphasis on clinicopathologic analysis and follow up.

Design: A search was made through the surgical pathology files of our institution for patients who had open or robotic/laparoscopic partial nephrectomy procedures between 2007 and 2010. Clinicopathologic parameters and follow up information was obtained.

Results: 136 patients were identified, who had a total of 142 procedures (6 patients had repeat partial nephrectomies, 5 contralateral and 1 ipsilateral kidney). 2/136 patients (2%) underwent subsequent ipsilateral completion radical nephrectomy, 1 of whom was the only patient with a positive renal parenchymal margin. The mean patient age was 57 years (range, 19-84 years), with a male to female ratio of 2.1:1. Of the 142 partial nephrectomy procedures, 91 (64%) were open, and 51 (36%) were robotic/laparoscopic. The mean greatest tumor size was 3.7 cm (range, 1.2-8.2 cm). The most common diagnosis was renal cell carcinoma (RCC) 130/142 cases (92%) including; clear cell RCC 86/130 cases (66%), papillary RCC 31/130 cases (24%), chromophobe RCC 7/130 cases (5%), multilocular cystic RCC 3/130 cases (2%), mucinous tubular and spindle cell carcinoma 2/130 cases (2%) and RCC unclassified 1/130 cases (1%). The remaining 12/142 cases were; angiomyolipoma 5/142 cases (3%), oncocytoma 5/142 cases (3%), simple renal cyst 1/142 cases (1%), and cystic nephroma 1/142 cases (1%). Among the RCC cases the stages were as follows; pT1a 84/130 cases (65%), pT1b 39/130 cases (30%), pT2a 4/130 cases (3%), and pT3a 3/130 cases (2%). Duration of follow up ranged from 3 to 40 months. During the follow up period, only 2/136 patients (2%) developed metastatic RCC (lung and clavicle).

Conclusions: Although over 90% of patients had malignant renal tumors, the outcome was excellent in the majority of cases. Our study demonstrates that partial nephrectomy, either open or robotic/laparoscopic, is a viable option for a select group of patients with malignant or benign renal tumors who may not need to undergo radical nephrectomy.

937 Evaluation of ERG Expression in Tumors from Various Organs

H Liu, J Shi, M Wilkerson, X Yang, F Lin. Geisinger Medical Center, Danville, PA; Northwestern University, Chicago, IL.

Background: ERG is a recently described immunohistochemical marker for prostatic adenocarcinoma. Expression of ERG has also been suggested to correlate with the poor prognosis of prostatic adenocarcinoma with Gleason score of 6 (3+3) by some investigators. However, the published data on ERG expression in tumors from other organs were limited. In this study, we investigated the expression of ERG in a large series of carcinomas from various organs using a single immunostaining system (Dako).

Design: Immunohistochemical evaluation of the expression of ERG (Epitomics, Cat. No. AC-0105RUO) on 1,094 cases of carcinomas from various organs, and normal prostatic tissue (N= 20) and normal seminal vesicles (N=20) using tissue microarray sections was performed. The staining intensity was graded as weak or strong. The distribution was recorded as negative ($<$ 5% of tumor cells stained), 1+ (5-25%), 2+ (26-50%), 3+ (51-75%), or 4+ ($>$ 75%).

Results: The positive staining results (%) and the total number of cases for each entity (N) are summarized in Table 1. Forty of 90 prostatic adenocarcinomas (Gleason score 3+3) were positive for ERG, with 25 of 40 cases showing diffuse and strong nuclear staining (3 or 4+). Only 1 lung adenocarcinoma showed 2+ nuclear staining. All others cases including normal prostatic tissue and seminal vesicles in this study were negative for ERG.

Table 1. Summary of Immunostaining Results on 1,094 Cases

Tumor	ERG (positive cases and %)
Seminoma (N=30)	0
Embryonal CA (N=24)	0
Yolk sac tumor (N=12)	0
Lung neuroendocrine CA (N=61)	0
Lung ADC (N=50)	1/50 (2%)
Lung SCC (N=49)	0
Papillary thyroid CA (PTC, N=47)	0
Follicular thyroid CA (FTC, N=37)	0
Medullary thyroid CA (MTC, N=10)	0
Anaplastic thyroid CA (ATC, N=5)	0
Clear cell RCC (N=82)	0
Papillary RCC (N=20)	0
Colonic ADC (N=43)	0
Esophageal ADC (N=30)	0
Gastric ADC (N=21)	0
Pancreatic ADC (N=50)	0
Urothelial CA (N=31)	0
Prostatic ADC (N=90)	40/90 (44%)
Cholangiocarcinoma (N=11)	0
Breast ductal CA (N=99)	0
Breast lobular CA (N=48)	0
Endocervical ADC (N=17)	0
Endometrial CA (N= 38)	0
Ovarian serous CA (N=56)	0
Hepatocellular CA (N=18)	0
Pancreatic endocrine neoplasm (N=15)	0
Skin melanoma (N=100)	0

ADC—adenocarcinoma; CA—carcinoma; RCC—renal cell carcinoma

Conclusions: Our data demonstrate that ERG is a highly specific but not very sensitive marker 1) to confirm the diagnosis of prostatic adenocarcinoma, since normal prostate does not express ERG, and 2) to identify the prostatic primary when working on a tumor of unknown origin.

938 Histological Heterogeneity of Clear Cell Renal Cell Carcinoma (CCRCC). A Complete Morphological Analysis of 47 Tumors

Ji Lopez, G Muniz, R Guarch, N Camarasa, M Caceres, V Moreno, L Garcia-Prats, R Orozco. Hospital de Cruces, Univ of the Basque Country (UPV/EHU), Barakaldo, Bizkaia, Spain; Hospital Virgen del Camino, Pamplona, Spain; Hospital Peset, Univ of Valencia, Spain; Hospital General Yagüe, Burgos, Spain; Hospital Txagorritxu, Vitoria-Gasteiz, Spain; Hospital San Jorge, Huesca, Spain; Hospital San Juan de Dios, Ciudad de Guatemala, Guatemala.

Background: CCRCC are known to be histologically heterogeneous but no study quantifying this fact in a large group of unselected cases has ever been performed. There is concern that limited kidney tumor sampling protocols in general pathology practice may give a partial and insufficient view of tumor heterogeneity. The aim of this study is to define and quantify the extent of tumor heterogeneity in a series of totally sampled CCRCC.

Design: Sixty-four (64) consecutive renal cell tumors from seven hospitals were totally sampled over a three months period in 2011. 47 (73.5%) of this group were CCRCC. A total of 1439 H&E slides of CCRCC were collected and reviewed applying AJCC staging and Fuhrman nuclear grade. Cases were classified as homogeneous or heterogeneous carcinomas depending on the presence of one or more different cell types and grades in different areas of the same tumor. Basic clinical and pathologic data were retrieved in all cases.

Results: Males predominated in the series (31M/16F), the average age being 62.5 years (range 27-83). Average tumor diameter was 5.9 cm (range 2-19) and average number of paraffin blocks per case was 30.6 (range 3-130). Organ-confined tumors were predominant (59.5%) in the series. Twenty eight CCRCC (59.5%) were histologically heterogeneous with the main histology consisting in Grade 1 and 2 conventional clear and/or eosinophilic cells arranged in nests, cords and pseudoglands. Secondary patterns in these tumors included Grade 3 and 4 areas (17 cases, 60%), sarcomatoid areas (2 cases, 7%), and oncocytoid areas (1 case, 3.5%). Small clear cells (35.7%), necrosis (32.1%), syncytial cells (21.4%), bony metaplasia (14.2%), and papillae (7%) were also focally detected. Homogeneous CCRCC (19 cases, 40.5%) were all entirely composed of conventional Grade 1 and 2 clear/eosinophilic cells. More than one third (36%) of low grade (G1/2) CCRCC had minor high grade (G3/4) areas.

Conclusions: A significant number of CCRCC are composed of different cell types with variable grades that can be incompletely sampled with current protocols. This fact may contribute to the unexpected poor behaviour of some CCRCC. Our data suggest that as many as one third of low grade CCRCC will contain high grade foci if extensively sampled.

939 Prostate Adenocarcinomas Aberrantly Expressing p63 Are Negative for ERG Protein Expression and ERG Gene Rearrangement

TL Lotan, MC Haffner, JL Hicks, AO Osunkoya, GJ Netto, AM De Marzo, JI Epstein. Johns Hopkins School of Medicine, Baltimore, MD; Emory University School of Medicine, Atlanta, GA.

Background: We have recently described a group of prostatic adenocarcinomas (PCa) that show diffuse expression of p63, a protein present in prostatic basal cells and absent from the vast majority of PCa. Despite positivity for basal markers p63 and bcl-2, these tumors also express a number of luminal markers, with uniform expression of androgen receptor (AR) and positivity for luminal cytokeratins rather than high molecular weight basal-type keratins. Given that these tumors express AR and androgen-regulated PSA and that androgen-induced gene rearrangements involving the *ERG* locus occur in nearly half of typical acinar PCa, we investigated whether p63-expressing PCa also harbor *ERG* gene rearrangements.

Design: A total of 27 p63-expressing tumors, including 12 radical prostatectomy specimens, 14 needle biopsies and one transurethral resection of the prostate (TURP), were immunostained to determine presence or absence of nuclear ERG protein. Additionally, fluorescence in situ hybridization (FISH) using a break apart probe for 5' and 3' *ERG* was performed on a tissue microarray (TMA) constructed from a subset of 7 of the radical prostatectomy specimens. These cases were scored for presence of *ERG* gene rearrangement through deletion or translocation.

Results: None of the 27 p63-expressing PCa cases expressed nuclear ERG protein by immunohistochemistry (0/27), despite the fact that adjacent endothelial cells were strongly positive, providing an internal positive control in all cases. Consistent with lack of ERG protein expression, FISH was negative for *ERG* gene rearrangement in the subset of all 7 p63-expressing tumors tested (0/7). Compared to a control group of more than 800 cases of usual acinar PCa at our institution, where approximately one half of all cases are positive for ERG protein and harbor *ERG* gene rearrangement, absence of ERG protein expression in all 27 p63-expressing cases was highly statistically significant ($p < 0.001$).

Conclusions: Prostate tumors with aberrant p63-expression comprise an unusual subgroup with a mixed luminal and basal immunophenotype. Despite an apparently intact androgen signaling axis, these tumors completely lack ERG protein expression, and in a subset, we have confirmed that this is due to lack of *ERG* gene rearrangement. This data strongly suggests that p63-expressing PCa represents a molecularly distinct subclass of PCa. Further study of this rare tumor type may yield important insights into the role of p63 in prostatic epithelial and tumor biology.

940 Urine Cytology and Fluorescent In Situ Hybridization of Upper Urinary Tract Malignancies: A Report of Cases and Literature Review

CA Lum, C Gima, R Kaneshiro, E Matsubara, D Wei, R Maruyama, P Tauchi-Nishi. Queens Medical Center/Hawaii Pathologists Laboratory/University of Hawaii, Honolulu, HI; Showa University Northern Yokohama Hospital, Yokohama, Japan; Queens Medical Center, Honolulu, HI; Shimane University, Izumo, Japan.

Background: Primary upper urinary tract urothelial carcinoma comprises approximately 5% of all urothelial cancers and 7-8% of renal tumors. Compared to its bladder counterpart, these malignancies present diagnostic challenges that may effect delays in detection, resulting in advanced stage at diagnosis with worsened prognosis. In this study, we investigate the utility of cytologic examination and Urovysion™ FISH in identifying these upper tract malignancies.

Design: A retrospective review of our database revealed 376 patients during the period of April 2008 to March 2011 with biopsy proven urothelial cancers. Fifty-nine (16%) of these patients were diagnosed with ureteral or renal pelvis primaries. During this same period, 325 patients underwent 443 Urovysion™ FISH studies with 202 concomitant cytologic exams.

Results: Twenty of the 376 urothelial cancer patients were had prior positive FISH results. Six (30%) had upper urinary tract malignancies with 9 of 13 FISH exams positive (sensitivity 69.2%). Sixteen of 30 cytologic studies revealed abnormal cells (sensitivity 53.3%). For voided urine specimens, FISH sensitivity (83.3%) exceeded cytology (21.4%). Combined cytology and FISH testing yielded a higher predictive value (sensitivity 83.3%). No false positive cytologic or FISH exams were observed. FISH testing proved more sensitive for high grade (75.0%) than low grade tumors (60.0%). Low grade carcinomas demonstrated a higher percentage homozygous 9p21 loss, while high grade malignancies showed 4 or more chromosomal gains per cell. Our review revealed 4 patients with renal cell carcinomas. Tumor size had no bearing on FISH positivity, and none involved the renal pelvis. Both cases exhibited polysomy for chromosomes 3, 7, and 17; no homozygous 9p21 loss was noted. There were no discernible differences in karyotypic abnormalities between urothelial and renal cell carcinomas.

Conclusions: Urovysion™ FISH contributed to the diagnosis of upper tract malignancies, and demonstrated higher sensitivity than cytology, especially in the setting of voided urine specimens. Combined cytology and FISH testing yielded enhanced cancer identification. Urovysion™ FISH may also prove useful as an adjunct in the detection of renal cell carcinomas, and further studies may be warranted.

941 Prognostic Significance of Periacinar Retraction Cleaving in Prostatic Adenocarcinoma

V Macias, A Kajdacsy-Balla. University of Illinois at Chicago, Chicago, IL.

Background: Periacinar retraction cleaving is one of the proposed additional supportive diagnostic criteria in prostate cancer. Some studies have shown its potential prognostic significance in several tumors. A recent report indicates that extensive retraction predicts biochemical recurrence-free survival in prostate carcinoma. This study examines the presence and extent of cleaving in a nested case-control prostate cancer cohort to evaluate its predictive value.

Design: Formalin fixed, paraffin embedded tissues from prostatectomy specimens from the Cooperative Prostate Cancer Tissue Resource were analyzed (n=386). Patients with PSA recurrence (n=193) were paired 1:1 for year of surgery, race, age, Gleason grade and pathological stage with patients without recurrence (n=193). All cases were free of known metastasis at the time of surgery and had ≥ 5 years follow-up. Only neoplastic acini and nests with retraction in $\geq 50\%$ of circumference were counted as positive for cleaving. Based on the proportion of clefts within the tumor, the extent was graded as 0 (absent to rare); 1+ (1 to 25%); 2+ (26% to 50%); 3+ (51% to 75%); and 4+ ($>75\%$). Groups were compared for differences by the paired Wilcoxon Signed-Rank Test.

Results: Overall, periacinar cleaving was noted in 45.08% of the recurrence cases, and 38.34% of the non-recurrence cases; and proportions (scale 1-4) between the two groups were 36.27%, 4.14%, 2.60%, and 2.07% versus 30.57%, 3.63%, 2.07%, and 2.07%. However, no significant differences between the two groups were found by statistical analysis ($p=0.28$).

Conclusions: In contrast with previous reports on carcinoma of the prostate and other organs, our results do not demonstrate significant associations between the presence or the extent of clefting with outcome after subjects were matched by age, race, Gleason score and pathologic stage.

942 Extraction of Metabolites Can Be Successfully Performed without Affecting Histopathologic Evaluation in Prostate Needle Biopsies

C Magi-Galluzzi, SM Farzarano, EA Klein, J McDunn, B Neri. Cleveland Clinic, Cleveland, OH; Metabolon, Inc, Durham, NC.

Background: Potential application of metabolomic profiling in prostate cancer (PCA) relies on the identification of differentially accumulated metabolites in PCA compared to non-neoplastic tissue. Metabolomic profile of prostate biopsies (PBx) taken ex-vivo from radical prostatectomy (RP) and cystoprostatectomy (CP) specimens was analyzed to identify metabolites able to discriminate negative biopsies from men with and without PCA.

Design: Twelve PBx per patients were taken from 8 RP and 2 CP specimens and incubated at room temperature overnight each into a separate cryovial pre-loaded with 80% methanol/20% water. Following incubation, each PBx was removed from the solution, transferred to formalin, processed via standard histopathology methods, and stained with hematoxylin and eosin. Immunohistochemistry (IHC) for p63, CK903, racemase, and ERG was performed in 28 PBx. Methanolic solutions were analyzed for metabolites by gas chromatography/mass spectrometry and ultrahigh performance liquid chromatography/tandem mass spectrometry.

Results: Patient median age, PSA, and Body Mass Index (BMI) were 61 years, 6.24 ng/mL, and 27, respectively. All patients were White except for one CP patient who was Hispanic. Tissue was well preserved for histopathologic evaluation in all cases. PCA was found in 23 of 120 (19%) cores; high-grade prostatic intraepithelial neoplasia in 12 (10%) and atypical glands suspicious for cancer in 5 (4%). IHC confirmed preserved immunoreactivity of tissue, although the intensity of staining was weaker than positive controls in 18% of cases. Methanolic extracts were successfully analyzed for biochemical composition and 205 small molecules were measured across all major biochemical classes (amino acids, carbohydrates, lipids, nucleotides, cofactors, xenobiotics). A comparison of relative levels of compounds in PCA containing vs. non-PCA containing PBx showed significant differences for some of the compounds, such as sarcosine, kynurenine and succinylcarnitine. Of interest, levels of select steroid and polyamine catabolites were significantly higher in non-PCA than in PCA cores.

Conclusions: Microscopic diagnostic examination of tissue is important to correlate metabolomic profile with pathologic findings. This method whereby needle cores are methanol extracted prior to formalin fixation preserves tissue for successful histopathologic and IHC evaluation and provides high quality metabolite profiles for biochemical characterization of disease.

943 Impact of Race on the Incidence and Prognosis of Variants of Prostate Adenocarcinoma: A 35 Year SEER Analysis

DM Marcus, PJ Rossi, AB Jani, M Goodman, AO Osunkoya. Emory University School of Medicine, Atlanta.

Background: Racial disparities have been well described in conventional prostatic adenocarcinoma (PCA), however the impact of race on incidence and outcomes of patients with variants of PCA has not been well characterized. We used the Surveillance, Epidemiology, and End Results (SEER) database to evaluate the impact of race on the incidence and prognosis of five variants of PCA.

Design: A search was made through the SEER 17 database to identify cases of mucinous PCA, ductal PCA, signet ring cell PCA, neuroendocrine PCA, and adenosquamous PCA from 1973 to 2008. For comparison, we also identified cases of conventional PCA. We calculated age-adjusted incidence rates and overall survival (OS) for each variant. Incidence and survival in African Americans and Caucasians were compared using rate ratios (RRs) and Kaplan Meier analyses respectively, accompanied by tests for significance.

Results: We identified 790,937 cases of conventional PCA, 806 cases of mucinous PCA, 692 cases of ductal PCA, 502 cases of neuroendocrine PCA, 130 cases of signet ring cell PCA, and 27 cases of adenosquamous PCA. Incidence was higher in African Americans compared to Caucasians for mucinous PCA (RR = 1.63, p = 0.004), ductal PCA (RR = 1.49, p = 0.017), and conventional PCA (RR = 1.45, p < 0.001). By contrast, incidence of neuroendocrine PCA was lower in African Americans compared to Caucasians (RR = 0.54, p = 0.016). There was no statistically significant difference in the incidence of adenosquamous PCA and signet ring cell PCA. There was a statistically significant difference in OS in mucinous PCA for Caucasians (5 year OS 77.2%, 95% confidence interval [CI] 73.1 - 80.6%) compared to African Americans (5 year OS 64.8%, 95% CI: 54.9-73.1%, p < 0.001), and no statistically significant difference in OS was seen in the other variants of PCA.

Conclusions: There are statistically significant differences in incidence and outcomes in some variants of PCA when stratified by race. African Americans have a higher incidence of mucinous PCA and ductal PCA compared to Caucasians. In contrast, African Americans have a lower incidence of neuroendocrine PCA compared to Caucasians. African Americans are associated with lower OS compared to Caucasians with mucinous PCA. Additional epidemiological studies examining variants of PCA in concert with race are needed to elucidate the etiology of these disparities.

944 Macrophage Related Markers Expression in MITF/TFE Family Renal Translocation Carcinoma, Melanotic Xp11 Translocation Renal Cancer and Pure Epithelioid PEComa (so Called Epithelioid Angiomyolipoma) of the Kidney

G Martignoni, D Segala, E Munari, M Pea, S Gobbo, M Brunelli, F Bonetti, C Zampini, C Ghimenton, O Hes, P Camparo, S Pedron, C Pastena, M Chilosi, JN Eble, P Argani. University of Verona, Verona, Italy; Ospedale Orlandi, Bussolengo, Italy; Ospedale Civile Maggiore, Verona, Italy; Charles University and University Hospital, Plzen, Czech Republic; Hopital Foch, Suresnes, Paris, France; Indiana University School of Medicine, Indianapolis, IN; Johns Hopkins Medical Institutions, Baltimore, MD.

Background: Cathepsin K is a lysosomal protease recently described in MITF/TFE family renal translocation carcinomas (tRCC) and angiomyolipoma of the kidney both classic and epithelioid (pure epithelioid PEComa (PEP)). Both tRCC and angiomyolipoma are neoplasms expressing MITF/TFE family transcription factors. Moreover t(6;11) TFEB+ tRCC and PEP constantly immunostain for the melanogenesis markers HMB45 and MART1 such as melanotic Xp11 tRCC. These three tumors can show overlapping morphological and immunohistochemical features and their differential diagnosis can be challenging. In this study we investigated the expression of macrophage markers (CD68-PGM1, CD68-KP1, cathepsin K, CD163) in a series of tRCC, PEP and melanotic Xp11 tRCC, in order to assess their utility to distinguish them.

Design: We studied the immunohistochemical expression of CD68-PGM1, CD68-KP1, cathepsin K and CD163 in 21 tRCC (including 9 PRCC TFE3+ tRCC and 12 t(6;11) TFEB+ tRCC), 5 melanotic Xp11 tRCC and 13 PEP.

Results: All PEP, all t(6;11) TFEB+ tRCC, and all but two, PRCC TFE3+ tRCC express strongly and diffusely cathepsin K whereas the 5 melanotic Xp11 tRCC were weakly positive. CD163 resulted positive in 3 out of 7 PEP and in none of 4 t(6;11) TFEB+ tRCC, 4 PRCC TFE3+ tRCC and 1 melanotic Xp11 tRCC. CD68-KP1 was expressed in all 22 tested tumors (13 PEP, 4 t(6;11) TFEB+ tRCC, 1 melanotic Xp11 tRCC, 4 PRCC TFE3+ tRCC) whereas CD68-PGM1 immunostained all 13 PEP, but none of the other neoplasms.

Conclusions: 1) Cathepsin K is consistently expressed in PRCC TFE3+ tRCC, t(6;11) TFEB+ tRCC, melanotic Xp11 tRCC and PEP; 2) CD68-PGM1 is a useful tool for the differential diagnosis between PEP and all the other tRCC, including the HMB45 positive t(6;11) TFEB+ tRCC; 3) the CD68-PGM1 negativity in melanotic Xp11 tRCC seems to relate this tumor more closely to tRCC rather than PEP.

945 Signet Ring Cell Adenocarcinoma of Urinary Bladder: Clinicopathologic Features of Patients Undergoing Radical Cystectomy

SN Masineni, SA Boorjian, I Frank, P Thapa, JC Chevillet. Mayo Clinic, Rochester, MN; Mayo Clinic, Rochester, MN.

Background: Signet ring cell carcinoma (SRCC) is a rare subtype of urothelial carcinoma involving the urinary bladder that has been reported to have a worse prognosis than typical urothelial carcinoma (UC). However, few studies have examined the outcome of patients with SRCC treated by radical cystectomy (RC). In this study, we compared the clinical and pathologic features of a large series of patients of SRCC and UC treated by RC.

Design: A clinical and pathologic review of 3436 patients undergoing RC for bladder cancer at the Mayo Clinic between 1980 and 2011 identified 43 (1.3%) patients with SRCC. The pathologic and clinical features of SRCC and UC were compared including cancer-specific (CS) outcomes. In addition, a case-control analysis was performed where a patient with SRCC was matched with at least 3 patients with UC for age at surgery, year of surgery, TNM stage and ECOG status. Survival estimates were compared using Log rank test.

Results: There were 35 patients with SRCC that had adequate clinical follow-up. Patients with SRCC presented at a higher T stage (p < 0.0001) and were more likely to receive perioperative and adjuvant chemotherapy than patients with UC (p < 0.0001). Most patients (91%) with SRCC presented with pT3a or higher. Overall patients with SRCC had a worse 5-year CS survival than patients with UC (5-yr CS survival 34% vs 55%, respectively; p = 0.04). However, in the case-control analysis, there was no difference in CS outcome between patients with SRCC and UC (5 yr CS survival 34% vs 31%, respectively; p = 0.63).

Conclusions: Patients with SRCC treated surgically present at a higher tumor stage and are more likely to receive chemotherapy than patients with UC. Overall, patients with SRCC have a worse CS survival than patients with UC but when matched for prognostic features, there is no statistically significant difference in outcome.

946 Long-Term Clinical Outcome of Inverted Urothelial Papilloma Including Cases with Focal Papillary Pattern: Is Continuous Surveillance Necessary?

JP Maxwell, C Wang, A Kulaga, A Yilmaz, K Trpkov. Calgary Laboratory Services and University of Calgary, Calgary, AB, Canada.

Background: Inverted papilloma (IP) of the urinary tract is a benign urothelial neoplasm. A controversy, however, exists regarding the need for continuous cystoscopic surveillance, because there are conflicting reports regarding the potential of IP for recurrence and progression. Additionally, it is uncertain if IP with focal papillary pattern (mixed IP/urothelial papilloma morphology) have different clinical outcome than the traditional IP.

Design: We retrieved all cases with a diagnosis of IP from our institutional information system between 01/2000 and 12/2009. All cases with a previous history of higher grade urothelial neoplasm or diagnostic ambiguity were excluded. We identified 35 *de novo* ('primary') IP, including 3 cases with mixed (IP/urothelial papilloma) features, which represented the study cohort. 34/35 were consecutive routine cases seen in our centralized urology and uropathology practice for the region and only 1 case was from our consult files.

Results: The average patient age was 60 years (range, 26-88), with a male/female ratio of 1.9/1. IP were located in the bladder in 86% (30/35) patients. In 14% (5/35) patients, the primary location was in the urethra (4 male; 1 female). Focal papillary architecture was identified in three patients, age 51, 52 and 78 years (2 male; 1 female). The greatest dimension of the IP, based on the gross description, ranged from 0.1 to 3 cm. The IP with mixed morphology measured 0.8, 1.5 and 3 cm in greatest dimension. The follow-up ranged from 11 to 132 months (mean 66; median 68). Only one 81-years old patient with an initial diagnosis of IP had a recurrent IP diagnosed after 9 months (both with traditional IP morphology). No recurrence or progression was documented in any other patients with an initial diagnosis of IP (traditional or mixed). Of note, the only patient with recurrence had an initial IP that measured only 0.3 cm in greatest dimension, which raises the possibility of incomplete initial resection. Two subsequent biopsies of this patient at 21 and 32 months were negative for bladder tumor.

Conclusions: The absence of progression of IP on long-term follow-up in this study argues strongly against the need of continuous surveillance for patients in which: 1.) the diagnosis is established using strict diagnostic criteria, 2.) the completeness of the resection can be ascertained and 3.) when no previous or synchronous urothelial malignancies are documented. Rare IP with mixed morphology seem to follow the same benign course as the traditional IP.

947 Reproducibility Assigning Grade in Noninvasive Papillary Urothelial Neoplasms among Dedicated Genitourinary Pathologists: A Single-Institution Study Based on the 2004 WHO Classification

R Mehra, A Amin, LL Gellert, A Gopalan, Y Chen, SW Fine, SK Tickoo, VE Reuter, H Al-Ahmadie. Memorial Sloan-Kettering Cancer Center, New York, NY.

Background: The 2004 WHO classification is the most commonly used system to diagnose and grade bladder lesions. Inter- and intra-observer variability in assessing tumor grade in non-invasive papillary urothelial neoplasms (PUN) is well known. Despite its inherent subjectivity, as subspecialization becomes more prevalent, greater degree of concordance among "experts" and decreased inter-observer variability is expected if pathologists routinely consulted with each other for tumor grading. This study attempts to determine the inter-observer variability in grading PUN among dedicated genitourinary (GU) pathologists practicing at a single institution.

Design: 50 cases of PUN were prospectively selected by a senior member of the team, 4 years prior to the study. Cases were independently reviewed by 6 GU pathologists blinded to patient identity, prior diagnosis and clinical outcome. Based on the 2004 WHO classification, lesions were classified as hyperplasia, papilloma, papillary urothelial neoplasm of low malignant potential (PUNLMP), low grade (LGPU) or high grade papillary urothelial carcinoma (HGPUC). Consensus was defined as agreement among at least 4 of 6 pathologists. Free-marginal kappa for interobserver variability was calculated.

Results: Overall, there was good agreement among the 6 GU pathologists ($\kappa=0.64$). Based on our definition, consensus was achieved in 84% (42/50) of cases. Unanimous agreement (UA) or agreement among 5 of 6 pathologists was seen in 42% (21/50) of cases, each.

Of the 8 cases without consensus, discrepant cases included LGPU vs HGPUC (5) and PUNLMP vs LGPU or HGPUC (3). UA was observed in 11 LGPUCs, 8 HGPUCs and 2 urothelial papillomas. A diagnosis of PUNLMP was rendered by at least 1 pathologist 6 times but consensus was reached only once for this category.

Conclusions: In spite of subspecialization and consultation among GU pathologists, considerable inter-observer variability exists in the grading of PUN based on the 2004 WHO classification. This is particularly true in evaluating low grade lesions, mostly PUNLMP. It is evident that even experienced pathologists are reluctant to assign a papillary urothelial neoplasm to a non-malignant category. Novel molecular markers might help in reducing diagnostic variability as well as reflect the true progression/recurrence of these lesions. We hypothesize that grade plus marker will lead to increased interobserver concordance and risk stratification. The search and subsequent evaluation of these markers is ongoing.

948 Renal Lymph Nodes for Tumor Staging: Appraisal of 861 Adult Nephrectomies with Microscopic Examination of Hilar Fat

V Mehta, JJ Speiser, KM Mudaliar, MM Picken. Loyola Univ Med Ctr, Maywood.

Background: The role of lymphadenectomy in the management of renal cell carcinoma (RCC) is emerging. While sentinel lymph node (LN) detection is the standard of practice in several cancers, mapping of sentinel LNs has not been utilized in the management of RCC. Studies in porcine models have shown that lymphatic drainage is not uniform. Thus, sampling of LNs during nephrectomy for malignancy is an open issue. Although gross examination of hilar tissue to assess the nodal status is performed routinely, it is not known whether this approach is adequate. Our aim was to evaluate the LN status in nephrectomy specimens.

Design: All radical nephrectomies performed over a 10-yr period were reviewed, with particular attention paid to the identification and number of hilar and other LNs and their tumor involvement. As per protocol, the entire hilar tissue was submitted for histology. If hilar LNs were grossly visible, they were submitted separately by the surgeon or by the pathologist. We also reviewed cases with regional lymphadenectomy. The LN metastases were correlated with the grade & stage of tumor.

Results: Among 861 nephrectomies, including several cytoreductive procedures, in 226 cases 1924 LNs were recovered (avg. 8.5 LNs/kidney). 1-22 hilar LNs were identified in 88 cases (40%); of which LNs were grossly seen in 37 cases (83 LNs). Metastases were detected in 32/37 cases with enlarged LNs (67/83 LNs=80%). All of these cases had a higher tumor stage [pT2 x 3; pT3 x 7; pT4 x 5]. The Fuhrman's nuclear grade was II/IV (6 cases), III/IV (20 cases) and IV/IV (6 cases), 55 (25%) nephrectomies with LN yield, showed microscopic hilar LNs (187). All of these LNs were negative for metastases. 99 (43%) of patients had regional lymphadenectomy (gross 853 and microscopic 611:

periaortic, paracaval, interaortocaval, common iliac and external iliac. The number of identified LN ranged from 1-45. In 39/99 cases (39%) there were metastases (20% of 853 gross LNs). All of these cases had a higher tumor stage [pT2 x 6; pT3 x 27; pT4 x 6]. The Fuhrman's nuclear grade was II/IV (6 cases), III/IV (24 cases) & IV/IV (9 cases). Cases with negative LN were pT1a(x9), pT1b(x14), pT2(x23), pT3(x12), pT4 (x2).

Conclusions: Microscopic hilar LNs, seen in 25% of cases were all benign, while grossly visible hilar LNs were positive in 80%. LN positivity correlated with tumor stage but not grade. Thus, searching for occult LNs is not practical. In patients who are not at high risk for LN metastases and do not have grossly visible LNs at the time of surgery, regional lymphadenectomy and its associated morbidity may be avoided.

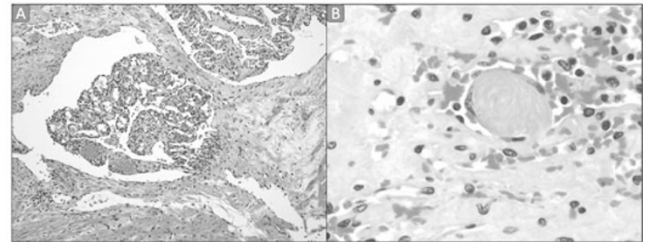
949 Primary Benign Vascular Tumors and Tumor-Like Lesions of the Kidney: A Clinicopathologic Analysis of 16 Cases

V Mehta, V Ananthanarayanan, T Antic, T Krausz, G Venkataraman, MM Picken. Loyola University Medical Center, Maywood; University of Chicago, Chicago.

Background: Primary benign vascular lesions of the kidney are uncommonly encountered in routine surgical pathology practice. They can, however, mimic malignancy or be an incidental finding adjacent to a malignancy.

Design: 16 specimens harboring 17 primary benign renal lymphatic/vascular lesions were identified from our files from 1999-2011 and subjected to a detailed pathologic evaluation and clinico-pathologic correlation.

Results: There were 9 males and 7 female patients (M:F =1.2:1) with age range of 33-75 years (mean 55 years). The radiologic finding in most cases was the presence of either a cystic (6 cases) or a solid (10 cases) mass suspicious for neoplasia. Lesions ranged from 0.5cm to 9.5cm (mean 2.8cm) and were all solitary except 2. There were 6 arteriovenous malformations (AVM), 4 capillary hemangiomas, 5 lymphangiomas and 1 solid intravascular papillary endothelial hyperplasia (i.e. Masson's hemangioma, fig. B) and 1 anastomosing hemangioma (fig.A). Five AVMs were located in the kidney parenchyma and 1 in the pelvi-ureteric system. Additional associated lesions ranged from renal stones to renal cell carcinoma in 2 cases (1 lymphangioma and 1 AVM). One AVM was associated with a capillary hemangioma in the vicinity, another with a history of renal cell carcinoma in the contralateral kidney. The Masson's hemangioma was arising in an intra-renal hematoma. AVMs were identical to their somatic soft tissue counterparts. Capillary hemangiomas and lymphangiomas were noninfiltrative and lacked cytologic atypia and mitotic activity. Except for a renal pelvic AVM, all other lesions radiologically mimicked malignancy. The patients had undergone partial or radical nephrectomies except for the renal pelvic AVM which was laparoscopically excised. None of the cases had any syndromal/systemic associations to our knowledge.



Conclusions: Benign vascular lesions of the kidney are rarely seen in routine surgical pathology practice, partly because a vast majority of them are medically treated by embolization. However lesions mimicking renal malignancy are subjected to surgery. They may exist as isolated lesions or coexist with, malignant lesions, either in the ipsilateral or the contralateral kidney.

950 TMPRSS2-ERG Gene Fusion in Prostate Cancer of Central Zone Origin

MP Mikulasovich, ML Stanton, CC Guo, MT Deavers, IN Prokhorova, BA Czerniak, P Troncoso. The University of Texas MD Anderson Cancer Center, Houston, TX.

Background: The incidence of prostate cancer originating from the 3 prostate zones varies. Most tumors arise from the peripheral (PZ) and transition (TZ) zones; <5% are considered of central zone (CZ) origin. Previous studies showed that the *TMPRSS2-ERG* gene fusion status differs substantially between carcinomas of PZ and TZ origin: 30-70% vs. ≤12%. Only limited information is available about the *TMPRSS2-ERG* gene fusion status in tumors of CZ origin.

Design: We reviewed radical prostatectomy specimens containing foci of possible CZ origin. Only specimens with tumor foci located exclusively within the CZ (identified by its anatomic location and distinct morphologic features) were selected for histologic characterization and *TMPRSS2-ERG* gene fusion analysis, conducted by using break-apart fluorescence in situ hybridization (FISH) and immunohistochemical analysis (IHC) for ERG protein expression using the ERG antibody (9FY, Biocare Medical, Concord, CA).

Results: We studied a total of 31 specimens with 32 CZ tumor foci (1 specimen had 2 CZ foci). The patients' median age at prostatectomy was 60 years (range, 47-74). The total number of tumor foci in the specimens ranged from 2 to 8 (median, 4). Besides the CZ foci, all specimens had additional tumor foci arising from the PZ + TZ (n = 21), PZ (n = 9), or TZ (n = 1). The CZ tumor foci were nondominant and organ confined in all cases. The CZ tumor foci ranged from <1.0 mm to 10.0 mm with a mean volume of 0.007 cm³ (range, 0.001-0.048 cm³). The mean total tumor volume was 1.099 cm³ (range, 0.030-5.566 cm³). The Gleason score of the CZ tumor foci was 6 in 29 cases, 7 (3+4) in 1 case, and 7 (4+3) in 2 cases. High-grade prostatic intraepithelial neoplasia (HGPIN) in the CZ was identified in 94% of the cases. *TMPRSS2-ERG* gene fusion was detected in 32% (n = 9) of the 28 cases analyzed by FISH. Of those 9 cases with

gene fusion, 5 were caused by gene deletion and 4, by gene translocation. Twenty-two foci analyzed by FISH (8 positive, 14 negative) were also available for ERG protein expression by IHC. The results were concordant in 20 of the 22 (91%) cases.

Conclusions: In this limited study, *TMPRSS2-ERG* gene fusion was present in 32% and 36% (FISH and IHC results, respectively) of prostate cancers arising from the CZ, with good correlation between the 2 techniques. These results are similar to the incidence range reported for PZ tumors. The association of prostate cancers with HGPIN and the similar incidence of *TMPRSS2-ERG* gene fusion in PZ and CZ tumors together suggest that similar molecular mechanisms underlie the development of carcinoma in both zones.

951 Validation of New Staging System for Patients with Invasive Urothelial Carcinoma of the Prostate

R Miodinovic, AA El Latif, AJ Stephenson, D Hansel. Cleveland Clinic, Cleveland, OH.

Background: To investigate whether the outcome of patients undergoing radical cystectomy (RC) with contiguous involvement of the prostatic urethra by urothelial cancer of the bladder (UCB) varies by the extent of ductal/stromal invasion, and to verify the changes in the new staging system.

Design: A retrospective review identified 103 consecutive patients who underwent RC at two high-volume hospitals who were found to have contiguous involvement of the prostatic urethral ducts +/- stroma with UCB. Patients were divided into two groups according to extent of prostatic invasion: 1) superficial N=48 (ductal involvement [N=6], glandular invasion [N=7] or focal stromal invasion [N=35]), and 2) deep N=55 (deep stromal invasion [N=32], extra capsular invasion or seminal vesicles invasion [N=23]). Multivariable Cox proportional hazards model was used to determine the association of extent of prostatic involvement with mortality after controlling for age, institution, pathological stage, surgical margin status, and lymph node status.

Results: The median follow-up was 18 months (IQR: 8-37). Lymph node metastasis was observed in 27% and 40% of patients in groups 1 and 2, respectively. The 5-year overall survival for groups 1 and 2 was 63% and 40%, respectively ($p=0.02$). In multivariable analysis, patients with deep stromal invasion had a significantly worse mortality than those with superficial involvement of the prostatic urethra/stroma (HR: 2.6; 95% CI: 1.2-5.9).

Conclusions: Patients with superficial involvement of the prostate by contiguous UCB have a significantly improved survival in comparison to deep invasion. This supports the recent changes in staging system in which patients with ductal and focal stromal invasion are classified as pT2 stage.

952 Consecutive Progression from Intratubular Germ Cell Neoplasm, Unclassified (IGCNU) to Seminoma and Ultimately to Embryonal Carcinoma of the Adult Testis: An Allelotyping Analysis of Cases with Embryonal Carcinoma Accompanied by Co-Existing Seminoma and/or IGCNU Components

K Miyai, S Yamamoto, K Iwaya, O Matsubara, EJ Mark. National Defense Medical College, Tokorozawa, Saitama, Japan; Massachusetts General Hospital and Harvard Medical School, Boston, MA.

Background: The pathogenesis of embryonal carcinoma remains a matter of debate in adult testicular germ cell tumors (TGCTs). Some believe single consecutive progression from intratubular germ cell neoplasm, unclassified (IGCNU) to seminoma and embryonal carcinoma. Others believe that seminoma and embryonal carcinoma derive independently from IGCNU.

Design: From a cohort study of 18 patients with TGCT of embryonal carcinoma, a total of 25 co-existing histological components, consisting of 11 seminoma and 14 IGCNU components, were identified. We performed allelotyping analysis to clarify the genetic relationship between testicular embryonal carcinoma components and co-existing seminoma and/or IGCNU components. Their matched DNA was subjected to allelotyping analysis using 20 polymorphic markers located on 12 chromosome arms such as 3q, 5q, 6p, 9p, 10q, 11p, 12p, 12q, 13q, 17p, 17q and 18q.

Results: The concordance rate in the allelic pattern (loss of heterozygosity [LOH] or retention of heterozygosity) was 80% between embryonal carcinoma components and co-existing seminoma components, and 71% between embryonal carcinoma components and co-existing IGCNU components. Referring to Jacobs et al, the probability that IGCNU, seminoma, and embryonal carcinoma components in a specific case lose individually the same allele at a specific locus can be calculated as $1/2 \times p_1 \times p_2 \times p_3$, where p_1 , p_2 , and p_3 represent the frequencies of LOH at that locus in IGCNU, seminoma, and embryonal carcinoma components, respectively. It would be very unlikely that identical LOH pattern would be found both in embryonal carcinoma components and in co-existing seminoma or co-existing IGCNU components (probability < 0.05). Therefore, these findings indicated a clonal relationship among these components. Moreover, for all informative loci, the total frequency of LOH was 21% in IGCNU, 30% in seminoma, and 46% in embryonal carcinoma components ($p < 0.05$, respectively).

Conclusions: Our allelotyping analysis of cases with embryonal carcinoma accompanied with co-existing seminoma and/or IGCNU components suggests consecutive progression from IGCNU to seminoma and ultimately to embryonal carcinoma of the adult testis.

953 Expression of Androgen and Estrogen Receptors and Its Prognostic Significance in Urothelial Neoplasm of the Urinary Bladder

H Miyamoto, JL Yao, A Chaux, Q Yang, LA McMahon, Y Zheng, K Izumi, GJ Netto. University of Rochester, Rochester, NY; Johns Hopkins Medical Institution, Baltimore, MD.

Background: Men have a significantly higher risk of bladder cancer than women, whereas female patients have been shown to present with less favorable tumor

characteristics than male patients. Steroid hormone receptor signals have been implicated in bladder carcinogenesis and cancer progression. Although there are several reports showing the expression of androgen receptor (AR) and estrogen receptors (ERs) in bladder cancer, recent studies have demonstrated conflicting results and the prognostic significance remains unclear.

Design: We investigated the expression of AR, ER α , and ER β in 188 bladder tumor specimens, as well as matched 141 non-neoplastic bladder and 14 lymph node metastasis tissues, by immunohistochemistry. We then evaluated the relationships between their expression and clinicopathologic features available for our patient cohort.

Results: AR/ER α /ER β was positive in 80%/50%/89% of benign urothelium, 50%/67%/41% of benign stroma, 42%/27%/49% of primary tumors, and 71%/64%/71% of metastatic tumors. Significantly lower expressions of AR/ER α were found in high-grade (36%/23%) and muscle-invasive (33%/19%) tumors than in low-grade (55%; $P=0.0232/38\%$; $P=0.0483$) and non-muscle-invasive (51%; $P=0.0181/35\%$; $P=0.0139$) tumors, respectively. Significantly higher expressions of ER β were found in high-grade (58%) and muscle-invasive (67%) tumors than in low-grade (29%; $P=0.0002$) and non-muscle-invasive (34%; $P<0.0001$) tumors, respectively. There was no significant difference in expression pattern of each receptor between bladder tumors from male versus female patients. Additionally, there was a statistically significant inverse relationship between ER α expression and ER β expression in bladder cancer ($P=0.0216$), whereas no significant correlations between expressions of AR and ER α or ER β were seen. Kaplan-Meier and log-rank tests further revealed that positivity of ER β , but not AR or ER α , was associated with recurrence of low-grade tumor ($P=0.0072$), progression of low-grade tumor ($P=0.0005$), non-muscle-invasive high-grade tumor ($P=0.0020$), and muscle-invasive tumor ($P=0.0010$), or disease-specific mortality in patients with muscle-invasive tumor ($P=0.0073$).

Conclusions: Compared to benign bladders, significant decreases in the expression of AR, ER α , or ER β in bladder cancer were seen. Loss of AR or ER α was strongly associated with higher grade/more invasive tumors, while ER β expression was increased in high-grade/invasive tumors and predicted worse prognosis.

954 GATA3 Is Down-Regulated in Bladder Cancer yet Strong Expression Is an Independent Predictor of Poor Prognosis in Invasive Tumor

H Miyamoto, K Izumi, JL Yao, Q Yang, LA McMahon, N Gonzalez-Roibon, A Chaux, DG Hicks, GJ Netto, D Tacha. University of Rochester, Rochester, NY; Johns Hopkins Medical Institution, Baltimore, MD; Biocare Medical, Concord, CA.

Background: GATA3, a zinc finger transcription factor and an estrogen receptor (ER)-regulated gene, plays a critical role in breast tumorigenesis. GATA3 has recently been suggested as a marker for urothelium/urothelial neoplasm. However, little is known about the prognostic significance of GATA3 expression and its correlation with ER expression in bladder tumor.

Design: We immunohistochemically stained for GATA3 in 145 bladder tumor specimens and matched 106 non-neoplastic bladder tissues for which the expression levels of androgen receptor (AR), ER α , and ER β had been assessed. We then evaluated the association between GATA3 expression and clinicopathologic features available for our patient cohort.

Results: GATA3 was positive in 125/145 [86%; 13 (9%) weak, 44 (30%) moderate, and 68 (47%) strong] urothelial neoplasms, which was significantly lower than in benign urothelium [104/106 (98%); 3 (3%) weak, 30 (28%) moderate, and 71 (67%) strong] ($P=0.001$). Fifty (98%) of 51 low-grade tumors were GATA3-positive, whereas 75 (77%) of 98 high-grade carcinomas were GATA3-positive ($P=0.001$). Similarly, 78 (98%) of 80 non-muscle-invasive tumors expressed GATA3, compared with 47 (72%) of 65 muscle-invasive tumors ($P<0.001$). In contrast, among 68 cases treated with cystectomy, significantly lower expression of GATA3 was found in pN0 tumors [32/47 (68%)] than in node-positive tumors [20/21 (95%)] ($P=0.027$). There was no significant difference in the GATA3 expression pattern between bladder tumors from male vs. female patients. Kaplan-Meier and log-rank tests further revealed that overall positivity ($P=0.049$) or strong positivity ($P=0.019$) of GATA3 correlated with progression of muscle-invasive tumors. GATA levels were not strongly associated with prognosis in patients with low-grade and/or non-muscle-invasive tumors. Multivariate analysis identified high GATA3 expression as a strong prognosticator for progression ($P=0.052$) and cancer-specific survival ($P=0.040$) of muscle-invasive tumors. Moreover, there were statistically significant correlations between the expression of GATA3 vs. AR ($P=0.006$) or ER α ($P=0.025$), but not ER β ($P=0.473$).

Conclusions: Compared to benign urothelium, a significant decrease in the expression of GATA3 in urothelial neoplasms was seen. Loss of GATA3 was associated with high-grade and/or muscle-invasive tumors, while strong expression was an independent predictor of poor prognosis. We also found that GATA3 co-expressed with AR and ER α in bladder tumors.

955 Expression of DC-SCRIPT/ZNF366 Protein in Prostatic Adenocarcinomas (PACS): DC-SCRIPT Signaling Is Associated with High Tumor Grade, Advanced Stage and Biochemical Disease Recurrence

W Mneimneh, BVS Kallakury, GM Sheehan, M Feurstein, CE Sheehan, HAG Fisher, RP Kaufman, T Nazeer, JS Ross. Albany Medical College, Albany, NY; Georgetown University Hospital, Washington, DC.

Background: Dendritic cell specific transcript, a novel protein encoded by an 8-kb mRNA, is a transcription coregulator which upon binding to hormones, plays a key role in physiologic processes including growth and differentiation. DC-Script expression has been shown to have an independent prognostic value in the development and progression of human breast cancer. However, studies on DC-script protein expression in human carcinogenesis are extremely limited with almost no available data on its prognostic value in any other human cancers including prostatic carcinoma. In this study, we

evaluated DC-script protein expression by immunohistochemistry in human prostatic adenocarcinoma and correlated staining results with standard prognostic variables such as tumor grade, stage and disease recurrence.

Design: Formalin-fixed, paraffin-embedded sections from 132 PACs were immunostained by automated methods (Ventana) using goat anti-human DC-SCRIPT/ZNF366 antibodies (R&D Systems, Minneapolis, MN). Cytoplasmic immunoreactivity was scored based on intensity and percentage of positive cells, in a semi-quantitative scoring system, in both tumor and adjacent benign epithelium of each case. Moreover, tumor and benign tissue scores were compared in each case, and cases were subsequently classified accordingly in three categories: tumor (T) = benign (B) T=B, T>B, and T < B. Results were correlated with clinicopathologic variables.

Results: Cytoplasmic DC-SCRIPT immunoreactivity was noted as follows: [T>B 87/132 (66%), T=B 45/132 (34%), T < B 0%] and correlated with high grade [76% high grade vs 59% low grade, p=0.043] and advanced stage [79% advanced vs 61% early, p=0.047]. Intense diffuse tumor immunoreactivity was noted in 26/132 (20%) [all 26 cases were in the T>B subgroup; 26/87 (30%) of all T>B cases] and correlated with high grade [28% high grade vs 14% low grade, p=0.052] and biochemical disease recurrence [29% recur vs 11% non-recur, p=0.011]. On multivariate analysis, intense diffuse tumor immunoreactivity (p=0.05) and advanced stage (p=0.009) independently predicted biochemical disease recurrence.

Conclusions: These findings indicate that, similar to studies in breast cancer, DC-script protein expression is an independent adverse prognostic factor for patients with surgically resected prostate cancer. Further study of this transcriptional regulator and correlation with hormonal therapy response appears warranted.

956 Glandular Inclusions in Hernia Sacs of Children and Adults: Potential Source of Diagnostic Error: Report of 21 Cases, 3 Involving Females

D Mockler, P Kane, S Hwang, A Heimann, C Tornos. Stony Brook University Medical Center, Stony Brook, NY.

Background: Glandular inclusions in hernia sacs are more commonly seen in children and usually represent Mullerian duct-derived structures. Morphologically, they can be classified as vas deferens-like, epididymis-like and Mullerian-like. To date, most reports have described them in males younger than age 19. Our study was designed to determine whether benign inclusions are also found in adults and females and to study their morphology.

Design: We performed a computer search at our institution of all cases coded with the diagnosis of hernia sac with an additional diagnosis, from 1/1/1981 until 1/1/2011. Slides and reports were reviewed in all cases. Immunohistochemical stains were prepared if needed to confirm the diagnosis.

Results: We found 21 cases containing benign glandular inclusions. Six of them were vas-deferens-like (4 in children and 3 in adult males; ages 30, 62 and 71), 3 epididymis-like (all in male children ages 11 weeks, 3 months and 5 months), 9 Mullerian-like (all in males, 3 adults ages 20, 20 and 30, and 6 children ages 3 months to 8 years). We also found 3 cases with mesothelial inclusions, all in females; ages 9 weeks, 28 years, and 39 years. Classification of inclusions as mesothelial was confirmed with calretinin stains.

Conclusions: The presence of benign glandular inclusions in hernia sacs can occur, not only in male children, but also in females and adults. In males, the lesions are morphologically similar to vas deferens, epididymis or Mullerian remnants. In females, on the other hand, inclusions are mesothelial in origin and are strongly positive for calretinin. Awareness of these lesions can avoid their misinterpretation as metastatic adenocarcinoma or transected true anatomic vas deferens.

957 Expression of Novel Renal Tubular Associated Markers in Nephrogenic Adenoma (NA) of the Urothelial Tract: Potential Utility in Distinction from Its Malignant Mimics

SK Mohanty, N Nese, M Amin, M Aron, R Parakh, R Gupta, P Zhang, D Luthringer, MB Amin. Cedars-Sinai Medical Center, Los Angeles, CA; Beaumont Medical Center, Royal Oak, MI.

Background: NA of the bladder, urethra and renal pelvis is believed to represent renal tubular satellites/outposts in response to injury or metaplastic response to urothelial injury. Lesions have a range of histologic patterns, form a mass lesion, may have an infiltrative growth and morphologically mimic malignant lesions such as clear cell carcinoma of the bladder (CCC), urothelial carcinoma with glandular differentiation or nested pattern (UCa) and prostatic adenocarcinoma (PCa). This study aims at analyzing the utility of novel renal tubule-associated markers in differentiating NA from its malignant mimics.

Design: hKIM-1, Pax2, Pax8, racemase and S100A1 are renal tubule associated markers. The entire renal tubular system including the Bowman's capsule expresses Pax2, Pax8 and S100A1. hKIM-1 is expressed in injured proximal renal tubules and racemase is expressed primarily in proximal convoluted tubules. We analyzed the utility of a panel of immunohistochemical (IHC) markers [renal-associated markers - hKIM-1, Pax2, Pax8, racemase, S100A1; urothelial-associated marker S100p and MIB-1 (Ki67)] in the distinction of NA (n=39) from its histologic mimics: CCC (n=4), UCa (n=6) and PCa (n=14). The staining results were recorded in a semiquantitative fashion (0: negative, 1+: 1-25, 2+: 26-50, 3+: 51-100% and intensity as weak, moderate and strong). A MIB-1 (Ki-67) proliferation index (% positive in 100 cells counted) was ascertained for each case.

Results: IHC results are summarized in the table expressed as percentage positive. 13% of NA negative or weak for Pax2, Pax8 and racemase were strongly positive for hKIM-1. The range of MIB-1 proliferation index for NA, CCC, PCa, UCa was 1-4%, 20-50%, 5-30% and 10-40%, respectively.

Categories	hKIM-1	Pax-2	Pax-8	Racemase	S100A1	S-100p	Mean Ki-67
NA	67	87	74	59	95	0	1
CCC	0	25	0	50	50 (weak)	100 (usually 1+)	25
PCa	0	0	0	100	0	0	7
UCa	0	0	0	33 (weak)	0	0	25

Conclusions: The consistent IHC expression of renal tubular markers supports morphologic observations and cytogenetic data that NA of the urothelial tract is of renal tubular origin. Depending on the histologic pattern of NA, a judicious IHC panel of hKIM-1, Pax2, S100A1 (supporting NA), S100p (supporting UCa), PSA and PSMA (supporting PCa) and high MIB-1 proliferation (supporting CCC and UCa), has diagnostic utility in the distinction of NA from its malignant mimics.

958 Diagnostic Utility of a Comprehensive Immunohistochemical Panel To Differentiate High Grade Urothelial Carcinoma (UCa) from Prostatic Adenocarcinoma (PCa)

SK Mohanty, D Luthringer, AM Gown, M Aron, MB Amin. Cedars-Sinai Medical Center, Los Angeles, CA; PhenoPath Laboratories, Seattle, WA.

Background: The distinction between high-grade UCa and high-grade PCa in transurethral resection (TUR) specimens particularly from the bladder neck can be extremely challenging. The diagnostic difficulty is compounded by cases felt clinically to be PCa which are immunohistochemically (IHC) negative for prostate specific antigen (PSA). Accurate characterization is necessary as treatment modalities are significantly different (cystoprostatectomy/chemotherapy for UCa and hormonal/radiation therapy for PCa). The aim of this study was to evaluate the potential appropriateness of a broad immunohistochemical panel in differentiating high-grade UCa from high grade PCa.

Design: With IRB approval, the institutional pathology database was searched for high grade UCa and high-grade PCa on TUR specimens. Cases were then subjected to a panel of eleven established and emerging IHC markers including urothelial-associated markers: GATA3, S100p, IMP3, p63, CK7, CK20, CK5/6, uroplakin III, and prostate-associated markers: PSA, prostate specific membrane antigen (PSMA) and androgen receptor (AR). The staining results were recorded in semiquantitative fashion as estimated percentage of tumor cells immunoreactive with the antibodies (0: negative, 1+: 1-25, 2+: 26-50, 3+: 51-100% and intensity as weak, moderate and strong). IMP3 staining was considered positive when 10% of neoplastic cells were immunolabeled by the stain.

Results: 14 cases of high-grade UCa and 12 cases of high-grade PCa were identified. The details of key IHC results are summarized in the table as percentage positivity in the tumors. CK7, IMP3, CK5/6 and Uroplakin in UCa was 93, 71, 57 and 14% vs. 17, 7, 0 and 0% in PCa.

Category	GATA3	S100p	p63	CK20	PSA	PSMA	AR
UCa	100	86	57	57	0	0	14
PCa	0	0	0	25	33	100	100

Conclusions: A majority of high-grade PCa are PSA negative requiring a panel of IHC markers to confirm PCa and in its distinction from UCa. Urothelial lineage-associated markers, GATA3 and S100p, are relatively sensitive and specific for urothelial differentiation in the context of the differential diagnosis of UCa and PCa. A panel comprising of urothelial-associated markers (GATA3, S100p and p63 or CK20) and prostate-associated markers (PSMA, PSA and AR) has diagnostic utility in the therapeutically critical distinction of high-grade PCa from UCa.

959 FOXA1 Promotes Tumor Progression in Prostate Cancer and Represents a Novel Hallmark of Castrate Resistant Prostate Cancer

M Montani, J Gerhardt, G Kristiansen. University of Bern, Bern, Switzerland; University Hospital of Zurich, Zurich, Switzerland; University Hospital Bonn, Bonn, Germany.

Background: Forkhead box protein A1 (FOXA1) modulates the transactivation of steroid hormone receptors and thus may influence tumor growth and hormone responsiveness in prostate cancer. Therefore, we investigated FOXA1 expression in a large cohort of prostate cancer patients of different stages in order to correlate it to clinical parameters, PSA relapse free survival and hormone receptor expression.

Design: We investigated a cohort of 529 Patients who underwent radical prostatectomy, transurethral resection or resection of organ metastasis of prostate cancer or benign hyperplasia (primary carcinomas (n=207), castrate-resistant prostate cancer (n=27), lymph node and distant metastases (n=39), benign prostatic hyperplasia (n=15)). A tissue microarray (TMA) was constructed. Follow-up data was obtained for the group of primary carcinomas. Immunohistochemical stainings of FOXA1, AR, ER, PR, PSA a.o. was evaluated. To determine if FOXA1 expression has an influence on prostate cancer cell proliferation, LNCaP and PC-3 cells were transfected with FOXA1 specific siRNAs and cells were counted. DNA synthesis rate was determined by measuring BrdU incorporation. FOXA1 expression during cell migration was elucidated in a transmigration assay towards fibronectin. We reanalyzed the proliferation and migration behavior of FOXA1 high and low LNCaP cells upon androgen treatment.

Results: FOXA1 was overexpressed in metastases and particularly in castration resistant cases. Interestingly, FOXA1 was expressed at lower levels in both normal and neoplastic transitional zone tissues. FOXA1 levels correlated with higher pT stages and Gleason scores as well as androgen and estrogen receptor expression. FOXA1 overexpression was associated with faster biochemical disease progression, which was even pronounced in cases with low AR levels. Finally, siRNA based knockdown of FOXA1 decreased cell proliferation and migration. Moreover, in vitro tumorigenicity was only inducible by androgens in the presence of FOXA1, substantiating a functional cooperation between FOXA1 and AR.

Conclusions: In conclusion, FOXA1 expression is associated with tumor progression, de-differentiation of prostate cancer and poorer prognosis as well as cellular proliferation and migration and androgen signaling. These findings suggest FOXA1 overexpression as a novel mechanism to induce castration resistance in prostate cancer.

960 Cytogenomic Analysis of Translocation Renal Cell Carcinomas Reveals Distinct Molecular Subtypes with Similarities to Other Renal Cell Tumors

FA Monzon, G Malouf, J Couturier, V Molinier, P Escudier, P Tamboli, D Lopez-Terrada, M Picken, M Garcia, N Tannir. The Methodist Hospital, Houston, TX; MD Anderson Cancer Center, Houston, TX; Institut Curie, Paris, France; Hopital Saint Joseph, Paris, France; Institut Gustave Roussy, Villejuif, France; Texas Children's Hospital, Houston, TX; Loyola University Medical Center, Chicago, IL; University of Colorado, Aurora, CO.

Background: Translocation renal cell carcinoma (RCC) is a subtype of kidney cancer characterized by translocations involving *TFEB* or *TFE3* genes. Little is known about the whole genome and epigenetic characteristics of these tumors. Translocation RCC shows heterogeneity in clinical behavior with some patients having highly aggressive tumors. We performed genomic characterization of a cohort of translocation RCCs to investigate if molecular subtypes of these tumors exist.

Design: Cytogenomic analysis was performed with 250K Nsp SNP microarrays (Affymetrix) on 19 tumor specimens of translocation RCC (Age <18 (n=6); Age >=18 (n=13) and 2 established cell lines (UOK109, UOK146). Changes in global DNA methylation level were measured by using pyrosequencing of highly repetitive LINE-1 sequences on 27 tumor samples. Results were correlated with clinical and demographic information.

Results: Three distinct molecular subtypes were identified. Eight patients and one cell line (42%) showed 3p loss in a background of chromosomal imbalances commonly seen in clear-cell RCC. Three patients and the other cell line (19%) showed profiles similar to papillary RCC with gains of 7 and/or 17. The remaining 8 patients showed either a diploid genome or unique cytogenomic profiles. Three cases showed uniparental disomy lesions (UPD). Patients with 3p loss showed poor overall survival (OS) (Median OS: 12.7 month vs not reached) (p=0.03). There was no association between 3p loss and other clinic-pathological variables. Young patients (<18 years) displayed fewer numbers of genetic abnormalities as compared to older patients (p=0.02). Line-1 methylation was found to be lower in adult patients (71.1% vs 76.7%, p=0.02).

Conclusions: Our results show that subsets of translocation RCC are characterized by genetic profiles similar to those of clear-cell and papillary RCC. Evaluation of VHL mutation in tumors with 3p loss is underway. Tumors with 3p loss appear to show more aggressive behavior. We also identified Line-1 hypomethylation in adult tumors. These findings could explain the clinical heterogeneity observed in translocation RCC patients and could potentially be used to determine treatment strategies.

961 Correlation of Immunohistochemical Expression of Protein-Coding Genes RAD23B, SIM2S, Notch3, BID and FBP with Biochemical Recurrence in Patients Following Radical Prostatectomy for Prostatic Adenocarcinoma

CS Moreno, S Sannigrahi, J Cheng, W Zhou, JA Petros, TW Gillespie, AO Osunkoya. Emory University School of Medicine, Atlanta.

Background: One of the challenges in prostate cancer research is the development of effective predictors of tumor recurrence following radical prostatectomy, to determine whether immediate adjuvant therapy is warranted. This is even more important in patients who have negative margins and may be lost to follow up. To date very few biomarkers have been identified that accurately predict the possibility of tumor recurrence or biochemical failure in this setting.

Design: A panel of five biomarkers (RAD23B, SIM2S, Notch3, BID and FBP) were selected based on cDNA-mediated Annealing, Selection, extension and Ligation (DASL) assay. A TMA was constructed from 94 radical prostatectomy cases with available detailed follow-up data. Five TMA sections were stained with antibodies to RAD23B, SIM2S, Notch3, BID, and FBP. Intensity of the various immunohistochemical stains were scored blindly as follows; 0-negative, 1+ (weak), 2+ (intermediate) and 3+ (strong). The expression of these markers was correlated with biochemical recurrence (BCR). The expression of these markers was correlated with biochemical recurrence (BCR) using Fisher's exact test with samples divided into categories 0-2+ vs. 3+ for staining and positive vs. negative for BCR.

Results: Median patient age was 64 yrs (range 47-74yrs). Median Pre-operative PSA was 6.6 (range 1.6-72.6). Gleason scores were as follows: 12/97 cases (3+3=6), 53/97 cases (3+4=7), 23/97 cases (4+3=7), 7/97 cases (4+4=8), 1/97 cases (4+5=9), and 1/97 cases (5+4=9). There were 59 Caucasian and 31 African-American cases, with the remaining 7 of unknown race. There were 61/97 cases without BCR and 34/97 cases with BCR. Increased expression of RAD23B (p = 0.023) and SIM2S (p = 0.021) demonstrated statistical significance by Fisher's exact test for discriminating between patients with BCR and those without BCR. Expression of BID (two-tailed p-value = 0.357), NOTCH3 (p = 0.237), and FBP (p = 0.237) did not demonstrate statistical significance between patients with BCR and those without BCR. Interestingly, there was no statistically significant correlation between any of the markers and pathologic stage, Gleason score, patient race, or pre-operative PSA levels.

Conclusions: RAD23B and SIM2S may be useful immunohistochemical biomarkers in the prediction of BCR in patients following radical prostatectomy, irrespective of pathologic stage, Gleason score, patient race, or pre-operative PSA levels. Patients with tumors that demonstrate increased expression of these markers may benefit from close follow-up after radical prostatectomy.

962 CDX2 Is Superior to Alpha-Fetoprotein in Yolk Sac Tumors (YST) Both in Adult and Pediatric Patients: Study with Emphasis on Morphologic Patterns

G Naderkhani, A Pinto, K Trpkov, T Bismar, A Yilmaz. Calgary Laboratory Services and University of Calgary, Calgary, AB, Canada.

Background: YST can be diagnostically challenging due to its diverse morphologic patterns. Alpha-fetoprotein (AFP), a traditional YST marker, has also some limitations. CDX2, an antibody often used in intestinal adenocarcinomas, has recently been reported to be positive in adult testicular and ovarian YST, but it has not been studied in pediatric YST. We studied CDX2 expression both in adult testicular and pediatric YST.

Design: We compared the expression of CDX2 and AFP in 28 GCT: 22 adult testicular YST and 6 pure pediatric testicular (1) and extratesticular (5) YST. In adults, YST component ranged from 10% to 100%. The YST patterns were as follows: microcystic (75%), glandular (39%), myxomatous (36%), papillary (32%), macrocystic (25%), endodermal sinus (21%), solid (21%), and polyvesicular vitelline (11%). We used as negative controls, the non-YST components of mixed GCT and 6 additional pure GCT (4 seminoma, 2 embryonal), all confirmed by positive OCT 3/4. Extent of staining was scored as 0 (<5%), 1+ (5%-10%), 2+ (11%-50%) and 3+ (>50%). Staining intensity was graded from 0-3+.

Results: CDX2 was positive in 100% (6/6) of pediatric YST: No cases 0 or 1+, 3 cases each with 2+ and 3+. Mean intensity was 3. AFP stained 83% (5/6) pediatric YST: 1 with 0, 1 with 1+, 3 with 2+ and 1 with 3+. Mean intensity was 2.6. In adults, 91% (20/22), expressed CDX2: 2 (9%) with 0+, 4 (18%) with 1+, 8 (36%) with 2+ and 8 (36%) with 3+ staining. The mean intensity of CDX2 staining was 2.5. In adult YST, AFP stained 95% (21/22) cases: 1 (5%) with 0+, 6 (27%) with 1+, 11 (50%) with 2+ and 4 (18%) with 3+ staining. The mean intensity of AFP staining in the adult YST component was 2.5. Regarding the expression of CDX2 vs AFP in different YST patterns, CDX2 was superior in myxomatous (70% vs 0%), papillary (89% vs 55%) and macrocystic (71% vs 14%) patterns. Both antibodies were comparable in microcystic (90% vs 95%), endodermal sinus (66% vs 66%), polyvesicular (66% vs 33%) and solid (66% vs 66%) patterns. Seminomas and embryonal carcinomas were uniformly negative for both antibodies. CDX2 was expressed only in intestinal component of teratomas.

Conclusions: We found that CDX2 is an excellent marker for pediatric YST, which was not reported previously. We also confirmed that CDX2 is a useful marker identifying YST component in adult GCT. CDX2 is superior to AFP in detecting the commonly overlooked YST patterns such as myxomatous papillary and macrocystic. In contrast to AFP, CDX2 has distinct nuclear expression without background staining.

963 Correlation between ERG Fusion Protein and Androgen Receptor Expression in Prostate Cancer; Possible Role in Diagnosis and Therapy

AH Navaei, PP Aung, BA Walter, P Pinto, MJ Merino. NCI/NIH, Bethesda.

Background: Prostate cancer (PC) is the second cause of cancer and cancer deaths in males in US. Recent discovery of fusion genes brought a new look to the pathogenesis of PC. Gene fusions occur nearly in 60% of PC with the TMPRSS2:ERG being the most common. Evidence supports the role of ERG fusion in tumorigenesis, progression and invasion of PC via effecting pathways such as C-MYC, PI3K/PTEN/AKT axis, uPA, TLR4 and Androgen receptor (AR) mediated signaling. Fusion related ERG over expression is dependent on existence of AR. In this study we evaluate by IHC, AR and ERG fusion on prostate core biopsies and prostatectomies with a wide range of pathological grades to investigate clinicopathological applications as well as their possible role in therapy.

Design: Ninety two biopsies and corresponding prostatectomies from 38 patients were studied as well as 2 lymph node metastasis. IHC was performed utilizing two highly specific ERG mAbs (EPR 3864; Epitomics, CA) and 9FY (Biocare LLC, CA). Fifty six matching biopsies and the corresponding prostatectomies were stained with AR mAb (AR441, Dako, CA). Percentage and intensity of staining rated from 0 to 3. Correlation with FISH for ERG fusion was done.

Results: Twelve of the 92 biopsies were benign, 15 had atypical glands and PIN, 43 were adenocarcinomas (AC) Gleason 6-7 and 32 were Gleason 8-10. Twenty two of 75 AC stained for ERG (29%); 17 were Gleason 6-7 (77%) and 5 Gleason 8-10 (23%). None of benign biopsies stained with ERG. Forty four of 59 matching biopsies with AC; 20/27 (45%) Gleason 6-7, 17/17 (38%) Gleason 8-10 and 9/11 atypical glands stained with AR (p<0.05). Among matching biopsies 8/25 (32%) Gleason 6-7, 3/17 (17%) Gleason 8-10 and 1/9 (11%) atypical glands stained with both ERG/AR. All ERG positive biopsies were also positive with AR however 1 prostatectomy and 2 biopsies were ERG positive but AR negative. The two lymph node metastasis were positive for ERG/AR expression, consistent with the prostatectomy.

Conclusions: We conclude from our study that ERG assessment by IHC is useful for characterization of ERG status in prostate biopsies, and that the presence of fusion protein correlates with AR expression. These markers may assist in diagnosis since none of the benign biopsies stained with ERG. AR negative, ERG positive cases are rare. There is excellent correlation for ERG/AR staining between biopsies and prostatectomy specimen which suggests that the staining may have important clinical utility and assist in the development of new therapeutic targets.

964 Interrelation of Cell Cycle Markers in Squamous Cell Carcinomas of the Penis

GJ Netto, AL Cubilla, R Sharma, J Hicks, KL Lecksell, A Chau. Johns Hopkins University, Baltimore, MD; Instituto de Patologia e Investigacion, Asuncion, Paraguay.

Background: Previous studies have suggested a link between tumor morphology and expression of specific cell cycle markers in penile squamous cell carcinoma (SCC). However, studies assessing the intercorrelation between molecular pathways involved in cell proliferation and apoptosis are scant. Herein, we evaluated the status

and intercorrelation of 5 cell cycle and apoptosis related markers in a large series of penile carcinomas.

Design: One-hundred and twelve penile SCC were used to build 4 tissue microarrays. TMA spots were scanned using the APERIO system and uploaded to the TMAJ platform (<http://tmaj.pathology.jhmi.edu>). The following cell cycle and apoptosis related markers were evaluated by immunohistochemistry: p16^{INK4a}, p53, MDM2, Cyclin-D1, and Ki-67. For each marker, extent (percent of positive cells) was assessed in each spot, and an average value was calculated per case. Pairwise correlation coefficients (CC) were estimated for all markers. Strength of correlation was interpreted as follows: < 0.3, weak; 0.3–0.5, moderate; > 0.5, strong.

Results: Extent of p16^{INK4a} expression was positively correlated with Ki-67 (CC = 0.39, P < .001) and negatively correlated with p53 (CC = -0.28, P = .003) and cyclin-D1 (CC = -0.48, P < .001). In addition, extent of p53 expression was positively correlated with Ki-67 (CC = 0.22, P = .02) and cyclin-D1 (CC = 0.48, P < .0001). Cyclin-D1 intercorrelation with p16^{INK4a} and p53 was similar across histologic subtypes of penile cancer. No significant associations were found for all the other pairwise correlations. Tumors with warty and/or basaloid morphology had higher levels of p16^{INK4a} and Ki-67 (both P = .001) compared to keratinizing SCC.

Conclusions: Increased Ki-67 was positively correlated with the expression of both p16^{INK4a} and p53. The negative correlation between p16^{INK4a} and cyclin-D1 is expected. The positive correlation between cyclin-D1 and p53 and the negative correlation between p16^{INK4a} and p53 indicates a crosstalk between pathways during penile carcinogenesis. This crosstalk seems to be independent of tumor morphology.

965 The Epidermal Growth Factor Receptor (EGFR) Is Frequently Overexpressed in Penile Squamous Carcinomas

GJ Netto, AL Cubilla, R Katz, KL Lecksell, R Sharma, A Chaux. Johns Hopkins University, Baltimore, MD; Instituto de Patologia e Investigacion, Asuncion, Paraguay.

Background: Overexpression of the epidermal growth factor receptor (EGFR) has been described in a variety of tumors but experience in penile squamous cell carcinomas (SCC) is scant. Current adjuvant and neoadjuvant treatment options for penile cancer can be improved by the identification of new targets of therapy. Herein, we evaluated EGFR expression in a large set of penile SCC.

Design: EGFR immunorexpression was evaluated in 112 cases of penile SCC, from which 4 tissue microarrays (TMA) were built. TMA spots were scanned using the APERIO system and uploaded to the TMAJ platform (<http://tmaj.pathology.jhmi.edu>). Scanned images were digitally-analyzed with ImageJ (<http://rsbweb.nih.gov/ij>) and the immunomembrane plug-in (<http://imtmicroscope.uta.fi/immunomembrane>). Staining completeness (0–10 points) and intensity (0–10 points) were added for a combined score (0–20 points). Cases were classified as: EGFR negative, 0–3 points; low expression, 4–8 points; high expression, 9–20 points.

Results: 50 cases (45%) showed high EGFR expression, 49 cases (44%) demonstrated low EGFR expression, and 13 cases (11%) were negative. No association was observed with histologic subtype (Fisher's P = .55) or histologic grade (Fisher's P = .62).

Conclusions: EGFR is frequently overexpressed in penile SCC, with high levels in almost one half of the cases. EGFR expression is not related to histological subtype or grade. These results suggest a potential role for EGFR inhibitors in the treatment of patients with penile carcinomas.

966 Combined *In Situ* Hybridization and Immunohistochemistry for the Detection of Human Papillomavirus (HPV) Infection in Penile Carcinomas

GJ Netto, AL Cubilla, R Sharma, J Hicks, KL Lecksell, A Chaux. Johns Hopkins University, Baltimore, MD; Instituto de Patologia e Investigacion, Asuncion, Paraguay.

Background: Approximately one half of penile carcinomas are HPV positive. Polymerase chain reaction (PCR) assay is the gold standard for HPV detection. Alternative methods of detection that are less technically demanding and less costly are desirable especially in developing countries. Herein, we evaluated a combination of *in situ* hybridization and immunohistochemistry for defining HPV status in penile cancers.

Design: Forty-eight cases of penile squamous cell carcinoma (SCC), with previously determined HPV status by SPF-10 PCR assay, were included in a set of 4 tissue microarrays (TMA). Presence of high-risk HPV (HR-HPV) was assessed by *in situ* hybridization (ISH). Additionally, immunorexpression of 5 cell cycle control markers (p53, p16^{INK4a}, MDM2, cyclin-D1, and Ki-67) was evaluated. TMA spots were scanned using the APERIO system and uploaded to the TMAJ platform (<http://tmaj.pathology.jhmi.edu>). Discrimination of markers for defining HPV status was estimated using receiver operating characteristic (ROC) curves, and performances were compared by changes in the area under the ROC curve (AUC).

Results: Positive HR-HPV by ISH and increased p16^{INK4a} and Ki-67 expression were significantly associated with HPV status (P < .008). ROC analyses are shown in the table, with 95% confidence intervals in parenthesis.

	% Sensitivity	% Specificity	AUC
p16 ^{INK4a} alone	65 (38, 86)	90 (74, 98)	0.77 (0.65, 0.90)
HR-HPV ISH alone	47 (23, 72)	100 (89, 100)	0.73 (0.61, 0.86)
Ki-67 alone	65 (38, 86)	71 (52, 86)	0.68 (0.54, 0.82)
p16 ^{INK4a} and HR-HPV ISH	35 (14, 62)	100 (89, 100)	0.68 (0.56, 0.79)
p16 ^{INK4a} or HR-HPV ISH	76 (50, 93)	90 (74, 98)	0.83 (0.72, 0.95)
p16 ^{INK4a} and Ki-67	59 (33, 82)	94 (79, 99)	0.76 (0.63, 0.89)
p16 ^{INK4a} or Ki-67	71 (44, 90)	68 (49, 83)	0.69 (0.55, 0.83)
Ki-67 and HR-HPV ISH	35 (14, 62)	100 (88, 100)	0.68 (0.56, 0.79)
Ki-67 or HR-HPV ISH	76 (50, 93)	71 (52, 86)	0.74 (0.60, 0.87)

Conclusions: As a stand-alone marker, p16^{INK4a} performed better than HR-HPV ISH or Ki-67 to define presence of HR-HPV. Specificity was high for p16^{INK4a} and HR-HPV ISH positivity (90% and 100% individually; 100% when both positive). Positivity for

either p16^{INK4a} or HR-HPV ISH (rather than requiring both to be positive) had the best AUC performance. The latter combination could serve as an acceptable surrogate to the gold standard PCR assay.

967 Comparison of Latent Prostate Cancer Detected at Autopsy between Pre- and Post-Prostatic Specific Antigen (PSA) Era

M Okayasu, H Takahashi, B Furusato, M Kido, S Mizukami, M Furusato, H Hano. The Jikei University School of Medicine, Minato-ku, Tokyo, Japan.

Background: The prevalence of latent prostate cancer (LPC) found only at autopsy has been explored only in relatively old reports (from the 1980s and 1990s) in Asian prostate cancer research. The LPC has been widely recognized as well differentiated microscopic cancer. To determine whether significant differences now exist in LPC between periods before and after the advent of serum PSA screening for Asian prostate cancer detection, we compared 2 groups of men undergoing autopsy during the 2 periods.

Design: The Jikei University institutional autopsy records were searched for cases that had undergone prostate dissection at autopsy to identify prostate cancer. A total of 500 men were available between 1983 and 1992 (cohort A), and 89 men were available between 2009 and 2011 (cohort B) for this study. We calculated the incidence of LPC and compared the pathological parameters, including grade distribution and the proportion of tumor volume (TV) between the 2 cohorts. In addition, the frequency of phosphorylated AKT (pAKT) expression in cohort B was analyzed by immunohistochemistry.

Results: In cohort A, the prevalence of LPC was 22% (104/500 cases) compared with 40% (36/89 cases) in cohort B. In cohort A, the average TV was 230.4mm³ (range: 4.8–18,463mm³), which increased to 1280.02 mm³ (range: 0.5–19,091.2 mm³) in cohort B. Cases showing significant TV (>500 mm³) accounted for only 9.6% in cohort A, but increased to 22.2% (8/36) in cohort B. There was no trend observed in the grade distribution between the 2 cohorts. In addition, the expression of pAKT was detected in 12/26 available cases (46.2%) of cohort B, the incidence was quite similar to clinically detected prostate cancer (49%: our data from the Japanese cases). Expression of pAKT was detected in 100% (6/6) of the cases with TV>500 mm³, and in 30% (6/20 cases) with TV<500mm³ in cohort B, respectively (p=0.0026).

Conclusions: In recent years, autopsy rates have been decreasing at our institution. Though PSA screening has become standard, the prevalence and TV of LPC have increased quite dramatically in Japan, which may raise questions about the usage of PSA screening. We also found that certain percentage of LPC seems to be similar to the clinical cancer, especially in the post-PSA cohort (i.e. from its size and the cancer-related protein expression). Therefore, further studies are required to determine whether this finding is reproducible in multi-institutional analysis and clinically important.

968 Non-Invasive Papillary Urothelial Neoplasms of the Bladder: A Study of Tumors with Borderline Features

JM Oliver-Krasinski, J Hou, LR Harik. Columbia University - New York Presbyterian Hospital, New York, NY.

Background: The 2004 WHO/ISUP system is currently used for grading non-invasive papillary urothelial neoplasms of the bladder (PUNB) and classifies them into papilloma, papillary urothelial neoplasms of low malignant potential (PUNLMP), papillary urothelial carcinoma low grade (LG) and high grade (HG). Although most tumors can be classified into these categories with ease, some tumors show borderline features and are subject to interobserver variability, which is problematic in the setting of LG versus HG, a distinction that changes subsequent patient therapy.

Design: 99 cases of PUNB are identified between 1990 and 2010. Only patients with initial presentations of non-invasive PUNB are included. Patients with less than 2 year follow up (F/U) are excluded unless they have developed recurrence or progression. Tumors are classified as borderline tumors if they are either 1) Predominantly LG with focal HG (<50% HG), 2) Architecturally and cytologically LG but have areas of mitoses >5/10HPF, or 3) Show marked nuclear pleomorphism but are architecturally LG, with low mitotic count and absence of necrosis or presence of focal punctate necrosis. Recurrence is defined as occurring after 3 months of F/U. Progression is defined as progression in grade, or stage (invasion or metastases).

Results: The average age is 68y (35–86y); M:F: 2.8:1; F/U: 68.7 mo (5.7–243 mo), median=56 mo. The cases are classified as PUNLMP (n=5), LG (n=33), borderline tumors (LG/HG) (n=39) and HG (n=22) (table 1). Within the borderline tumors, category 1 tumors show similar rates of recurrence and progression as LG. Category 2 tumors show a high rate of recurrence and grade progression, however none progressed by stage. Category 3 tumors show similar rates of recurrence and grade progression as LG; however, the rate of stage progression is intermediate between LG and HG.

Table 1. Subclassifications of PUNB: recurrence and progression

	Cases	Recurrence N (%)	Grade Progression N (%)	Stage Progression N (%)
LG	33	23 (70)	5 (15)	2 (6)
Borderline total	39	28 (72)	5 (13)	4 (10)
LG/HG mix, <50% HG (1)	15	10 (67)	0 (0)	1 (6)
LG, increased mitoses (2)	9	9 (100)	3 (33)	0 (0)
LG, increased nuclear atypia (3)	15	9 (60)	2 (13)	3 (20)
HG	22	17 (77)	-	7 (32)

Conclusions: Tumors which are mixtures of LG and <50% HG fair like LG. Borderline lesions with nuclear atypia have a higher stage progression rate than LG. Borderline tumors which are mitotically active show a higher recurrence rate than LG. Further studies on borderline tumors are required to identify optimal patient therapy.

969 Microvascular Pericyte Density Predicts Prostate Cancer Progression

U Ozerdem, EM Wojcik, C Ersahin, GA Barkan. Loyola University Medical Center, Chicago, IL.

Background: The progression of tumor neovascularization is critical to continued tumor progression. It is critical to note that the walls of neovascular blood vessel capillaries are composed of two principal cell types: vascular endothelial cells and pericytes. Pericytes form an outer sheath surrounding the endothelial cells. Nascent pericytes express PDGF receptor-beta while nascent blood vessels and lymphatic endothelial cells express CD34. This investigation deals with establishing a quantitative analysis of PDGF receptor-beta and CD34 expression in prostate cancer as a tangible prognostic tool.

Design: We used a tissue microarray, which represented 49 patients with Gleason scores 0 (normal prostate tissue), 6, 7, 8, 9, and 10. These prostate cancer samples represented prognostic stages II, III, and IV (AJCC Manual 2010, p. 457). Tissue microarray slides were immunostained with PDGF receptor-beta and CD34. Immunostained slides were imaged with a high resolution digital camera. Digital images were analyzed by using NIH ImageJ1.44 image analysis software to quantify PDGF receptor-beta and CD34 expression. Microvascular density was measured for each patient as a percentage of the area covered by pericytes or endothelial cells to the area of the microarray spot. Statistical analyses were performed using Graphpad Prism. The microvascular pericyte density (MVPD) or microvascular endothelial density (MVED) scores in each position of tissue microarray were compared across each prognostic group.

Results: The mean MVPD score was 0.70%, 0.98%, 2.00%, 2.87%, 3.79%, and 4.33% in patients with Gleason scores 0, 6, 7, 8, 9, and 10, respectively. MVPD was significantly different between patients with different Gleason scores ($p < 0.001$). The mean MVPD score was 2.05%, 3.02%, and 3.30% in patients with stage II, III, and IV prostate cancer, respectively ($p < 0.05$). The mean MVED score was 0.74%, 1.19%, 2.04%, 3.02%, 3.97%, and 4.44% in patients with Gleason scores 0, 6, 7, 8, 9, and 10, respectively. MVED was significantly different between patients with different Gleason scores ($p < 0.001$). Mean MVED was 2.31%, 3.23%, and 3.29% for patients with stage II, III, and IV prostate cancer, respectively ($p < 0.05$).

Conclusions: MVPD and MVED scores can easily be utilized as practical prognostic tools in prostate cancer. Potentially, MVPD and MVED scores can be used to identify the patients who would benefit from targeted anti-pericyte, anti-endothelium, and anti-lymphangiogenesis therapies. *This project has been supported by an institutional research grant.*

970 Gleason Score at Surgical Margin Is Not an Independent Predictor of Biochemical Recurrence after Radical Prostatectomy

S Paluru, V Iremashvili, SA Umar, S Lokeshwar, M Manoharan, R Satyanarayana, MS Soloway, M Jorda. University of Miami, Jackson Memorial Hospital, Miami; University of Miami, Jackson Memorial Hospital, Miami.

Background: A positive surgical margin is known to increase the risk of prostatic adenocarcinoma (PA) recurrence after surgery. Gleason score at surgical resection margin (GSM) may independently affect postoperative outcome; this association however has not been confirmed. The objective of this study is to retrospectively analyze the association between GSM and biochemical recurrence (BCR) after radical prostatectomy (RP).

Design: We identified 154 RPs with positive surgical resection margin (SRM) and different Gleason patterns amounting to scores of 7 (3+4, 4+3) and 8 (3+5 and 5+3). Since GSM may impact BCR, these cases were selected for their disparate Gleason patterns. All slides with positive margins were reviewed and the GSM was recorded for each case. The BCR-free survival in patients with same overall Gleason score (GS) and different GSM was estimated using the Kaplan-Meier method and results were compared with the log-rank test. To determine if the GSM has independent predictive value with regards to biochemical outcome, we also compared the predictive performance of two multivariate Cox regression models. One model comprised traditional pathologic and clinical variables, including pathologic stage and GS, lymph nodes status, visually estimated percent of carcinoma, length of surgical margin and preoperative PSA. The other model added GSM to the first model variables. The predictive performance of these two models was quantified using the Harrell's c-index.

Results: Thirteen (12%) of 109 patients with PA GS 7 (3+4) and GS 8 (3+5) had GSM of 7 (4+3) or 8 (5+3). Twenty-eight (62%) of 45 patients with PA GS 7 (4+3) and GS 8 (5+3) had GSM of 7 (3+4). Over a median follow-up of 4.2 years, 52 (34%) patients had BCR. No difference in BCR-free survival was found between the two models. GSM was not significantly associated with BCR-free survival in the multivariate analysis ($p = 0.285$). A marginal increase in predictive performance of the multivariate model was noted after inclusion of GSM (c-index changed from 0.689 to 0.691).

Conclusions: GSM is not associated with biochemical outcome after radical prostatectomy in both univariate and multivariate analyses. GSM does not add predictive accuracy to the standard model containing established prognostic factors. We found no evidence to support the inclusion of GSM in routine pathologic reporting of radical prostatectomy specimens.

971 Her2 Amplification Is Associated with a High Risk of Progression in Non-Muscle-Invasive Bladder Cancer

C-C Pan. Taipei Veterans General Hospital, Taipei, Taiwan.

Background: Her2/*neu* amplification and overexpression have been studied mainly in invasive and metastatic bladder cancers, but its significance in non-muscle invasive bladder cancer (NMIBC) has not been substantially investigated. The study was conducted to evaluate the prognostic value of Her2 amplification in NMIBC.

Design: Immunohistochemistry for *neu* and fluorescence in situ hybridization (FISH) using Her2/CEP17 probe (PathVysion) were performed on 8 cases of papillary urothelial

neoplasm of low malignant potential (PUNLMP), 108 cases of low-grade papillary urothelial carcinoma (LPUC) and 169 cases of high-grade papillary urothelial carcinoma (HPUC). The immunoreactivity for *neu* was assessed by the percentage of tumor cells showing complete membranous positivity. Amplification was defined following the ASCO/CAP guideline (Her2/CEP 17 ratio > 2.2). The status of Her2 amplification was correlated to progression of detrusor muscle invasion (progression from Ta/T1 to T2-4, metastasis or cancer-specific mortality).

Results: None of the PUNLMPs and LPUCs showed Her2 amplification. Fifteen (8.9%) of HPUCs showed Her2 amplification. Eleven (73.3%) of Her2-positive HPUCs progressed into muscle-invasive or metastatic disease. The cumulative incidence of progression at 5 years was 80.9% in Her2-positive HPUCs, as opposed to 40.1%, 14.8% and 2.2% in T1 Her2-negative HPUC, Ta Her2-negative HPUC, and LPUC/PUNLMP, respectively ($p < 0.0001$). When overexpression of *neu* was defined using a cut-point of 50%, the concordance rate between immunohistochemistry and FISH was 100%.

Conclusions: Her2 amplification and overexpression can discern a subset of NMIBC with high risk for progression. These patients may be eligible for target therapy if the tumor progressed.

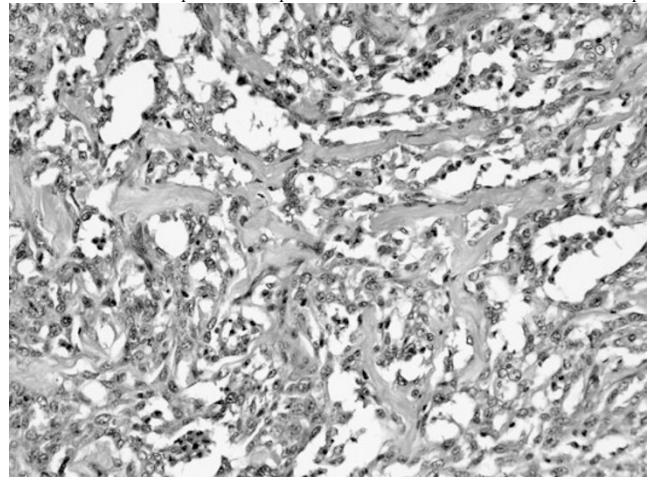
972 Pseudoangiosarcomatous (Acantholytic) Variant of Urothelial Carcinoma of the Urinary Bladder

GP Paner, RM Cox, M Large, AJ Cohn, N Gokden, ND Smith, T Krausz, JK McKenney, GD Steinberg. University of Chicago, Chicago, IL; University of Arkansas, Little Rock, AK; Stanford University, Stanford, CA.

Background: We present an unusual morphologic pattern of urothelial carcinoma of the bladder. Although rare instances of this morphology had been reported in other organ carcinomas, only one example in the bladder has been previously described in the literature.

Design: Six radical cystectomies obtained from the surgical pathology files of two institutions formed the basis of this study.

Results: Patients included 5 males and 1 female ranging from 47 to 78 years old (mean 63 years). Histologically, the tumor was characterized by florid vascular-like formations of invasive carcinoma cells. There were elongated jagged and larger nests of cells with abundant central acantholysis and dyscohesion. Complete cell loss imparted an appearance of interanastomosing network of vascular-like channels lined by residual plump hobnailing cells reminiscent of epithelioid angiosarcoma. In addition, dyscohesion or cracking in smaller elongated nests formed slit-like spaces and occasionally, intracytoplasmic vacuoles were also seen. When in the muscle, the tumor tended to infiltrate in between and wrapped around smaller muscle bundles. The acantholytic areas were often accompanied by abundant acute inflammatory cells. Other admixed morphologies included squamous (3/6, 20-40% of tumor), small cell neuroendocrine (1/6, 15% of tumor) and sarcomatoid (1/6, 50% of tumor) differentiations. Pseudoangiosarcomatous pattern was similarly seen in the squamous component. Immunohistochemical stains in 3 tumors for Fli-1, CD31 and CD34 were all negative. AJCC pT stages were as follows: pT3a (2), pT3b (2) and pT4a (2) and 2/6 had lymph nodal metastasis at time of surgery. 1 patient had concomitant Gleason score 9 and pT3 prostate adenocarcinoma. Follow-up available in 4 patients (mean 6.7 months) showed metastasis in 1 patient and 2 patients died at 2 months and 4 months follow-up.



Conclusions: We present an unusual morphologic pattern of bladder carcinoma with striking resemblance to a malignant vasoformative tumor. Knowledge of this pattern is important to avoid misdiagnosis particularly in smaller TURBT samples. It appears that this morphology is associated with higher tumor stage and suggests a poorer outcome.

973 Application of ERG/TFF3/HMWCK Triple Immunostain: A Novel Diagnostic Biomarker in Prostate Needle Biopsies

K Park, F Demichelis, Y-L Chiu, MA Rubin, JM Mosquera. Weill Medical College of Cornell University, New York; University of Trento, Trento, Italy.

Background: Trefoil factor 3 (TFF3) expression is associated with various cancers and found to be over-expressed in a subset of prostate cancer (PCa). Functional studies suggest that *TMPRSS2-ERG* fusion down-regulates TFF3 expression in hormone-naïve prostate cancer. Through these *cis* interactions on chromosome 21, we posit a mutually exclusive expression of ERG and TFF3. Given this inverse relationship in

expression, we developed a triple immunohistochemistry (IHC) assay for ERG, TFF3, and high-molecular weight cytokeratin (HMWCK), and evaluated its utility as a PCa specific biomarker.

Design: ERG, TFF3, and HMWCK antibodies were sequentially applied on three tissue microarrays (TMAs), composed of 103 localized PCa and 50 benign prostate samples. Intensity scores for both nuclear ERG and cytoplasmic TFF3 expression were assigned. Statistical analysis was performed on TMA results. In addition, 21 prostate biopsy samples containing small atypical glands and minute foci of carcinoma were stained using the same IHC protocol.

Results: ERG and TFF3 were expressed in 43% (44/103) and 73% (75/103) of PCa, respectively; co-expression was observed in 21% (22/103) of PCa samples, and 6% of PCa samples (6/103) failed to express ERG or TFF3. The mutually exclusive expression of ERG (nuclear) or TFF3 (cytoplasmic) was statistically significant (p -value < 0.0001 from Chi-Square test) with 90% of ERG-negative tumors (53/59) demonstrating TFF3 expression. 5 benign cases demonstrated TFF3 expression and none were positive for ERG. Sensitivity and specificity of ERG and TFF3 in detecting PCa was 94% and 90%, respectively. In addition to morphology, HMWCK expression in basal cells distinguished TFF3-positive benign glands from cancerous glands. TFF3 and ERG expression was not associated with Gleason grade, tumor stage, or rate of biochemical recurrence. IHC protocol was successful in prostate biopsies, demonstrating its application in clinical practice.

Conclusions: We observed that TFF3 is over-expressed in 73% of primary PCa, significantly more in ERG-negative tumors than ERG-positive ones, and 94% of tumor cases in this study cohort had over-expression of either ERG or TFF3. Combined with HMWCK, we have developed a highly sensitive and specific *in situ* PCa diagnostic biomarker. The feasibility of this triple stain for molecular characterization of PCa, and as a supplemental diagnostic tool for prostate needle biopsies should be further expanded.

974 Concurrent *AURKA* and *MYCN* Amplification in Primary Prostate Adenocarcinoma Is Associated with the Development of Lethal Neuroendocrine Prostate Cancer

K Park, H Beltran, TY MacDonald, ST Tagawa, DM Nanus, MA Rubin, JM Mosquera. Weill Medical College of Cornell University, New York, NY.

Background: Neuroendocrine prostate cancer (NEPC) is an aggressive variant of prostate cancer that most commonly arises from existing prostate adenocarcinoma (PCa), with likely clonal origin. There is currently no effective therapy with most patients surviving less than one year. Recent work identified the overexpression and amplification of Aurora kinase A (*AURKA*) and N-myc (*MYCN*) in metastatic NEPC, evidence that they cooperate to directly induce a neuroendocrine (NE) phenotype in PCa, and are targetable with Aurora kinase inhibitor therapy (AKI). We evaluated primary prostate tumors of patients that later developed lethal NEPC and metastases for presence of *AURKA* and *MYCN* alterations.

Design: 180 primary PCa tumors were evaluated, of which 64 tumors were from patients who later developed NEPC (low serum PSA, increased serum Chromogranin A, metastatic disease). These included 19 acinar PCa, and 45 mixed small cell/ acinar to pure small cell carcinoma. 8 metastatic tumors were available, 6 of which had matching primary PCa for evaluation. Histology of metastases included 6 mixed small cell/acinar to pure small cell carcinoma (pleura, pelvic bone/soft tissue, epidural, colon), and poorly differentiated adenocarcinoma (liver, brain, spine). Fluorescence *in situ* hybridization (FISH) using centromeric and target gene probes was performed and correlated with histological findings. 20 benign prostate tissue samples were used as controls.

Results: *AURKA* and concurrent *MYCN* amplification were identified in 75% of evaluable primary PCa of patients that later developed NEPC. In contrast, *AURKA* and *MYCN* amplifications were identified in 5% of 116 cases of an unselected PCa cohort. When metastatic NEPC was compared to primary PCa of same patient, there was 100% concordance of *AURKA* and *MYCN* amplification. In metastatic tumors with mixed features, there was 94% concordance between *AURKA* and *MYCN* amplification. 0% benign prostate harbored *AURKA* and *MYCN* amplification.

Conclusions: *AURKA* and *MYCN* amplification occurs early and is nearly always concurrent despite their location in separate chromosomes. Its presence in primary PCa identifies patients predisposed to the development of an aggressive and lethal NEPC variant. These patients may benefit from early intervention with AKI therapy. Therefore, *AURKA* and *MYCN* amplification may be new prognostic and predictive biomarkers.

975 Evaluation of Novel ERG/SPINK1 IHC and 4-Color Quantum-Dot Based ERG/P TEN FISH in Radical Prostatectomy Specimens

K Park, N Palanisamy, T MacDonald, J Siddiqui, AM Chinnaiyan, MG Sanda, H Ye, MA Rubin, JM Mosquera. Weill Medical College of Cornell University, New York, NY; University of Michigan, Ann Arbor, MI; Beth Israel Deaconess Medical Center and Harvard Med School, Boston, MA.

Background: *TMPRSS2-ERG* gene fusions and SPINK1 overexpression have been reported in approximately 50% and 10% of prostate cancer (PCa). We investigated tissue extent of both biomarkers in radical prostatectomy (RP) specimens using novel dual ERG/SPINK1 IHC and 4-color quantum-dot based ERG/P TEN FISH. The study was conducted with tissue from patients enrolled in the Early Detection Research Network (EDRN), a well-characterized clinical cohort suitable for further validation studies.

Design: 236 H&E slides corresponding to different areas of 101 dominant and 122 secondary tumor nodule(s) from 101 RP specimens were reviewed. ERG/SPINK1 IHC and ERG/P TEN FISH were performed on Discovery and Benchmark XT platforms (Ventana). Semi-quantitative evaluation of nuclear ERG and cytoplasmic SPINK1 expression was performed: >20% staining extent and 2-3 intensity (scale 0 to 3) was considered positive. ERG (break-apart assay; red-5' and green-3') and P TEN (orange-P TEN; yellow-Centromere 10) signals were automatically deconvolved using an interferometer, and each gene status was determined using spectral imaging software.

Results: 24/101 cases had one dominant tumor nodule only, 31/101 had one dominant and one secondary nodule, and 46/101 had one dominant and two secondary nodules. By IHC, 59/101 (58%) RP cases demonstrated at least one ERG-positive tumor nodule, and 8/101 (8%) cases showed at least one SPINK1-positive tumor.

Nuclear ERG staining was always strong-diffuse, and cytoplasmic SPINK1 staining was strong-focal. ERG and SPINK1 expression was mutually exclusive in all cases. 34/101 (34%) RP specimens demonstrated neither ERG nor SPINK1 expression. By FISH, ERG rearrangement was observed in 98% of ERG positive tumors by IHC, approximately 30% of which demonstrated ERG translocation through deletion. Homozygous and hemizygous P TEN deletions were observed in both ERG-rearranged and non-rearranged tumors. However, P TEN deletions were not observed in SPINK1-positive cases.

Conclusions: To our knowledge, this is the first study designed to validate the feasibility of multiplex biomarker tissue-assays on all distinct tumor nodules in RP specimens from a clinical cohort. We demonstrate that both ERG/SPINK1 IHC and 4-color quantum-dot based FISH assays show sensitive and specific detection of dual protein expression and multiple gene rearrangements, respectively. Further studies to validate clinical correlation of these assays are ongoing.

976 Immunohistochemical Evaluation of ERG Expression in Metastatic Carcinoma of the Prostate

ER Parrilla-Castellar, JC Chevillat, M Kohli, TJ Sebo, RE Jimenez. Mayo Clinic, Rochester, MN.

Background: *TMPRSS2-ERG* is the most common gene fusion occurring in prostate cancer (PCa), and results in the expression of a truncated protein product of the oncogene ERG. Immunohistochemical detection of this protein product has been demonstrated to have a high correlation with *TMPRSS2-ERG* gene fusion status in primary prostatic tumors. Feasibility of ERG expression assessment and its frequency in metastatic PCa have not been extensively evaluated.

Design: We reviewed 75 cases of metastatic PCa and performed immunohistochemistry for ERG utilizing a monoclonal antibody. ERG expression was evaluated as positive if nuclear staining was observed. Overall survival from date of diagnosis was assessed using the Kaplan-Meier method and the log-rank test. Multivariate analysis was carried-out using a Cox regression model. Clinical end-points included date of death or date of last follow-up.

Results: Metastatic sites of involvement included bone (54%), lung (20%), liver (19%), brain (4%), gastrointestinal tract (1%), bladder (1%), and lymph node (1%). Overall, ERG was positive in 20 cases (27%), including 9/40 bone, 6/16 lung, 2/14 liver, 2/3 brain, 1/1 bladder, and 0/1 colon. Lung cases represented 30% of ERG-positive cases, compared to 18% of ERG-negative case ($p=0.341$). All tumors showed high-grade morphology (Gleason grade 8-10), and no morphologic features distinguished ERG-positive cases. ERG expression did not correlate with survival in either univariate or multivariate analysis.

Conclusions: Frequency of ERG expression in metastatic PCa is similar to reported rates of *TMPRSS2-ERG* gene fusion in this setting. ERG positivity is not predictive of site of metastasis or survival after detection of metastasis. Since *TMPRSS2-ERG* status could potentially influence the modality of systemic therapy, its determination by immunohistochemical evaluation of ERG expression may be a viable and affordable option in patients with metastatic PCa.

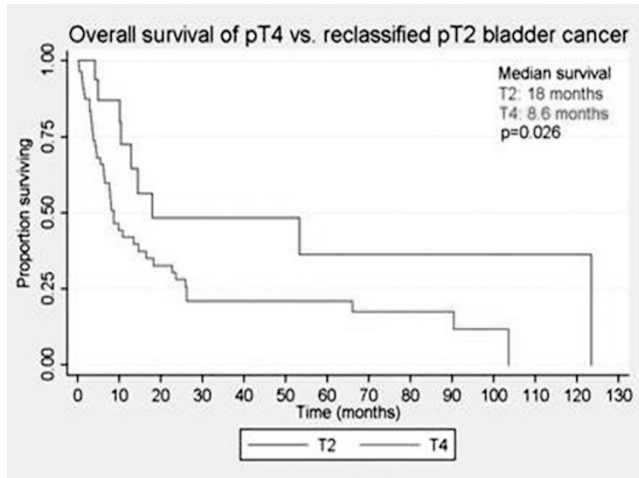
977 Overall Survival after Radical Cystectomy for Bladder Cancer Using the New AJCC Pathologic Classification for Prostatic Stromal Invasion

AR Patel, MC Large, S Prasad, JA Cohn, A Tatjana, JB Taxy, ND Smith, GD Steinberg, GP Paner. University of Chicago, Chicago, IL.

Background: In 2010, the American Joint Committee on Cancer (AJCC) reclassified primary staging for bladder cancer to include prostatic stromal invasion directly from bladder cancer and exclude subepithelial invasion of the prostatic urethra as pT4 staging status. We sought to determine whether the changes were reflective of overall survival between pT4 disease and the newly classified pT2 prostatic stromal invasion.

Design: We retrospectively extracted patients in our institutional cystectomy database with pT4 disease. Additionally, we queried the pathology database for all cystectomy specimens with prostatic urethral involvement. We systematically reclassified patients according to the new AJCC staging guidelines and divided the cohort into 2 groups: pT4 (n=56) and reclassified pT2 (n=21). Our primary endpoint was overall survival. We examined demographic factors and pathologic factors for each group.

Results: The two groups did not differ with respect to age, race, Charlson comorbidity index, or tumor size. However, the reclassified pT2 group compared to the pT4 group had a lower rate of lymph node involvement (15% vs 55%, $p=0.002$) and any positive margins (30% vs 62%, $p=0.008$). Median overall survival for reclassified pT2 versus pT4 was 18 months versus 8.6 months, $p=0.026$.



Conclusions: The new AJCC staging for urothelial carcinoma prostatic stromal invasion corresponds to a difference in pathologic outcomes as well as in overall survival for our population. Our results support continued use of the new AJCC staging system for bladder cancer.

978 Expression of Syndecan-1 (CD138) in Bladder Cancer with Emphasis on Conventional Urothelial Carcinoma and Urothelial Carcinoma with Squamous Differentiation

S Patel, AO Osunkoya, C Ormenisan, GM Oprea-Ilies. Emory University, Atlanta, GA.
Background: Syndecan-1(CD138) is a member of the family transmembrane heparan sulfate proteoglycans, which are involved in cell-to-cell adhesion and the interaction of cells with the extracellular matrix, cell migration and angiogenesis. Altered CD138 (Syndecan-1) expression has been described in carcinogenesis of various tumors in which it correlates with gain of malignant characteristics and adverse outcome. Syndecan-1(CD138) expression has also been described in Plasmacytoid variant of Urothelial Carcinoma (UCa). However, Syndecan-1(CD138) expression has not been well characterized in conventional UCa and UCa with squamous differentiation.

Design: Tissue microarrays (TMA) were constructed from 155 bladder tumor specimens retrieved from 82 patients. 40/155 cases (26%) demonstrated at least focal squamous differentiation. Immunohistochemical stains for Syndecan-1(CD138) was performed on the TMAs, and intensity, percentage, and pattern of staining in tumor cells was documented. Data was recorded with respect to tumor type, grade, stage, patient age, gender, and clinical outcome when available (39 cases). Preliminary statistical analysis was performed by Chi-square analysis. Kaplan-Meier survival plots were constructed, and disease-free survival was compared via log-rank test.

Results: There was a statistically significant correlation between cytoplasmic granular staining and UCa with squamous differentiation by chi-square ($p < 0.001$), with a kappa statistic of 0.686 ($p < 0.001$). 3+ cytoplasmic granular staining was associated with non-papillary architecture ($p = 0.001$), high T-stage ($p = 0.02$), and high M-stage ($p = 0.02$) but not with tumor grade, patient age, or gender ($p > 0.05$).

Conclusions: 1. UCa with squamous differentiation demonstrates statistically significantly increased cytoplasmic granular expression of Syndecan-1(CD138) relative to conventional UCa. Syndecan-1(CD138) may be involved in the pathogenesis of squamous differentiation in UCa, and may conceivably play a role in the aggressive phenotype in this variant of UCa.

2. Anti-Cd138 agents may be useful in treating these more aggressive urothelial tumors.

979 Comparative Analysis of 12-Core Biopsy Results and Tumor Location in Prostatectomy Specimens

L Pelaez, V Iremashvili, M Jorda, M Manoharan, DL Rosenberg, MS Soloway. University of Miami, Miller School of Medicine, Miami, FL.

Background: The 12-core transrectal prostate biopsy scheme has emerged as a standard of care. However, quality of sampling may vary in different areas of the prostate included in this procedure. We have analyzed the diagnostic performance of individual prostate biopsy cores.

Design: The study included 250 men who underwent radical prostatectomy at our institution. All participants had a systematic 12-core transrectal prostate biopsy containing lateral and medial cores from each side of the apical, medial and basal thirds of the prostate. After obtaining a 2 mm apical margin the prostatectomy specimens were step-sectioned at 3 to 5-mm intervals in transverse planes into separate blocks. Outlines of each cancer area were drawn on the slides under the microscope and then copied to paper diagrams for prostate sectioning. Biopsy results were matched with histologic maps of the prostatectomy specimens. Sensitivity, negative predictive value (NPV), and overall accuracy were calculated for each biopsy core location and compared between different groups of cores. In addition, patients in the upper quartile of prostate weight were compared to the rest of the cohort.

Results: While in the prostatectomy specimens cancer was found more frequently in the apex, biopsy cores obtained from this third of the prostate were less likely to be positive than mid and basal samples. As a result sensitivity, NPV, and overall accuracy were significantly lower for apical cores. Average NPV and overall accuracy of basal and mid lateral biopsies were inferior to those of medial biopsies on the same levels. However, sensitivity of these lateral cores was similar to that of the medial cores. It should be

noted that during pathological examination cancer was much more frequently found in the lateral areas of mid- and basal prostate compared to the medial ones. Sensitivities of apical and mid cores were significantly lower in patients with larger prostates.

Conclusions: Our study has demonstrated significant variations in the quality of sampling of different areas included into the current 12-core transrectal biopsy scheme. Decreased accuracy in lateral mid and basal cores results from higher frequencies of cancer in corresponding prostate areas, and therefore additional samples should be taken at these locations. In addition, diagnostic accuracy of apical cores may be improved through better targeting of the prostatic apex. This may be particularly important in patients with larger prostates.

980 Cytogenomic Analysis Is a Useful Adjunct Diagnostic Tool for Difficult Renal Oncocytic Tumors

AL Peterson, A Ayala, JY Ro, SS Shen, LD Truong, FA Monzon. The Methodist Hospital, Houston, TX.

Background: The differential diagnosis of renal oncocytic neoplasms includes clear cell renal cell carcinoma (ccRCC with granular, eosinophilic or rhabdoid features), type II papillary RCC, chromophobe RCC (chRCC) and oncocytoma. In some of these tumors morphology and immunoprofile studies may not render a definitive diagnosis. An accurate diagnosis is essential for proper patient management, especially targeted therapy. Renal tumor subtypes have been shown to have specific chromosomal gains and losses. We studied the feasibility of using cytogenomic arrays as an adjunct in the diagnosis of difficult oncocytic renal tumors.

Design: We evaluated 26 archived renal neoplasms with oncocytic features using Affymetrix 250K Nsp mapping arrays. Tumors were independently reviewed by 4 genito-urinary (GU) pathologists. Cytogenomic data was interpreted based on previously reported genomic imbalances characteristic for each renal neoplasm. These findings were compared to the morphologic diagnosis of the expert panel.

Results: Classic cytogenomic patterns of renal neoplasm subtypes were identified in 92% (24/26) of the cases. All cases in which the pathologist's panel reached a diagnostic consensus (n=11) were concordant with the molecular findings. Two cases diagnosed as RCC unclassified by the panel had cytogenomic profiles consistent with ccRCC. A majority consensus was reached in 31% (n=8) of the cases with concordant molecular findings in 62% (5/8) of these cases. The remaining 27% (n=7) of cases did not have a majority consensus and represented cases for which the differential was oncocytoma, chRCC, mixed/hybrid tumor or unclassified. The majority of these cases (n=4) had cytogenomic profiles of oncocytomas. One of these cases had a profile not classic for known renal neoplasms; however the limited number of affected chromosomes suggested an oncocytoma diagnosis.

Conclusions: Cytogenomic arrays provided chromosomal profiles that allowed classification in 92% of all difficult oncocytic renal tumor cases. In cases in which expert GU pathologists could not achieve a consensus, the use of chromosomal profiles allowed for diagnostic classification in 87% and suggested a diagnosis in the rest. We conclude that cytogenomic analysis with SNP microarrays is a useful tool to aid in the diagnosis of oncocytic renal cell neoplasms that are difficult to classify morphologically. This technique is feasible and now available to resolve these difficult cases in the clinical setting.

981 Acquired Mitochondrial DNA Mutations in Metastatic Prostatic Adenocarcinoma

JA Petros, RS Arnold, LD True, LW Chung, AO Osunkoya. Emory University School of Medicine, Atlanta; Cedars-Sinai Medical Center, Los Angeles; University of Washington, Seattle.

Background: Mitochondrial DNA (mtDNA) mutations are present in patients with prostatic adenocarcinoma both as modulators of inherited predisposition to disease, and as somatically acquired mutations in the primary tumors. In animal models, it has been suggested that additional mtDNA mutations can markedly influence metastatic capability of tumor cells. The presence of additional acquired mtDNA in metastatic prostatic adenocarcinoma in humans has not been studied.

Design: In order to determine whether additional mutations occur in the process of metastasis in humans, we performed mtDNA sequencing of bone metastasis from three patients with known mtDNA mutations (Patient 1: G9477A; Patient 2: C4458A, C8532T and Patient 3: G7521A, G8854A), that died of metastatic prostatic adenocarcinoma. All bone specimens were confirmed to contain cancer on routine histological analysis. Decalcified, fixed sections were subjected to laser capture microdissection to obtain pure metastatic cancer for sequencing of specific mitochondrially encoded genes. In order to determine which mutations were associated with malignant progression, control tissue (normal kidney) was also sequenced from each patient.

Results: Metastatic prostatic adenocarcinoma to bone contained multiple pathogenic mutations in key mitochondrial genes that were not present in corresponding normal tissues. These mutations include protein synthesis mutations (in both ribosomal RNA and tRNAs) as well as amino-acid altering missense mutations in respiratory complexes 1 and 4. Both homoplasmic and heteroplasmic alterations were seen. One alteration in particular appeared to be especially prevalent in metastatic prostatic adenocarcinoma in all patients; the A10398G (Thr114Ala) mutation of the NADH Dehydrogenase Subunit 3 (ND3) mitochondrial gene.

Conclusions: This is the first study to demonstrate that metastatic prostatic adenocarcinoma is characterized by a high level of acquired pathogenic mutations in the mitochondrial genome. A specific individual mutation (A10398G), appears to be particularly common as a somatic mutation in metastatic prostatic adenocarcinoma to bone. It is therefore conceivable that this mutation may be involved in cancer cell alteration in a manner that enhances the metastatic phenotype.

982 Values of Expression of SOCS-3 in Prostatic Biopsies

F Pierconti, T Cenci, F Pinto, PF Bassi, LM Larocca. Catholic University of Sacred Heart, Rome, Italy.

Background: In a recent study we found that the promoter of *SOCS3* was methylated in 39.2% of prostate cancer, while all benign prostatic hyperplasias (BPH) and normal controls had an unmethylated pattern. *SOCS3* promoter methylation significantly associated with intermediate-high grade Gleason score and with an unfavorable clinical outcome. In order to validate our results in prostatic biopsies, we analyzed *SOCS3* protein expression in a series of biopsies including BPH and prostatic adenocarcinoma. **Design:** *SOCS-3* protein expression was analyzed by immunohistochemistry in 20 BPH and in 90 prostate cancer biopsies: 54 prostatic carcinoma with Gleason score 7, 18 with Gleason score <7 and 18 with Gleason score >7. *SOCS3* methylation status was analyzed with Methylation-Specific PCR (MSP-PCR). Slides were incubated with monoclonal antibody *SOCS3* (1E4) (1.5 mg/ml; Abnova, Taiwan). The *SOCS3* staining intensity were evaluated by two pathologist (FP and LML) in three different way: positive; negative; weak intensity (two different pattern: weak staining in all neoplastic glands and mixed areas with positive and negative neoplastic glands). Colonic mucosa were used as positive control. We statistically analyzed the correlation between our results and clinical data.

Results: *SOCS3* positive staining were found in all cases of BPH, all cases of adenocarcinoma with Gleason score <7 and in 14 cases with Gleason score 7, negative staining were found in all cases of adenocarcinoma Gleason score >7 and in 10 cases with Gleason score 7. Weak *SOCS3* staining were found in 30 cases of adenocarcinoma Gleason score 7. Tumors *SOCS3* negative were significantly more aggressive than *SOCS3* positive ones in terms of TNM stage and positivity of surgical margin. Moreover, among cases with Gleason score 7, negative staining of *SOCS3* identifies a subgroup of tumor with more aggressive clinical behavior (increase number of T3) than positive ones. **Conclusions:** In prostatic biopsies immunohistochemical analysis of *SOCS3* protein identify among prostatic adenocarcinoma Gleason score 7:

A subgroup of tumor negative staining for *SOCS3* with aggressive clinical behavior and thus object of strict follow-up and suitable to demethylating agents therapy. A subgroup of tumors with weak *SOCS3* staining, not identified by methylation analysis, probably corresponding to an intermediate stage of tumor turning towards shutdown of *SOCS3*, whose clinical behavior requires a long follow-up to be clearly evaluated.

983 Nephrogenic Adenoma Showing a Flat Pattern. Description of a New Histological Variant of a Rare Benign Lesion Using PAX-2 and PAX-8 Immunohistochemistry

S Pina-Oviedo, JY Ro. The Methodist Hospital, Houston, TX.

Background: Nephrogenic adenoma (NA) is a rare benign lesion of the bladder that mostly occurs in males. Its histogenesis is uncertain but possible origin from mesonephric embryologic remnants of the bladder, metaplastic urothelial changes after chronic inflammation, or renal cell shedding and implantation into the bladder have been postulated. Several histological patterns including a tubular, tubulocystic, polypoid and papillary patterns have been described. NA consists of tubules, cysts or papillae lined by flat to polygonal cells with large nucleus and middle-sized nucleolus, occasionally separated by stroma with associated chronic inflammation. Although a benign entity, NA is a gross and microscopic mimicker of malignant lesions. By immunohistochemistry, NAs are positive for the renal tubule markers PAX-2, PAX-8, AMACR, CD10 and CK7, and negative for urothelial (thrombomodulin, p63) and/or prostate markers (PSA). We described for the first time the presence of NA with a flat pattern adjacent to tubular and papillary NAs, and the utility of PAX-8 along with PAX-2 for the diagnosis of this lesion.

Design: Fifteen (15) cases of NA were retrieved from the archives of our institution. The following immunostains were performed: PAX-8, PAX-2, thrombomodulin and p63. Appropriate positive and negative controls were used.

Results: PAX-8 immunostain was positive in 9 cases (60%) of NAs; PAX-2 was positive in 14 (93%) of the cases. Thrombomodulin and p63 were positive in 1 case (<1%), each. By immunohistochemical evaluation with PAX-2 and PAX-8, we were able to identify that at least 9 cases (60%) of NAs not only presented tubular or papillary patterns, but also featured a flat pattern that extended into the adjacent urothelium or spreaded in a Pagetoid fashion.

Conclusions: We report the presence of NA with a flat pattern in at least 60% of our cases after immunohistochemical evaluation of adjacent areas of tubular or papillary NAs. PAX-8, along with PAX-2, may be also considered as a marker for the detection and diagnosis of NA. PAX-2 and PAX-8 expression also supports the hypothesis of its possible renal epithelial origin. Recognition of a flat pattern in NA may be important for differential diagnosis, however, its clinical implications are uncertain.

984 Pigmented Microcystic Chromophobe Renal Cell Carcinoma: A Peculiar Morphological Variant. Clinicopathologic, Immunohistochemical, and Molecular Cytogenetic Study of 33 Cases

FJ Queipo, A Panizo, A Tienza, I Rodriguez, JJ Sola, J Pardo. Clinica Universidad de Navarra, Pamplona, Spain; Complejo Hospitalario de Navarra "A", Pamplona, Spain.

Background: The chromophobe renal cell carcinoma (CRCC) is a tumor that exhibits two different morphologic subtypes. Pigmented microcystic and cribriform (PMCRCC) is a new morphologic subtype recently described. The aim of this study is to investigate the clinical, histologic, IHC and cytogenetic profile of 33 cases of PMCRCC.

Design: We identified 33 cases in 32 patients of PMCRCC variant. In all cases we performed a detailed clinical, morphological, and IHC study. Chromosomal abnormalities of chromosomes (CHRO) 7 and 17 were evaluated by automated dual-color silver-enhanced in situ hybridization (SISH) on paraffin-embedded tissue.

CHRO imbalance was defined on the basis of changes in both CHRO index and signal distribution: when only one of these was altered, this was classified as a tendency to gain or loss.

Results: Age range was 41 to 83 yrs, 28 males and 4 women. 14 cases were in the right kidney, 16 in the left and 1 bilateral. The diameter of the tumors ranged between 1 and 10 cm (mean 4 cm). 23 were pT1, 6 pT2, and 2 pT3. Grossly the tumors were solid, with a brown dark color. Microscopically, tumors consisted of eosinophilic cells arranged in microcysts or microalveoli in a cribriform pattern, and focally formed adenomatous structures. Necrosis foci were seen in 5 cases. All tumors showed extracellular dark brown pigment, although in some cases also in the tumor cytoplasm. The pigment stained with Masson Fontana and focally with iron stain. There were microcalcifications in all cases. No case presented sarcomatoid transformation. All tumors were positive for CK7, EMA, and Claudin-7. Tumors were negative for RCC, AMACR, HMB45, and S100. Tumors showed both multiple monosomies and polysomies. Monosomy of CHRO 17 was seen in 2/24 cases, and 12 showed a trend towards loss. Monosomy of CHRO 7 was present in 1/16 cases. Polysomy of chromosome 17 and 7 was found in 1/24 and 10/16 cases, respectively. The median follow-up of the 32 patients was 47.5 months (range 3-156): 30 were alive without disease, and 2 were alive with hepatic metastasis. **Conclusions:** The PMCRCC constitute a morphologically distinctive and unusual variant that expands the spectrum of the CRCC. PMCRCC show an immunohistochemical profile and monosomy of CHRO 17 corresponding to usual forms of CRCC. However polysomy of CHRO 7 was common, unlike CRCC. This study confirms that these tumors have a low aggressive behavior, with absence of sarcomatoid dedifferentiation, and exceptional distant metastases.

985 Nephrogenic Adenoma: An Immunohistochemical Study

W Quinones, A Zober, Y Yao, Z Bing. Hospital of University of Pennsylvania, Philadelphia, PA.

Background: Nephrogenic adenoma (NA) is a rare benign lesion commonly occurring in the urinary bladder. NA may be derived from detached renal tubular cells implanting along the urothelial tract in previously injured areas. NA can be confused with lesions with papillary architectures including urothelial papilloma, papillary urothelium neoplasm with low malignant potential, and low-grade papillary urothelial carcinomas. NA involving deep lamina propria and/or superficial muscle can mimic metastatic prostatic adenocarcinoma, urothelial carcinoma with bland histology including nest variant of urothelial carcinoma and microcystic urothelial carcinoma, and clear cell adenocarcinoma.

Design: Twenty one cases of NAs were retrieved from the archives of hospital of the University of Pennsylvania. Immunohistochemistry for PAX8, p63, CK903 and PSA were performed on routine tissue sections according to the standard immunohistochemistry protocols. Intensity of the nuclear staining for PAX8 and p63 and the cytoplasmic staining for CK903 and PSA were evaluated and graded as 0, 1+, 2+, and 3+. Extent of staining was assigned as focal (<25%), nonfocal (25% to 75%), or diffuse (>75%).

Results: PAX8 showed diffuse moderate to strong (2+/3+) nuclear staining in all of NAs (n=21) and negative in the normal urothelium (n=15). Nuclear staining for p63 was not seen in any case of NAs examined (n=19) and was diffuse and strong (3+) in the normal urothelium (n=14). High molecular weight keratin CK903 showed weak (1+) diffuse staining in all of the nephrogenic adenomas examined (n=19) and diffuse and strong positivity in the normal urothelium (n=16). PSA staining was negative in both of the NAs (n=21) and normal urothelium (n=16).

Conclusions: We evaluated a panel of immunohistochemical markers in 21 cases nephrogenic adenomas. A panel composed of PAX8, p63 and PSA appears to be sensitive and specific in differentiating NA from its mimics of urothelial and prostatic origins.

986 Cytogenomic Molecular Profiles of Tubulocystic Carcinoma of the Kidney

G Quiroga-Garza, AG Ayala, L Truong, MB Amin, K Arora, I Alvarado-Cabrero, K Cuevas-Ocampo, FA Monzon. The Methodist Hospital Weil Medical College, Cornell University, Houston, TX; Cedars-Sinai Medical Center, Los Angeles, CA; Mexican Oncology Hospital, IMSS, Mexico City, DF, Mexico.

Background: Tubulocystic renal cell carcinoma is not yet included in the latest WHO classification of renal neoplasms. Considered a variant of collecting duct carcinoma, now is regarded as an independent pathologic entity. Studies have reported chromosomal imbalances in this tumor similar to those seen in papillary RCC, but a genome-wide chromosome copy number analysis has not been performed previously.

Design: Eight cases of tubulocystic carcinoma were identified from institutional archives under IRB approved protocols. H&E-stained slides were reviewed, confirming the diagnosis and outline of the tumor and nontumorous components, which were microdissected from 10um unstained sections. After total DNA extraction from each specimen, DNA copy number variation and loss of heterozygosity were analyzed using Affimetrix 250K Nsp genotyping arrays.

Results: Clinicopathological information was available for six cases (6/8). Five male and one female patients, ages 39 to 70 years (mean: 54.5); tumor size was 2.5 to 6.5 (mean: 3.8). In two patients, there were associated synchronous tumors (papillary RCC and clear cell RCC). All tumors showed chromosomal abnormalities, with the number of affected chromosomes ranging from 1 to 12. Loss of chromosome 9 and gain of chromosome 17 were observed in all cases except one (88%). Gain of chromosome 16 was seen in 5 of 8 cases (62%) and gain of 8 was seen in 4 of 8 cases (50%). Uniparental disomy was present in two of the examined cases.

Conclusions: Tubulocystic carcinoma of the kidney not only shows distinct clinicopathological features, but appears to be characterized by recurrent loss of chromosome 9 and gain of 17. This differs from the profile of other renal cell tumors, particularly collecting duct carcinomas, supporting the concept that tubulocystic

carcinoma is a different tumor entity. Cytogenetic studies in collecting duct carcinoma have not shown consistent chromosomal abnormalities. Although gain of chromosome 17 is also observed in papillary renal cell carcinoma, only one of the 8 tubulocystic carcinoma showed gain of 7, suggesting that these two tumors are not related at the genetic level. Our results suggest that the recurrent chromosomal imbalances seen in tubulocystic carcinoma can be used in the differential diagnosis from other cystic renal neoplasms.

987 Primary Clear Cell Adenocarcinoma of the Urethra: A Clinicopathologic Study of 16 Cases

P Rao, BA Czerniak, CC Guo. The University of Texas MD Anderson Cancer Center, Houston, TX.

Background: Primary clear cell adenocarcinoma of the urethra is a rare neoplasm. Limited clinicopathologic data are available for this distinct tumor.

Design: We retrospectively searched our pathology database from 1987 to 2011 and found 16 cases of primary urethral clear cell adenocarcinoma. None of the patients had a previous history of vaginal carcinoma. The pathology specimens included biopsy (n=7) and resection specimens (n=9), and histologic and immunohistochemical slides were reviewed. Clinical information was collected from patients' medical records.

Results: All but one of the patients were women. The mean age at diagnosis was 63 years (range, 46–71 years). Hematuria was the most common presenting symptom (n=7). In 8 cases, the tumor arose within a urethral diverticulum. Histologically, the tumors showed tubular, papillary, nested, or hobnail growth patterns. The tumor cells were characterized by high-grade nuclear atypia and clear or slightly eosinophilic cytoplasm. Of the 5 cases for which immunohistochemical stains were available, all were strongly positive for CK7 and negative for CK20. Tumor stage was available for 11 patients based on pathologic and clinical examinations and revealed that the tumors invaded the muscularis propria (T2, n=3), periurethral adipose tissue and anterior vaginal wall (T3, n=6), or adjacent organs (T4, n=2). Six patients developed metastasis, to regional lymph nodes (n=4), bone (n=1), or liver (n=1). Follow-up information was available for 13 patients: 5 were free of disease at a mean of 31 months 2 were alive with disease after 10 and 16 months, respectively; 4 died of disease in a mean of 14 months; and 2 died of unrelated causes.

Conclusions: Primary clear cell adenocarcinoma of the urethra is a rare tumor with a strong predilection for women. The tumor often arises within a urethral diverticulum and presents as a deeply invasive lesion. Recognizing this tumor in small biopsy specimens may be challenging, and secondary involvement of the urethra by a vaginal primary should be clinically excluded.

988 Renal Tumors in Patients with Von Hippel-Lindau Disease – A Single Institutional Study over 15 Years

P Rao, FA Monzon, E Jonasch, P Tamboli. MD Anderson Cancer Center, Houston, TX; Baylor College of Medicine, Houston, TX.

Background: Von Hippel-Lindau (VHL) disease is an autosomal dominant disorder. Patients with this disease are typically prone to develop renal tumors, CNS hemangioblastomas, retinal angiomas and pheochromocytomas. We present the largest series of cases from a single institute documenting the pathology of renal tumors arising in patients with VHL disease, encompassing a 15 year period (1996-2011).

Design: We identified 30 patients from our VHL clinic database that had a documented history of a surgical resection. All patients had a clinical diagnosis of VHL. Histologic slides from 16 nephrectomy specimens were available for review.

Results: Mean age at diagnosis was 37 years (range 10-56). Patients included 6 women and 10 men. Other clinical stigmata of VHL disease included CNS hemangioblastomas (n=10), retinal angiomas (n=7), pancreatic cysts (n=7) and adrenal pheochromocytomas (n=2). Eight patients had 2 or more clinical stigmata of VHL, in addition to a renal tumor. Nine patients presented with bilateral renal tumors. Pathologic stages included pT1 (n=10), pT2 (n=1), pT3 a or b (n=5). Five patients presented with multiple renal tumors (5 or more). The most common histologic subtype was clear cell RCC (n=12) followed by clear-cell papillary RCC (n=3) and chromophobe RCC (n=1). Most tumors were of low Fuhrman nuclear grade (1 or 2) with only one tumor displaying Fuhrman nuclear grade 4 features. The latter was the sole case of chromophobe RCC in our series which displayed extensive sarcomatoid differentiation. It was not uncommon for multiple tumors within a single resection specimen to display varying Fuhrman nuclear grades, often ranging from 1-3. Only 2 patients developed metastatic disease; 1 to the lung and bone (pT3b chromophobe RCC; time to metastasis 6 mos) and the other to the retroperitoneum (pT3a clear cell RCC; time to metastasis 36 mos). Genomic analysis (using SNP arrays) of a subset of these tumors is currently underway.

Conclusions: Von Hippel-Lindau has traditionally been known to be associated with multiple bilateral clear cell renal cell carcinomas, which are often extensively cystic. Our study demonstrates that although clear cell RCC remains the most common histologic subtype, other histologic subtypes including clear-cell papillary RCC and chromophobe RCC may also be associated with this syndrome. Most tumors behave in an indolent fashion and prognosis is related to tumor stage at diagnosis.

989 Clear Cell Papillary Renal Cell Carcinoma in Von Hippel-Lindau Disease

P Rao, FA Monzon, E Jonasch, BA Czerniak, P Tamboli. MD Anderson Cancer Center, Houston, TX; Baylor College of Medicine, Houston, TX.

Background: Clear cell papillary RCC is a renal neoplasm that has recently received widespread recognition in the literature. There have been several reports of this tumor arising in a sporadic setting and in patients with end-stage renal disease. However there is limited information available about the clinical, pathologic characteristics and genetic characteristic of this tumor in the setting of Von Hippel-Lindau (VHL) disease.

Design: We identified 29 patients from our VHL clinics database, who underwent resection at our institution. All patients had a clinical diagnosis of VHL. Histologic slides from 16 nephrectomy specimens were available for review.

Results: Three of sixteen patients had tumors that met the histologic criteria for clear cell papillary RCC. Two of the three patients presented with multiple bilateral cystic tumors. The third patient had a single renal tumor, in addition to an adrenal pheochromocytoma. All of the tumors in two patients were of the clear cell papillary type. One patient (#3) had multiple tumors, which included clear cell papillary and clear cell subtypes. The histology of in all cases was similar to that which has been previously reported for clear cell papillary RCC. Of note, all tumors were diffusely and strongly positive for CK7 and negative for racemase. All tumors showed at least focal staining for CD10, which is reportedly less common in tumors arising in the sporadic setting. The results are summarized in Table 1.

Summary of clinicopathologic data

Age/ Gender	Other clinical stigmata of VHL	Tumor configuration/ Laterality	Number of tumors	Tumor size (cm)	Fuhrman grade	Pathologic stage
1 22/F	Pheochromocytoma, hemangioblastomas	Cystic/bilateral	1	3.5	2	pT1
2 39/F	Hemangioblastoma	Cystic/bilateral	Multiple	0.6-5.3	2	pT1 (all tumors)
3 38/F	Hemangioblastoma	Cystic/bilateral	Multiple	0.4-6.5	2	pT1 (all tumors)

Comparative genomic analysis (using SNP arrays) of these clear cell papillary RCC's and clear cell RCC's is currently underway.

Conclusions: Von Hippel-Lindau disease has traditionally been known to be associated with multiple bilateral clear cell renal cell carcinomas, which are often extensively cystic in nature. This is the first reported series of cases documenting the presence of clear cell papillary RCC in patients with Von Hippel-Lindau disease. Genomic analysis will help us to better understand the biology of this unique tumor and compare it to typical clear RCC in this inherited disorder.

990 Extra-Renal Cancer Metastasizing to Primary Renal Neoplasms: A Rare Entity with Important Implications for Clinical Management

JP Reynolds, M Latour, J Zhang, XJ Yang, M Zhou. Cleveland Clinic, Cleveland, OH; CHUM, Montreal, QC, Canada; Mayo Clinic, Rochester, MN; Northwestern University, Chicago, IL.

Background: Extra-renal cancer rarely metastasizes to primary renal neoplasms and may be mistaken for a high grade component of the primary renal neoplasm. Recognition of these metastatic components is critical for proper patient management. Our study describes the clinicopathologic features of these tumors that may aid their recognition.

Design: 9 cases of extra-renal cancer metastatic to primary renal neoplasms were retrieved from the surgical pathology files of authors' institutions. Clinicopathologic information and follow-up data were reviewed.

Results: 9 patients (5 male, 4 female) had a mean age of 61.7 (range 47-74) years. 8 underwent nephrectomy, and 1 underwent biopsy. The primary renal tumors were clear cell renal cell carcinoma (CCRCC) in 5 cases and oncocytomas (OC) in 4 cases. The average size of the primary renal neoplasms was 53 (range 17-100) mm. Metastatic cancer included one adenocarcinoma (esophagus), two squamous cell carcinomas (lung), one urothelial carcinoma, three invasive ductal carcinomas (breast), one papillary thyroid carcinoma (PTC), and one diffuse large B cell lymphoma. In all cases, the metastatic tumors were present primarily within the renal tumor vasculature and formed a "second" population of cells that were significantly different from the primary renal neoplasms. 3 cases had multiple tumor foci, and 6 had a solitary metastatic focus. The size of the largest metastatic focus ranged from 4 to 70 mm. Immunohistochemistry staining was necessary to confirm the diagnosis in all cases. The average duration of follow-up is 16 (range 2-72) months. Two patients were dead of the extra-renal cancer, five alive with the extra-renal cancer. Only one patient was alive with CCRCC. One has no evidence of disease (PTC metastatic to CCRCC).

Conclusions: Extra-renal cancers metastatic to primary renal neoplasms are rare but important to recognize. In addition to obtain important clinical history, the presence of a "second" population of cells within renal tumor vasculature should prompt a consideration of metastatic extra-renal cancer. The clinical outcomes in these patients were primarily determined by the extra-renal cancer.

991 All New Antiangiogenic Therapies Can Induce "Preeclampsia-Like Syndrome"

N Rioux-Leclercq, T Dolley-Hitze, N Lorcy, M-A Belaud-Rotureau, F Jouan, C Vigneau. CHU Pontchaillou, Rennes Cedex 9, France; Institut Génétique et Développement de Rennes, Rennes, France.

Background: Anti-VEGF targeted therapies are used in metastatic carcinomas. However, renal side effects seem to be underestimated. According to the clinical and physiopathological similarities between preeclampsia and renal side effects of anti-VEGF therapies, we postulated that glomerular protein abnormalities described in the preeclampsia might be seen in kidneys developing renal side effects under antiangiogenic drugs. We report a series of patients treated by anti-VEGF therapies for cancer and undergoing a renal biopsy (RB) because of renal side effects.

Design: RB performed in several centers in France for proteinuria or renal failure under antiangiogenic drugs have been collected in Rennes. 17 RB and 5 kidneys samples from nephrectomy under antiangiogenic drugs have been included.

Results: Patients presented a proteinuria and/or renal failure and a hypertension after/ under antiangiogenic treatment. Renal biopsies have been realized mainly 14.2 +/- 9.7 months after treatment. 15/17 patients were treated by RAS blockers at the time of the biopsy. Mean proteinuria was 3.14 +/- 2.4 g/d and mean creatininemia was 146 +/- 128 µmol/L. There was mild or no biological sign of (thrombotic microangiopathy)TMA. For the 5 kidneys treated by antiangiogenic therapies before surgery, none but one

exhibited proteinuria nor hypertension. All but one kidney showed chronic TMA, 3 with acute microthrombosis and 5 with acute tubular necrosis (ATN). Serum creatinemia of patients with more than 20% ATN was higher than serum creatinemia of patients with only glomerular TMA. All of the biopsies from nephrectomies, showed only ATN due to surgical clamping. All RB showed a mild to dramatic decrease of nephrin, podocin and synaptopodin immunostained expression. Even when the patient was treated by a RAS blocker, there was no re-expression of those proteins. Moreover, there is no correlation between expression of these proteins and existence of ATN.

Conclusions: Our series underlines the importance of regular checking by arterial tension, urinary dipstick and creatininemia measurements for all patients treated by any anti-VEGF therapy. This checking might allow to detect early TMA, and allow or not the safe continuation of the therapy.

992 Practice-Based Differences in Ancillary Stain Usage When Evaluating Prostate Needle Core Biopsies

BD Robinson, RK Yantiss. Weill Cornell Medical College, New York.

Background: High molecular weight keratin (HMWCK), p63, and AMACR immunostains are often combined in a triple stain to aid prostatic adenocarcinoma (PCa) detection in needle core biopsies. However, their judicious use is necessary to prevent escalating costs when multiple biopsies are obtained, particularly if the results do not impact patient care. The purpose of this study was to evaluate patterns of ancillary stain utilization among various pathology practice models.

Design: We reviewed 400 recent outside pathology reports for patients referred to our institution from academic centers (n=63), community hospitals (n=68), commercial laboratories (n=158), and private urology groups (n=111). The following features were recorded for each part of the case: total number of cores, diagnosis, number of PCa+ cores, Gleason score (GS), percent PCa involvement, and perineural invasion (PNI). Use of ancillary stains was deemed appropriate in potentially difficult cases (*i.e.* GS \leq 7, \leq 20% involvement, and no PNI) or when results would alter clinical management, namely definitive therapy *versus* active surveillance (*i.e.* \leq 2 PCa+ cores with GS \leq 6 and \leq 50% core involvement). Ancillary stains were always considered appropriate in PCa+ cases.

Results: A diagnosis of PCa was rendered in 388 cases, including 159 in which at least 1 immunostain was used to facilitate the diagnosis. Of these, academic centers used ancillary stains the least (15%), followed by community hospitals (35%), reference laboratories (44%) and private urology groups (56%). Academic centers used immunostains in an appropriate fashion based on the above criteria, but community hospitals, reference laboratories, and private urology groups frequently obtained triple stains in PCa cases with high GS, extensive disease, or PNI (18%, 20%, 40%, respectively). These groups also used triple stains on multiple additional tissue blocks in situations that did not impact management (17%, 10%, 33%, respectively). There were no significant differences between practice groups with respect to number of cores obtained, PCa+ cores, GS, disease extent, or PNI in cancer cases.

Conclusions: Pathologists may be tempted to confirm a diagnosis of PCa with immunostains even when it is readily apparent on H&E stained sections. The increased costs incurred are often compounded by use of multiple triple stains on other blocks, the results of which may not impact treatment decisions. Pathologists can help contain healthcare costs by understanding the algorithms of prostate cancer management and limiting use of ancillary stains to situations that affect patient care.

993 Is Renal Angiomyoadenomatous Tumor (RAT) a New Entity? Clinicopathologic, Immunohistochemical and Molecular Cytogenetic Study of 3 Cases

I Rodriguez, A Panizo, FJ Queipo, I Amat, MR Mercado, M Gomez, J Pardo. Complejo Hospitalario de Navarra "A", Pamplona, Spain; Clínica Universidad de Navarra, Pamplona, Spain.

Background: Several low-grade renal cell tumors have been described. Recently, RAT (renal angiomyoadenomatous tumor), a tumor composed of admixture of an epithelial component and leiomyomatous stroma has also identified. The aim of this study is to investigate 3 new cases of RAT.

Design: We performed a detailed clinical, morphological, IHC, and molecular study. Copy numbers of chromosomes (CHRO) 7 and 17 were evaluated by automated dual-color silver-enhanced in situ hybridization. CHRO imbalance was defined on the basis of changes in both CHRO index and signal distribution. Sequencing of von Hippel-Lindau gene was also carried out.

Results: There were 2 female and 1 male patients; age ranging from 45 to 57 years, and the size from 0.7 to 2 cm. All 3 tumors were located in the right kidney (stage pT1a). One patient had a history of von Hippel Lindau disease (VHL). None had signs of tuberous sclerosis. All patients remain alive and free of recurrent or metastases after median follow-up of 5 months (range 1-25.5 months). Grossly the tumors were solid, well-defined, and grayish. Tumors were composed of admixture of epithelial cells with clear cytoplasm and prominent smooth muscle-rich stroma. Epithelial cells formed tubules or tubulopapillary structures endowed with blister-like cytoplasmic processes. All tubular structures were lined and surrounded by fine capillary network. Prominent benign leiomyomatous stroma was present in all cases. Perirenal, renal sinus, vascular invasion, tumor necrosis, and sarcomatoid dedifferentiation were not observed. All cases were positive for CK7, HMCK, CK19, EMA, PAX8, and CD10. Stromal component was positive for SMA, desmin, and h-caldesmon. CD34 and CD31 highlighted a rich capillary network surrounding the epithelial component. No positivity was observed for AMACR, RCC, TFE3, HMB45, and S100. All cases were diploid for CHRO 17 and 7 and 1 showed a trend towards polysomy of CHRO 7 by SISH. 1 tumor showed mutation in the VHL gene (patient with VHL).

Conclusions: RAT appears most likely a distinct entity based on their morphologic, IHC, and molecular features. The association of the epithelial component with the capillary network is unique and can serve as a diagnostic clue. The immunophenotype (CK7+,

CK19+, HMCK+, RCC-, AMACR-) is sufficiently distinct to allow easy separation from ccRCC and pRCC. Our findings suggest that RAT may be biologically indolent tumors with absence of distant metastases and sarcomatoid transformation.

994 Comparison of ERG Oncoprotein Expression among Matched Cohorts of African-American and Caucasian-American Prostate Cancer Patients

P Rosen, D Pfister, D Young, G Petrovics, Y Chen, A Dobi, D McLeod, S Srivastava, I Sesterhenn. Walter Reed National Military Medical Center, Bethesda, MD; University Hospital, Rheinisch-Westfälische Technische Universität, Aachen, Germany; Center for Prostate Disease Research, Uniformed Services University of the Health Sciences, Bethesda, MD; Joint Pathology Center, Silver Spring, MD.

Background: The ERG proto-oncogene is frequently overexpressed in Prostate Cancer (CaP) following genomic fusion, which places ERG under the control of the TMPRSS2 promoter. Recent studies show higher frequency of ERG rearrangement or ERG oncoprotein expression in CaP of Caucasian-American (CA) patients compared to African-American (AA) patients. The frequency of the ERG oncoprotein expression in prostate tumors of matched CA and AA CaP patients is evaluated to better understand the biological basis for differences in prostate cancer between the two populations.

Design: Ninety-one AA CaP patients were matched for age, Gleason sum and pathologic stage to 91 CA CaP patients. All underwent radical prostatectomy between 1993 and 2010. Whole mount prostate specimens were used for immunohistochemical detection of the ERG oncoprotein by an ERG monoclonal antibody (clone 9FY). Individual foci of tumors were noted as either positive or negative. ERG staining data was linked to clinico-pathologic data.

Results: Fifty-nine of 91 CA patients (64.8%) and 41/91 (45.0%) AA patients had at least one focus of tumor positive for ERG in a whole-mount prostate section ($p = 0.0073$). The index tumor was positive for ERG expression in 55/89 (61.8%) CA and 24/85 (28.2%) of AA patients ($p < 0.001$). Seventy-seven of 183 (42.1%) individual foci were positive in CA versus 51/196 in AA (26.0%; $p < 0.001$). There was a trend towards increased biochemical recurrence in CA patients with ERG positive index tumors.

Conclusions: The prevalence of ERG oncoprotein expression is significantly higher among Caucasian-American patients. Differences in pattern of ERG positivity of index and non-index tumors between Caucasian-American and African-American prostate cancer patients and trends towards decreased biochemical recurrence-free survival suggest a more accelerated growth of ERG-positive tumors in Caucasian-American patients. Differences in ERG expression have the potential to delineate biological distinctions of CaP in these patient populations.

995 Prevalence and Patterns of ERG Expression in Matched Cohorts of African-Americans and Caucasian-Americans with Prostate Cancer

PA Rosen, D Pfister, D Young, G Petrovics, A Dobi, Y Chen, DG McLeod, S Srivastava, IA Sesterhenn. Walter Reed National Military Medical Center, Bethesda, MD; Center for Prostate Disease Research, Bethesda, MD; University Hospital, Rheinisch-Westfälische Technische Universität, Aachen, Germany; Joint Pathology Center, Silver Spring, MD.

Background: The ERG proto-oncogene is frequently overexpressed in Prostate Cancer (CaP) as a result of a genomic rearrangement that places ERG under the control of the TMPRSS2 promoter. The initial report of quantitative ERG mRNA expression in micro-dissected prostate tumor cells showed significantly higher ERG expression in CaP of Caucasian-Americans (CA) patients vs. African-American (AA) patients (Petrovics *et al.*, *Oncogene*, 2005). Recent studies (Magi-Galluzzi *et al.*, *Prostate*, 2011; Elliott *et al.*, *USCAP Mtg.*, 2011) have also shown higher frequency of ERG rearrangement or ERG oncoprotein expression in CaP of CA patients. We evaluate the frequency and pattern of the ERG oncoprotein expression in prostate tumors of matched CA and AA CaP patients to better understand the biological basis for differences in prostate cancer between the two populations.

Design: Matched for age, Gleason and pathologic stage were 91 AA and 91 CA CaP patients. All underwent radical prostatectomy between 1993 and 2010. Whole mount prostate specimens were used for the immunohistochemical detection of the ERG oncoprotein by a monoclonal antibody (clone 9FY). Individual foci of tumors were noted as either positive or negative. ERG staining data was linked to clinico-pathologic data. Biochemical recurrence was defined as at least 2 PSA's of 0.2 ng/mL or higher at least 8 weeks from surgery.

Results: Comparing CA to AA CaP patients, more had at least one focus of tumor that was ERG (+) (64.8% vs. 45.0%; $p = 0.0073$), more had ERG (+) index tumors (61.8% vs. 28.2%; $p < 0.001$) and a higher percentage of individual tumor foci were ERG (+) (42.1% vs. 26.0%; $p < 0.001$). There was a trend towards increased biochemical recurrence in CA CaP patients with ERG (+) index tumors.

Conclusions: Between matched cohorts, ERG expression is more prevalent among CA CaP patients. Differences in the pattern of ERG expression in CaP and differing trends in biochemical recurrence between CA and AA patients with ERG (+) index tumors suggest a dominant clonal selection of ERG-positive tumors in CA patients. These differences in ERG expression have the potential to delineate biological distinctions of CaP in the two patient populations.

996 Significantly Lower Expression Levels of Androgen Receptor (AR) Are Associated with Erythroblastosis Virus E26 Oncogene Related Gene (ERG) Negative (-) Prostate Cancer (PCa)

JN Rosenbaum, SA Drew, W Huang. University of Wisconsin-Madison, Madison.

Background: ERG overexpression is correlated with the ERG-TMPRSS2 fusion gene, a mutation known to be present in about 50% of PCa. AR is a known regulator of the ERG-TMPRSS2 fusion gene. Despite knowledge of these relationships, limited data is available on AR expression in PCa in relation to ERG status.

Design: Two prostate tissue microarrays (TMA) were used: progression TMA (pTMA) and outcome TMA (oTMA). The pTMA consists of 384 cores: 43 stage 2 PCa, 30 stage 3 and 4 PCa, 22 metastatic PCa (Mets), 25 high grade intraepithelial neoplasia (HGPIN), 24 benign prostate hyperplasia (BPH) and 48 benign prostate tissues (BPT). The oTMA consists of 462 duplicate cores from 48 BPT and 183 PCa (125 without recurrence, 38 with biochemical recurrence and 20 with cancer recurrence either local or distant). Antibodies to e-cadherin (Biocare Medical, 1:100), AR (Biocare Medical, 1:50) and ERG (Epitomics, 1:200) were assayed using a bright field multiplex IHC. TMA sections were stained with the three antibodies and counterstained with hematoxylin. E-cadherin was used to define the epithelial compartment. The TMA slides were scanned with the Vectra™ platform. Biomarker expression analysis was performed with Vectra™ software – both Nuance and inForm™. IBM SPSS Statistics 20 was used for data analysis.

Results: Nuclear AR expression levels were significantly increased in PCa tissue compared to BPT ($p < 0.01$) with highest level in PCa Mets and PCa with cancer recurrence. ERG expression levels were also significantly increased in PCa compared to BPT ($p < 0.01$); however, no clear correlation with either PCa progression or outcome was observed. 49% PCa in pTMA expressed ERG (ERG+) and 53% of PCa in oTMA were ERG+. Comparing ERG+ to ERG- PCa in each subcategory of the two TMAs, AR expression levels in ERG- PCa were significantly lower than those in ERG+ PCa ($p < 0.01$).

Conclusions: Significantly lower AR expression in ERG- PCa suggests a dosage effect of AR in the development of ERG-TMPRSS2 fusion.

997 Do Adenocarcinomas of the Prostate with Gleason Score (GS) ≤ 6 Have the Potential To Metastasize to Lymph Nodes?

HM Ross, ON Kryvenko, JP Simko, TM Wheeler, JI Epstein. The Johns Hopkins Hospital, Baltimore; Baylor College of Medicine, Houston; Henry Ford Hospital, Detroit; UCSF, San Francisco.

Background: Although rare, GS ≤ 6 in radical prostatectomies (RP) have been reported with pelvic lymph node (LN) metastases. However, there are no studies as to whether pelvic LN metastases occur in tumors GS ≤ 6 using the ISUP modified Gleason scoring system.

Design: We searched the RP databases at 4 large academic centers for entirely submitted RPs GS ≤ 6. 14,444 cases from 1975-2010 were identified. Cases from Institution #1 were split into two groups with December 2004 as the breakpoint, reflecting when the modified ISUP Gleason grading scheme was in press.

Results: Institution #1: 10,935 men were identified with GS ≤ 6 at RP: 7,332 pre-ISUP and 3,603 post-ISUP. In the pre-ISUP group, there were 19 (0.26%) cases with positive LNs, whereas there was only 1 case (0.03%) with a positive LN in the post-ISUP group. 18/19 pre-ISUP cases had non-focal extraprostatic extension (EPE) with 4 invading seminal vesicles. The 1 post-ISUP case had focal EPE. Histological review of 17/19 cases (2 cases unavailable for review) pre-ISUP and the one post-ISUP case showed higher grade than originally reported. Of the 17 pre-ISUP reviewed cases, 3 were upgraded to 4+3=7 with small/large cribriform and poorly formed glands. 10 cases were upgraded to 3+4=7 with either glomeruloid structures, small/large cribriform glands, or ductal features. 3 cases had tertiary pattern 4 with small cribriform glands. 1 case had a prominent colloid component that had been previously left ungraded that currently would be graded as 4+5=9 with large cribriform glands and solid sheets of cells within mucin. The single post-ISUP case had a cribriform gland of tertiary pattern 4. Institutions 2-4: Out of 3,509 men with GS ≤ 6 at RP, 1 pre-ISUP (slides not available for review) and 1 post-ISUP had a positive LN. The post-ISUP case was called 3+4=7 on biopsy. Although the RP was initially graded as 3+3=6, review showed GS 3+4=7 with small cribriform glands.

Conclusions: Under-grading primarily accounts for lymph node positivity with GS ≤ 6, which has decreased significantly since the adoption of the ISUP grading system in 2005. Out of over 14,000 totally embedded RPs from multiple institutions, there was not a single case of a GS ≤ 6 tumor with LN metastases. In contrast to prevailing assumptions, Gleason score ≤ 6 tumors do not appear to metastasize to lymph nodes. Rather, Gleason patterns 4 or 5, as better defined by the current ISUP modified grading system, is required for metastatic disease.

998 Clinical Follow-Up of 101 Patients with Isolated HGPIN Immunostained for ERG

DH Russell, D Tacha, A Dobi, IA Sesterhenn, D McLeod, S Srivastava, JT Moncur. Walter Reed National Military Medical Center, Bethesda, MD; Biocare Medical, Concord, CA; Joint Pathology Center, Silver Spring, MD; Uniformed Services University of the Health Sciences, Bethesda, MD.

Background: The [9FY] antibody to the ERG oncoprotein is a sensitive surrogate marker for the *TMPRSS2-ERG* gene fusion in prostate cancer. We assessed the utility of this antibody in patients with isolated high grade prostatic intraepithelial neoplasia (HGPIN).

Design: All available prostate needle biopsy cases with isolated HGPIN from Walter Reed Army Medical Center (3/05-12/10) were stained for ERG (Brown), CK5+p63 (Purple) and P504S (Red) (ERG-4, Biocare Medical). Out of 139 total cases with only HGPIN, 169 slides from 101 cases were available. The number of core biopsies per case with HGPIN averaged 1.7 (range 1-10) out of 12 cores.

Results: Of 101 patients, eight (8%) had ERG+ HGPIN. Each patient had only one focus of HGPIN that was ERG+. Seven of the eight patients had other cores with ERG- HGPIN. Five of the eight patients with ERG+ HGPIN were rebiopsied, with an average time to initial rebiopsy of 12 mos (range 3-43 mos). On initial rebiopsy (12 cores performed), all five patients had HGPIN (range 1-3 cores) without invasive adenocarcinoma. One patient's HGPIN exhibited features consistent with intraductal carcinoma in three cores and was ERG+ in all three cores. The HGPIN in the other four rebiopsied patients (range 1-2 cores/case) was ERG-. One of the five patients with

ERG+ HGPIN was rebiopsied a third time (after 30 mos) and had adenocarcinoma. The index tumor in this patient's prostatectomy was ERG-. In the 93 patients with HGPIN that was ERG-, 34 underwent rebiopsy after an average of 15 mos (range 3-60 mos). Eight patients (24%) had adenocarcinoma on rebiopsy. Nine patients (26%) had isolated HGPIN on rebiopsy, and 17 (50%) had benign biopsies.

Conclusions: While the number of patients with ERG+ HGPIN was small, the percentage with invasive adenocarcinoma on initial rebiopsy (0%) was less than the percentage with adenocarcinoma after a diagnosis of ERG- HGPIN (24%). A larger study is needed to further assess the significance of ERG+ HGPIN, but this relatively small study suggests that ERG+ HGPIN is not associated with an increased risk of adenocarcinoma on rebiopsy, compared to patients with ERG- HGPIN. The relatively low frequency of ERG+ HGPIN in the current study likely reflects sampling issues and the focal nature of ERG positivity in HGPIN.

999 Microvessel Density Correlation with Gleason Score in Prostatic Adenocarcinoma – A Computer Assisted Image Analysis in Whole-Mount Prostatectomies

ME Salama, M Heilbrum, C Dechet, LJ Layfield, T Liu. University of Utah/ARUP, Salt Lake City, UT; University of Utah, Salt Lake City, UT.

Background: Angiogenesis has been well recognized as a fundamental element of a multistep process in the evolution of cancer progression, invasion, and metastasis. Previous studies on angiogenesis in prostate cancer revealed that angiogenesis plays a role in the progression of prostate cancer. Microvessel density (MVD), a measurement of prostate cancer angiogenesis, has been shown to be a predictor of metastasis and survival. Thus, targeting angiogenesis has been the subject of several clinical investigations, however pathological and morphologic studies are lacking. In this Study, we analyzed the correlation between MVD and Gleason score.

Design: The study consisted of 12 cases of prostate adenocarcinomas from patients (mean age: 61 years) who have undergone research MRI studies with the use of an endorectal coil 3.0T. All of the specimens were entirely submitted in a whole-mount (4.5 mm section thickness) fashion, from apex to base. Slides were reviewed to determine location, size and Gleason score of carcinoma of each plane. Slides were stained with CD31 antibody (clone JC/70A, Dako, Carpinteria, CA) and were scanned using the Aperio CS Scanscope, and analyzed with Aperio's vessel algorithm (Aperio Technologies, Inc., Vista, CA, USA). MVD defined as the area occupied by number of vessels divided by the total analysis area represented in μm^2 . Each area of Gleason score 3 and 4 was manually marked on the digitally scanned CD31 slides and value of MVD were recorded. For each stained level the MVD findings were compared according to Gleason score. T-test was used for analysis.

Results: Totally, 45 foci of Gleason pattern 3 tumor and 27 foci of Gleason pattern 4 tumor were analyzed in this study. MVD is statistically significantly higher in Gleason 4 areas ($0.009662 \pm 0.00002458/\mu\text{m}^2$) than that in Gleason 3 areas ($0.0004841 \pm 0.000007509/\mu\text{m}^2$) with a P value of 0.0091.

Conclusions: MVD in prostate cancer is closely related to Gleason grade with higher MVD noted in Gleason 4 tumor compared to Gleason 3 tumor. MVD appears to be associated with tumor aggressiveness. The benefit of angiogenesis inhibitors has become a reality in several tumor types, with significant potential in prostate cancer with higher Gleason score.

1000 Malignancies Arising in Allograft Kidneys

R Saleeb, H Faragalla, K Sy, GM Yousef, R Stewart, CJ Streutker. University of Toronto, Toronto, ON, Canada; St. Michael's Hospital, Toronto, ON, Canada.

Background: Cancer in the post kidney transplant population has been a rising concern in many publications, causing a debate regarding the need for increased post transplant surveillance. Renal carcinoma is one of the most common cancers to occur in the transplant population, almost always arising in diseased native kidneys. Rarely, tumors arise in the transplanted kidney. Our case series reports four cases of malignancy in allograft kidneys.

Design: The renal transplantation data base at St. Michael's Hospital, Toronto, Canada, containing 1584 patients, was reviewed for diagnoses of malignancies arising in the post transplant period. Cases of tumors arising in the allograft were identified, and the reports and pathology slides were reviewed.

Results: Four cases of malignancies arising in the allograft kidney were identified in the transplant population; this is a significant proportion (3.9%) of the total post-transplant malignancies (101 malignancies in 1584 patients). One tumor was a high grade urothelial carcinoma in the pelvis of the donor kidney 9 years post transplant and 6 years post BK virus infection. The other 3 cases were renal cell carcinomas, developing 1 year, 9 years, and 16 years post-transplant. The first was a clear cell carcinoma, Fuhrman Grade 3, pT1a, the second a renal cell carcinoma with areas of both clear cell and papillary architecture, Fuhrman Grade 3, pT1b and the third was a pure papillary renal cell carcinoma, Fuhrman Grade 1, pT1a. Tissue from the four tumors was submitted for DNA testing which showed that samples from all 4 tumours had two distinct profiles, suggestive of donor origin with infiltration by recipient lymphocytes.

Conclusions: Previous reports suggest that malignancies in allograft kidneys (other than post transplant lymphoproliferative disorders) were rare. We identified 4 tumours, three renal cell carcinomas and one urothelial carcinoma, in 1584 transplant patients. Tumors developed 1-16 years after transplantation. One patient had prior BK virus infection: there is a correlation in previous literature between BK virus infection and urothelial carcinoma. While the rate of malignancy in allograft kidneys is small, screening of the donor kidneys by ultrasound and/or urine cytology may be of use in detecting these lesions.

1001 Genome Expression Profiling of Holoclones Derived from Prostate Cancer

Y Salley, M Gallagher, S Elbaruni, P Smyth, C Spillane, CM Martin, W Watson, OM Sheils, JJ O'Leary. Trinity College Dublin, Dublin, Ireland; Conway Institute, University College Dublin, Dublin, Ireland.

Background: Prostate cancer is one of the five most prevalent malignancies in all male age groups worldwide. Prostate cancer is a heterogeneous disease and is the second most common cause of cancer resulting in male deaths caused by cancer and is the most commonly diagnosed cancer in Irish males. There are over 1500 new cases diagnosed every year in Ireland, the second leading cause of fatal cancer in Irish men (NCRI, 2010). Stem-like cells have been identified in several malignancies including prostate cancer and are thought to drive primary tumorigenesis through self-renewal and differentiation. Additionally, persistence of stem cells post-therapeutic intervention has been proposed as an explanation for metastasis and recurrence. Holoclones are a tightly packed clone of small cells generally thought to contain stem cells and progenitors. The aim of this study was to generate a whole genome expression profile of holoclone derived cell lineage in prostate cancer.

Design: In this study, holoclones were cultured using a high salt-soft agar assay for LNCaP (metastatic carcinoma) and PC-3 (non-metastatic adenocarcinoma) cell lines. Microarray analysis was carried out on cell lines and holoclone derived cells (n=4) and analysed by XRAY software using the criteria; $FDR \leq 0.05$ and $FC \pm 2$. Gene ontology of biological processes and pathways was generated with DAVID and PANTHER. Genes were selected and validated using a quantitative Real Time TaqMan® PCR method.

Results: Holoclones were generated from cell lines (LNCaP, PC-3) using a high salt-soft agar assay. PC-3 versus PC-3 holoclones demonstrated 228 significant differentially regulated genes and LNCaP versus LNCaP holoclones demonstrated 44 significant differentially regulated genes and validations were confirmed.

Conclusions: Various genes were identified and validated which represent stemness, differentiation and EMT as well as numerous other biological processes involved in cancer progression establishment, progression and maintenance. These gene and their relevant functions have been found to be either significantly downregulated or upregulated specifically in the PC-3 and LNCaP holoclones indicating that these cells have specific expression profiles for each holoclone/founder set cancer stem cell holoclone potential.

1002 Perinucleolar Clearing (PNC) with Macronucleoli Is Not a Feature of Some Benign Mimics of Prostate Cancer

H Samaratunga, D Samaratunga, J Yaxley, J Perry Keene, D Payton, B Delahunt. Aquesta Pathology, Brisbane, QLD, Australia; Royal Brisbane Hospital, Brisbane, QLD, Australia; Wellington School of Medicine and Health Sciences, Wellington, Otago, New Zealand.

Background: Nucleolar prominence has been found to be a useful feature in the diagnosis of prostate cancer. However, benign mimics also display prominent nucleoli. Nucleolar characteristics in these lesions on needle biopsy have not been adequately studied.

Design: 100 needle biopsies with $\leq 20\%$ Gleason score $3+3=6$ prostatic adenocarcinoma (including 38 with only small foci or $<5\%$) in one core were compared with 20 cases of adenosis and 37 of partial atrophy for presence of prominent but small nucleoli identified at $\times 400$ magnification and for very large, often eosinophilic nucleoli (macronucleoli) including those with perinucleolar clearing (PNC) easily identified at $\times 100$ or $\times 200$ magnification. The mean percentages for each were estimated visually and recorded as absent; 0, rare; $<10\%$, frequent; $10-50\%$ and common; $>50\%$.

Results: Carcinoma had prominent nucleoli in 98%, macronucleoli in 65% and macronucleoli with PNC in 46% of cases whereas adenosis had 25%, 0% and 0% and partial atrophy had 32%, 0% and 0% respectively. Macronucleoli and macronucleoli with PNC in cases with only small foci of cancer were 63% and 47% respectively. Prominent nucleoli were frequent or common in 63% of carcinoma, 10% of adenosis and 6% of partial atrophy.

Conclusions: Presence of frequent prominent nucleoli suggests a more likely diagnosis of carcinoma. Macronucleoli with or without PNC in a focus argue against a benign diagnosis. Typically, other features of carcinoma in these cases will assist with a cancer diagnosis. In cases with limited such features, an outright benign diagnosis is not warranted

1003 Metabolic Syndrome and Prostate Inflammation in Benign Prostate Hyperplasia

R Santi, M Gacci, L Vignozzi, M Carini, M Maggi, G Nesi. University of Florence, Florence, Italy.

Background: Features of metabolic syndrome (MetS), including hypertension, type 2 diabetes mellitus, abdominal obesity and dyslipidemia have all been associated with an increased risk of benign prostatic hyperplasia (BPH). Inflammation may also play a role in BPH and represents a common finding in prostate specimens for BPH. The aim of this study was to evaluate the possible association between components of MetS and the presence of an inflammatory infiltrate in prostate specimens from transurethral or open prostatectomy for BPH.

Design: In a series of 70 consecutive patients (mean age: 79.6 years; mean BMI: 26.5) MetS was defined according to NCEP-ATPIII criteria. All surgical specimens were weighed at the time of surgery. According to the standardized classification system of chronic prostatitis of NIH, the following parameters were assessed: prevalent anatomic location (stromal, periglandular, glandular), grade score (mild [1], moderate [2], severe [3]) and extent (focal [$<10\%$], multifocal [10-50%], diffuse [$>50\%$]) of the inflammatory infiltrate and the presence/absence of glandular disruption. Patients with moderate to

severe inflammation (grade 2-3 or extent $>10\%$ or presence of glandular disruption) were compared to those with mild inflammation (grade 1 or extent $<10\%$ and absence of glandular disruption).

Results: Fifty-six (80%) prostates showed moderate to severe inflammation. NCEP-ATPIII-defined MetS was detected in 23 (32.9%) patients. The presence of MetS increased the occurrence of moderate to severe inflammation even after the adjustment for age ($p=0.05$). Among MetS components, low HDL-cholesterol and high triglyceride serum levels were the most important predictors of prostate inflammation ($p=0.02$ and $p=0.022$, respectively). Moreover, the weight of prostatic adenoma significantly correlated with the extent ($p=0.026$) and the anatomic location ($p=0.017$) of inflammatory infiltrate and with the presence of glandular disruption ($p=0.008$).

Conclusions: We highlighted a statistically significant relationship between both low HDL-cholesterol and high triglyceride serum levels with the presence of an inflammatory infiltrate in adenomatous prostatic tissue. Severe inflammation was also significantly associated with increase in prostate weight. These data indicate that metabolic syndrome may play a key role in the pathogenesis of BPH and underline the importance of assessing HDL in men with BPH.

1004 E-Cadherin, Snail and Slug Expression in a Series of Non-Muscle Invasive Bladder Carcinomas with Long-Term Follow up

R Santi, T Cai, M Pepi, M Paglierani, R Bartoletti, G Nesi. University of Florence, Florence, Italy; Santa Chiara Hospital, Trento, Italy.

Background: Pathologic grading according to the 2004 WHO/ISUP proposal has been regarded as a useful tool to classify urothelial tumors into prognostically distinct categories. Unraveling molecular pathways of development for bladder carcinomas may further improve classification results. Previous reports have investigated the relationship between the expression of Snail and Slug transcription repressors and clinicopathologic features of non-muscle invasive bladder cancers.

Design: The study population consisted of 43 patients (38 men and 5 women, mean age 67.4 years), receiving transurethral resection for non-muscle invasive urothelial carcinoma. Histologic slides were reviewed and tumors were classified according to the 2004 WHO/ISUP system. Immunostaining for E-cadherin, Snail and Slug proteins was performed in all cases, and both staining intensity and percentage of positive cells were recorded. Grades according to the intensity of staining included 0, 1+, 2+, and 3+ while the percentage of positive cells was separated into 0 (0%), 1 (1% to 33%), 2 (34 to 66%), and 3 (67 to 100%). Staining results were then classified into 2 groups: weak staining (any intensity with percent category 0-1) and strong staining (intensity 2-3 with percent category 2-3).

Results: High-grade (HG) carcinomas were 21/43, with nine invasive cases (pT1). Low-grade (LG) carcinomas were 22/43, with no invasive cases (pTa). The mean follow-up period was 113.3 months. Among the 9 HGpTa cases with recurrence, strong Snail expression was detected in 7 (77.9%). Out of the 16 LGpTa patients who experienced recurrence, 11 (68.7%) showed strong positivity for Snail. Among the 9 HGpT1 cases, recurrence was observed in 4 cases and 3 (75%) of these intensely stained for Snail. With regard to immunohistochemical Snail status, Kaplan-Meier analysis demonstrated significantly different recurrence rates between patients with strong reactivity and those with weak reactivity ($p=0.003$). E-cadherin and Slug expression did not correlate with any of the clinicopathologic parameters considered.

Conclusions: Overexpression of Snail may represent a clinically relevant mechanism of cancer progression in bladder urothelial carcinoma.

1005 Immunohistochemical Profiles of Urothelial Carcinomas from Upper Urogenital Tract Versus Lower Tract. Does PAX8 Have Any Role?

J Schwartz, R Malhotra, P Zhang, M Amin. William Beaumont Hospital, Royal Oak, MI.

Background: Metastatic urothelial carcinoma (UCa) is diagnosed by histologic features and sometimes with the aid of immunohistochemical (IHC) markers such as CK7 and CK20. PAX2 and PAX8 are recent markers that have shown expression in renal tumors. PAX8 in addition has been shown to be positive in 8-23% of UCAs of kidney suggesting possible role in differentiating from lower tract UCAs. While most studies showed negative PAX-8 IHC staining in UCa of bladder, a recent single study showed 10% cases positive. We wished to evaluate the role of PAX8 in combination with other IHC markers in the diagnosis of UCa in a metastatic setting.

Design: A representative paraffin block was selected from 60 cases of UCa of kidney/ureter (n=20), urinary bladder (n=20) and metastatic UCa (n=20). Six immunostains were performed on these cases - PAX-2, PAX8, CK7, CK20, p-63 and uroplakin. Immunostains were graded visually for extent of staining 0 (0%), 1+ (1-33%), 2+ (34-66%) and 3+ ($>67\%$); and for intensity of staining as 1+ (weak), 2+ (moderate) and 3+ (strong).

Results: There was no PAX2 staining noted in any urothelial carcinoma. PAX8 positivity was noted in 12% (2/17) of UCa from kidney/ureter. No PAX-8 staining was noted in UCa of bladder. PAX8 staining was noted in 5% (1/19) in metastatic UCa, presumably from bladder primary. UCa from the kidney/ureters showed positivity for CK7 in 95% (19/20), CK20 in 71% (12/17), p63 100% (17/17) and uroplakin 18% (2/11). UCa from the urinary bladder showed positivity for CK7 in 95% (19/20), CK20 65% (13/20), p63 94% (17/18) and uroplakin 36% (4/11). Metastatic UCa showed positivity for CK7 in 100% (11/11), CK20 100% (7/7), p63 78% (7/9) and uroplakin 39% (5/13). PAX-8 immunostaining was noted in normal urothelium of the renal pelvis and in collecting tubules of kidney. Staining in normal mucosa is absent in bladder except for rare foci of basal cells.

Conclusions: PAX-2 positivity is not a feature of urothelial carcinoma and positivity should exclude urothelial primary. PAX8 on the other hand is positive in 17% in our hand. PAX8 positivity when present is invariably present as weak staining in rare isolated cells, suggesting little utility. While positivity of the more classic markers p-63, CK7 and CK20 has great value in determining urothelial tumors in a metastatic setting, this

does not differentiate upper tract tumors from lower tract tumors. The positivity for PAX8 noted in normal urothelium of upper urogenital tract was confirmed in our study, however, this did not translate into positivity in UCas arising from this site.

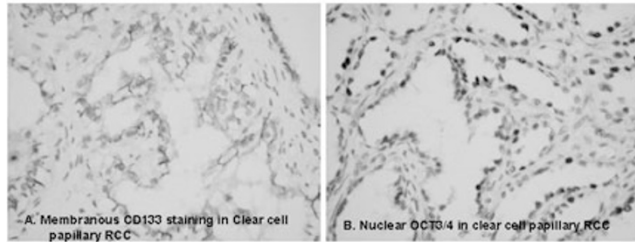
1006 Immunohistochemical Profile of Stem/Progenitor Cell Marker C133 in Variants of Renal Tumors

JD Schwartz, MB Amin, PL Zhang. William Beaumont Hospital, Royal Oak, MI; Oakland University William Beaumont School of Medicine, Rochester, MI.

Background: CD133, a stem/progenitor cell marker, is expressed diffusely in normal glomerular parietal epithelium (GPE) as well as in a small percent of normal renal tubular epithelium. Cancer stem cells have been proposed to undergo malignant transformation from benign stem cells, since only stem cells may carry sufficient genetic properties for unlimited tumor proliferation. The intent of this study was to investigate the immunohistochemical expression of CD133 in variants of renal tumors.

Design: Seven groups of renal tumors (n = 84, tumor cross sections) were immunohistochemically stained for CD133 (monoclonal AC133 antibody at 1:20 and rabbit polyclonal CD133 antibody at 1:500, in order to achieve similar positivity in normal GPE). The percent of membranous CD133 expression in tumor cells was graded as follows: 1+ <33%, 2+, 33-66% and 3+ >66%.

Results: Using monoclonal CD133, diffuse membranous positivity was found in clear cell papillary renal cell carcinoma (CCP-RCC) (10/10, 100%, 3+ in 8, 2+ in 1 and 1+ in 1) (Panel A), and often in XP11.2 translocation carcinoma (5/9, 56%, 3+ in 1, 2+ in 1 and 1+ in 3) and papillary RCC (8/15, 53%, 3+ in 2, 2+ in 1 and 1+ in 5). CD133 was also expressed in a small percent of Wilms' tumor (4/14, 28%, 1+ in epithelial component of 4 cases), clear cell RCC (3/21, 14%, 3+ in 1 and 1+ in 2), chromophobe RCC (1/7, 14%, 1+ in 1), and oncocytoma (1/5, 20%, 1+ in 1). Polyclonal CD133 staining confirmed the above findings. Stem cell transcription factor OCT3/4 staining revealed nuclear positivity in 9/10 CCP-RCC (90%, 3+ in 4, 2+ in 4, 1+ in 1 and 0 in 1) (Panel B) but it was rarely positive in the remaining types of renal tumors.



Conclusions: Our findings support the notion that cancer stem cells exist in the majority of renal tumors, although positive staining rates varied among different tumor types. In addition, CD133 and OCT3/4 expression in the majority of CCP-RCCs further support that this tumor is an independent entity of RCC derived from distal nephron tubules (taken together with its positive CK7 but negative P504S stains reported by others, and negative kidney injury molecule-1 staining found in our previous study).

1007 Ductal Adenocarcinoma of the Prostate in 1051 Radical Prostatectomy Specimens. Histopathological Features and Prognostic Relevance

A Seipel, F Wiklund, P Wiklund, L Egevad. Karolinska Institutet, Stockholm, Sweden.

Background: Ductal adenocarcinoma of the prostate (DAC) is a histological subtype of prostatic carcinoma thought to be associated with a relatively poor prognosis. The prevalence of DAC varies widely in the literature (0.4% - 12.7%). We aimed to evaluate the prognostic significance of histopathological patterns of DAC and to identify relevant diagnostic criteria.

Design: 1156 men underwent radical prostatectomy at the Karolinska Hospital 1998 - 2005. Men with neoadjuvant treatment or unavailable slides or follow-up were excluded and 1051 cases remained for review. Tumors were classified as DAC of classical type (DACC), borderline type (DACB) or prostatic carcinoma with ductal features (PCDF). A DACC had tall, columnar, pseudostratified epithelium, elongated, oval nuclei with prominent nucleoli, papillary, glandular or cribriform architecture and more than focal extent. A DACB showed most features but lacked elongated nuclear shape or classical architecture. A PCDF lacked elongated nuclei and had either DAC-type architecture or pseudostratified epithelium with high-grade atypia. Cox models were used to assess association of DAC subtypes and histopathological features with biochemical recurrence.

Results: DACC, DACB and PCDF were seen in 2.6% (27), 4.0% (42) and 1.6% (17) of 1051 radical prostatectomy specimens. DAC was almost always mixed with prostatic acinar adenocarcinoma (PAC) and only 0.2% (2/1051) contained pure DAC. Papillary, glandular and cribriform architecture was seen in 72%, 36.6% and 62.2%. Zonal origin was peripheral, transition, central zones or unclear in 57%, 7%, 1.2% and 34.8%. Location was periurethral, peripheral or both in 69.8%, 3.5% and 26.7%. DAC constituted 10% - 100% (mean 40%) of the main tumor. Necrosis was seen in 31.3%, stromal invasion of DAC in 52.3% and intraductal spread in 91.9%. In assessment of biochemical recurrence, DACC, DACB och PCDF had a HR of 1.5 (0.8-2.9), 1.4 (0.8-2.5) and 1.2 (0.5-2.7), respectively. Location, % DAC, necrosis, stromal invasion or GS of PAC component were not predictive of recurrence. In DACC/DACB and PAC, extraprostatic extension was seen in 66.7% and 42.4% (p <0.001) and seminal vesicle invasion in 13.0% and 5.0% (p = 0.0045), respectively.

Conclusions: The results suggest that DAC is more aggressive than an average PAC. It is proposed that DAC should include DACC and DACB, thus 6.6% of all prostate

cancers. Cancer with DAC type architecture only and cancer with conventional architecture and pseudostratified high-grade epithelium without elongated nuclei should not be included in DAC.

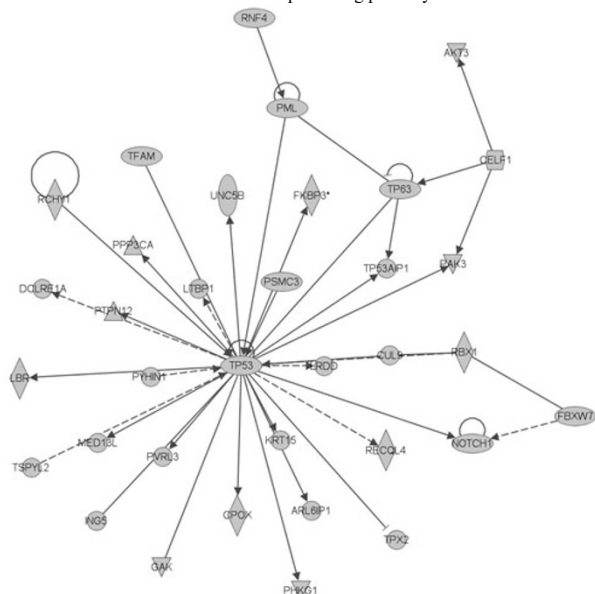
1008 Comprehensive Molecular Oncogenomic Profiling & microRNA Analysis of Prostate Cancer

S Sethi, D Kong, G Dyson, W Saks, F Sarkar. Wayne State University, Detroit, MI.

Background: Comprehensive molecular oncogenomic and microRNA (miRNA) profiling of tumors can provide tumor specific oncogenomic and miRNA signatures which can be useful to improve diagnostic accuracy, refine prognostic and predictive capabilities, and may serve as therapeutic targets. In prostate cancer (Pca) such a comprehensive analysis has not been reported.

Design: DNA and RNA obtained from scant amounts of fresh frozen Pca tumor tissue samples (n=36) were profiled by (1) mutation analysis using Sequenom Massarray & OncoCarta VI panel that profiles 238 common cancer mutations in 19 oncogenes (known predictors of response or resistance to targeted therapies)(2) whole-genome gene expression microarrays & (3) single nucleotide polymorphisms (SNP) microarrays with genome-wide coverage. miRNA analysis was done on RNA from FFPE Pca tumor tissues using RT-PCR. Data was statistically analyzed & correlated with clinical & pathologic variables.

Results: Massarray analysis identified a *MET* oncogene mutation, variant *T992I*, in a 49 year old patient with Gleason score 7 (4+3) tumor. Of the 47,224 genes analyzed by gene expression & SNP microarrays, 74 were significant in predicting high tumor grade (p<0.0001) and *ILMN_1754102*; *TGIF1* was the most significant gene. Of 731,442 SNP's analyzed, 1,022 significantly predicted high tumor grade by ordinal regression analysis (p<0.01) and 638 by logistic regression analysis (p<0.01). Ingenuity Pathway analysis revealed the significant genes (p<0.05) were involved in biological pathways for "Gene Expression, Cell Cycle, Cancer", "Inflammatory Response, Cell Death, Infection Mechanism" and "Cellular Assembly, Organization, Gene Expression, Cancer". Gene *p53* was found to be at the center hub of predicting pathways.



Loss of miR-34a expression was found in Pca tissues consistent with the central role of *p53*.

Conclusions: Using high throughput genomic profiling & expression analysis of genes & miRNAs, we found that *p53* gene is at the center hub of all pathways & loss of miR-34a was consistent with *p53* function in Pca. Moreover, *MET* oncogene mutation is a novel finding, hitherto unreported in Pca & these molecular evidence may have a significant clinical impact on diagnosis, prognosis & in designing targeted therapies to achieve the goal of personalized medicine.

1009 Antibody Based Detection of ERG Gene Fusions in Prostate Cancer: An Immunohistochemical Study Comparing C- and N-Terminus ERG Antibodies

RB Shah, R Lonigro, B Brummell, J Siddiqui, B Spaulding, A Chinmiayan, R Mehra. Caris Life Sciences, Irving; University of Michigan, Ann Arbor, MI; Dako Corporation, Carpinteria; Memorial Sloan Kettering Cancer Center, New York.

Background: *TMPRSS2: ERG* gene fusion, a highly specific molecular event is seen in ~50% of prostate cancers (Pca) and ~20% of HGPIN lesions intermingled with adjacent Pca demonstrating identical gene fusions. Recent studies have demonstrated excellent correlation between positive immunohistochemical (IHC) reaction with novel ERG antibody and underlying *ERG* gene rearrangement in Pca. The goal of this study is to compare the sensitivity of two commercially available antibodies (C- and N- terminally directed) for detection of gene fusion positive Pca and to correlate ERG protein expression with molecular class of gene fusions.

Design: A tissue microarray (TMA) containing 294 cores from 93 patients with Pca was analyzed using ERG FISH 3' and 5' break apart probes and were classified as negative, rearranged with insertion or deletion mechanism or amplified. IHC was performed using

clone EPR3864 generated to C-terminus (aa 393-479) and clone 9FY produced to the N-terminus (aa 42-66) of the ERG protein. The antibodies were optimized using serial dilutions and the immunostaining was compared on TMAs. The patient was classified as positive for ERG if at least one PCA core from that patient had any nuclear staining. Status of ERG protein expression was correlated with presence of gene fusions and molecular class of gene fusions.

Results: A total of 73 patients (290 and 285 cores for C- and N-terminal antibodies respectively) had both FISH and antibodies results available. A total of 41/43 (95%) PCA with gene fusions showed predominantly strong ERG IHC staining with the C-terminal antibody while 10/43 (24%) of PCA with gene fusions showed variable staining results using N-terminal antibody ERG expression (sensitivity 95% versus 24%, $p < 0.001$). Both C- and N-terminus ERG antibodies were not associated molecular class of gene fusions.

Antibody	Insertion (%)	Deletion (%)	Not rearranged (%)
C-terminus	24/25(96)	17/18(94)	3/30(10)
N-terminus	8/25(32)	2/18(11)	1/29(3)

Comparisons of ERG protein expression by C- and N-terminus antibodies in different classes of gene fusions

Conclusions: The monoclonal antibody directed against C-terminus of ERG was shown to be significantly more sensitive than an antibody to N-terminus for the detection of gene fusion regardless of underlying class of gene fusions. We propose the use of C-terminally directed antibody for optimal antibody based evaluation of gene fusions in prostate cancer.

1010 Variability of Smoothelin Expression in Muscularis Propria of the Urinary Bladder: A Diagnostic Pitfall

UN Sheikh, MI Zulfiqar, A Shahab, PJ Kowalski, H Qu. Saint John Hospital & Medical Center, Detroit, MI.

Background: Smoothelin is a smooth muscle-specific cytoskeletal marker expressed strongly in terminally differentiated smooth muscle cells. It has been postulated that in the urinary bladder, immunohistochemistry for smoothelin may help separate conventional and hyperplastic muscularis mucosa (MM) from the true muscularis propria (MP) to aid in accurate cancer staging. We studied the expression pattern of smoothelin in the MP and investigated the possible impact of tumor invasion, chronic inflammation, and fibrosis, on the expected staining pattern.

Design: A total of 24 cystectomies were retrieved from St. John Hospital's surgical pathology archive. Out of these 24 cases, 70 full-thickness representative sections were selected with 1 to 6 sections per case. Of these 70 sections, 14 were from dome, 11 from trigone, 12 from ureteric orifice, and 33 from the remainder of the bladder. The MP was divided into the upper {superficial 50% (UMP)} and lower {deep 50% (LMP)}, and was further evaluated in H&E slides for the presence of invasive carcinoma, chronic inflammation, and fibrosis. These sections were subsequently immunostained with antibody to smoothelin (R4A mab; Cell Marque Corp, CA). The staining score was evaluated for staining intensity (0 to 3+) and % positive cells (focal, moderate or diffuse). Smooth Muscle Actin (SMA) was done in 5/10 of the sections containing significant fibrosis to confirm MP.

Results: With smoothelin, the MP typically showed moderate to strong (2 to 3+) and diffuse staining in 57/70 (81%) and 28/70 (40%) of LMP and UMP, respectively. In the 28 UMP sections, tumor invasion, inflammation, fibrosis and scarring were either absent or minimal. In the remaining 42 UMP sections, which stained negative to weak (0 to 1+), tumor invasion, extensive inflammation, or fibrosis and scarring were seen in 21/42 (50%) sections. SMA showed diffuse positivity in all of those UMP bundles, which had lost their reactivity to smoothelin due to fibrosis. However, in 19% of LMP and 10% of UMP, no definitive factor was seen that affected the smoothelin staining.

Conclusions: Our data shows that MP smoothelin expression varies considerably. This variability is likely related to the presence of tumor invasion, chronic inflammation, and fibrosis. Since most of these changes occur frequently in the UMP, a critical determinant for cancer staging especially in the setting of transurethral resections of bladder tumors (TURBTs), smoothelin staining is highly unpredictable. In conclusion, caution should be taken when using this antibody as a decision making tool for MP in TURBTs.

1011 Differential Expression of the Transferrin Receptor in Renal Cell Neoplasms: A Novel Marker of Aggressive Behavior

NM Shillingford, S Lu, S Mangray, R Tavares, MB Resnick, E Yakirevich. Warren Alpert Medical School of Brown University and Rhode Island Hospital, Providence, RI.

Background: The transferrin receptor (TfR, CD71) is a cell surface glycoprotein related to cell growth and iron-requiring processes, including DNA synthesis, electron transport, and cell proliferation. Overexpression of TfR has been described in various malignancies including carcinomas of the lung, breast, colon, pancreas, and bladder, however its expression in tumors arising in the kidney has not been examined. The goal of this study was to evaluate the expression pattern and prognostic significance of TfR in different histologic subtypes of renal cell neoplasms (RCNs).

Design: Paraffin embedded microarray specimens from 205 consecutive patients with RCNs were analyzed for TfR expression by IHC. A mouse anti-TfR monoclonal Ab (Clone H68.4, 1:500) from Invitrogen was used as the primary Ab. Cases were stratified into 143 clear cell renal cell carcinomas (CRCC), 8 CRCC with sarcomatoid features (SCRCC), 19 papillary RCC type 1 (PRCC1), 6 papillary RCC type 2 (PRCC2) 15 chromophobe RCC (CHRCC), and 14 oncocytomas (OC). The immunoreactivity was assessed based on a combined score of the extent and intensity on a scale of 0-3+.

Results: Strong predominantly cytoplasmic TfR expression was present in the distal convoluted tubules of the normal kidney, whereas proximal convoluted tubules and glomeruli were negative. In the RCNs the staining pattern was both membranous and cytoplasmic. TfR expression was found in all SCRCC, in the majority of PRCC2 (83%), in 59% of CRCC, 53% PRCC1, 47% CHRCC, and 36% of OC ($P = 0.002$). Within the SCRCC group the vast majority of positive cases demonstrated strong

immunoreactivity (2+ and 3+). None of the OCs showed strong expression. Strong TfR expression was higher in PRCC2 as compared to PRCC1. TfR overexpression was strongly associated with tumors of high nuclear grade (Fuhrman grade 3 and 4, $P = 0.006$) and advanced stage (stage 3 and 4, $P = 0.05$). Univariate survival analysis revealed a significant direct correlation between TfR overexpression and poor overall survival in the CRCC group ($P = 0.03$).

Transferrin Receptor Expression in Renal Tumors

TfR	CRCC	SCRCC	PRCC1	PRCC2	CHRCC	OC
Positive	85/143(59%)	8/8(100%)	10/19(53%)	5/6(83%)	7/15(47%)	5/14(36%)
Strong (2+,3+)	35/143(25%)	7/8(88%)	4/19(21%)	3/6(50%)	2/15(13%)	0/14(0%)

Conclusions: TfR is differentially expressed in the various histologic subtypes of RCNs. TfR overexpression was more commonly seen in the aggressive histologic subtypes of renal cell carcinoma, including SCRCC and PRCC2 and proved to be a poor prognostic indicator in CRCC.

1012 Mitosis Phase Enrichment with Identification of Mitotic Centromere-Associated Kinesin as a Therapeutic Target in Castration-Resistant Prostate Cancer

K Sircar, H Huang, L Hu, Y Liu, J Dhillon, D Cogdell, A Aprikian, N Navone, P Troncoso, W Zhang. MD Anderson Cancer Center, Houston, TX; UT Arlington, TX; McGill University, Montreal, QC, Canada.

Background: Hormone sensitive prostate cancer (HSPC), though initially treatable, eventually progresses to castration resistant prostate cancer (CRPC), which is the lethal phase of this disease. The recently described transcriptomic switch to an androgen receptor mediated mitosis program in CRPC suggests that mitotic proteins may be rationally targeted at this lethal phase of disease progression. We sought to study mitosis phase protein expression in CRPC and identify novel anti-mitotic targets in CRPC using genomic, proteomic and functional approaches.

Design: We examined human CRPC samples (n=51) for expression of the mitosis phase marker p-histone H3 (SC-8656, 1:100) and the centrosomal marker γ -tubulin (Abcam 27074, 1:400). We performed gene expression profiling (Agilent 44K) of chemotherapy-resistant CRPC samples (n=25) and compared our results with those from publicly available primary chemotherapy-naïve CRPC (n=10) and HSPC (n=149) datasets. Target validation was performed using immunohistochemistry with functional characterization using si-RNA to our target in LNCaP and C42-B cell lines treated with and without Docetaxel chemotherapy.

Results: Mitosis-phase and centrosomal markers were upregulated at the protein level in CRPC compared with untreated, high Gleason grade hormone-sensitive prostate cancer ($P < 0.0001$). Gene expression data showed enrichment of mitosis-phase genes and pathways with progression to both castration-resistant and chemotherapy-resistant disease. The mitotic centromere-associated kinesin (MCAK/KIF2C) was identified as a novel mitosis-phase target in prostate cancer that was overexpressed in multiple CRPC gene-expression datasets. KIF2C showed increased protein expression with clinical progression of prostate cancer to CRPC. Si-RNA mediated knockdown of KIF2C arrested the growth of prostate cancer cells and sensitized CRPC cells to Docetaxel chemotherapy.

Conclusions: Mitosis phase is upregulated at the transcript and protein levels with progression to CRPC chemoresistant disease. Mitotic centromere associated kinesin (KIF2C) was identified as a novel therapeutic target in CRPC that may complement standard of care Docetaxel chemotherapy.

1013 Sarcomatoid Renal Cell Carcinoma Shows a Distinct Transcriptomic Profile That Is Not Associated with Epithelial to Mesenchymal Transition Markers

K Sircar, T Majewski, K Wani, J McDonald, K Baggerly, P Tamboli, B Czerniak, K Aldape. University of Texas MD Anderson Cancer Center, Houston, TX.

Background: Renal cell carcinoma (RCC) accounts for 13000 cancer deaths yearly in the USA with prognosis most strongly correlated to pathologic tumor stage. Sarcomatoid transformation, a histologic change that occurs in approximately 5% of RCC, is long known to predict for an aggressive clinical course with limited therapeutic options and a median overall survival of under 17 months even in localized disease. Further advancement that requires a molecular understanding of sarcomatoid change in RCC has been hindered, in part, by the difficulty in obtaining suitable sarcomatoid RCC tissues. We sought to characterize the transcriptome of sarcomatoid RCC, particularly with respect to epithelial to mesenchymal transition (EMT) markers and in comparison with clinically advanced non-sarcomatoid RCC.

Design: Archived clinical samples from 23 patients with sarcomatoid RCC were selected that had at least 15% sarcomatoid (S) and epithelioid (E) components. The epithelioid component was restricted to clear cell RCC histology. As controls, we used the epithelial component (E*) from 54 patients with non-sarcomatoid clear cell RCC (stage 4, n=40; stages 1-3, n=14). Lesional foci (E*, E, S) were macrodissected from formalin fixed paraffin embedded tissues and RNA was extracted using the DASL protocol. The transcriptomic profile of all lesions (n=100: 23 E, 23 S, 54 E*) was assessed by whole genome gene expression microarray (Illumina Array HumanRef-8 v3).

Results: Unsupervised clustering analysis showed no significant differences in global gene expression between the epithelioid (E) and sarcomatoid (S) groups in sarcomatoid RCC. Supervised analysis for 68 EMT probes likewise showed no association between E and S groups or the E* and E/S groups. Most non-sarcomatoid RCC (E*, n=45/54) showed separation from sarcomatoid RCC with two expression patterns seen: high in E*, low in E/S; high in E/S only. A subset of non-sarcomatoid RCC (E*, n=9/54) that were all stage 4 (n=9/40) did, however, show overlap with sarcomatoid RCC: high in both E* and E/S.

Conclusions: This first ever genome wide transcriptional profiling study of sarcomatoid RCC showed that the histologically separable epithelioid and sarcomatoid components could not be distinguished by gene expression pattern, including for EMT genes. Our data suggests two signatures for tumor aggressiveness in clear cell RCC with a subset of advanced non-sarcomatoid RCC showing a molecular transition to a sarcomatoid phenotype.

1014 The Value of Napsin A in the Work-Up of Renal Neoplasms

AR Smith, S Patel, JF Silverman. Allegheny General Hospital, Pittsburgh, PA.

Background: Napsin A is an aspartate protease that is expressed in the cytoplasm of normal renal, thyroid and lung epithelium and has proven utility in the diagnosis of pulmonary adenocarcinomas. PAX 8 is a transcription factor seen in tissues of Mullerian, renal and thyroid origin and is used in the evaluation of adenocarcinomas of unknown primary origin. While the PAX family of transcription factors including PAX 8 have been well studied, there are no studies discussing the combined utility of PAX 8 and Napsin A in the evaluation of renal neoplasms. Additionally, there are only two discordant studies evaluating the application of Napsin A in a limited spectrum of renal neoplasms. Therefore, we evaluated the utility of immunohistochemistry (IHC) for Napsin A and PAX 8 in a spectrum of renal neoplasms.

Design: Napsin A and PAX 8 were applied to archived tissue from various renal neoplasms. Reactivity was scored in a four tiered manner with positive results defined as scores of 1 (< 25 % of cells staining with minimal intensity), 2 (moderately intense staining in 25 – 50 % of the cells) and 3 (strong staining in > 50 % of the cells). Internal positive and negative controls were present in the surrounding normal renal tissue of each specimen chosen. The classification of each renal neoplasm was established by histologic and IHC studies. A Fischer test using Graphpad Prism software was used for statistical analysis.

Results:

Renal Neoplasm	Napsin A # positive (% positive)
clear cell RCC	5/20 (25%)
papillary RCC	15/18 (83%)
chromophobe RCC	1/11 (9%)
oncocytoma	7/7 (100%)

Napsin A distinguishes papillary renal cell carcinoma (RCC) from clear cell RCC ($p < 0.05$; $p = 0.0004$), and chromophobe RCC from oncocytoma ($p < 0.05$; $p = 0.0003$). Napsin A reactivity was also seen in 1 of 2 collecting duct carcinomas, 1 of 2 multicystic RCC and 0 of 1 metanephric adenomas. All of the renal neoplasms examined were reactive for PAX 8.

Conclusions: Napsin A can be a useful discriminator between oncocytoma and chromophobe RCC and papillary versus conventional RCC, especially in the work-up of core needle biopsies of oncocytic renal neoplasms or problematic resected cases. Consistent with previous literature, Napsin A is also useful in an IHC panel that includes CK 7 for the identification of papillary RCC. PAX 8 did not contribute to the classification of renal neoplasms.

1015 Molecular Characterization of Gleason Pattern 3 Prostate Cancer with Co-Existing Adjacent Gleason Pattern 4 Cancer

AG Sowalsky, H Ye, SP Balk. Beth Israel Deaconess Medical Center, Boston, MA.

Background: Prostate cancer (PCa) often presents in multiple foci with different grades in the same individuals. It is unknown whether high grade PCa develops de novo or progresses from a lower grade tumor. The molecular features that determine different grades of PCa are not clear.

Design: Using 19 radical prostatectomy specimens of multifocal PCa that contain immediately adjacent G3 and G4 foci, we assessed whether adjacent G3/G4 foci share a common clonality through examining their 1) *TMPRSS2-ERG* fusion status, by screening 19 cases for ERG expression using immunohistochemistry and confirming fusion mRNA using qRT-PCR in 6 ERG-positive cases, 2) *TMPRSS2* and *ERG* genomic breakpoints using hybrid capture and sequencing of genomic DNA in 6 fusion positive cases, and 3) RNA expression profiles using Affymetrix ExonST arrays in 6 cases. Laser-capture microdissection was used to purify cancerous glands for genetic assays in this study.

Results: 1) All 19 cases of PCa with adjacent G3/G4 foci showed a concordant ERG expression pattern, regardless whether the adjacent G3/G4 foci were separated ($n=16$) or intermixed ($n=3$). 9 cases were concordantly positive for ERG expression with equal immunointensity, except in one case that the G3 focus showed a lower ERG immunointensity than the adjacent G4 focus. 10 cases were concordantly negative for ERG expression. ERG positive rate was 47% (9/19), which is in agreement with the reported frequency in the literature. We examined *TMPRSS2-ERG* fusion using qRT-PCR in 6 ERG-positive cases, which were all positive for *TMPRSS2-ERG* mRNA expression; 2) *TMPRSS2* and *ERG* breakpoints have been shown to be random in a ~25-kb region between exon 1 and exon 4 of *TMPRSS2* and ~75-kb region in intron 3 of *ERG*. We have submitted hybrid-captured *TMPRSS2* and *ERG* genomic DNA for breakpoint sequencing in 6 fusion positive cases. The sequencing results will be soon available, which will further validate the clonality; 3) ExonST arrays showed remarkably similar RNA expression profiles in adjacent G3/G4 foci in all 6 cases examined. A few genes showed a significant difference in expression levels in adjacent G3/G4 foci.

Conclusions: In cases of multifocal PCa, adjacent G3/G4 foci are much more likely to share the same clonal origin than to be two independent clones. Additional studies need to be done to identify molecular signatures to distinguish G4-associated G3 PCa from indolent G3 PCa.

1016 Improving Margin Status in Radical Prostatectomies through Performance Measurement and Multidisciplinary Knowledge Transfer (KT) Activities: A Population Level Approach to Quality Improvement

J Strigley, A Evans, M Yurcan, A Hunter, J Hart, J Mazuryk, L McKnight, M Raby, J Irish, J Chin, T McGowan, R McLeod, N Fleshner. Cancer Care Ontario, Toronto, Canada; McMaster University, Hamilton, Canada; University Health Network, Toronto, Canada; University Health Network and Mount Sinai Hospital, Toronto, Canada; University of Toronto, Toronto, Canada; London Health Sciences Centre, London, Canada; University of Western Ontario, London, Canada; Credit Valley Hospital, Mississauga, Canada; Mount Sinai Hospital, Toronto, Canada; Princess Margaret Hospital, Toronto, Canada.

Background: About 3,000 radical prostatectomies (RP) are performed annually in Ontario (male population = ~6.5M). As part of a 2007 RP guideline development process, a manual audit based on 2005/06 data ($n=2,074$) revealed a margin positivity rate (MPR) of 33% for organ confined (pT2) disease ($n=1,577$). Quality improvement (QI) strategies were developed to reduce this rate.

Design: A target of <25% MPR for pT2 was set by consensus. QI strategies included creation of pathology, surgery and radiation oncology champions in 14 regions, hosting provincial champion workshops, implementing a prostate cancer case based listserv, providing regional funding to support multi-disciplinary communities of practice (CoPs), providing hospital-level data and a performance measurement process that reports quarterly to regions and publicly on an annual basis. Starting in 2008, the RP margin positivity rates were monitored using the discrete data field synoptic reporting system developed in Ontario.

Results: The provincial pT2 MPR declined from 33.3% (2008-09 Q3) to 20% in 2010/11 ($n=1,772$). The reduction in MPR was seen in all regions of the province. However, significant variation between regions (13% to 35% in FY2010/11) and between hospitals within individual regions still exists.

Conclusions: Margin positivity rates are related to patient selection, pathological interpretation and surgical factors. Through a multi-faceted approach, we have successfully engaged the clinicians and pathologists and have achieved a significant improvement in overall pT2 MPR in Ontario. The clinical engagement with creation of CoPs and the regular monitoring and reporting of quality indicators were key factors in this population-level QI program. We are currently working with regions and hospitals to reduce both inter- and intra-regional variations in performance.

1017 Evaluation of Erg Expression in Isolated High Grade Prostatic Intraepithelial Neoplasia (HGPIN) and Benign Prostate Glands

JN Stall, N Palanisamy, J Siddiqui, AM Chinnaiyan, SA Tomlins, LP Kunju. University of Michigan, Ann Arbor, MI.

Background: ETS gene fusions (most commonly *TMPRSS2-ERG*) have been identified in approximately 50% of PSA-screened prostate cancers (PCA). By FISH, *ERG* rearrangements are also present in approximately 15% of high grade prostatic intraepithelial neoplasia (HGPIN), always adjacent to *ERG* rearranged PCA. As IHC studies have shown variable rates of ERG+ HGPIN (29-52%) in different cohorts, we studied the rate of ERG positivity in isolated HGPIN and benign prostate glands.

Design: From a retrospective cystoprostatectomy cohort, foci of isolated HGPIN ($n=67$) from 17 cases without PCA (54 slides), HGPIN with incidental PCA from 10 cases (32 slides), and benign prostate from 10 cases (10 slides) were stained with an anti-ERG antibody (clone EPR3864). An additional 55 needle biopsy cores from 5 benign cases with follow-up transperineal mapping biopsy (3/5 cases with PCA on the follow-up biopsy) were also stained for ERG. Staining of endothelial cells was used as an internal positive control and nuclear ERG staining was scored as positive or negative.

Results: Amongst men without PCA on cystoprostatectomy, 3 of 65 (4.5%) foci of isolated HGPIN were ERG+ (one of which had adjacent ERG+ small atypical glands). Amongst men with incidental PCA on cystoprostatectomy, ERG staining was observed in 1 of 20 (5%) foci of isolated HGPIN (which had adjacent ERG+ small atypical glands) and 2 of 18 (11%) HGPIN foci adjacent to PCA (both with adjacent ERG+ PCA); 1 of 10 (10%) PCA without adjacent HGPIN was ERG+. Amongst all 96 sections and 55 needle biopsy cores, only 2 morphologically benign glands were ERG+, one adjacent to cancer and one in the same section as cancer.

Conclusions: Truly isolated HGPIN is rarely ERG+, in contrast to published rates in HGPIN adjacent to cancer (29-52%), and ERG+ benign prostate glands are exceedingly rare. These findings further support ERG staining as being highly specific for prostatic adenocarcinoma. ERG+ isolated HGPIN in diagnostic biopsies suggests unsampled carcinoma, which may warrant closer clinical follow-up and/or evaluation.

1018 Landscape of Chromosome Number Changes during Prostate Cancer Progression

J Stomper, M Braun, W Vogel, D Boehm, V Scheble, F Fend, S Perner. University Hospital of Bonn, Bonn, Germany; University Hospital of Tuebingen, Tuebingen, Germany.

Background: Genetic instability resulting in both aneuploidy and polyploidy is discussed to be involved in prostate cancer (PCa) development and progression. However, a complete survey of numerical chromosomal changes in PCa is lacking so far. The aim of this study was to comprehensively characterize the ploidy status in PCa with regard to disease progression via fluorescence in situ hybridization (FISH). Since aneuploidy and aggressive disease are often associated with increased tumor cell proliferation, we also assessed the expression of two common mitosis markers within the same PCa cohort.

Design: We studied a cohort comprising 112 localized PCa, 75 PCa with 125 corresponding lymph node metastases, and 42 hormone-refractory distant metastases. Using dual-color FISH, we assessed the cohort for losses and gains of all 24 chromosomes. Conducting immunohistochemistry using the markers pHH3 and Ki67, we quantified the proliferation rate within the same cohort.

Results: We observed a sharp and significant increase in aneuploidy with advancing tumor stage ($p < 0.01$). Whereas 38.1% of localized tumors, 61.3% of lymph node metastasized primary PCa, and 80% of corresponding lymph node metastases displayed an aneuploid karyotype, almost all (97.6%) distant metastases were aneuploid. In general, gains (51.5%) of chromosomes were more common than losses (25.4%). Regarding characteristic copy number changes of single chromosomes, chromosomes X (31.8%), 21 (25.1%), 14 (22.7%), Y (22.2%), 16 (21.9%), 1 (20.6%), and 8 (20.2%) were most frequently altered. Additionally, we found that losses of chromosomes 20 (14.1%), 10 (5%), and 6 (4.9%) accounted for the most frequent monosomies. Noteworthy, an increased degree of cell proliferation was significantly associated with the extent of aneuploidy and higher tumor stage ($p < 0.01$).

Conclusions: Disease progression from localized to hormone-refractory PCa is poorly understood on the molecular level. Here, we accumulate evidence that genomic instability leading to aneuploidy may be a crucial factor in cancerogenesis and the metastatic cascade. Our results further indicate a potential association of increased cell proliferation and numerical chromosomal changes. Together, we provide new insight into the incompletely elucidated chromosomal landscape of PCa. More directly, our study suggests an approach that may help to identify patients at risk of unfavourable clinical course.

1019 Comparison of mTORC1 Pathway Immunoexpression between Chromophobe Renal Cell Carcinoma and Renal Oncocytoma

JZ Sugianto, D Rakheja, RF Yousef, Y Lotan, V Margulis, T Kinard, P Kapur. University of Texas Southwestern Medical Center, Dallas, TX.

Background: The mammalian target of rapamycin complex 1 (mTORC1) pathway is dysregulated in many human cancers, and agents targeting the mTORC1 are being clinically used. The mTORC1 pathway interacts with effectors of cell cycle progression and ultimately regulates protein translation and cell proliferation. We undertook this study to ascertain if there are any differences in the expression of mTORC1/PI3K/AKT pathway components between chromophobe renal cell carcinoma (ChRCC) and renal oncocytoma (RO).

Design: Standard immunohistochemical analysis was performed for p-S6, p-mTOR, p-4EBP1, HIF-1 α , p-AKT, and PI3K on sections of tissue microarrays constructed from 43 primary ChRCC and 51 primary RO treated at our hospital with nephrectomy (1998-2008). Duplicate 1.0 mm cores of representative tumor were obtained from each case to construct the tissue microarrays. Cytoplasmic expression was assessed for each marker as the percentage of positive cells (0-3) and intensity of staining (0-3). A final Histo-score was calculated as the product of intensity and percentage and correlated with clinic-pathologic parameters.

Results: The M:F ratio was 1.0 and 4.7, mean age at diagnosis was 55.3 and 64.9 years, and mean tumor size was 7.0 and 3.8 cm respectively for ChRCC and RO. Compared to normal proximal renal tubules, ChRCC showed increased expression of p-S6 in 6 (14.0%), p-mTOR in 28 (65.1%), p-4EBP1 in 14 (32.6%), HIF-1 α in 41 (95.3%), PI3K in 12 (27.9%), and p-AKT in 13 (30.2%) cases. RO showed increased expression of p-S6 in 4 (7.8%), p-mTOR in 39 (78.0%), p-4EBP1 in 12 (24.0%), HIF-1 α in 51 (100%), PI3K in 40 (80.0%), and p-AKT in 32 (64.0%) cases. There was significantly higher expression of PI3K ($P < 0.0001$) and p-AKT ($P = 0.0017$) in RO compared to ChRCC.

Conclusions: Our results indicate differential immunoexpression of PI3K and p-AKT in RO compared to ChRCC, indicating a difference in activation of PI3K/AKT signaling between the tumors.

1020 ALK Alterations in Adult Renal Cell Carcinoma: Frequency, Clinicopathologic Features and Outcome in a Large Series of Consecutively Treated Patients

WR Sukov, JC Hodge, CM Lohse, MK Akre, BC Leibovich, H Thompson, JC Cheville. Mayo Clinic, Rochester, MN.

Background: Chromosomal rearrangements involving *ALK* at 2p23 result in fusion with various partner genes leading to aberrant production of oncogenic protein products in multiple tumor types. Recently, the *ALK* product inhibitor crizotinib was shown to be an effective therapy in patients with *ALK*-rearranged non-small cell lung cancer. The goal of this study was to determine the frequency of *ALK* alterations in adult renal cell carcinoma (RCC) and define associated clinicopathologic features and outcome.

Design: RCCs from a cohort of 534 consecutive surgically treated adult patients were analyzed for alterations of *ALK* by fluorescence *in situ* hybridization (FISH).

Results: *ALK* rearrangements were identified in 2 of 534 (<1%) RCCs. Both tumors were papillary type RCC (PRCC) with similar histologic features and both patients had a poor outcome with death from disease in less than 5 years. *ALK* copy number gain was identified in 54 (10%) RCCs. In clear cell type RCC (CCRCC), *ALK* copy number gain was significantly associated with tumor size ($p = 0.02$) and nuclear grade ($p < 0.001$), and with a worse 10 year cancer-specific survival versus similar patients lacking *ALK* copy number gain ($p = 0.03$). In PRCC, *ALK* copy number gains was not associated with specific clinical or pathologic features or outcome.

Conclusions: *ALK* rearrangement is rare in adult RCC but may be associated with distinct histologic features and poor outcome. Another potential mechanism to elevate *ALK* expression, increased *ALK* gene copy number, was observed in 10% of adult CCRCC where it is associated with a higher tumor grade and poorer outcome. Additional studies are necessary to determine whether RCCs with *ALK* rearrangement and/or those with an increase in *ALK* copy number would benefit from *ALK* inhibitor treatment.

1021 Clinical and Pathologic Features Associated with Prognosis in Patients with Papillary Renal Cell Carcinoma

WR Sukov, CM Lohse, BC Leibovich, H Thompson, JC Cheville. Mayo Clinic College of Medicine, Rochester, MN.

Background: The most common classification system for papillary renal cell carcinoma (PRCC) divides these tumors into two distinct subtypes -type 1 or basophilic and type 2 or eosinophilic - based on specific histologic features. Features predictive of outcome in patients with PRCC vary by study; several studies indicate that type 2 PRCC are associated with a significantly worse prognosis than type 1. However, this is not a consistent finding, and there are issues related to PRCC tumor heterogeneity that make the identification of prognostic features difficult. Identification of prognostic features is further complicated by the lower frequency of PRCC. The purpose of the current study is to investigate a large series of patients with PRCC to determine the prognostic value of various clinical and pathologic features.

Design: Upon approval from the Institutional Review Board, we identified 395 consecutive patients from the Mayo Clinic Nephrectomy Registry treated with radical nephrectomy or nephron-sparing surgery for unilateral, sporadic, PRCC between 1970 and 2002. The clinical and pathologic features for each case were reviewed. The associations of clinical and pathologic features with death from PRCC were evaluated using Cox proportional hazards regression models and summarized with hazard ratios and 95% confidence intervals. Cancer-specific survival was estimated using the Kaplan-Meier method.

Results: At last follow-up, 45 patients died from PRCC at a median of 2.8 years following surgery. By univariate analyses symptoms, tumor thrombus, tumor size, perinephric/renal sinus fat invasion, regional lymph node involvement, distant metastasis, the 2010 TNM stage groupings, grade, tumor necrosis, sarcomatoid differentiation, and PRCC type were associated with death from RCC. Grade was more strongly associated with death from PRCC (hazard ratio 3.97; 95% CI 2.14-7.39; $p < 0.001$) than PRCC type (hazard ratio 2.16; 95% CI 1.20-3.89; $p = 0.010$). Multivariable analyses indicated that symptoms, tumor size, the 2010 TNM stage groupings, grade, and sarcomatoid differentiation were jointly significantly associated with death from RCC.

Conclusions: This large series of patients with PRCC identifies features associated with death from RCC, and confirms that grade is more predictive of outcome than PRCC type.

1022 PAX8 Mouse Monoclonal Antibody: A Comprehensive and Comparative Study on Normal and Neoplastic Tissues

D Tacha, D Zhou, R Bremer, L Cheng. Biocare Medical, Concord, CA; Indiana School of Medicine, Indianapolis, IN.

Background: PAX8 rabbit polyclonal (P) antibody is expressed in a high percentage of kidney and ovarian cancers; however, PAX8 (P) recognize B-cells, pancreatic cancers, carcinoids and some soft tissue tumors. B-cell expression can be especially problematic in lymph nodes when identifying tumors of unknown origin or distinguishing lymph node metastases. A new mouse monoclonal hybridoma PAX8 (M) antibody [BC12] has been developed for IHC. In this study PAX8 (M) was tested for specificity and sensitivity in over 1200 cases of normal and neoplastic tissues. In particular, PAX8 (M) vs. PAX8 (P) was compared in (RCC) and ovarian cancers.

Design: Formalin-fixed paraffin embedded whole tissues and TMA were constructed from archival tissues. Patient information included age, sex, diagnosis, grade and stage. Tissue was processed in the usual manner and immunohistochemistry (IHC) was performed using polymer detection. Cases were considered positive if nuclear staining was observed in $\geq 5\%$ of the cells.

Results: PAX8 (M), exclusively expressed in nuclei, demonstrated equal or superior sensitivity in both renal cell and ovarian carcinomas (Table 1 and 2). PAX8 (M) also demonstrated high sensitivity in endometrioid and thyroid cancers, 67.5% and 60.7% respectively. Low sensitivity of PAX8 (M) was observed in cervical and bladder cancers, 2.5% and 1.4% respectively. All other cancers evaluated, including lung, breast, prostate, stomach, liver, soft tissue, pancreas, testis, brain, colon, melanoma, lymphoma, adrenal, pituitary and rectal were negative. In normal tissue, PAX8 (P) stained lymph nodes, pancreas, and neuroendocrine cells of stomach and colon (confirmed by chromogranin). Conversely, PAX8 (M) was negative in each of these tissues.

Table 1: RCC

	PAX8 (M)		PAX8 (P)	
Diagnosis	Cases (+)	% (+)	Cases (+)	% (+)
Clear cell RCC	154/178	84.6%	148/178	83.1%
Papillary RCC	13/14	92.9%	12/14	85.7%

Table 2: Ovarian Cancer

	PAX8 (M)		PAX8 (P)	
Diagnosis	Cases (+)	% (+)	Cases (+)	% (+)
Serous cystadenocarcinoma	53/58	91.4%	53/58	91.4%
Endometrioid adenocarcinoma	27/37	72.9%	25/37	67.6%

Conclusions: These results demonstrate that PAX8 (M) is a highly specific and sensitive marker for renal ovarian and thyroid cancers. Importantly, PAX (M) does not stain B-cells, and does not recognize epitopes of pancreatic origin or neuroendocrine cells in stomach and colon.

1023 GATA3, p63 and S100P: An IHC Comparison Analysis in Bladder Cancer

D Tacha, R Bremer, C Yu, L Chen. Biocare Medical, Concord, CA; Indiana University School of Medicine, Indianapolis, IN.

Background: More than 90% of bladder cancers are urothelial (transitional) cell carcinomas (TCC), which originate in the mucous layer of surface cells of the bladder lining (transitional epithelial cells). Establishing urothelial origin of the tumor is critically important, especially when prostate cancer is also in differential diagnosis.

Several studies have shown p63 to be a sensitive marker for bladder cancers and negative in prostate and kidney cancers; however, only limited studies of GATA3 and S100P have been reported in bladder, prostate and kidney cancers. The aim of this study is to examine immunohistochemical staining characteristics of GATA3, p63 and S100P antibodies on bladder TCC, and compare staining expression of GATA3 and S100P on prostate and kidney cancers.

Design: Formalin-fixed, paraffin-embedded TMA's of bladder cancers were constructed in-house and purchased commercially, and processed in the usual manner for IHC analysis. All sections were retrieved in a modified citrate buffer, in a pressure cooker at 125°C. Mouse monoclonal antibodies GATA3 and p63, and rabbit polyclonal antibody S100P, were individually optimized using a 30 minute incubation. Detection was performed using a micro-polymer and visualization with DAB chromogen.

Results: The results of GATA3, p63 and S100P in TCC are summarized in Table 1.

Table 1: Transitional Cell Carcinoma: All grades

Antibody	Cases	Positive	(+) %	Negative	(-) %
GATA3	59	54	92%	5	8%
p63	59	53	90%	6	10%
S100P	59	55	93%	4	7%

Positive staining of each antibody, according to histologic grade is summarized in Table 2.

Table 2: Staining of GATA3, p63 and S100P in TCC according to histologic grade

Grade 1-3	GATA3	p63	S100P
Grade 1 (11 cases)	10 (91%)	11 (100%)	11 (100%)
Grade 2 (37 cases)	33 (89.2%)	32 (86.5%)	33 (89.2%)
Grade 3 (11 cases)	10 (90.1%)	9 (81.2%)	9 (81.2%)

GATA3 was 100% negative in prostate (n=68) and kidney cancers (n=69) and S100P was 100% negative in kidney cancer and 98.6% negative in prostate cancer.

Conclusions: GATA3, p63 and S100P are highly sensitive and specific biomarkers for urothelial carcinoma. The combination of this 3 biomarker panel may be employed to establish urothelial origin and will aid in cases of tumor of unknown origin.

1024 The Utility of ERG Antibody in the Assessment of Difficult Prostate Biopsies: How Often Does ERG Contribute to Resolving an Atypical Diagnosis beyond That Provided by Basal Cell Markers and AMACR?

Y Tadros, B Brummell, M Zhou, RB Shah. Caris Life Sciences, Irving, TX; Cleveland Clinic, Cleveland, OH.

Background: Recent studies have demonstrated high correlation between ERG protein expression with the *TMPRSS2: ERG* gene fusions, a specific molecular event seen in ~50% of prostate cancers and ~20% of HGPIN lesions intermingled with adjacent adenocarcinoma demonstrating identical gene fusions. We evaluated the diagnostic utility of ERG antibody in resolving difficult prostate biopsies beyond that provided by routinely utilized cancer marker AMACR and basal cell markers.

Design: 96 prostate needle biopsies with "atypical" glandular proliferation were stained with ERG (clone EPR3864), AMACR and basal cell cocktail antibodies. ERG and AMACR staining in atypical glands and adjacent benign/PIN glands was graded as negative or positive. For AMACR, only staining that was significantly stronger than that of background benign glands was considered positive. An initial consensus diagnosis was rendered as benign, atypical or cancer based on combined morphology, basal cell markers and AMACR. The impact of ERG antibody on this work up was than independently evaluated based on final interpretation.

Results: A total 72 biopsies with atypical glands were available for review for all markers. A final diagnosis benign, atypical and cancer was rendered following review of morphology and all markers in 7, 21, and 44 cases, respectively. Of 44 cancer diagnoses, 18 (42%) were positive for ERG, and 40(93%) were positive for AMACR. Of 21 atypical diagnoses none were positive for ERG and 18 (81%) were positive for AMACR. Of 6 benign diagnoses, none were positive for ERG and 5 (83%) were positive for AMACR. ERG expression in PIN glands was noted in 8 cases containing adjacent ERG positive(11%) and 1 ERG negative cancer(1%), while AMACR expression was noted in non-cancer glands in all diagnostic categories with a total of 21 (29%) cases. Positive ERG staining converted an initial atypical diagnosis to a final cancer diagnosis in 4/72 (6%) of cases and strengthened the cancer diagnosis in additional 5 cases (7%) where morphology was less than optimal despite AMACR expression and lack of basal cell staining.

Conclusions: ERG has limited independent advantage over traditionally utilized AMACR and basal cell markers. However, in small proportion of cases positive ERG expression helps establish a definitive cancer diagnosis. We propose utilization of ERG as a component of cocktail antibodies in optimal evaluation of difficult prostate biopsies.

1025 Incidence and Correlation of AKT and ERG Expressions in Japanese Prostate Cancer

H Takahashi, B Furusato, T Kimura, M Okayasu, S Mizukami, S Egawa, H Hano. The Jikei University School of Medicine, Tokyo, Japan.

Background: As prostate cancer carcinogenesis, 2 major pathways have been advocated. The one is PTEN deletion-AKT phosphorylation/activation pathway. In the previous study, we have shown that overexpression of phosphorylated AKT (pAKT) is associated with higher tumor stage and Gleason score, namely an aggressive tumors. Gene fusions involving ERG oncogene has been highlighted as another pathway. ERG overexpression is detected in approximately half of the prostate cancer cases in the Western population, but the incidence is not yet well known in the Asian patients. Also, the correlation of these 2 pathways is not well understood to date.

Design: A total of 131 clinical prostate cancer foci in 49 regular specimens (RS) and 82 in the constructed tissue microarray (TMA) were evaluated. Immunohistochemistry was performed with anti-AKT (phosphorylation form specific) and expression was evaluated. For RS, intensity and distribution were evaluated as grade 0 (none), 1 (weak/<10% of

the tumor), 2 (intermediate/10-49%), 3 (strong/>50%), 4 (very strong/>50%). Grades 2-4 were designated as expression (+). For the TMA, intensity was evaluated as negative (-), or positive (+). Immunohistochemistry was performed with anti-ERG and expression was evaluated as negative (-) or positive (+).

Results: In the RS and TMA, 24/49 cases (49.0%) and 36/82 cases (43.9%) showed positive with pAKT, respectively. Similarly, 8 cases (16.3%) and 15 cases (18.3%) showed positive with ERG in the RS and TMA, respectively. As a concordance of pAKT and ERG expression, only one case showed expression of both proteins in RS series and reverse-correlation between pAKT and ERG expressions was significant (p=0.02). In TMA series, concordance of these 2 protein expressions was not statistically significant.

Conclusions: Approximately, half of the Japanese cancer show pAKT expression and the incidence is quite similar between RS and TMA. On the other hand, ERG gene fusion seems to be a relatively rare event in the Japanese prostate cancer patients compared with the Western population. The PTEN/AKT pathway may play a major role in the carcinogenesis of the Japanese prostate cancer. It is suggestive that these 2 pathways seem to be independently working.

1026 Pathological Analysis of Testicular Germ Cell Tumor with Metastasis in Retroperitoneal Lymph Nodes

WP Tarrant, BA Czerniak, CC Guo. UT MD Anderson Cancer Center, Houston, TX.

Background: Retroperitoneal lymph nodes are the most common metastatic site for testicular germ cell tumor (GCT). To understand the relationship between the primary GCT and metastasis, we compared the histopathologic features of GCT between orchietomy and retroperitoneal lymph node dissection (RPLND) specimens.

Design: We retrospectively searched our surgical pathology files from 2002 to 2011 and identified 100 patients with testicular GCT who underwent RPLND for metastatic disease. The pathologic features of GCT in both orchietomy and RPLND specimens were evaluated. Patients' demographic and clinical data were collected from medical records.

Results: The mean age of patients at initial diagnosis was 28 years (range, 15-58 years). The mean size of testicular tumors was 5.2 cm (range, 0.5-20.0 cm). The orchietomy specimens showed mixed GCT (n=67), teratoma (n=21), seminoma (n=5), embryonal carcinoma (n=3), yolk sac tumor (n=1), and no viable tumor (n=8). The components in the mixed GCTs included teratoma (n=56), embryonal carcinoma (n=50), yolk sac tumor (n=48), seminoma (n=21), and choriocarcinoma (n=11). In addition, somatic malignant components were found in 5 orchietomy specimens. Most RPLND specimens showed extensive necrosis. The most common viable GCT component in the RPLND specimens was teratoma (n=90); in 21 of those cases, a teratomatous component was not observed in the corresponding orchietomy specimen. Other viable GCT components included embryonal carcinoma (n=15), yolk sac tumor (n=11), choriocarcinoma (n=1), and seminoma (n=1). Somatic malignant components were present in 5 RPLND specimens, but none of them had a somatic component in the corresponding orchietomy specimens. Overall, 13 patients died of disease at a mean of 42 months (range, 7-263 months) after RPLND, and 87 were alive at a mean of 80 months (range, 5-269 months). While only 1 of the 5 patients with somatic components in the primary GCT died of disease, 3 of the 5 patients with somatic components in the metastasis died.

Conclusions: Teratoma was the most common viable GCT component in the RPLND specimens. Some patients had a teratomatous component only in the RPLND specimen but not in the orchietomy specimen. Although this difference could be due to undersampling of the orchietomy specimen, the metastatic teratomatous component may also result from transformation of other non-teratomatous GCT components. In addition, our limited study suggests that the presence of a somatic component in the RPLND metastasis may portend a worse prognosis than such a component in the testicular primary tumor.

1027 ERG Protein Expression in Localized, Metastatic and Castration Resistant Prostate Cancer: A Comparative Immunohistochemistry and Fluorescent In-Situ Hybridization Study

LH Teng, C Wang, K Trpkov, A Yilmaz, LR Begin, S Liu, M Dolph, TA Bismar. Calgary Laboratory Services and University of Calgary, Calgary, AB, Canada; McGill University and Hôpital du Sacré-Coeur de Montréal, Montréal, QC, Canada.

Background: ERG gene rearrangements have been reported as the most common gene rearrangement in prostate cancer (PCA). Recently, some reports suggested that ERG protein expression is reflective of genomic ERG rearrangements but that ERG protein expression could also be detected in benign prostate tissue, albeit at a weak level.

Design: We characterize ERG protein expression in comparison to genomic ERG gene rearrangement in PCA using immunohistochemistry (IHC) and fluorescence in situ hybridization (FISH) to assess the potential diagnostic and prognostic value of anti-ERG antibody in the clinical setting. Two hospital-based cohorts including 344 patients, representing benign, high-grade prostatic intraepithelial neoplasia (HGPIN), localized, metastatic and castration resistant PCA were evaluated.

Results: ERG protein expression was detected in 6.8% (2/29) of HGPIN cases, 46.3% (190/410) in localized PCA, 36.1% (13/36) in lymph node metastatic PCA and 37.2% (181/486) in castration resistant PCA cases. In a subgroup of PCA demonstrating foamy-gland morphology, ERG protein expression was detected in only 18.6% (16/86). ERG protein expression and ERG gene rearrangements showed an overall consistency rate of 90.6% (714/788) in the evaluable cores (p<0.0001). The rates of ERG consistency were 100% in the benign glands and HGPIN and 96.1% (270/281) in localized PCA. The consistency rates were lower in the node metastatic and castration resistant PCA groups 76.9% (20/26) and 85% (323/380), respectively (p<0.001).

Conclusions: ERG protein expression appears to be exclusive for the neoplastic prostatic epithelium and showed high concordance between IHC and FISH in localized prostate cancer, suggesting a potential role as a biomarker for prostate cancer diagnosis. We found significantly lower consistency rates of ERG expression between IHC and FISH

in lymph node metastatic and castration resistant PCA which limits its value in these setting. The novel observation of lower rates of ERG protein expression in foamy gland PCA may suggest potential differences for this pattern of PCA at the molecular level.

1028 Immunohistochemical Expression of MCM2 Predicts Biochemical Recurrence in Prostate Cancer: A Tissue Microarray and Digital Imaging Analysis-Based Study of 428 Cases

A Toubaji, S Sutcliffe, A Chaux, K Leckell, J Hicks, AM De Marzo, EA Platz, GJ Netto. Johns Hopkins University, Baltimore, MD; Johns Hopkins Bloomberg School of Public Health, Baltimore, MD; Washington University in Saint Louis School of Medicine, Saint Louis, MO; Georgetown University Hospital, Washington, DC.

Background: Prostate cancer remains a major health problem in the United States. Established clinicopathological parameters, such as Gleason score, tumor stage and serum PSA levels, are currently the guiding tools for prognostication and disease management. Additional biomarkers that could increase accuracy of predicting disease progression, response to therapy, and survival are needed. The goal of this study was to evaluate MCM2 and Ki-67 immunorexpression as predictors of outcome in prostate cancer.

Design: 11 tissue microarrays were constructed using tumor and nontumor samples from 428 patients. Patients were divided into short-term (mean, 2.9 years) and long-term (mean, 14.1 years) follow-up groups. Endpoints were biochemical recurrence for the short-term group, and prostate cancer-related death for the long-term group. All men in the long-term follow-up group had biochemical recurrence at the time of recruitment. Tissue microarray spots were scanned and analyzed using the BLISS platform (Bacus Laboratories, Inc., Lombard, IL). MCM2 and Ki-67 levels were analyzed for i) percentage of positive cells, ii) intensity of staining, and iii) the product of percentage and intensity.

Results: Expression of both markers was higher in tumor than in nontumor glands. Percentage of MCM2 positivity was associated with Gleason score in both groups. Percentage and intensity of Ki-67 positivity were associated with Gleason score and pathologic stage only in the short-term group. Higher MCM2 percentages were associated with biochemical recurrence in the short-term group. In the long-term follow-up group, neither MCM2 nor Ki-67 levels (percentages or intensities) predicted prostate cancer death. Furthermore, no significant increase in the risk for cancer death was observed in patients with combined high MCM2 and high Ki-67 percentage expression.

Conclusions: Higher percentages of MCM2 and Ki-67 are associated with increased Gleason score. In patients treated by radical prostatectomy, high MCM2 levels are associated with biochemical recurrence. Once biochemical recurrence ensues, neither MCM2 nor Ki-67 predicts cancer-related death.

1029 Polybromo 1 (PBRM1) Expression in Renal Epithelial Neoplasms (REN) by Immunohistochemistry

M Tretiakova, M Kocherginsky, SE Eggener, AL Shalhav, T Antic, GP Paner. University of Chicago, Chicago.

Background: SWItching and Sucrose Non-Fermenting (SWI-SNF) genes play a key role in chromosomal stability, cellular proliferation and transcription, emerging as bona fide tumor suppressors. Most recently, mutations in PBRM1 gene which encodes BAF180 protein were identified in 41% of renal cell carcinomas (RCC), making PBRM1 the 2nd most frequently mutated gene after VHL (Nature, 2011). Herein, we examined BAF180 expression in a large set of REN using a novel commercially available antibody.

Design: TMA sections of 290 REN (130 clear cell [CCRCC], 79 papillary [PRCC], 52 chromophobe [ChRCC], 4 TFE3 translocation [tRCC] 5 clear cell papillary [PRCC] RCC and 20 oncocytomas [RO]) and 41 normal tissues from different organs including 14 kidneys were immunostained. Anti-BAF180 antibody suitable for paraffin sections was obtained from Sigma (rabbit IgG, 1:160), and tested according to manufacturer's recommendation. Reactivity with >5% of cell nuclei was considered positive, 5-50% - focal, and >50% - diffuse. Staining intensity was scored as weak or strong.

Results: From 290 tumors only 16.5% exhibited nuclear BAF180 reactivity which was strong in 5.5% and weak in 11% of cases. Expression of BAF180 in normal kidney (NK) was present in 57% cases and localized to distal tubules and glomeruli. Detailed BAF180 expression is shown in table 1. Group comparison showed significant difference in BAF180 expression between normal, benign RO and malignant RCC (p=0.019, Fisher exact test) with gradual decrease of % positive cases. This decreasing trend is further confirmed by logistic regression model (p=0.008). Among the 3 RCC histotypes the highest BAF180 expression was in PRCC and lowest in CCRCC (p=0.006).

Type	Negative	Strong diffuse	Strong focal	Weak diffuse	Weak focal
CCRCC	119 (91%)	0	2 (2%)	2 (2%)	7 (5%)
PRCC	60 (76%)	3 (4%)	7 (9%)	5 (6%)	4 (5%)
ChRCC	42 (81%)	0	3 (6%)	2 (4%)	5 (9%)
CPGCC	3 (60%)	0	0	1 (20%)	1 (20%)
IRCC	3 (75%)	0	0	0	1 (25%)
RO	15 (75%)	1 (5%)	0	2 (10%)	2 (10%)
NK	8 (57%)	0	0	3 (21.5%)	3 (21.5%)

Conclusions: Homozygous inactivation of PBRM1 via truncating gene mutations was expected to cause BAF180 expression loss in a significant subset of RCC cases but not in normal kidney or benign tumors. We found statistically significant decreasing trend in BAF180 expression from normal (42.9%) to benign RO (25.0%) to RCC (15.3%), with the lowest BAF180 levels in CCRCC (8.5%). However, overall low frequency of BAF180 expression in vast majority of REN and normal kidney suggest limited value of IHC in predicting mutational status of PBRM1 and warrant further genetic analysis of this promising tumor suppressor gene.

1030 Multiplex Ligation-Dependent Probe Amplification (MLPA) Assay – A Novel Approach for Renal Tumor Typing

M Tretiakova, P Reddy, T Antic, GP Paner, L Joseph. University of Chicago, Chicago.

Background: Distinction between eosinophilic chromophobe renal cell carcinoma (ChRCC) and renal oncocytoma (RO) can be difficult due to significant morphologic and immunophenotypic overlap. RO harbor infrequent loss of chromosomes 1 and Y, whereas ChRCC is characterized by extensive chromosomal alterations and commonly monosomy of one or more chromosomes 1, 2, 6, 10, 17 and 21 with 60-96% frequency. Here we test the utility of the DNA based MLPA in assessing gains and losses of all chromosomes on formalin-fixed paraffin embedded (FFPE) diagnostic tissues in a single tube assay.

Design: MLPA was used to analyze DNA extracted from tumor and matched normal kidney FFPE tissue from 19 patients including 6 classic ChRCC, 7 RO, and 6 cases with hybrid morphology (ChRCC-RO). The SALSA MLPA kit P036-E1 (MRC-Holland) contains a 49 probe mix which targets the subtelomeric regions of each arm of all 23 chromosomes, potentially measuring chromosomal copy number. The pattern of PCR amplicons and their signal strengths were compared (after normalization) to the reference normal samples and control cases with known chromosomal abnormalities.

Results: Five of seven RO (71%) cases showed no chromosomal abnormalities. Two RO cases showed loss of chromosome 20, and one RO had additional loss of chromosome 14. All six classic ChRCC cases showed multiple chromosomal monosomies in various combinations: chromosome 1 (4/6 cases), 2 (3/6 cases), 6 (2/6 cases), 10 (3/6 cases), 13 (2/6 cases), 17 (3/6 cases), X (3/6 cases), and Y (2/3 male patient cases). In addition, we detected loss of chromosomes 3, 5, 8, 12, 21 and 22 with frequency of 17% (1/6 cases each). Among 6 ChRCC-RO cases with overlapping morphologic features 2 cases had no gross chromosomal anomalies, whereas remaining 4 cases had loss of chromosomes 1, 20, 21 and Y in 2 cases, and chromosomes 14 and 17 loss once. Group comparison showed significant difference in chromosomal loss between all studied groups (p<0.05, Fisher exact test).

Conclusions: By MLPA all ChRCC cases showed multiple chromosomal losses with frequent monosomies of chromosomes 1, 2, 6, 10, 13, 17, X and Y, whereas in RO only 29% cases showed single or two chromosome losses. ChRCC-RO group divided with half cases showing chromosomal anomalies similar to ChRCC and half cases with no loss or chromosomal loss similar to RO with monosomy 14 or 20. Our preliminary results show that MLPA could serve as a simple cost-effective method for cytogenetic classification of morphologically challenging renal neoplasms and possibly to identify novel associations in "unclassified" tumors.

1031 Impact of Histologic Cystic Features in Clear Cell RCC (CCRCC) and Multilocular Cystic RCC (MCRCC) or Shall We Say – Neoplasm of Low Malignant Potential?

M Tretiakova, V Mehta, SS Shen, SJ Sirintrapun, JL Yao, I Alvarado-Cabrero, SE Eggener, AL Shalhav, T Antic, MM Picken, GP Paner. University of Chicago, Chicago; Loyola University Medical Center, Maywood; Methodist Hospital, Houston; Wake Forest University, Winston Salem; University of Rochester, Rochester; National Medical Center, Mexico City, Mexico.

Background: MCRCC as defined in the 2004 WHO classification is recognized as a tumor with excellent prognosis. However, the clinicopathological data for MCRCC remains limited. In addition, pathologic studies that specifically assesses the influence of histologic cystic change when partly present in CCRCC is also limited.

Design: The clinicopathological features of 46 MCRCC (from 6 institutions), 85 partially cystic CCRCC (from 2 institutions) and 47 solid CCRCC (as control) are herein presented. CCRCC with cystic change due to necrosis were not included.

Results: Patient mean ages were as follows: MCRCC (59.7 yrs.), partially cystic CCRCC (60.9 yrs.) and solid CCRCC (58.6 yrs.). Cystic change in partially cystic CCRCC was $\geq 25\%$ of the tumor. The cysts were predominantly septated, multilocular, and contained variable amount of fluid. Fuhrman nuclear grades were 1 (82%) or 2 (18%) for all MCRCC; for partially cystic CCRCC were 1 (22%), 2 (69%), 3 (9%) and 4 (0%); and for solid CCRCC were 1 (9%), 2 (53%), 3 (25%) and 4 (13%). All MCRCC were either AJCC pT stage 1 (96%) or 2 (4%). pT stage for partially cystic CCRCC were 1 (91%), 2 (2%), 3 (7%) and 4 (0%) and for solid CCRCC were 1 (60%), 2 (6%), 3 (34%) and 4 (0%). Sarcomatoid change was present only in solid CCRCC (4%). Follow up for MCRCC (excluding those with synchronous RCC) (available in 40/46 cases; mean 49.6 mos) showed no recurrence or metastasis. Follow up for partially cystic CCRCC (available in 75/85 cases; mean 55.5 mos) showed 4% recurrence and 1% metastasis. None of the patients with MCRCC or partially cystic CCRCC died of disease during the follow-up. In contrast, patients with solid CCRCC (available in 35/47 cases; mean 48.4 mos) showed 37% recurrence, 51% metastasis and 6% death rate.

Conclusions: This large series of MCRCC shows lower stage and grade and reaffirms its indolent behavior, and thus, supports a prior proposal of renaming this tumor in its pure form as *multilocular cystic renal cell neoplasm of low malignant potential*. Our results also showed that CCRCC with cystic change is associated with lower grade, lower pathologic stage, and confers better prognosis than solid CCRCC. We recommend that presence and extent of cystic changes be documented as a separate variable in the surgical pathology reporting of CCRCC.

1032 Correlation between Laterality of Pelvic Lymph Node Metastases and Tumor Laterality in Biopsy and Prostatectomy Specimens from Patients Undergoing Extended Pelvic Lymph Node Dissection (ePLND)

P Troncoso, S Matin, KN Babaian, IN Prokhorova, JW Davis. The University of Texas MD Anderson Cancer Center, Houston, TX.

Background: The optimal extent of lymph node dissection at the time of radical prostatectomy has been the subject of ongoing debate and study. Although older

nomograms have predicted which patients may not require a lymph node dissection, those guidelines were largely derived from dissections limited to the obturator fossa. The use of the extended template (i.e., obturator + external iliac + hypogastric nodes regions) generally doubles the number of lymph nodes retrieved and thus increases the likelihood of N1 disease detection. Because the operative time required for the extended template is longer, we sought to re-explore whether the extended dissection is required bilaterally or only unilaterally in the case of predominantly unilateral disease.

Design: Patients with N1 disease who underwent robot-assisted ePLND from November 2007 through August 2011 were included in our study. Preoperatively treated patients were excluded. The location, Gleason score (GS), and grades of the individual tumor foci in the mapped radical prostatectomy specimens (RPS) and tumor laterality in the biopsy specimens were related to the side of lymph node metastases in the ePLND.

Results: The median age of the 52 patients at prostatectomy was 62 years (range, 47–76). The median PSA was 7.85 ng/ml (range, 1.10–119). Most patients underwent an extended biopsy with a median of 12 cores. The biopsy GS was ≤ 7 in 32 patients and ≥ 8 in 20. The clinical stage was T1c in 22 patients, T2 in 29, and T3 in 1. The GS was 7 in 24 RPS and ≥ 8 in 28 RPS. The pathologic stage was pT2 in 10 patients, pT3a in 12, and pT3b in 30. The median numbers of lymph nodes obtained and of positive nodes, respectively, were 20.5 and 1. The tumor focus with the highest GS was exclusively unilateral in 13 patients, predominantly unilateral in 19, and bilateral in 20. Metastases contralateral to the side of the focus with the highest GS were present in 3 of 13 (23%) patients with exclusively unilateral disease and 7 of 19 (37%) with predominantly unilateral disease. Overall, 6 of 23 (26%) patients with unilateral disease in the biopsy specimen had contralateral metastases, including 3 of 14 (21%) patients with intermediate-risk and 3 of 9 (33%) with high-risk prostate cancer.

Conclusions: The occurrence of pelvic lymph node metastases contralateral to the focus of the highest GS supports the concept that, ePLND, when clinically indicated, should be performed bilaterally.

1033 Histopathological Tumor Features Associated with Her2 Amplified Urothelial Bladder Cancers

J Tschui, D Rotzer, R Seiler, A Fleischmann. Institute of Pathology, University of Berne, Berne, Switzerland; Department of Urology, University Hospital of Berne, Berne, Switzerland.

Background: Approximately 10% of invasive urothelial bladder cancers (UBC) are Her2 amplified. Anti-Her2 targeted therapies might become an option for these UBC, however, little is known about their morphological features.

Design: A cohort of 150 patients with UBC was evaluated by fluorescence in situ hybridization (FISH) for Her2 amplification. The histopathological features of the 13 amplified primary tumors (8.6%) were compared with 13 matched non-amplified primary tumors.

Results: Urothelial carcinomas with Her2 amplification presented with a broader variety of histomorphological subtypes than the control group, showing particularly a high frequency of micropapillary tumor components (10/13 patients). In contrast, the Her2 non-amplified tumors mainly presented the classical solid type of urothelial carcinoma and apart from two cases with sarcomatoid growth patterns, did not show a particular trend towards growth of any morphological subtype. In addition, Her2 amplified carcinomas demonstrated a high degree of intratumoral chronic inflammation while peritumoral inflammation was low.

Conclusions: UBC with Her2-amplification are morphologically heterogeneous, frequently demonstrate micropapillary growth and show strong intratumoral and weak peritumoral chronic inflammation. These features may help pathologists to identify UBC harboring Her2 amplification.

1034 Tyrosine Kinase Inhibitor-Induced Vasculopathy in Clear Cell Renal Cell Carcinoma as an Anti-Tumor Mechanism

T Tsuzuki, N Sassa, T Morikawa, A Fukatsu, Y Yoshino, R Hattori, R Shiroki, M Gotoh. Nagoya Daini Red Cross Hospital, Nagoya, Japan; Nagoya University, Nagoya, Japan; Fujita Health University, Toyoake, Japan; Komaki Municipal Hospital, Komaki, Japan.

Background: Tyrosine kinase inhibitors (TKIs) are one of the first-line drugs for the treatment of resectable or metastatic clear cell renal cell carcinoma (CCRCC). It is hypothesized that the mechanism underlying the anti-tumor effect of TKIs for CCRCC is inhibition of tumor neovascularization by blockade of the vascular endothelial growth factor receptor. However, the true mechanism underlying the anti-tumor effect of TKI is not fully explained.

Design: Nineteen patients were retrospectively administered TKI (sunitinib or sorafenib) for treatment of CCRCC. Sixteen of them underwent radical nephrectomy after neoadjuvant therapy with a TKI (sunitinib, 13; sorafenib, 3), and the remaining 3 died of the disease despite TKI administration (sunitinib, 2; sorafenib, 1), and their cadavers were subjected to an autopsy.

Results: The patient population was predominantly male (male to female ratio, 15:4). The mean patient age was 62 years (range, 27–76 years). Two types of regions were found in all the tumors: One characterized by necrosis and/or degeneration, which indicated anti-tumor activity, and the other by no or few pathological changes, which indicated absence of anti-tumor activity. The extent of degeneration and necrosis was varied across the different areas. Vasculopathy of tumor vessels was observed in or adjacent to the necrotic or degenerative area. Vasculopathy was of 2 types, defined by the following characteristics (1) concentric intimal thickening in medium-sized tumor vessels, which resulted in narrowing or occlusion of the lumen, or (2) by hyalinization in small-sized tumor vessels, which resulted in occlusion of the lumen. Little or no vasculopathy changes were observed in tumor vessels in areas affected by CCRCC, which indicated the absence of anti-tumor activity or low levels of activity.

Conclusions: This is the first report of vasculopathy in cases of TKI-treated CCRCC. Our data suggest that TKI induced vasculopathy in the tumor vessels initially, which

resulted in anti-tumor activity characterized by ischemic changes. Our data also suggest that the anti-tumor effects of TKI in CCRCC treatment may be better evaluated by the extent and intensity of vasculopathy rather than the extent of necrosis or degenerative changes in the tumor.

1035 Does SPOP-Mutated Prostate Cancer Have Specific Morphology?

KR Turner, K Park, S Bacca, Y-L Chiu, C Barbieri, F Demichelis, L Garraway, M Rubin, JM Mosquera. Weill Medical College of Cornell University, New York, NY; The Broad Institute of Harvard and MIT, Cambridge, MA; Harvard Medical School, Boston, MA.

Background: Recurrent inactivating mutations of the *SPOP* gene are present in 14% of whole exome-sequenced prostate cancer (PCa), making it the most common mutation in this type of cancer thus far. Most recent data from our group suggests that *SPOP* mutations define a distinct molecular class of ETS-negative prostate cancer with aggressive behavior and potential therapeutic targets. We sought to determine if this common mutation is associated with a morphological phenotype.

Design: Whole-exome sequencing was performed in 118 unselected PCa cases from one institution. Of these, 11 (9.3%) demonstrated *SPOP* gene mutation. Blinded to mutation status, two reviewers assessed all prostatectomy slides from 11 *SPOP*-mutated cancers and 11 non-*SPOP*-mutated cases with similar Gleason scores and pathologic stage. Dominant and secondary tumor nodule(s) from each prostatectomy specimen were assessed for presence or absence of 15 morphological features of PCa: Intraductal spread, cribriform morphology, blue-tinged mucin, crystalloids, high nucleocytoplasmic ratio, macronucleoli, foamy gland features, collagenous micronodules, small cell/neuroendocrine differentiation, perineural invasion, extraprostatic extension, signet-ring like cell features, ductal morphology, glomerulations, and comedonecrosis. To identify associations between morphology and *SPOP* mutation-positive status, Fisher's exact tests were performed with p-values corrected for multiple comparisons using the step-down Bonferroni method.

Results: No morphologic features were associated with *SPOP* mutated PCa. The cribriform morphology, while not statistically significant, was present in 64% of *SPOP* mutants compared to 18% of non-mutants ($p=0.08$). Foamy gland morphology showed a significant negative association with *SPOP* mutation, with 18% of *SPOP* mutated cases exhibiting this feature compared to 72% of control cases ($p=0.03$). However, when p-values were adjusted to account for multiple comparisons, the statistical significance of this finding was lost.

Conclusions: This study is the first to examine morphological features of PCa harboring *SPOP* mutations. Foamy gland morphology was less commonly identified in *SPOP* mutated cases; while cribriform morphology was more commonly identified in *SPOP* mutated cases when compared with controls. Future studies employing a larger sample size will be required to establish whether these preliminary findings are statistically significant.

1036 Differential Expression of Integrins in Intraductal Spread, Cribriform, and Non-Cribriform Patterns of High Grade Untreated and Treated Prostate Cancer

V Tzelepi, M Karlou, S Wen, A Hoang, C Scopa, C Logothetis, E Efsthathiou, P Troncoso. University of Patras, Patras, Greece; MD Anderson Cancer Center, Houston.

Background: The presence of intraductal spread (IDS) or cribriform (CR) morphologic patterns in prostate cancer (PCa) represents an adverse prognostic feature in untreated and treated patients. However, the molecular features of these patterns, in comparison to high grade non-CR pattern have not been studied in detail. IDS and CR patterns are unique in that tumor cell spatial organization results in their minimal contact with the stroma. We have hypothesized that high grade (HG) PCa loses stromal dependence and becomes epitheliocentric accounting for therapy resistance. Integrins (IT) are transmembrane receptors that mediate cell adhesion and activation of intracellular signaling cascades and represent potential candidates for therapeutic targeting in PCa. Aberrations in IT signaling have been associated with the progression, emergence of castration resistance and metastasis of PCa and may be implicated in the phenotype of CR vs. non-CR pattern of HG PCa.

Design: We used PCa xenografts with CR and non-CR morphology as discovery platforms to identify differences in the expression of the mRNA of various IT components (a1-3, a5-8, a10, aE, aX, av, b1-5, b7, b8) with qRT-PCR. Expression of aX, b1 and b3 were validated with immunohistochemistry in tissue microarrays (TMA) that were constructed from the prostatectomy specimens of patients with untreated (N=62) and short term (2-4 months) (N=29) and long term (5-12 months) (N=18) androgen ablation treated HG PCa. IDS, CR and Gleason Grade 4, non-CR (fused glands) patterns were included in the TMA.

Results: Expression of ITb3, b5 and aX was higher ($p<0.001$, $p=0.014$ and $p=0.03$), whereas ITb1 was marginally lower ($p=0.09$) in the xenograft with non-CR compared to that with CR morphology. Immunohistochemistry in untreated human tumors showed that stromal expression of ITb3 was higher in non-CR compared to IDS and CR ($p<0.001$). Additionally, epithelial expression of ITb1 in untreated and treated tumors was lower ($p<0.001$ and $p=0.033$) and stromal expression in untreated tumors was higher ($p<0.001$) in non-CR compared to IDS and CR. No difference was noted between IDS and CR patterns in any of the markers tested.

Conclusions: A downregulation of IT expression was frequently noted in IDS/CR pattern of HG PCa. IDS and CR patterns seem to share biologic properties as shown by their similarities in IT expression. The role of IT expression in the pathogenesis and prognosis of the IDS/CR and non-CR patterns in treated and untreated tumors warrants further study.

1037 DeltaNp63 Isoforms of p63 in Aberrant Diffuse p63 Positive Prostate Cancer

K Uchida, HM Ross, JI Epstein, T Lotan, PB Illei. The Johns Hopkins Hospital, Baltimore.

Background: p63 typically labels prostatic basal cells in benign glands and is negative in adenocarcinoma of the prostate. Prostatic adenocarcinoma with aberrant diffuse p63 expression is extremely rare and poorly understood. The only series of this entity is of 21 cases compiled from a busy consult service. On H&E-stained slides, the tumor typically shows a distinctive morphology composed predominantly of glands, nests, and cords with atrophic cytoplasm, hyperchromatic nuclei, and visible nucleoli. Although the lesion does not express high molecular weight cytokeratin (HMWCK), p63 staining in the tumor with use of a PIN4 cocktail can obscure the loss of HMWCK and may be a diagnostic pitfall. The p63 protein is present in at least 6 major isoforms. Of these, TAP63 and deltaNp63 are the best characterized N-terminal variants, with deltaNp63 mRNA expressed at more than 100-fold higher levels than TAP63 in the normal prostate. While the p63 antibody recognizes both protein variants, a recently available p40 antibody only recognizes deltaNp63. In an attempt to aid in the diagnosis of p63 positive adenocarcinomas, we studied the p40 antibody to see if it was a more specific marker that does not show aberrant positivity.

Design: Immunohistochemistry for p40 was performed on 23 cores with aberrant p63 positive prostate adenocarcinoma from 16 patients. In all cases, parallel sections were additionally stained with p63 to confirm that the cancer present on deeper sections aberrantly expressed p63.

Results: 15/16 cases (94%) consisting of 21/23 cores showed diffuse expression of both p40 and p63 in the prostate adenocarcinomas. One case (two cores) was positive for p63 but entirely negative for p40. This case was morphologically identical to the other 15 cases. The basal cells in adjacent benign prostate glands in all cases stained uniformly for both p63 and p40, which were both negative in the overlying secretory cells.

Conclusions: DeltaNp63, as detected by the p40 antibody, is expressed in the majority of p63 positive prostate adenocarcinomas. This is consistent with the partial basal-like immunophenotype of these unusual tumors. From a diagnostic perspective, the use of the p40 antibody provides only a small advantage over the currently in use p63 antibody. Our one p40 negative p63 positive case may represent expression of the TAP63 isoform in the tumor. We are also currently further characterizing these tumors by looking at other basal/stem/progenitor cell markers.

1038 Comparison of Partial Sampling Methods in Radical Prostatectomy Specimens

SA Umar, V Iremashvili, L Pelaez, S Yasir, S Paluru, S Lokeshwar, M Manoharan, M Soloway, M Jorda. The University of Miami, Jackson Health System, Sylvester Comprehensive Cancer Center, Miami, FL.

Background: Extraprostatic extension (EPE) and surgical resection margin (SRM) status of a radical prostatectomy (RP) specimen directly impacts subsequent post-surgical patient management. There is no consensus as to whether partial sampling can provide sufficient information about these two parameters. Furthermore, no agreement has been reached in regards to which partial sampling method is most informative. The aim of our study was to evaluate different methods of partial sampling described in the literature and their association with rates of missed positive SRMs and/or EPE.

Design: We reviewed 697 entirely sampled RP specimens with positive SRM and/or EPE. Using schematic templates accompanying each case, we were able to analyze four previously described partial sampling methods: A) three representative sections of the gland B) alternate "slices" C) alternate "slices" representing the posterior aspect of the gland in addition to one of the mid-anterior D) every "slice" representing the posterior aspect of the gland in addition to one of the mid-anterior, supplemented by additional sections based on tumor size. The rates of positive SRM and EPE that could be identified using each of these techniques were compared to the actual rates obtained by entire sampling using the McNemar test.

Results: Of 697 completely sampled RP specimens (mean number of slides examined = 31), solely positive SRMs were identified in 387 (55.5%) cases, solely EPE in 136 (19.5%) cases, and both were identified in 174 (25%) cases. The partial sampling methods would have required examination of an average of 16 (A), 18 (B), 13 (C) and 20 (D) slides. All alternative sampling methods were associated with missing a significant number of the analyzed aggressive pathological features ($p < 0.001$ for all pairs of comparison), however the numbers of missed cases varied considerably. Positive SRMs (561 patients) and EPE (310 patients) would have been missed in 98 (18%) and 142 (46%) patients using method A, 78 (14%) and 94 (30%) using method B, 125 (22%) and 146 (47%) using method C, and 36 (6%) and 22 (7%) using method D.

Conclusions: Partial sampling method D consisting of every "slice" representing the posterior aspect of the gland in addition to one of the mid-anterior, supplemented by additional sections based on tumor size, appears to be superior to the other evaluated methods, missing 7% or less of cases with positive SRMs and/or EPEs.

1039 Molecular Classification Helps Discriminate between Oncocytomas and Chromophobe Renal Carcinomas Using Meta-Analysis of Gene Expression Microarrays

VA Valera Romero, BA Walter Rodriguez, MJ Merino. National Cancer Institute, National Institutes of Health, Bethesda, MD.

Background: Renal oncocytoma and chromophobe renal cell carcinomas are tumors that may share some morphologic features. Given the differences in prognosis, several attempts have been made to identify unique molecular markers based on gene expression studies. The results have been limited by the reduced number of cases included in

each study. In this study, we attempted to find unique gene expression profiles of renal oncocytomas and chromophobe RCC by systematically combining and analyzing publicly available microarray data.

Design: Microarray datasets containing the MeSH identifiers "Chromophobe" and "Oncocytoma" were queried in the NCBI Gene Expression Omnibus (GEO) database. Original, raw intensity files from single-platform (Affymetrix®) studies were retrieved. Only non-redundant samples were used for analysis. Built-in quality control probes were used to ensure comparability. After data preprocessing, gene expression signatures were investigated by unpaired T-test analysis with stringent conditions for false discovery rate and gene fold-changes. A classifier based on gene expression pattern was built and externally validated. Analyses were conducted with Genespring® and R/Bioconductor software.

Results: Seventeen databases were initially identified. From these, 10 databases were based on Affymetrix® gene microarray technology, and 4 non-redundant databases were used for analysis, comprising 34 chromophobe tumors, 40 oncocytomas, and 38 normal samples. Uniform array data preprocessing, 5291 genes were found differentially expressed. After data reduction by PCA, 121 genes responsible for the highest variability among samples were used for building a classifier. Apolipoprotein E (APOE, 3.9-fold), Aquaporin 6 (AQP6, 9.4-fold) and Phosphoenolpyruvate Carboxykinase 1 (PCK1, 15.1-fold) showed higher expression in oncocytomas. Osteoactivin (GPNMB) and Claudin 8 (CLDN8) showed increased expression in chromophobe tumors (9.2 fold and 14.2-fold respectively). The combination of genes helped to accurately classify tumors with an overall accuracy of 94%.

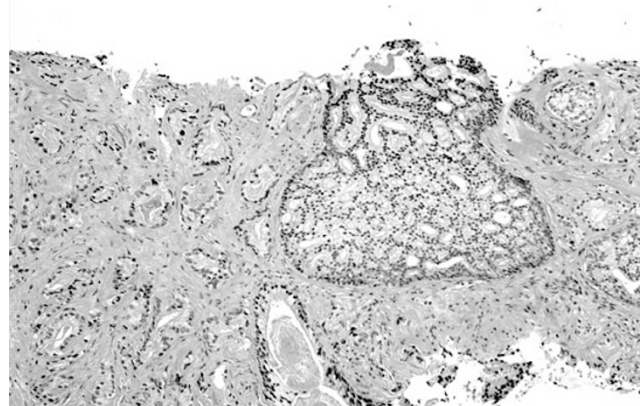
Conclusions: In this study, we have identified unique gene expression patterns comparing chromophobe RCC tumors and renal oncocytomas reanalyzing original, publicly available raw microarray data. The results demonstrated that gene expression profiling can be used to differentiate benign and malignant renal oncocytic tumors with high accuracy.

1040 Biopsy Diagnosis of Intraductal Carcinoma Is Prognostic in Intermediate and High Risk Prostate Cancer Patients Treated by Radiation

TH Van der Kwast, N Aldaoud, L Collette, J Sykes, M Bolla, RG Bristow. Princess Margaret Hospital, University Health Network, Toronto, Canada; Jordan University of Science and Technology, Irbid, Jordan; EORTC Headquarter, Brussels, Belgium; Grenoble University Hospital, Grenoble, France.

Background: Intraductal carcinoma of the prostate (IDC-P) is associated with high grade prostate cancer. In radical prostatectomy specimens, the presence of intraductal carcinoma of the prostate is an independent prognosticator for biochemical recurrence. We investigated the frequency and prognostic significance of IDC-P in biopsies and transurethral resections of two patient cohorts prior to radiotherapy.

Design: Cohort 1 consisted of 118 patients with intermediate risk prostate cancer treated by radiotherapy, with biochemical recurrence as endpoint (median follow-up 6.5 year). Cohort 2 consisted of 132 high risk patients, enrolled in a randomized trial (EORTC 22863) comparing radiotherapy alone to radiotherapy with long-term androgen deprivation (LTAD) with clinical progression free survival as primary endpoint (median follow-up 9.1 year). The presence of IDC-P was identified after central review of the available HE-stained slides.



Multivariable regression modelling and Kaplan Meier analysis was performed with IDC-P as dichotomous variable.

Results: In this retrospective study IDC-P was identified in 19% and 22% of cohort 1 and 2 tissues, respectively. IDC-P was a strong prognosticator for early (< 36 months) biochemical recurrence (HR 7.3; $p = 0.007$) in cohort 1 and for clinical disease-free survival in both arms of cohort 2 (radiotherapy arm: HR 3.5; $p < 0.0001$; radiotherapy plus LTAD arm: HR 2.8, $p = 0.018$). IDC-P retained significance after stratification for reviewed Gleason score in the radiotherapy arm (HR 2.5; $p = 0.03$). IDC-P was a strong prognosticator for metastatic disease (radiotherapy arm: HR 5.3; $p < 0.0001$; radiotherapy plus LTAD arm: HR 3.6; $p = 0.05$).

Conclusions: IDC-P in diagnostic prostate samples of patients with intermediate or high risk prostate cancer is an independent prognosticator for progression free survival and metastatic disease, after radiotherapy. We suggest that the presence of IDC-P in prostate biopsies should routinely be reported.

1041 Handling and Processing of Prostate Needle Biopsies (PNBx) in Europe: A Web-Based Survey by the European Network of Urology (ENUP)

M Varma, F Algaba, DM Berney, P Camparo, E Comperat, DFR Griffiths, G Kristiansen, A Lopez-Beltran, R Montironi, L Egevad. University Hospital of Wales, Cardiff, United Kingdom; Fundació Puigvert-University Autonomous, Barcelona, Spain; St Bartholomew's Hospital, London, United Kingdom; Hôpital Foch, Paris, France; UPMC Paris VI la Pitié, Paris, France; University Hospital Bonn, Bonn, Germany; Cordoba University Medical School, Cordoba, Spain; Polytechnic University of the Marche Region, Ancona, Italy; Karolinska Institutet, Stockholm, Sweden.

Background: Little information is available regarding the handling and processing of PNBx in laboratories across Europe.

Design: A web based survey of 23 questions related to the procuring, handling and processing PNBx was emailed to members of ENUP and British Association of Urological Pathologists.

Results: Responses were received from 241 laboratories in 17 countries in Europe, including 151 from continental Europe (CE) and 90 from UK/Ireland(UK/I). A few routines were almost universally adopted; buffered formalin (96.5% of centers) and right vs. left side identification (100%).

PNBx were most commonly taken by urologists (93.8%) or radiologists (23.7%) but in 8.7% were also taken by non-medical persons such as radiographer, nurse or biomedical assistant. The latter was more common in UK/I [21.1% (nurse 15.6%)] compared to CE (2%). The most common PNBx protocol was 12 cores per patient (42.3%).

PNBx were received loose in fixative (55.6%), attached to paper (22.4%) or between sponges (21.2%). Cores were most commonly received in separate containers (40.8%) and processed 1 core/block (42.3%) with 3 levels/block (54.2%), 1 H&E section/level (49.4%) and retention of unstained spare sections for possible immunohistochemistry (56.1%). Unstained spares were most commonly retained for over a year (40.9%) but 36.2% discarded spares within 1 month of reporting. Only 2 (0.8%) respondents routinely performed immunohistochemistry on all PNBx. Special techniques for flattening cores were employed during embedding by 12.4%, most commonly use of metal tampers.

As compared to UK/I, laboratories in CE more commonly receive each core in a separate container (CE: 55.3% vs. UK/I: 15.9%), process one core/block (57.6% vs. 16.7%), examine fewer levels/block (<3 levels: 42.9% CE, 6.7% UK/I), examine more H&E sections/level (>1 section: 61.1% vs. 19.3%), less often retain unstained spares (38% vs. 86.5%) and more often discard spares within a month of reporting (48.2% vs. 26.8%).

Conclusions: There are significant differences in procurement, handling and processing of PNBx in laboratories across Europe. This data can help development of best practice guidelines.

1042 The Utility and Diagnostic Accuracy of Ureteroscopic Biopsy in Diagnosing Upper Urinary Tract Urothelial Carcinoma

V Vashistha, DL Zynger. The Ohio State University Medical Center, Columbus, OH.

Background: Ureteroscopic biopsies of the ureter, renal pelvis, and ureteropelvic junction (UPJ) have become more pervasive for the diagnosis of upper urinary tract lesions. Tissue obtained from these locations is often minute and can be difficult to histologically evaluate. Our aim was to assess the accuracy of endoscopically obtained biopsies of the ureter, renal pelvis, and UPJ.

Design: Pathology and surgical procedural reports for all patients who had undergone upper urinary tract biopsies at our institution from 2008 to 2011 were retrospectively reviewed. We recorded the specimen clinical history, tissue size, and pathological stage and grade. The initial biopsy diagnosis was compared to the procedural surgical impression and follow-up pathology. Diagnoses that were discordant with follow-up pathology were re-reviewed and immunohistochemically analyzed using ki67, CD44s, CK20, and p53. Initial biopsy tumor stage and grade were compared to subsequent nephroureterectomy or ureterectomy specimens. Differences between tissue sizes were evaluated using a *t*-test.

Results: Ureteroscopic biopsies (n=83) had a sensitivity of 85.7% for the ureter (n=58), 87.5% for the renal pelvis (n=23), and 100% for the UPJ (n=2). No false positives were identified, with a specificity of 100% for all 3 locations. 8 cases were considered false negatives. After histologic re-review and immunostaining, only 1 of the false negative samples suggested diagnostic error yielding a diagnostic accuracy of 98.8%. The remaining 7 false negatives did not contain tumor and were therefore falsely negative due to insufficient sampling. The mean size was 0.8 cm for true positives, 0.3 cm for true negatives, and 0.6 cm for false negatives with a statistically significant difference between true positives and true negatives (p=0.001). 30 patients underwent surgical resection, with 23 (76.6%) having tumor in the initial biopsy. Comparing grade of the initial biopsy and resection, 82.6% (19/23) had concordant grade (grade higher in resection, n=3; grade lower in resection, n=1). A comparison of the stage identified 57.9% (11/19) with concordant stages (stage higher in resection, n=8).

Conclusions: Endoscopic biopsy is sensitive and specific for diagnosing malignancies of the upper urinary tract. The majority of errors are due to insufficient tissue sampling; consequently, performing immunostains does not provide further diagnostic information.

1043 Features of Atypical Glands on Initial Prostate Biopsy as Positive or Negative Predictors of Malignancy on Subsequent Prostate Biopsy

S Venigalla, C Zhao, H Miyamoto. University of Rochester, Rochester, NY.

Background: Patients whose prostate biopsy reveals the presence of atypical glands suspicious for prostatic carcinoma (AGSC) are subject to close monitoring and repeat biopsies, perhaps unnecessarily, as clinicians do not have a clear basis for understanding and stratifying the significance of these findings. The value of histologic atypia on an initial prostate biopsy in predicting the detection of prostate cancer on subsequent biopsies should thus be further studied.

Design: In a retrospective, blinded manner, we examined the initial biopsies of 82 patients (93 foci) reported as AGSC. Five factors assessed in these biopsies include the size of the nucleoli of cells composing AGSC (graded on a scale of 1-4 with "1" denoting small, inconspicuous nucleoli and "4" denoting macronucleoli), the presence of high-grade prostatic intraepithelial neoplasia (HGPIN) adjacent to or separate from AGSC, the number of AGSC, the presence of intraluminal crystalloid, mucin, or dense secretions within AGSC, and the presence of basal cells in AGSC highlighted by immunohistochemical staining.

Results: On subsequent biopsies, 31 (38%) patients were found to have prostate cancer (PCA) while no carcinoma was identified in the remainder (62%) of cases (NOCA). Nucleolar grade was significantly higher (p=0.010) in PCA cases (mean ± SD: 2.43 ± 0.80) than in NOCA cases (mean ± SD: 1.98 ± 0.70). Adjacent (p=0.235) and separate (p=0.132) HGPINs were found in 8/37 (22%) foci and 8/31 (26%) cases in PCA, respectively, and in 6/56 (11%) foci and 6/51 (12%) cases in NOCA, respectively. The number of atypical glands was similar (p=0.950) between PCA (mean ± SD: 7.03 ± 5.35) and NOCA (mean ± SD: 7.09 ± 4.18). The presence of intraluminal crystalloid, mucin, or dense secretions in AGSC did not show a statistically significant correlation between PCA [5/37 (14%)] and NOCA [13/56 (23%)] (p=0.293). Immunohistochemical stains demonstrated patchy basal cells in 17/39 (44%) of NOCA whereas basal cells were absent in 24/27 (89%) PCA (p=0.006).

Conclusions: On an atypical initial prostate biopsy, the size of nucleoli in AGSC is a positive predictor of prostate cancer on subsequent biopsy. On the other hand, as expected, even patchy staining of basal cells in AGSC represents a negative predictor of prostate cancer. However, HGPIN adjacent to or separate from AGSC, the total number of AGSC, and intraluminal materials do not reliably predict the subsequent diagnosis of prostate cancer.

1044 ERG Expression in 175 Prostatic Carcinomas and 270 Carcinomas from Different Primary Sites

M Verdu, R Roman, M Calvo, N Rodon, B Garcia, P Merce, X Puig. BIOPAT. Biopatologia Molecular, SL, Grup Assistencia, Barcelona, Spain; Hospital de Barcelona, SCIAS, Grup Assistencia, Barcelona, Spain; Histopat Laboratoris, Barcelona, Spain; Universitat de Barcelona(UB), Barcelona, Spain.

Background: ERG gene rearrangement, detected by FISH or RT-PCR, has been identified as a highly specific alteration, present in 40-50% of prostate carcinomas (PCa). Recent studies describe a novel anti-ERG antibody, whose positive staining by immunohistochemistry (IHC) highly correlates with the ERG rearrangement. The standardization of an IHC assay would have significant diagnostic and prognostic value. Marked variations in rates of PCa among populations in the world suggest the involvement of genetic factors. The aim of this study was to identify the incidence of this rearrangement in a Spanish population and to test the specificity of the IHC ERG evaluation for PCa.

Design: Tissue microarrays (TMA's) of a wide variety of normal and neoplastic tissues were tested. TMA's were analyzed by IHC performed by ABC immunoperoxidase staining, using a rabbit monoclonal antibody (ERG, clone EPR3864). The expression of ERG protein was scored as negative, weak, moderate or strong, using vascular endothelial cells as internal control. A case was judged positive if any of the evaluable cores showed a positive staining, whichever its intensity.

Three prostate TMA's were constructed using prostatectomy specimens, and their Gleason score (GS) and extent of invasion (pT) were routinely determined. These TMA's included, besides samples of malignant cases (175), specimens with prostatic hyperplasia (25) and high grade prostatic intraepithelial neoplasia (HGPIN) (10).

In addition, TMA's of the most common tumors in Spain (breast, colon, lung and bladder) were also tested (270 samples in total).

Results: In our study 44% (76/171) evaluable cases of PCa showed ERG expression, most of them presenting strong staining (61/76). No ERG expression was observed in any of the HGPIN samples, as reported by others. ERG expression was independent of GS (p=0.735) and pT (p=0.128). There was no ERG expression found in any other type of tumor, with the exception of one bladder cancer single sample which showed focal expression.

Conclusions: The frequency of ERG detected in our study correlated with that published in other Caucasian populations. The expression of ERG protein is exclusively detected on prostatic adenocarcinoma, corroborating the specificity of ERG rearrangement for these tumors. Thus, in addition to its prognostic significance, the use of ERG detection by IHC may be useful in routine practice to complement the panel of prostatic carcinoma.

1045 "Hybrid Oncocytic/Chromophobe Renal Cell Tumours" Do Not Display Genomic Features of Chromophobe Carcinomas

A Vieillefond, n Pote, F Mege-Lechevallier, M Sibony, p Camparo, v Molinie, j Couturier. Hopital Cochin, Paris, France; Hopital Edouard Herriot, Lyon, France; Curie Institute, Paris, France; Hopital Foch, Suresnes, France; Hopital Saint-Joseph, Paris, France.

Background: "Hybrid" oncocytic/chromophobe tumours (HOCT) of the kidney are rare tumours of uncertain diagnosis and prognosis, presenting with histological characteristics of both renal oncocytoma (RO), and chromophobe renal-cell carcinoma (ChRCC). Various terminology have been used in the literature: "atypical oncocytoma", "oncocytoma with chromophobe areas", "tumours with overlapping histology" but the real frequency of HOCT is not known. Based on morphology, and immunohistochemistry, pathologists consider a morphologic spectrum with RO and ChRCC at its ends, and HOCT in between. Based on genomic and cytogenetic datas, RO and ChRCC are two distinct genetic entities, but HOCT were never studied.

The aim of our study is to determine the genomic profile of so-called HOCT using array-CGH.

Design: A series of 42 kidney tumours of the RO/ChRCC group was selected. 30 RO and ChRCC were easily diagnosed and 12 tumours were diagnosed as "HOCT" (2

in BHD patients). HOCT were defined as tumours with admixture of oncocytes and chromophobe cells or with cells with "hybrid" morphology. Colloidal iron and CK7 stainings were analyzed.

For Array-CGH, DNA extraction was done from frozen tumoral samples. Cases were analysed either on a 5K BAC/PAC DNA microarray or on 4x72K NimbleGen® arrays. Genome profiles were visualised using the SignalMap® software (NimbleGen®).

Results: In the majority of HOCT tumours, Hale (colloidal iron) staining, displayed an apical positivity, in 80 to 100% of cells, all sporadic tumours except in the two BHD patients. In sporadic tumours, 10% to 100% of cells were CK7-positive, 5 cases contain more than 80% of CK7-positive cells. In BHD tumours, a mosaic pattern was observed. Array-CGH profiles: in 5 sporadic HOCT as well as in the two BHD cases, no chromosome imbalances were observed. One case showed only a gain of chromosome 18. The 4 other cases showed a small number of chromosome imbalances always involving a loss of 1p or of the whole chromosome 1. No characteristic combined losses of ChrRCC were seen.

Conclusions: HOCT display hybrid morphology, histochemical and immunohistochemical profiles and a good clinical outcome. Genomic features of so called HOCT show no link with ChrRCC. In case of difficult histological diagnosis in the RO/ChrRCC group, genome profiling is recommended to exclude a true ChrRCC.

1046 How Immunohistochemistry Can Help To Identify Renal Tumors Associated with SDHB Syndrome

BA Walter, VA Valera, K Pacak, M Linehan, MJ Merino. NCI, NIH, Bethesda.

Background: Renal cell carcinoma (RCC) is composed of several histologic subtypes. While the majority occur sporadically, about 5% are associated with hereditary syndromes. Lately, our understanding of RCC-predisposing syndromes has improved and genes associated with specific tumors have been discovered. However, there are no specific IHC stains to assist in the identification of each tumor type. Germline mutations in genes that code for the succinate dehydrogenase complex subunits (*SDHB*, *SDHC* and *SDHD*) are associated with a high risk of head and neck paragangliomas, extra-adrenal pheochromocytomas and RCC. SDHB protein by IHC can definitely assist in identifying renal tumors and patients that are part of the SDHB syndrome.

Design: Ninety tumors representing the wide histologic spectrum of RCC were evaluated, including 10 oncocytomas, 36 clear cell RCC (ccRCC) (10 with hx of VHL), 10 chromophobe RCC, 5 Hybrid tumors with BHD mutation, 13 HLRCC, 3 Papillary type and 13 cases of RCC with known SDHB mutation. Complete sections of the tumors were used to evaluate SDHB protein expression by IHC. Two different antibodies were used to recognize different binding sites of the target protein, (N-terminal 4-150 aa) and (C-terminal 165-273 aa) (Sigma-Aldrich, USA).

Results: Ten oncocytomas and 67 RCC of different subtypes stained positive with both SDHB antibodies. Normal renal tubules showed a moderate fine granular cytoplasmic staining as a control. Oncocytomas showed a stronger intensity in the cytoplasm, followed by ccRCC high Furman grade. All the other ccRCC associated or not with VHL mutation, HLRCC and chromophobe cases were also positively stained. Hybrid tumors were intensely staining the eosinophilic cells. All of the RCC with known SDHB mutation were negative with both antibodies. These patients, ranged in age from 15 to 61 years with a female predominance. Histologically 11/13 cases (70%) showed oncocytic features with groups of clear cells; only two cases also had a spindle cell component. Most of the oncocytic cells have a unique intracytoplasmic inclusion which was confirmed by EM.

Conclusions: We concluded that IHC staining of RCC with SDHB markers can be of great help to identify patients that can be part of the SDHB syndrome. All our cases stained negative by IHC with both markers, meanwhile all the different types of RCC, including tumors that are part of other hereditary syndromes stained positive. Early identification of patients with SDHB syndromes will definitely allow to improve survival by proper screening of the families.

1047 Mitochondria Respiratory Chain Gene Expression Analysis in Renal Cell Carcinoma

BA Walter Rodriguez, VA Valera Romero, M Linehan, MJ Merino. NCI/NIN, Bethesda; NCI/NIH, Bethesda.

Background: Mitochondrial dysfunction has been proposed as a major pathogenetic mechanism in solid tumors including renal cell carcinomas (RCC). The underlying mechanism is related to both energy production and reactive oxygen species generation by the organelle. The most common morphologic and functional alterations include copy number changes and mt-DNA mutations. However, mRNA expression changes have not been well characterized in RCCs.

Design: A group of 21 renal tumors of different histologies including benign oncocytomas were evaluated. Alterations in the non-coding displacement (D) loop mitochondrial DNA (mt-D Loop) and the 12S mitochondrial ribosomal (rRNA)(RNR2) were evaluated by RT-PCR, as well as the expression of the following subunits of the respiratory complex: NADH dehydrogenase 1/2 (complex I), Cytochrome B subunit of the complex III, complex cytochrome c oxidase (COX2) (complex IV) and the mRNA expression of the complex II. HIF-1 A as a surrogate marker of hypoxia activation was assessed in the tumor by IHC.

Results: Analysis of the mt-D Loop mitochondrial content showed that oncocytomas have an increased expression level (7.10 fold-change) in comparison with ccRCC and SDHB mutation-related RCCs (0.18 and 0.58 fold-change). The 12SrRNA expression was also high in Oncocytomas (10.32 fold-change) and decreased in the ccRCC and SDHB-RCC cases (0.56 and 0.85 fold-change), respectively. Complex I subunits evaluated include, ND1 and ND2 genes. ND1 and ND2 expression showed in the oncocytomas high expression level (7.65 and 1.66 fold-change), whereas ccRCC and tumors with SDH mutations showed low expression levels (for ND1 0.24 and 0.22 fold-change and for ND2 0.16 and 0.57 fold-change, respectively). Expression of mRNA

of Complex II showed expression level in all the three groups of tumors (oncocytoma, ccRCC and SDHB related tumors). In the SDHB mutated cases, HIF 1 staining shows nuclear positivity only the tumoral cells in the periphery of the tumor mass that is displacing the adjacent normal renal tissue, all the rest of tumor was negative. The clear cell RCC cases, and the oncocytomas showed nuclear accumulation in all tumor cells.

Conclusions: In RCCs, alterations in the expression of mitochondria protein components of respiratory chain are frequent but not in mt copy number. Tumors showed in general low expression level in most the genes. Consistent with the increase in mt content, oncocytomas showed increased expression of most complexes. Hypoxia pathway activation due to HIF1alpha accumulation was not found in RCC with SDH mutation.

1048 Perineural Invasion (PNI) in Prostate Cancer Patients Who Are Potential Candidates for Active Surveillance: A Validation Study

C Wang, J Zhang, A Yilmaz, TA Bismar, K Trpkov. Calgary Laboratory Services and University of Calgary, Calgary, AB, Canada.

Background: One study recently showed that the presence of PNI on positive needle biopsy in patients considered for active surveillance should not represent an exclusion criterion (*J Urol* 2011;186:470-3). We sought to validate this finding in a large cohort of patients who fulfilled the Epstein biopsy criteria for active surveillance, but proceeded to radical prostatectomy.

Design: We retrieved from our institutional prostate cancer database the biopsy, prostatectomy and the clinical data of 845 patients who met the Epstein criteria (biopsy Gleason score ≤ 6 (no pattern 4), 2 or fewer positive cores and $\leq 50\%$ involvement of any positive core). All patients had standard ten-core biopsy and radical prostatectomy (specimens completely embedded) in our institution between 07/2000 and 06/2010. We compared the clinical, biopsy and prostatectomy data in patients with and without PNI on needle biopsy. Means were compared between the PNI and no PNI groups using the Student's t-test for continuous variables. For categorical variables, proportions were compared between the groups using chi-square or Fisher's exact test. All tests were two-sided, and the P values were considered significant at less than 0.05.

Results: PNI was present in 63 (7.4%) biopsies. Preoperative and prostatectomy findings are shown in Tables 1 and 2.

Table 1. Clinical and biopsy findings in patients with and without PNI on biopsy

	PNI (n=63)	no PNI (n=782)	P-value
Age (years), Mean	60.3	59.4	0.33
PSA ng/ml, Mean	6.2	6.5	0.57
Gland vol. cc, Mean	45	46.1	0.72
2-core positive (%)	57.1	36.8	0.001
Total % cancer on biopsy	2.5	1.8	<0.001

Table 2. Prostatectomy findings in patients with and without PNI on biopsy

	PNI (n=63)	no PNI (n=782)	P-value
Organ confined (%)	95.2	96.4	0.50
Positive margins (%)	20.6	16.4	0.39
TU vol. (gland %)	8.2	7.3	0.36
Gleason ≤ 6 (%)<<	57.1	66.8	0.13*
Gleason 3+4 (%)	39.7	29	
Gleason 4+3 (%)	1.6	3.1	
Gleason ≥ 8 (%)	1.6	1.1	

*Gleason ≤ 6 vs Gleason > 6

No significant differences were found between the PNI and no PNI groups when separate analysis was performed for the 1-core and 2-core positive patients.

Conclusions: We confirm that the presence of PNI on biopsy should not be used to exclude patients from active surveillance if the Epstein biopsy criteria are met. Although patients with PNI presented more frequently with 2-core positive biopsies and had higher total volume of cancer on biopsy, we found no statistically significant differences in the clinical and prostatectomy findings in patients with PNI compared to patients without PNI on biopsy.

1049 Primary Papillary Urothelial Neoplasm of Low Malignant Potential (PUNLMP) Including PUNLMP with Inverted Growth: Outcome Analysis

C Wang, JP Maxwell, A Yilmaz, TA Bismar, K Trpkov. Calgary Laboratory Services and University of Calgary, Calgary, Canada.

Background: Few single-center studies addressed the long-term clinical outcome for patients with PUNLMP. Many of the previous studies, however, included both *de novo* (Primary-PUNLMP) and Secondary-PUNLMP, diagnosed during surveillance for higher grade urothelial neoplasm. The previous studies typically included less than 100 patients.

Design: We searched our institutional information system for all Primary-PUNLMP including PUNLMP with inverted growth, diagnosed between 01/2000 and 12/2009. All cases with a previous history of higher grade urothelial neoplasm (Secondary-PUNLMP) were excluded. The follow-up (F/U) was obtained by review of the electronic medical records in our centralized urology and uropathology practice for the region. On F/U, recurrence was defined as any subsequent neoplastic bladder lesion. Progression was defined as subsequent high-grade or invasive recurrent tumor, including carcinoma in-situ or dysplasia.

Results: We identified a total of 196 Primary-PUNLMP (all bladder location except 1 in renal pelvis), including 12 (6%) with inverted pattern. Mean patient age was 64 years (median 66, range 19 to 92) with M:F ratio of 1.8:1. Mean F/U was 65 months (range 10 to 133). Recurrence was documented in 45 (23%) patients (median number of recurrences 1, range 1-7); 35 (18%) of recurrences were without progression. Multiple recurrences occurred in 37% (13/35) patients who did not progress. In 10 (5%) patients, there was progression to high-grade carcinoma: 7 non-invasive and 3 invasive, of which 1 into lamina propria and 2 into muscularis propria. In 6 patients progression occurred directly into high-grade, while in 4, progression occurred after subsequent PUNLMP (2) or low-grade (2) carcinoma. All patients who progressed were male with a mean

age of 71 years (range, 50-87). All recurrent neoplasms after Primary-PUNLMP were in the bladder, except one case in the renal pelvis. The mean time to recurrence without subsequent progression was 31 months (range, 5-87). The mean time to progression was 39 months (range, 4-101). None of the patients with Primary-PUNLMP with inverted growth pattern had a documented recurrence or progression. No progression with metastatic disease was found in any patient.

Conclusions: We found an overall recurrence rate of 23% and a progression rate of 5% in a large contemporary cohort of Primary-PUNLMP. Ongoing surveillance is particularly warranted for older males (≥ 50 years) diagnosed with Primary-PUNLMP. The subgroup of patients with Primary-PUNLMP with inverted growth pattern had a good outcome in this study.

1050 Utilization of Immunohistochemistry in Prostate Needle Biopsies: Quality Assurance and Cost Implications

K Watson, C Wang, A Yilmaz, TA Bismar, K Trpkov. Calgary Laboratory Services and University of Calgary, Calgary, AB, Canada.

Background: The use of immunohistochemistry (IHC) for high molecular weight keratin (HMWK) and AMACR has been studied extensively as an aid in establishing diagnosis on prostate needle biopsy. However, the quality assurance and the cost implications have not been previously addressed in great detail.

Design: We retrieved pathology reports of 748 prostate biopsies signed over a six-month period (12/10 to 05/11) in our academic practice. We identified the biopsies and the blocks in which IHC for HMWK and AMACR was ordered. We evaluated the rates and the turn-around time for IHC cases, the final diagnosis rendered on individual specimens (CANCER, ATYP, ATYP/PIN, PIN and BENIGN), the prostate biopsy departmental consultation rate and the consultation rate when IHC was used. We performed cost analysis for the average cost per biopsy and for the annual IHC cost for prostate biopsies in our lab.

Results: Overall, 39.4% (295/748) of prostate biopsies and 12% (539/4488) of biopsy blocks required IHC evaluation (average 1.8 block/IHC case). The biopsies with IHC were signed-out on average 1.7 work days later (8.6 days with IHC vs. 6.9 days without IHC). The diagnostic breakdown for individual blocks evaluated by IHC was: CANCER 47.7%, ATYP 10.8%, ATYP/PIN 6.9%, PIN 12.4% and BENIGN 22.2%. In cases with final CANCER diagnosis in individual blocks, 79% were assigned Gleason 6, 14.4% Gleason 7 and 6.6% Gleason 8-10. Regarding the cancer extent on individual cores, IHC aided in establishing minimal cancer diagnosis ($\leq 5\%$ core) in 39.8% and non-minimal cancer ($> 5\%$ core) in 60.2% positive cores. IHC supported the diagnosis in 74% (55/74) of single-core positive biopsies. Departmental consultation was performed in 18.3% (137/748) of prostate biopsies; IHC was used in 68% (93/137) of these. In 98% (51/52) of all ATYP cases (ATYP+ATYP/PIN) both IHC and consultation were performed. Using the estimated cost of \$31 per immunostain in our lab, the average IHC cost per biopsy was \$22.30. The estimated annual cost for prostate biopsy IHC was \$33,450 (1500 prostate biopsies annual lab volume).

Conclusions: Approximately 40% of prostate biopsies in our institution required IHC which did not affect the turn-around time significantly. Diagnosis CANCER or ATYP (ATYP+ATYP/PIN) were rendered in 65.4% of individual blocks assessed by IHC. IHC was used to establish a diagnosis of CANCER in large proportion of either minimal or single-core positive cases. IHC was used in 68% of cases requiring departmental consultation. We calculated an average IHC cost per prostate biopsy of \$22.30.

1051 Clinicopathologic and Immunohistochemical Characteristics of Invasive Low Grade Urothelial Carcinoma

KE Watts, DE Hansel. Cleveland Clinic, Cleveland, OH.

Background: Papillary urothelial carcinomas (UC) are broadly categorized into low and high-grade categories, with the former generally occurring as non-invasive lesions and the latter with or without invasion. Low-grade papillary UC may rarely be associated with invasion, although the properties that distinguish these lesions from the less aggressive, more prototypical papillary low-grade UCs is unclear. We therefore examined the clinicopathologic and immunohistochemical features associated with the uncommon subset of invasive low-grade papillary UC.

Design: The electronic archives were searched for cases of invasive low grade papillary UC between 2001 and 2008 and the appropriate slides reviewed. Clinical and outcomes data were extracted from the electronic medical record. Immunohistochemical stains for p53, CK20, E-cadherin, and CD44 were performed on routine formalin-fixed paraffin-embedded sections.

Results: Twelve cases of invasive low-grade papillary UC were identified. All but one of the patients were male (mean age 64 yrs; range 37-82 yrs). Five patients had a subsequent non-invasive low-grade papillary UC, with recurrence at an average of 9.6 months after initial diagnosis, 1 had a subsequent high-grade invasive UC on radical cystectomy, and 4 had no evidence of recurrence. One patient was found to have metastatic disease at the time of diagnosis and a second developed metastatic disease within 17 months; both of these patients died of their disease. Two cases showed invasion of the muscularis propria (MP) and 10 showed superficial invasion of the lamina propria. All cases showed diffuse expression of nuclear p53 and maintained E-cadherin expression throughout the lesion. Immunostaining for CK20 was more variable, with 5 cases showing strong diffuse staining throughout the papillary component (including 1 case with MP invasion) and 6 cases showing focal non-umbrella cell staining. CD44 was weakly present in a basilar distribution in 3 cases, whereas 3 other cases showed focal strong non-basilar expression, and 6 showed focal weak non-basilar staining; complete absence of CD44 staining was not seen in any case.

Conclusions: Immunohistochemical stains for p53 in cases of invasive low-grade papillary UC showed a similar pattern of expression to that associated with invasive high-grade papillary UC, suggesting its possible utility in predicting low-grade papillary

UC cases that are likely to display more aggressive biological behavior. Further investigation into the differences of E-cadherin, CK20 and CD44 staining patterns in this unusual subset of cases is warranted.

1052 Incidence and Clinicopathological Characteristics of Intraductal Carcinoma of the Prostate Detected in Prostate Biopsies: A Prospective Cohort Study

KE Watts, J Li, C Magi-Galluzzi, M Zhou. Cleveland Clinic, Cleveland, OH.

Background: Intraductal carcinoma of the prostate (IDC-P) is a distinct clinicopathological entity characterized by expansile proliferation of cancer cells within preexisting prostatic ducts and acini. It is strongly associated with aggressive high grade and high volume prostate cancer (PCa). It is critical to recognize IDC-P, especially in prostate biopsy (PBx). We aimed to study the incidence and clinicopathological characteristics of IDC-P detected in PBx in prospectively collected cases.

Design: IDC-P was defined as a lumen-spanning proliferation of malignant cells within prostatic glands with at least partial basal cell lining. From November 2009 to September 2011, PBx with IDC-P were prospectively collected and their clinicopathological features evaluated.

Results: 33 IDC-P cases were identified out of 1176 PBx (2.8%), including 3 (9%) cases without an associated invasive PCa, 16 (48%) associated with Gleason score 7 (GS 7) PCa, 4 (12%) with GS 8 PCa, and 10 (30%) with GS 9 PCa. The mean age of IDC-P patients was 65 (range 46-79) years and mean serum PSA was 16.2 (range 0.4-105.6) ng/mL. The mean number of biopsy cores involved by PCa was 7.2 (range 1-14). Treatment information was available in 30 patients: 19 men were treated with non-surgical therapy, including radiation, androgen deprivation and chemotherapy; 9 underwent radical prostatectomy (RP). Extraprostatic extension (EPE), seminal vesicle invasion (SVI) and lymph node metastasis (LN) was observed in 6/9 (67%), 4/9 (44%) and 1/9 (11%), compared to the predicted mean risk of 41%, 12% and 5% for EPE ($p=0.173$), SVI ($p=0.002$) and LN ($p=0.383$) on Partin Tables. Tumor volume in 75% RP was greater than 2 mL. Two patients with IDC-P only in PBx were treated with radiation and had normalized PSA after treatment.

Conclusions: IDC-P is rare (2.8%) and is even rarer (0.26%) as an isolated finding in PBx. It is strongly associated with high grade and high volume PCa. Majority of patients were managed non-surgically. The incidence of SVI is significantly higher than that predicted by Partin Tables, suggesting that IDC-P identified in PBx may provide additional prognostic information.

1053 Unclassified Renal Cell Carcinoma and Invasive High Grade Urothelial Carcinoma: Is the Distinction Possible by Immunohistochemistry and Clinically Important?

KE Watts, JP Reynold, P Carver, M Zhou. Cleveland Clinic, Cleveland, OH.

Background: The differential diagnosis for a poorly differentiated carcinoma in the kidney includes renal cell carcinoma (RCC) and urothelial carcinoma (UC). Such distinction is presumed to be clinically important as the chemotherapeutic and surgical regimens for them are different. This study aimed to investigate: 1) whether a panel of immunostain markers could differentiate between poorly differentiated RCC and UC, and 2) whether the distinction between the two is clinically important?

Design: A tissue microarray was constructed to include 11 unclassifiable RCC (including 3 with features of collecting duct RCC), 2 renal UC and 16 invasive high grade pelvic UC and was stained with a panel of markers (PAX-8, K903, p63, CK7, CK20). Clinical information was obtained by chart review and patient contact.

Results: The mean age of RCC and UC patients was 60.3 (range 45-81) years and 70.1 (range 54-95) years. The male/female ratio was 9/2 for RCC and 13/5 for UC patients. PAX-8, K903, p63, CK7 and CK20 were positive in 10, 0, 0, 2 and 2 of 11 RCC, and 3, 9, 18, 17 and 7 UC, respectively. Therefore, a PAX-8 positive/K903 negative/p63 negative phenotype identified 10/11 (90.9%) RCC, and a PAX-8 negative/K903 or p63 positive phenotype identified 15/18 (83.3%) UC. The follow-up for RCC patients was an average of 11 months, and in UC patients was an average of 10.4 months. 9/11 (81.9%) RCC patients and 13/18 (72.2%) UC patients died of disease, which was not found to be statistically significant ($p=0.55$).

Conclusions: Immunostains using a panel of markers (PAX-8, K903 and p63) could reliably distinguish poorly differentiated RCC and invasive high grade UC. However, all these patients had extremely poor prognosis; therefore, the distinction between the two tumors seem to be of limited clinical prognostic significance.

1054 Phenotypic Characterization of Primary Testicular Diffuse Large B-Cell Lymphoma

PT Went, T Menter, M Ernst, S Dirnhofer, A Barghorn, A Tzankov. Institute of Pathology, Basel, Switzerland; Institute of Pathology, Liestal, Switzerland; Medica, Zürich, Switzerland.

Background: Primary testicular lymphoma is rare, consisting of 3-5% of primary extranodal lymphomas. Different lymphoma types can occur; however, diffuse large B-cell lymphoma (DLBCL) represents by far the most frequent subtype. Patients with DLBCL may not benefit equally from Rituximab therapy as patients with nodal DLBCL. According to recent studies, the incidence of DLBCL is increasing. To investigate if this is paralleled by a shift in histological morphology, we systematically analyzed the morphology and phenotype of DLBCL on the background of recently described subtypes.

Design: Forty-three patients from three different Swiss hospitals were included in this study. The tumors were diagnosed between 1972 and 2009. The protein expression profile was assessed by immunohistochemistry.

Results: 39 of the tumors showed centroblastic and one immunoblastic morphology, three were not classifiable. All cases (n=43) were positive for CD79a. According to

the Tally algorithm, 83% (n=36) were phenotypically classified as non-GC type. All tumors were EBER negative. 70% (n=30) of the tumors showed active STAT signaling by expression of either pSTAT1 or pSTAT3, but not pSTAT5. P53 staining was positive in five tumors, but p21 staining was negative in all cases, indicating the absence of TP53 mutation. Mean mitotic index was 18/mm², median MIB1 labeling index was 40% (+/-25%). Tumors with lymphoepithelial lesions in seminiferous tubules showed a higher mitotic activity, although the association was weak. Interestingly, one tumor was positive for Oct4. All 43 cases were negative for NUT1 and PLAP. Only limited clinical data were available: mean age at diagnosis was 69 years (range: 43-87 years, n=41). There was no side predilection of the tumors. One tumor was bilateral at diagnosis, one tumor presented simultaneously in the testis and the CNS. Of ten tumors, five did not relapse (mean follow up time 48 months, min 0, max 132). Five tDLBCL relapsed, thereof two in the contralateral testis, two in the CNS and one in the skin.

Conclusions: We conclude that in tDLBCL centroblastic morphology and a non-GC phenotype predominates. There was no change of morphology or protein expression profile over time. No sign of TP53 mutations was detected. STAT signaling pathway is active and mediated through STAT3 and STAT3. To avoid misdiagnosis, a marker panel should be utilized, as rare cases can be positive for the germ cell tumor marker Oct4.

1055 miRNA Profiling in Metastatic Renal Cell Carcinoma Reveals a Tumor Suppressor Effect for miR-215

NMA White, HWZ Khella, J Grigull, S Adzovic, YM Youssef, RJ Honey, R Stewart, KT Pace, GA Bjarnason, MAS Jewett, AJ Evans, M Gabriel, GM Yousef. St. Michael's Hospital, Toronto, ON, Canada; University of Toronto, Toronto, ON, Canada; York University, Toronto, ON, Canada; Sunnybrook Health Sciences Center, Toronto, ON, Canada; Princess Margaret Hospital, Toronto, ON, Canada; London Health Sciences Center, London, ON, Canada.

Background: Renal cell carcinoma (RCC) is the most common neoplasm of the adult kidney. Metastatic RCC is difficult to treat. The five-year survival rate for metastatic RCC is <10%. Recently, microRNAs (miRNAs) have been shown to have a role in cancer metastasis and potential as prognostic biomarkers in cancer.

Design: We performed a miRNA microarray to identify a miRNA signature characteristic of metastatic compared to primary RCC. Results were validated by quantitative real time PCR. Target prediction analysis and gene expression profiling identified many of the dysregulated miRNAs could target genes involved in tumor metastasis. The effect of miR-215 on cellular migration and invasion was shown in a RCC cell line model.

Results: We identified 65 miRNAs that were significantly altered in metastatic when compared to primary RCC. Nine (14%) miRNAs had increased expression while 56 (86%) miRNAs showed decreased expression. miR-10b, miR-196a, and miR-27b were the most downregulated while miR-638, miR-1915, and miR-149* were the most upregulated. A non-supervised 2D-cluster analysis showed that a sub-group of the primary tumors clustered under the metastatic arm with a group of miRNAs that follow the same pattern of expression suggesting they have an inherited aggressive signature. We validated our results by examining the expressions of miR-10b, miR-126, miR-196a, miR-204, and miR-215, in two independent cohorts of patients. We also showed that overexpression of miR-215 decreased cellular migration and invasion in a RCC cell line model. In addition, through gene expression profiling, we identified direct and indirect targets of miR-215 that can contribute to tumor metastasis.

Conclusions: Our analysis showed that miRNAs are altered in metastatic RCC and can contribute to kidney cancer metastasis through different biological processes. Dysregulated miRNAs represent potential prognostic biomarkers and may have therapeutic applications in kidney cancer.

1056 Relative Quantification of Protein Expression in Metastatic Clear Cell Renal Cell Carcinoma Tissue Using iTRAQ LC-MS/MS Analysis

NMA White, O Masui, L DeSouza, O Krakovska, A Matta, KWM Siu, GM Yousef. St. Michael's Hospital, Toronto, ON, Canada; York University, Toronto, ON, Canada.

Background: Renal cell carcinoma (RCC) is the most common neoplasm of the adult kidney. Metastatic RCC is difficult to treat. The five-year survival rate for metastatic RCC is <10%. There are currently no biomarkers in use for clinical diagnosis or prognosis of clear cell renal cell carcinoma (ccRCC).

Design: We performed iTRAQ (isobaric tags for relative and absolute quantitation) analysis on six pairs of primary ccRCC and normal matched kidney from the same patient in addition to six metastatic RCC samples. Samples were homogenized, clarified, trypsinized, labeled, and pooled. The pooled labeled digests were then separated by offline strong cation exchange chromatography, followed by on-line reverse phase nano-liquid chromatography mass spectrometry (LC-MS/MS) analyses in triplicate. An exclusion list was used to minimize redundancy in subsequent iterations and consisted of the mass-to-charge (m/z) ratios and elution times of peptides that had been identified in the previous iteration(s). MS data were analyzed by ProteinPilot.

Results: Using a cut-off of 5% local false discovery rate, a total of 1,256 non-redundant proteins were identified in a total of five sets, from which 456 proteins were confidently quantified (p<0.05). 39 proteins were differentially expressed in the majority of cancer (primary and metastatic) samples versus the non-malignant pool, while another 20 were differentially expressed in the majority of metastatic versus primary samples. Three overexpressed proteins chosen as best candidates as potential ccRCC prognostic biomarkers are currently being independently verified by western blot and tissue microarray analysis. All differentially expressed proteins will be used as foci in a pathway analysis to elucidate their possible roles in tumorigenesis.

Conclusions: The identification of clinical markers for RCC patients will have a great impact on patient care since it will significantly reduce the risk of complications of late stage disease and will lead to significant reduction of the cost of treating advanced metastatic disease. Also, the mechanism of RCC metastasis remains to be elucidated.

Bioinformatic analysis of dysregulated proteins in metastatic RCC will shed light on the pathways that contribute to this malignancy leading to a further understanding of RCC pathogenesis and forming the foundation for the design of new targeted therapies.

1057 NANOG Immunohistochemical Expression in Tumors

M Wilkerson, F Lin, J Shi. Geisinger Medical Center, Danville, PA.

Background: The NANOG gene is located on human chromosome 12p13. The NANOG protein product is a homeobox DNA binding transcription factor that prevents differentiation of embryonic stem cells. Down regulation of the NANOG gene expression allows cell differentiation to occur. NANOG protein expression has been described in testicular intratubular germ cell neoplasia (ITGCN), classic seminoma, and embryonal carcinoma, but is not expressed in yolk sac tumors or teratomas. Published data on NANOG expression in other tumors is limited. In this study, we investigated the expression of NANOG protein in a large series of tumors from various organs using a single immunostaining system (Dako).

Design: Immunohistochemical evaluation of NANOG protein expression [Novus Biologicals, Nanog antibody (5A10)(NBPI-04320)] was performed on 998 tumors from various organs using tissue microarray sections. The staining intensity was graded as weak or strong. The distribution was recorded as negative (<5% of tumor cells stained), 1+ (5-25%), 2+ (26-50%), 3+ (51-75%), or 4+ (>75%).

Results: The positive staining results (%) and the total number of cases for each entity (N) are summarized in Table 1. Fifty-four of 998 cases demonstrated positive nuclear staining for NANOG protein and these cases consisted of testicular ITGCN, embryonal carcinoma, and classic seminoma.

Table 1. Summary of NANOG immunostaining in 998 cases

Tumor	N	# Positive	% Positive
Testicular ITGCN	17	17	100
Testicular classic seminoma	23	22	95.7
Testicular embryonal CA	16	15	93.8
Testicular yolk sac tumor	6		
Testicular spermatocytic seminoma	1		
Testicular Leydig cell tumor	3		
Urothelial CA primary to bladder	31		
Pulmonary neuroendocrine CA	62		
Pulmonary ADC	97		
Pulmonary squamous cell CA	45		
Pancreatic ductal ADC	46		
Pancreatic endocrine CA	14		
Clear cell renal cell CA	30		
Papillary renal cell CA	16		
Infiltrating duct CA of breast	123		
Infiltrating lobular CA of breast	48		
Esophageal ADC	24		
Gastric ADC	13		
Colonic ADC	27		
Hepatocellular CA	17		
Cholangiocarcinoma	5		
Melanoma	72		
Papillary CA of thyroid	41		
Follicular CA of thyroid	31		
Prostatic ADC	124		
Ovarian serous ADC	15		
Endocervical ADC	13		
Endometrial ADC	38		
Total tumors	998	54	5.4

ADC=adenocarcinoma; CA=carcinoma

Conclusions: Our data demonstrate that NANOG is a highly sensitive and specific marker for undifferentiated testicular germ cell tumors including ITGCN, classic seminoma, and embryonal carcinoma. NANOG does not appear to be expressed in testicular yolk sac tumors, or in tumors from other organs.

1058 Multilocular Cystic Renal Cell Carcinoma: Similarities and Differences in Immunoprofile Compared to Clear Cell Renal Cell Carcinoma

SR Williamson, S Halat, JN Eble, DJ Grignon, A Lopez-Beltran, R Montironi, PH Tan, M Wang, S Zhang, GT MacLennan, L Cheng. Indiana University School of Medicine, Indianapolis; Oschner Medical Center, New Orleans; Cordoba University, Cordoba, Spain; Polytechnic University of the Marche Region (Ancona), Ancona, Italy; Singapore General Hospital, Singapore; Case Western Reserve University, Cleveland.

Background: Multilocular cystic renal cell carcinoma (RCC) is an uncommon renal neoplasm, composed of thin fibrous septa lining multiple cystic spaces, associated with an excellent prognosis. Clear cells with generally low-grade nuclear features line cystic spaces and may be present within fibrous septa. Solid mass-forming areas are by definition absent. Findings in a recent study suggested that multilocular cystic RCC is a subtype of clear cell RCC. Immunohistochemical staining characteristics, however, have not been well elucidated.

Design: We studied 19 cases of multilocular cystic RCC, classified according to the 2004 WHO System. Immunohistochemistry was performed on an automated immunostainer for CD10, CK7, alpha-methylacyl-CoA-racemase (AMACR), epithelial membrane antigen (EMA), cytokeratin CAM 5.2, carbonic anhydrase IX (CA-IX), estrogen/progesterone receptors (ER & PR), smooth muscle actin (SMA), PAX-2, and vimentin. Nineteen cases of grade 1-2 clear cell RCC were stained for comparison.

Results: Multilocular cystic RCC and control cases of clear cell RCC showed the following results, respectively: CD10 (58%, 94%), CK7 (89%, 26%), AMACR (16%, 47%), vimentin (42%, 16%), ER (10%, 10%), EMA, CAM 5.2, CA-IX, PAX-2 (all 100%), PR and SMA (both 0%).

Conclusions: Tumors showed expression of common clear cell RCC markers CA-IX, EMA, and PAX-2, in support of the hypothesis that multilocular cystic RCC is a subtype of clear cell RCC. In contrast to clear cell RCC, tumors were less likely to express

CD10 (58%) and more likely to express CK7 (89%). Of note, coexpression of CA-IX and CK7 represents a point of overlap with the recently described clear cell papillary RCC, which also may show a prominent cystic architecture. However, no cases of the latter have exhibited deletion of chromosome 3p by molecular testing.

1059 Urethral Caruncle: Clinicopathologic Features of 41 Cases

SR Williamson, MR Conces, R Montironi, A Lopez-Beltran, M Scarpelli, L Cheng. Indiana University School of Medicine, Indianapolis; Polytechnic University of the Marche Region (Ancona), Ancona, Italy; Cordoba University, Cordoba, Spain.

Background: Urethral caruncle is a benign polypoid mass, occurring at the urethral meatus in primarily postmenopausal women, characterized by hyperplastic epithelium overlying a variably fibrotic, vascular, and inflamed stroma. Although a conclusive association with malignancy, other urologic disorder, or systemic disease has not been established, often the lesion carries a challenging clinical differential diagnosis that includes malignancy. Conversely, unexpected malignancy is sometimes identified in tissue specimens from lesions believed to represent urethral caruncle.

Design: We examined clinical and histopathologic characteristics in 41 patients. Medical records were assessed for presentation, clinical diagnosis, associated urothelial carcinoma, prior radiation treatment, tobacco use, immunologic or urologic disorder, and treatment strategy/outcome.

Results: Average patient age was 68 (range 28–87 years). Presenting symptoms included pain (37%), hematuria (27%), and dysuria (20%). Thirteen patients were asymptomatic (32%). Clinical diagnosis favored malignancy in 10% of cases. Concurrent or subsequent urothelial carcinoma was present for five patients (12%), involving sites elsewhere in the urinary tract. No patient had synchronous or metachronous urethral carcinoma. Histologic features included mixed hyperplastic urothelial and squamous lining, overlying a variably fibrotic, edematous, inflamed, and vascular stroma. Invaginations of urothelium extending into the stroma were common (68%), showing rounded nests with cystic or glandular luminal spaces, similar to urethritis cystica or urethritis glandularis. Intestinal metaplasia was not seen. Two lesions included an organizing thrombus, one with intravascular papillary endothelial hyperplasia or Masson tumor. Twenty patients were treated with topical medications prior to tissue diagnosis without resolution. Three patients were treated for recurrence (7%).

Conclusions: Urethral caruncle is a polypoid urethral lesion that may clinically mimic a variety of benign and malignant conditions. Tissue diagnosis is important, as the clinical differential diagnosis includes malignancy in a subset of cases. We found no conclusive association with urothelial carcinoma, smoking, or previous pelvic irradiation.

1060 Telomere Shortening Distinguishes Inverted Papilloma of the Urinary Bladder from Urothelial Carcinoma with Inverted Growth

SR Williamson, S Zhang, A Lopez-Beltran, R Montironi, L Cheng. Indiana University School of Medicine, Indianapolis; Cordoba University, Cordoba, Spain; Polytechnic University of the Marche Region (Ancona), Ancona, Italy.

Background: Inverted papilloma of the urinary bladder is considered to be a benign neoplasm, characterized by thin inter-anastomosing cords of invaginating urothelial cells, often similar in morphologic appearance to florid von Brunn's nests or cystitis cystica/glandularis of the usual type. However, urothelial carcinoma may occasionally demonstrate a similar inverted growth pattern, creating a challenging differential diagnosis and raising the question of whether the two entities are related. As telomere shortening has been implicated in the development of epithelial malignancy, we investigated relative telomere length in inverted papilloma and urothelial carcinoma with an inverted growth pattern.

Design: Formalin-fixed, paraffin-embedded tissue sections from 59 cases were studied, including 26 cases of inverted papilloma, 9 cases of urothelial carcinoma with inverted growth, and 12 cases of cystitis glandularis. Normal urothelium from the same slide for each of the designated lesions was used as a normal control. Quantitative fluorescence in situ hybridization (FISH) was performed on interphase nuclei utilizing a telomere-specific peptide nucleic acid probe to assess telomeric signal intensity. The relative telomere length was presented as ratio (%) between each lesion and its normal control.

Results: Relative telomere lengths for urothelial carcinoma with inverted growth, inverted papilloma, and cystitis glandularis were 27%, 89%, and 93%, respectively. A statistically significant reduction in relative telomere length between urothelial carcinoma with inverted growth and inverted papilloma was present ($p < 0.001$), while no significant difference was detected between normal urothelium, and cystitis glandularis, and inverted papilloma.

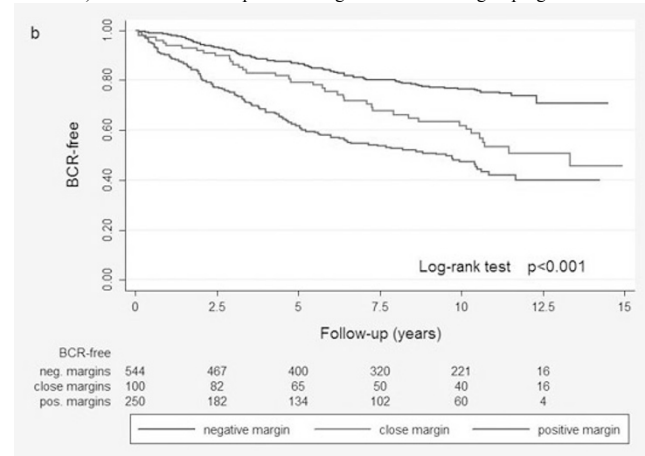
Conclusions: Significant telomere shortening in urothelial carcinoma with inverted growth compared to inverted papilloma contrasts the two lesions and supports the notion that inverted papilloma is a benign neoplasm. Despite the morphologic similarities of the two lesions, they may not share a common pathogenetic mechanism of development. Our findings also suggest telomere FISH may be useful biomarker in distinguishing inverted papilloma from urothelial carcinoma with inverted growth.

1061 Close Surgical Margins after Radical Prostatectomy Are an Independent Predictor of Prostate Cancer Recurrent

G Wirth, J Lu, S Wu, DM Dahl, AF Olumi, WS McDougal, RH Young, C-L Wu. Massachusetts General Hospital, Boston, MA.

Background: The term close surgical margin (CSM) refers to a tumor extending close to (less than 0.1 mm) the inked margin of the radical prostatectomy specimen without reaching it. Current guidelines state that CSM should simply be reported as negative. The clinical significance of CSM has not been fully studied. This study is to evaluate the impact of CSM on the long-term risk of biochemical recurrence following radical prostatectomy.

Design: We identified 1195 consecutive patients who underwent radical prostatectomy for localized prostate cancer in our institution. In 894 of these patients, associations between margin status and location, Gleason score, pathological stage, pre-operative PSA, prostate weight, and age with the risk of biochemical recurrence were examined. **Results:** Six-hundred forty-four of 894 patients (72%) had negative margins. Of these patients, 100 (15.5%) had CSM. In the group with PSA failure, median time to recurrence was 3.5 years. In the group without recurrence, median follow-up was 9.9 years. Cumulative recurrence-free survival differed significantly among the three types of margins (positive, negative and close) ($p < 0.001$). On multivariate analysis, CSM constituted a significant, independent predictor of recurrence (HR 2.23 95%CI 1.08-4.99). Gleason score and positive margins were the strongest prognostic factors.



Conclusions: In this cohort, CSM were independently associated with a two-fold risk of postoperative biochemical recurrence. Further evaluation of the clinical significance of CSM is indicated, as they might be an indicator of local recurrence and of relevance when considering salvage therapy.

1062 Utility of the ERG Immunostain in Conjunction with a PIN4 Cocktail in Classifying Atypical Glandular Lesions in Extended Prostatic Core Biopsies

A Wu, A Young, S Tomlins, A Chinnaiyan, LP Kunju. University of Michigan, Ann Arbor, MI.

Background: The TMPRSS2:ERG gene rearrangement is present in approximately 45% of prostatic adenocarcinomas (PCa). Previously, we characterized an immunostain (IHC) utilizing a monoclonal antibody directed against ERG (EPR3864) as showing diagnostic utility for the detection of ERG rearranged PCa.

Design: Our study examined the utility of the ERG IHC in conjunction with a PIN4 cocktail in classifying atypical lesions in extended (≥ 12) prostatic core biopsies in a large tertiary care center over a 6 month period. All atypical lesions were immunostained with PIN4 cocktail and ERG. Lesion classification pre IHC and post IHC and IHC results were recorded.

Results: Forty four core biopsies were examined including 84% (37/44) with atypical glandular proliferations (25 atypical small acinar proliferations (ASAPs) and 12 atypical large glands); and 16% (7/44) with minute foci of PCa. After IHC, the final diagnoses were 34% (15/44) atypical glandular proliferations (12 ASAPs and 3 atypical large glands); 36% (16/44) PCa (13 minute foci of PCa and 3 PCa with pseudohyperplastic or atrophic features); and 30% (13/44) benign mimics (including partial atrophy and adenosis). Basal markers were negative (100%) and AMACR was positive (95%) in nearly all PCa. All benign mimics showed patchy positivity with basal markers and a subset (25%) were AMACR positive. ERG was positive in 50% (8/16) of all PCas including 62% (8/13) of minute foci of PCa and was negative in all benign mimics. Of all lesions classified as atypical glandular lesions after IHC, one was ERG positive and was classified as atypical small glands adjacent to high grade PIN (PINATYP). In 7% (3/44) of cores, the ERG positivity contributed directly to the diagnosis of PCa, as the foci were very small (2-3 acini). ERG was positive in glands outside the atypical foci in 2 (5%) cases; weak staining was present in a benign gland directly adjacent to a focus of PCa and strong staining was present in HGPIN glands separate from a focus of PINATYP.

Conclusions: Over 50% of the morphologically atypical lesions could be definitively resolved as PCa or benign mimics after IHC with PIN4 cocktail and ERG. ERG was positive in 50% of all PCa, confirming our previous findings, and was negative in all benign mimics. ERG is highly specific for PCa but can stain a subset of HGPIN. Therefore, when utilized in the proper context (HGPIN or PINATYP is excluded), ERG can help diagnose a subset of minute foci of PCa which would otherwise be classified as ASAPs based on morphology and PIN4 cocktail alone.

1063 Clinicopathologic Features of Adenocarcinoma of the Prostate in Men 45 Years Old or Younger Treated by Radical Prostatectomy

J-J Yang, SM Falzarano, K Streater Smith, M Zhou, EA Klein, C Magi-Galluzzi. Cleveland Clinic, Cleveland, OH.

Background: Prostate cancer is typically a disease of older men, with most cases diagnosed in men older than 50 years. Studies have indicated that tumors diagnosed

in younger patients may be associated with unfavorable features. We examined contemporary cases of PCA in men aged 45 years or younger who underwent radical prostatectomy (RP) at our institution.

Design: We queried our radical prostatectomy (RP) database for men diagnosed with PCA from 2000 to 2011. Patients aged 45 years old or younger at the time of RP were included in the study. Race, family history, preoperative and postoperative characteristics were evaluated.

Results: Of the total 4527 men who underwent RP at our institution between 2000 and 2011, 122 (2.7%) were aged 45 years or younger. Patients' median age and preoperative PSA were 44 years (range 36-45), and 4.18 ng/ml (range 0.70-90.80), respectively. Race was recorded for 118 men and distribution was as following: 93 (76%) Whites, 23 (19%) Blacks, and 2 (2%) Hispanics. Positive family history was present in 53 (43%) men: 39 (42%) Whites, 11 (48%) Blacks, 1 (50%) Hispanic, and 2 of unknown race. Biopsy (Bx) Gleason score (GS) was 6 in 92 (76%), 7 in 26 (21%), 8 in 2 (2%), and 9 in 1 (1%). Number of positive Bx cores was <3 in 53 (52%) and ≥3 in 49 (48%) patients. Highest percentage of Bx core involvement was ≤50 in 76 (72%) and >50 in 29 (28%). Eighty-nine (74%) men met the D'Amico criteria for low-risk (LR), 26 (22%) for intermediate-risk (IR) and 5 (4%) for high-risk (HR) disease. RP GS was 6 in 49 (40%), 7 in 67 (55%), ≥8 in 6 (5%). Organ confined (OC) disease was found in 98 (73%) RP specimens: 79 (89%) LR, 18 (69%) IR, and 1 (20%) HR. SVI was present in 5 (4%) cases: 4 HR and 1 IR. Node metastases were detected in 3/46 (6%) cases: 2 HR and 1 IR. Tumor volume was low (<0.5 cc) in 26 (21%), medium (0.5-2.0 cc) in 74 (61%), and extensive (>2.0 cc) in 22 (18%) cases. Margin of resection was positive in 28 (23%) specimens.

Conclusions: Our findings indicate that PCA in men 45 years old or younger tend to present with favorable tumor features and represents potentially curable disease in the majority of case, particularly when meets preoperative low-risk criteria. Family history appears to play an important role in the younger population.

1064 Isolated Secondary Urothelial Dysplasia of the Bladder, a Clinicopathologic Characterization

J-J Yang, E Diaz, D Hansel. Cleveland Clinic, Cleveland, OH.

Background: Isolated secondary urothelial dysplasia is a poorly characterized entity, with no consensus on its progression rate and clinical management. Very little data is published on secondary urothelial dysplasia, with most not differentiating between concurrent secondary dysplasia (dysplasia with concomitant recurrent urothelial carcinoma) versus isolated secondary dysplasia (dysplasia as a sole finding on surveillance biopsy/TUR, in patients with established urothelial carcinoma diagnosis. Concurrent secondary dysplasia, by definition, is 100% progression, and thus should not be included in a secondary progression rate study. This explains the current wide variation in progression rate in published data, from 30 – 100%.

Design: The pathologic and clinical database of our institution was queried for specimens with a diagnosis of isolated secondary dysplasia of the bladder from 1995 to 2007. Isolated secondary urothelial dysplasia was defined as sole diagnosis of dysplasia on surveillance biopsy/TUR, in patients with prior urothelial neoplasia (carcinoma in-situ, low grade urothelial carcinoma and/or high grade urothelial carcinoma). Specimens were reviewed to determine histopathologic features associated with relapse/progression to CIS, low or high grade carcinoma. Patient follow-up was obtained by a retrospective review of clinical records.

Results: 47 patients with isolated secondary urothelial dysplasia of the urinary bladder were identified, with specimens consisting of surveillance biopsy or TUR. Treatment of the initial CIS, low or high grade carcinoma included TUR (37%), TUR+BCG (45.7%), TUR+mitomycin (8.7%), TUR+BCG+mitomycin (4.3%), TUR+chemotherapy (4.3%). Average time between primary diagnosis to finding isolated secondary dysplasia is 2.8 years. As of 2011, the rate of recurrence/progression is 52%, the rate of non-recurrence is 41%, not available 7%. Urine cytology after treatment of primary neoplasia and prior to secondary dysplasia is negative (35%), atypical (24%), positive (6%), or unavailable (35%). The most common features that contributed to a diagnosis of secondary urothelial dysplasia included architectural disorder and increased nuclear size 3-4 times normal.

Conclusions: Isolated secondary urothelial dysplasia is poorly characterized, and its true progression rate is essentially unknown. With our cohort of 46 patients, we find the rate of relapse/progression to be 50%, far less than the 100% of published series that mixed in concurrent secondary dysplasia. This progression rate is notably higher than the 6% progression rate of primary urothelial dysplasia in our earlier study.

1065 Expression of ERG Protein in Human Tumors Using a Highly Specific Anti-ERG Monoclonal Antibody

O Yaskiv, B Rubin, H He, P Carver, C Magi-Galluzzi, M Zhou. North Shore LIJ Laboratories, Lake Success, NY; Cleveland Clinic, Cleveland, OH; Cancer Biology and Glickman Urological Institute, Cleveland, OH.

Background: ERG protein expression, as the result of *TMPRSS:ERG* gene rearrangement in prostate cancer (PCa) and endogenous expression in vascular endothelial cells, is considered highly specific for both PCa and vascular lesions. However, only one study using a mouse anti-ERG antibody investigated the ERG protein expression in other human tissue and tumors. In this study, we studied the ERG expression using a different rabbit anti-ERG monoclonal antibody that is widely used for diagnosis and research of prostate carcinoma.

Design: ERG (Rabbit anti-ERG monoclonal antibody; clone EPR 3864, Epitomics) immunoreactivity was assessed on a tissue microarray comprising epithelial tumors (335 cases), vascular lesions (125 cases) and other non-vascular mesenchymal tumors (82 cases). Vascular endothelial cells were used as an internal positive control with assigned staining score of "strong positive". The expression of ERG protein in tumor cells was scored as negative, weak, moderate and strong.

Results: ERG protein expression was detected in 37% of prostatic adenocarcinoma, 100% of benign vascular tumors (84% strong and 16% moderate staining) and 100% of malignant vascular tumors (85% strong and 15% moderate staining). Additionally, we found moderate positivity in 40% (6/15) of grade I meningiomas, predominantly in fibrous type (5/6, 83%) and transitional type (1/2, 50%). These ERG-positive meningiomas were also positive for Flt-1. Other epithelial and non-epithelial tumors showed absence of ERG expression.

Conclusions: We characterized the ERG protein expression in a wide range of human tumors using a rabbit anti-ERG monoclonal antibody. Such knowledge is important for its clinical use as a prostate carcinoma and vascular specific immunohistochemical marker. ERG protein is detected in approximately 40% of prostate carcinomas and not in any other epithelial tumors. Therefore, a positive ERG immunostain supports the prostatic origin of the epithelial tumors. In addition, positive ERG immunostains are highly sensitive and specific for vascular and lymphatic endothelial cells and therefore can be used in the work-up of benign and malignant vascular lesions. Furthermore, about 40% of meningiomas are also positive for ERG immunohistochemically, probably due to cross-reactivity with Flt-1.

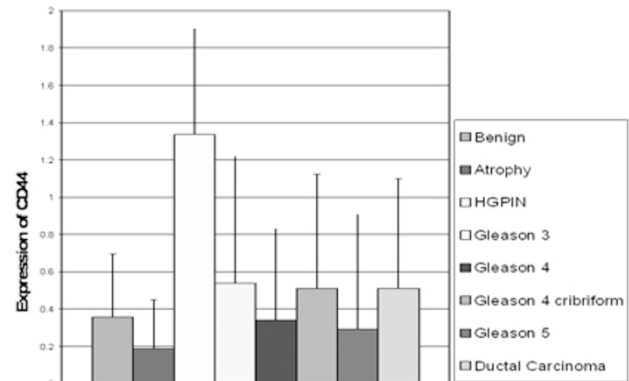
1066 Immunohistochemical Identification of Cancer Stem Cells in Human Prostate Carcinomas

M Yin, J Mays, R Falls. Brody School of Medicine at East Carolina University, Greenville, NC.

Background: Recent evidence indicates that cancer stem cells are responsible for tumor initiation and recurrence. Development of prostatic carcinoma (Pca) resistant to androgen-deprivation therapy has led to hypothesis that Pca contains a subpopulation of stem cells that do not express androgen receptor. Previous in vitro and in vivo studies using cell lines/xenograft tumor models provided compelling evidence that CD44 expression is associated with stem/progenitor cells. CD133 has been used to identify stem cells from leukemia and brain tumors. The purpose of this study is to identify the cancer stem cells in benign and malignant prostatic tissues using putative markers and correlate their expression with grades of tumor differentiation.

Design: Forty eight paraffin-embedded prostatectomy specimens with adenocarcinomas of different Gleason scores were randomly collected for immunohistochemical stains with putative stem cell markers CD44 and CD133. A composite score was calculated as a product of the staining intensity (0 – 3+) multiplying the percentage of positive cells.

Results: The basal cells of benign glands, which are known to have stem cell-like properties without androgen receptors and function as the progenitors of the secretory epithelial cells, are positive for CD44. Benign glandular epithelial cells and invasive carcinomas show a variable, small population of CD44-positive cells.



There was no statistical difference between benign and malignant glands of varying Gleason scores. Interestingly, high-grade prostatic intraepithelial neoplasia (HGPIN) demonstrate abundant epithelial expression of CD44. There was no CD133 staining seen in benign and neoplastic tissue.

Conclusions: CD44 positivity in basal cells confirms that CD44 identifies cells with stem cell-like properties. A small proportion of CD44-positive cells are present in benign and malignant components. Further characterization of these cells may lead to better understanding of tumorigenesis and targeted therapeutics. The study shows no relationship between the number of CD44-positive cells and tumor Gleason scores. The fact that larger numbers of HGPIN cells demonstrate CD44 expression warrants further studies.

1067 Clinical and Pathologic Parameters Predicting Seminal Vesicle Invasion (SVI) Based on 12 Core Prostate Needle Biopsy Protocol

JY Yoon, O Kryvenko, D Schultz, M Diaz Insua, N Gupta. Henry Ford Hospital, Detroit, MI.

Background: Prostate cancer with SVI indicates poor prognosis. In low risk patients, seminal vesicle sparing surgery provides better operative outcome for erectile function or continence. However, prediction of SVI from nomogram or imaging study may not be sufficient. It is generally known that prostate cancer frequently invades seminal vesicles from the prostate base. The aim of this study is to accurately predict SVI from base involvement and other variables based on 12 core biopsy protocol and evaluate the significance of medial base involvement to SVI.

Design: Patients with SVI on radical prostatectomy were identified in a period from 2009 to 2011. Only patients with corresponding previous 12 core biopsies were selected in the study. A control group consisted of consecutive patients who underwent 12 core biopsy protocol and did not show SVI in subsequent RP. T, X² and Fisher's Exact tests

were used for univariate analysis and logistic regression for multivariate analysis.
Results: A total of 55 patients had SVI. Mean serum prostate-specific antigen (PSA) was 8.36 in SVI vs 5.16 in NSVI with high incidence of PSA >10 ng/ml in SVI (16/55) vs NSVI (4/110). Clinical T stage above cT2a was seen in 60% of SVI vs 18.6% of NSVI ($p<0.001$). SVI group showed higher number of positive biopsy cores (6.45 in SVI vs 3.11 in NSVI, $p<0.0001$). The frequency of SVI was high when highest Gleason score on 12 core biopsy was ≥ 437 (67.3% in SVI vs 18.2% in NSVI, $p<0.0001$). Base biopsy was positive in 53/55 (94.5%) patients with SVI, compared with 67/110 (60.9%) patients without seminal vesicle invasion (NSVI) ($p<0.0001$). SVI was frequently seen with either medial or lateral base involvement, highest Gleason score of ≥ 437 at the base, high tumor volume in base biopsy and bilateral base involvement ($p<0.0001$). However, on multivariate analysis, only serum PSA, medial base tumor volume and high Gleason score in base were independent predictors of SVI.

Base involvement on biopsy

	B+ ≥ 437	MB + ≥ 437	LB+ ≥ 437	MB+ TV,%	LB+ TV,%	B+ Bilateral	B+ Unilateral
SVI +	30/52 (57.7%)	24/47 (51.1%)	24/47 (51.1%)	48.5%	52.1%	29/52 (55.8%)	23/52 (44.2%)
SVI -	7/67 (10.4%)	2/32 (6.2%)	6/60 (10%)	7.1%	16.9%	16/67 (23.9%)	51/67 (76.1%)

B:base, MB: Medial base, LB: Lateral base, TV: Tumor volume

Conclusions: Our results show that serum PSA, medial base tumor volume and high Gleason score on base biopsy may be useful predictors of SVI based on 12 core needle biopsy protocol.

1068 Correlation of Urine *TMPPSS2: ERG* and *PCA3* to ERG+ and Total Prostate Cancer Burden

AM Young, N Palanisamy, J Siddiqi, JT Wei, D Wood, AM Chinnaiyan, LP Kunju, SA Tomlins. University of Michigan, Ann Arbor, MI; University of Michigan Medical School, Ann Arbor, MI; University of Michigan Medical School, Ann Arbor, MI.

Background: *ERG* rearrangement, (most commonly resulting in *TMPPSS2:ERG* (*T2:ERG*) gene fusions), have been identified in approximately 50% of prostate cancers (PCa) and to date is the most specific prostate cancer biomarker. Quantification of *T2:ERG* in post-DRE urine, in combination with *PCA3*, improves the serum PSA performance for PCa prediction on biopsy. Previously, we have shown significant correlation between urine *T2:ERG* and maximum index tumor nodule dimension at prostatectomy.

Here we compared urine *T2:ERG* and *PCA3* to both ERG+ and overall tumor burden at prostatectomy to assess the cancer specificity of these urine biomarkers.

Design: Of 301 men presenting for biopsy assessed by transcription mediated amplification (TMA) for *T2:ERG* and *PCA3*, 41 (14%) underwent prostatectomy. All prostatectomies were mapped and all tumor nodules (including suspicious foci) were immunostained with an ERG antibody shown to be sensitive and specific for ERG rearranged cancer (EPR3864). For each prostatectomy, the total number, greatest linear dimension, Gleason score and ERG IHC status of all tumor nodules was documented. Correlations between clinicopathological data and urine *T2:ERG* and *PCA3* were determined.

Results: The 41 prostatectomies had a median of 3 tumor nodules (1-15) and 2.7 cm of total linear tumor dimension (0.5-7.1 cm). There was no significant difference between the number ($p=0.59$) or linear tumor dimension (1.2 cm vs. 0.9 cm, $p=0.36$) of ERG+ and ERG- nodules ($p=0.59$). Urine *T2:ERG* most correlated with the number of ERG+ foci and total ERG+ linear tumor dimension (both $r=0.67$, $p<0.0001$). Of patients with 0 cm, >0.1 to 1.0 cm, and >1.0 cm of total ERG+ linear tumor dimension, 1/8 (13%), 4/10 (40%) and 21/23 (91%) had urine *T2:ERG* >30. Urine *PCA3* showed weaker correlation with both tumor nodule number ($r_s=0.37$, $p=0.02$) and total linear tumor dimension ($r_s=0.27$, $p=0.08$).

Conclusions: We demonstrate a strong correlation between urine *T2:ERG* and total ERG+ tumor burden at prostatectomy. The weaker correlation between urine *PCA3* and total tumor volume suggests that this biomarker may be less cancer specific than *T2:ERG*. Hence, urine *T2:ERG* may be useful for risk stratifying men with elevated serum PSA, prior negative biopsy, or those considering active surveillance.

1069 Construction of Prognostic Model Incorporating Biological Markers To Predict Progression of Non-Muscle-Invasive Bladder Cancer

H-J Yu, C-C Pan. Cardinal Tien Hospital, New Taipei City, Taiwan; Taipei Veterans General Hospital, Taipei, Taiwan.

Background: Non-muscle invasive bladder cancers (NMIBC) run a variable course. The study was conducted to construct a robust multivariate model incorporating clinicopathologic factors and biological markers to predict the risk of progression.

Design: Immunohistochemistry for a series of biological markers (cyclin D1, p27Kip1, p21WAF1, EpCam, E-cadherin, Ki67, p53, *neu*, Cox2, p16, EGFR, PTEN, HSP27) were performed on 616 cases of NMIBC. Multivariate competing risk analyses including clinicopathologic variables (grade, stage, multiplicity, tumor size, prior history of bladder cancer) and expression of markers were performed. Prognostic model was constructed to predict progression based on the variables showing independent significance. Concordance index was calculated with internal validation using 200 bootstrapped resamplings.

Results: For patients without receiving intravesical instillation, the significant factors associated with progression were grade-stage, multiplicity, p53, *neu* and HSP-27. For patients receiving intravesical instillation, the significant factors were grade-stage, prior history of bladder cancer, Ki-67, *neu* and HSP-27. The concordance indices were 0.785 and 0.749 for patients without and with intravesical instillation, respectively. The accuracy was better than the models without including biological markers for the 2 groups (0.732 and 0.695), respectively.

Conclusions: Inclusion of relevant biological markers enhances the prognostication of NMIBC. Based on the multivariate models incorporating both clinicopathologic variables biological markers, NMIBC could be stratified satisfactorily into 3 distinctive groups of high, intermediate and low risk for progression.

1070 PSA and NKX3.1: A Comparative IHC Study of Sensitivity and Specificity in Prostate Cancer

C Yu, D Tacha, R Bremer, T Haas. Biocare Medical, Concord, CA; Mercy Health Sytems, Janesville, WI.

Background: Adenocarcinoma of the prostate can present as metastatic carcinoma, which typically can be confirmed in most metastatic sites by immunohistochemistry with PSA antibodies. A new anti-PSA rabbit monoclonal (RM) antibody has been developed, which theoretically combines the advantages of high affinity, due to its rabbit origin, and high specificity, resulting from its monoclonal nature. Additionally, NKX3.1 protein has recently been shown to be a superior and sensitive marker in the majority of primary and metastatic prostatic adenocarcinomas. This study compared the staining sensitivity of a mouse monoclonal PSA (M) cocktail, a new PSA (RM), and NKX3.1 rabbit polyclonal (P). The PSA (RM) was also tested for specificity in over 600 cases of various normal and neoplastic tissues.

Design: Formalin-fixed paraffin-embedded tissue microarrays (TMA) were deparaffinized in the usual manner, followed by antigen retrieval. PSA (M), PSA (RM) and NKX3.1 (P) were optimized for staining prostate cancers, using an HRP micro-polymer detection system and visualization with DAB.

Results: The PSA (RM) stained 163/167 (98%) cases of prostate cancer, including 94/94 cases with a Gleason score of 3 to 8, and 55/58 (95%) cases with a Gleason score of 9 or 10. All other cancers and normal tissues were 100% negative. Both PSA antibodies stained 67 of 70 (95%) cases and were negative in the same cases (Gleason score 9 and 10). A comparison of PSA (M) and NKX3.1 on 71 cases of prostate adenocarcinoma (Grade II-IV) is summarized in Table 1:

Tumor Grade	PSA (M)	NKX3.1
II	21/22	21/22
III	26/27	26/27
IV	19/22	20/22

Conclusions: The newly developed PSA (RM) was 100% specific and demonstrated equivalent staining to PSA (M), but in some cases provided sharper staining. The NKX3.1 (P) was slightly superior to PSA (M) in grade IV tumors. The strong nuclear staining of NKX3.1 results in easier interpretation of low expression cases, compared to the cytoplasmic staining of PSA, which can be ambiguous in these cases. PSA (RM) and NKX3.1 may be suitable for differential diagnosis, work-ups of tumors of unknown origin and multiplex stains.

1071 CD44 Full-Thickness Immunoreactivity Is More Sensitive Than CK5/6 for the Diagnosis of Flat Urothelial Lesions with Atypia

W Yu, SA Umar, S Yasir, M Jorda. University of Miami Miller School of Medicine, Jackson Memorial Hospital, Sylvester Comprehensive Cancer Center, Miami, FL.

Background: Flat urothelial lesions with atypia can pose a diagnostic dilemma when attempting to make the distinction between reactive urothelial atypia (RUA) and carcinoma in situ (CIS). A recent study suggested that CK5/6 may be a useful biomarker to help in this differential diagnosis. The aim of this study is to determine the diagnostic utility of CK5/6 in comparison to CD44 immunostain in the evaluation of flat urothelial lesions with atypia, since both immunostains demonstrate similar immunoreactive patterns.

Design: Thirty-seven transurethral resection of bladder (TURB) biopsies were evaluated. Twenty-eight (76%) cases comprised RUA with benign clinical follow-up and 9 (24%) CIS cases with classic histomorphologic features. All cases were evaluated by immunohistochemistry for CK5/6 (DAKO, RTU) and CD44 (DAKO, 1:25) using the LSAB method. Intensity and staining patterns were determined for each marker. Sensitivity and specificity for the diagnosis of RUA was determined.

Results: Full-thickness staining for CK5/6 was observed in 20 RUA cases. Negative or weak basal staining for CK5/6 was observed in 8 RUA cases and in all 9 CIS cases. Full-thickness staining for CD44 was observed in all 28 RUA cases and in 1 case of CIS. Negative or weak basal staining for CD44 was observed in 8 CIS cases. Sensitivity and specificity for the diagnosis of RUA were 71% and 100% for CK5/6 immunostain, and 100% and 89% for CD44, respectively.

Conclusions: Full-thickness staining for CD44 is more sensitive than full-thickness staining for CK5/6 for the diagnosis of RUA. CK5/6 does not add diagnostic value in this setting, and therefore should not be used as a substitute for CD44 in the traditional triple stain panel (CD44, CK20 and p53) employed in the differential diagnoses of flat urothelial lesions with atypia.

1072 Depth of Invasion of Urinary Bladder Cancer: Comparison of Direct Measurement Versus 2010 American Joint Committee on Cancer (AJCC) pT2 and 3 Classification

S Zarei, I Frank, SA Boorjian, S Kim, CJ Weight, R Tarrell, P Thapa, JC Cheville. Mayo Clinic, Rochester, MN.

Background: The clinical significance of sub-staging muscle invasive (AJCC pT2a and pT2b) and perivesical fat invasive (AJCC pT3a and pT3b) urinary bladder cancer remains uncertain. The objective of this study was to compare the cancer-specific (CS) outcome of pT2 and pT3 sub-staging and to compare the current AJCC staging system to a direct measurement of depth of invasion into muscularis propria and into perivesical fat.

Design: A search of the Mayo Clinic Cystectomy Registry identified 105 pT2N0 and 144 pT3N0 patients that underwent radical cystectomy or cystoprostatectomy between 1993 and 2003. The clinical and pathologic features of the cases were reviewed, and a measurement in millimeters (mm) of the depth of invasion into muscularis propria (for pT2 patients) and depth of invasion into perivesical fat (for pT3 patients) was recorded. Cancer-specific survival rates among pT2a/b and pT3a/b patient groups and depth of invasion (mm) were compared using the Kaplan-Meier method and Log rank test. Optimal cut-points for depth of invasion (in mm) were estimated using an interactive estimation process of finding the minimum p value with the maximum Hazard ratio.

Results: Of 105 of patients with pT2 bladder cancer (51 pT2a and 54 pT2b), there was no significant difference in CS outcome between pT2a and pT2b and no optimal cutpoint in mm that identified a difference in survival ($p=0.6$). Of 144 patients with pT3 bladder cancer (99 pT3a and 45 pT3b), there was no significant difference in CS survival ($p=0.4$). However, patients with invasion less than 3.5 mm into perivesical fat had a significantly improved CS survival compared to patients with invasion 3.5 mm and greater (CS survival at 5-yrs, 51% versus 33%, respectively; $p<0.03$). Finally, there was a significant difference in CS outcome between patients with overall classification of pT2 versus pT3 tumors (CS survival at 5-yrs, 68% vs. 42%, respectively; $p<0.0002$). **Conclusions:** There is no significant difference in CS survival when pT2 and pT3 tumors were stratified according to the AJCC sub-staging. However, for pT3 tumors, the direct measurement of depth of invasion into perivesical fat identified a significantly different CS survival difference at 3.5 mm. Therefore, pT2a/b should be consolidated into a single pT2 classification while the separation of pT3 into a and b should be based on a direct measurement of the depth of perivesical fat invasion.

1073 LMP2: An Immunohistochemical Marker for the Differential Diagnosis of Renal Oncocytoma and Chromophobe Renal Cell Carcinoma Eosinophilic Variant

G Zheng, A Chaux, R Sharma, G Netto, P Caturegli. Johns Hopkins Hospital, Baltimore, MD.

Background: LMP2, a subunit of the immunoproteasome, has been reported to be overexpressed in oncocytic lesions of the thyroid gland. In this study, we investigated LMP2 expression in non-thyroidal oncocytic lesions. Renal oncocytoma (RO) and the eosinophilic variant of chromophobe renal cell carcinoma (CHRCC-EV) share similar histological features but differ markedly clinically, but a reliable marker to distinguish the two is lacking.

Design: We selected from the Johns Hopkins surgical pathology archive 36 cases of RO and 49 cases of CHRCC, including 7 CHRCC-EV cases. Immunohistochemical staining for LMP2 was performed on routine and tissue microarray (TMA) sections using a standard protocol. Staining was scored for cellular location (nuclear versus cytosolic), intensity (from 0 to 3), and percent of area involved (from 0 to 100%). An H score was calculated by multiplying the intensity with the extent of the staining signal.

Results: A homogeneous cytoplasmic staining was noted in the majority of both RO cases (30 of 34, 88%) and CHRCC cases (37 of 49, 76%). On the contrary, a significant percentage of CHRCC cases (18 of 49, 37%) showed an appreciable nuclear staining (H score ≥ 0.1), which was instead only rarely observed in RO cases (2 of 36, 6%, $p=0.001$ by chi-squared test).

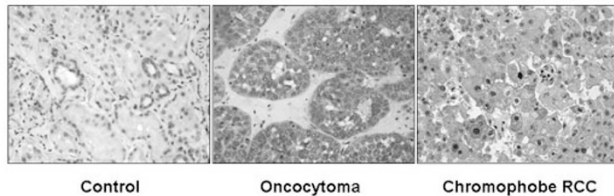


Figure 1 Representative stains of oncocytomas and chromophobe renal cell carcinoma with LMP2 antibody.

Importantly, all 7 CHRCC-EV cases showed an appreciable LMP2 nuclear staining (average H score > 1).

Conclusions: LMP2 is expressed cytosolically in the majority of RO and CHRCC cases, but its nuclear expression can be used to distinguish RO from the eosinophilic variant of CHRCC.

1074 Re-Evaluation of TFE3 Immunostaining in UOK 145 Cell Line and a Novel Subtype of PSF-TFE3 Translocation in Xp11 Translocation Renal Cell Carcinoma

M Zhong, B Zhu, M Brascisco, M Linehan, M Merino, C Cordon-Cardo, D Zhang, S Rohan, X Yang. Northwestern University, Chicago; University of São Paulo, São Paulo, Brazil; NCI, Bethesda; The Mount Sinai School of Medicine, New York.

Background: Xp11 translocation renal cell carcinoma (RCC) is a subtype of RCC characterized by translocations involving a breakpoint at TFE3 gene (Xp11.2). Moderate or strong nuclear TFE3 immunoreactivity has been approved as a specific diagnostic marker for this type of tumor. However, exclusive cytoplasmic localization of TFE3 fusion protein was reported in UOK 145 cell, a RCC cell line harboring PSF-TFE3 translocation. The purpose of this study is to investigate the discrepancy of the literatures, regarding TFE3 staining pattern in Xp11 translocation RCC.

Design: UOK 145 cell line and two other fresh frozen tissues from cytogenetic proved PSF-TFE3 translocation RCC were collected. All samples were subject for histopathologic evaluation, TFE3 IHC, RT-PCR and Sanger sequencing analysis.

Results: Strong nuclear TFE3 staining was demonstrated on all samples including UOK 145 cell line which has been previously reported with exclusively cytoplasmic TFE3 pattern. Previously reported cytoplasmic TFE3 pattern may due to experimental

artifacts, such as transient transfection, GFP interfering subcellular localization. On RT-PCR and Sanger sequencing, UOK 145 cell line and one of PSF-TFE3 translocation RCC were confirmed as previously reported PSF-TFE3 gene fusion with PSF exon 9 to TFE3 exon 6. Interestingly, a novel PSF-TFE3 gene fusion with PSF exon 9 to TFE3 exon 5 was detected in the other RCC sample.

Conclusions: 1. We demonstrated that UOK 145 cell, reported previously with exclusively cytoplasmic TFE3 pattern, is indeed with strong nuclear staining. In addition, one RCC sample with an identical gene fusion as UOK 145 cell line, showed the same nuclear staining.

2. We found a novel PSF-TFE3 gene fusion involving PSF exon 9 to TFE3 exon 5.

1075 Histopathological and Clinical Characterization of Intradiverticular Carcinoma in Urinary Bladder

H Zhong, G Azabdaftari, B Xu. Roswell Park Cancer Institute, Buffalo, NY.

Background: Intradiverticular bladder carcinoma accounts for only 1.5% of all carcinomas arising in the urinary bladder. Its histopathologic features and clinical outcomes are not well characterized due to its rarity. In this study, we analyze a relative large series of intradiverticular carcinoma of bladder with main focus on its histopathological features and clinical outcome.

Design: We identified 21 cases of intradiverticular carcinomas of urinary bladder diagnosed at our institution between 1995 and 2011. Hematoxylin-eosin stained slides were reviewed. Tumor subtype and staging was based on WHO classification of bladder cancer and AJCC Cancer Staging Manual. Clinicopathologic features and patient outcomes were obtained from a retrospective review of patient records.

Results: All patients are Caucasian. Patient's mean age was 68 years (42 to 85) with male to female ratio 20:1. Mean tumor size was 2.1 cm (0.5 to 5.5). 75% tumor involved the lateral walls. Histologically, 8 cases (38%) were non-invasive papillary urothelial carcinoma (UCC), 10 cases (48%) were infiltrating UCC and 3 cases (14%) were small cell carcinoma (SCC). All infiltrating tumors and 5 non-invasive ones were high grade carcinomas. Two SCCs had coexisting high grade infiltrating UCC. Urothelial carcinoma in situ was present in two infiltrating urothelial carcinomas and all three SCCs. Among invasive carcinoma, 9 cases were T1 and 4 cases were T3/4 tumors. More than half (57%) cases showed hypertrophic layer of muscularis mucosa. Synchronous extradiverticular urothelial carcinomas were observed in 5 out of 8 cases (63%) of non-invasive intradiverticular UCC and in 2 out of 10 cases (20%) of infiltrating UCC. Patient follow up (median 30 months) reveal that disease free time was similar between non-invasive and infiltrating UCC (21.5 and 27.5 months, respectively). However, the three SCC cases had much shorter disease free time (1.7 months). Both diseases free time and overall survival was significantly shorter in higher stage (stages III/IV) compared to that of lower stage carcinomas (10.8 and 17.2 months vs 26 and 30.2 months).

Conclusions: Non-invasive intradiverticular bladder carcinomas are more likely to have coexisting synchronous extradiverticular lesions. Hypertrophic muscularis mucosa is a common histological feature of intradiverticular bladder carcinoma, which can pose challenge in tumor staging. SCC recurs shortly after the procedure comparing to its UCC counterpart. Tumor stage remains a key prognostic factor in intradiverticular bladder carcinoma as in the conventional ones.

1076 C-Terminal Portion of Group 3 POTEs Antigen Correlates with Progression of Prostate Cancer

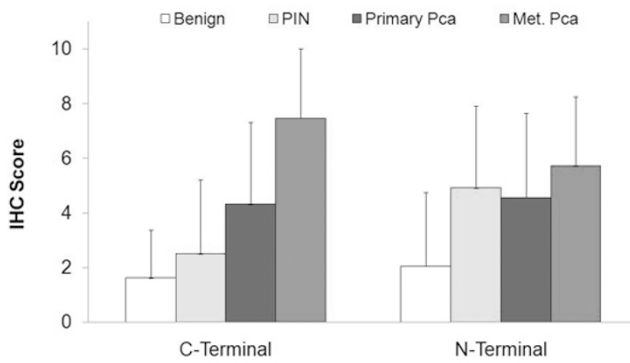
X Zhou, Z He, S Redfield, K Brown, S Bigler. University of Mississippi Medical Center, Jackson.

Background: POTEs, containing 3 domains and encoded by POTE gene family (expressed in prostate, ovary, testis and placenta) have been reported to be expressed in both normal and malignant prostate tissues. Whether the expression levels and which domain of POTEs correlate with the progression of prostate cancer is unknown. The aim of this study is to investigate the association of the expression levels of C- and N-terminals of group 3 POTEs with the progression of prostate cancer.

Design: Immunohistochemistry (IHC) for both C- and N-terminal antibodies was performed on tissue microarrays (TMA) including 260 specimens, which were divided into four groups: benign (34), PIN (36), primary prostate cancer (155) and metastatic prostate cancer (25). A semi quantitative IHC score, calculated by multiplying area score (0-3) and density score (0-3), was used as the expression level and compared among and between the groups.

Results: IHC signals were found in nucleoli for C-terminal and in cytoplasm for N-terminal. The IHC score for C-terminal was the highest in metastatic prostate cancer (7.5), which was dramatically higher than that in primary prostate cancer (4.3, $p=2.4 \times 10^{-5}$), PIN (2.5, $p=3.0 \times 10^{-7}$) and benign prostate (1.6, $p=1 \times 10^{-7}$).

Figure 1 The association of IHC scores for C- and N-terminals with prostate cancer progression



Increasing in the number and irregularity of nucleoli stained for C-terminal correlated with progression of prostate cancer.

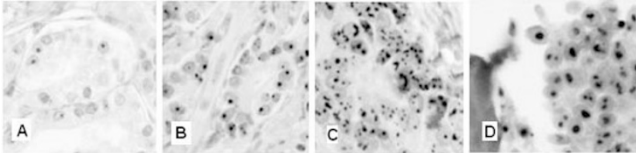


Figure 2 The association of C-terminal nucleolar IHC stain with progression of Pca

The IHC score for N-terminal was the lowest in the benign prostate (2.1), which was significantly lower than that in PIN (4.9, $p=3.3 \times 10^{-6}$), primary prostate cancer (4.6, $p=1.6 \times 10^{-6}$) and metastatic prostate cancer (5.7, $p=2 \times 10^{-7}$); however, there was no significant difference among PIN, primary and metastatic prostate cancer. IHC scores for both C- and N-terminals correlated with the Gleason's grade in primary prostate cancer. **Conclusions:** C-terminal portion of Group 3 POTEs is a nucleolar marker associated with progression of prostate cancer, from PIN to primary prostate cancer, to metastatic prostate cancer.

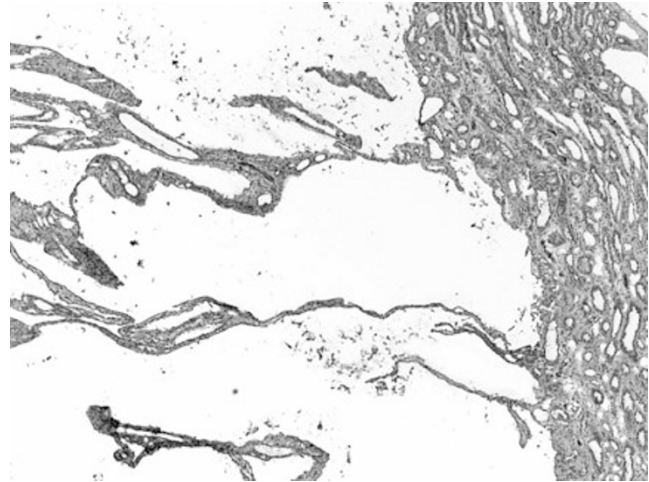
1077 Localized Cystic Disease of the Kidney Masquerading as Cystic Neoplasms

M Zhou, L Chen, R Fan, S Bonsib. New York University, New York, NY; Mayo Clinic Arizona, Scottsdale, AZ; Indiana University Medical School, Indianapolis, IN; Louisiana State University Health Sciences Center, Shreveport, LA.

Background: Cystic changes are common in both neoplastic and non-neoplastic kidney diseases. Some non-neoplastic cystic kidney lesions can be mistaken for cystic neoplasms clinically and radiographically. Accurate diagnosis is critical for patient management. We report the clinicopathological and radiological characteristics of 6 cases of a rare, non-genetic and non-progressive cystic disease, localized cystic disease of the kidney (LCD), that mimicked renal neoplasms and were treated surgically.

Design: LCD was defined as a non-genetic, non-progressive, non-neoplastic and localized cystic lesion. Six such cases were retrieved from the surgical pathology archives of authors' institutions and their clinicopathological and radiological characteristics were analyzed.

Results: Six patients had a mean age of 32.8 years (range 10-56) and included 3 males and 3 females. Two patients had gross hematuria while LCD was discovered incidentally in remaining 4 patients. No personal or family history of cystic renal disease was found in any patient. One patient had solitary kidney rendered by contralateral nephrectomy for renal cell carcinoma. Preoperative imaging studies showed multilocular cystic lesions with a mean size of 3.3 cm (range 2.1-6) and Bosniak II lesion in 3 and Bosniak III lesion in 3 patients. Partial and total nephrectomy was performed in 5 and 1 patients. All 6 lesions arose in the renal papillae without a capsule. Cystic changes also involved overlying cortex in 2 cases. Cysts were lined with cuboidal or flat cells identical to those lining the collecting ducts.



Some cysts were continuous with dilated collecting ducts. Significant inflammation was absent. Single 4-mm urolith was found in one case.

Conclusions: LCD is a rare, non-genetic, non-progressive, non-neoplastic and localized cystic lesion with a characteristic location within the renal papillae. Knowledge of its pathological features can help avoiding misdiagnosing it as cystic neoplasms and may assist preoperative imaging diagnosis.

1078 Intraoperative Frozen Section Evaluation of Ureteral and Urethral Margins: Studies of 212 Consecutive Radical Cystoprostatectomies for Men with Bladder Urothelial Carcinoma

H Zhou, JY Ro, LD Truong, AG Ayala, SS Shen. The Methodist Hospital, Weill Medical College of Cornell University, Houston, TX.

Background: Radical cystoprostatectomy with pelvic lymph nodal dissection is the standard procedure for men with invasive bladder cancer or non-invasive cancer that is resistant to intravesical therapy. Intraoperative frozen section is frequently used to guide the extent of surgery. However, it is still controversial whether intraoperative frozen sections of ureteral and urethral margins are necessary for all patients or a risk-based assessment is the best approach.

Design: A total of 212 men with bladder urothelial carcinoma treated by radical cystoprostatectomy with nodal dissection from 2003 to 2010 in our institution were reviewed. Clinicopathologic features studied include: patients' age, pathologic tumor stage, presence of carcinoma in-situ (CIS), and intraoperative frozen section diagnosis.

Results: The average age of patients in this series was 67.1 years (range 39.2 to 89.1). Tumor stage percentage distribution was as follows: pT0 (7.1%), pTis and pTa (20.3%), pT1 (10.9%), pT2 (19.8%), pT3 (35.4%) and pT4 (4.7%), pTx (1.9%). Among 212 patients, 203 had intraoperative frozen section of ureters, of which 17 (8.4%) had positive margin for CIS (16 cases) or invasive urothelial carcinoma (1 case). Logistic regression analysis showed that positive ureteral margin was not associated with patients' age or tumor stage, but was significantly associated with the presence of CIS in the bladder ($p<0.001$). In bladder cancer patients ($n=110$) who had concomitant CIS, 17 patients (15.5%) had positive frozen ureteral margin, in contrast, none of the patients ($n=93$) had positive frozen ureteral margin when they did not have concomitant CIS. In 37 patients who had urethral frozen sections, 3 patients (8.1%) had positive margin and all of them had concomitant CIS in the bladder.

Conclusions: Our study showed that the rates of positive ureteral and urethral margins during intraoperative frozen section are 8.4% and 8.1% respectively. The presence of concomitant CIS in patient with bladder cancer is highly associated with positive ureteral and urethral margins; therefore, intraoperative frozen section may be helpful in these patients. On the other hand, in patients without concomitant CIS, frozen section of ureteral margin is probably unnecessary.

1079 Clear Cell Renal Cell Carcinomas That Respond to Tyrosine Kinase Inhibitor Sunitinib Have Distinct microRNA Expression Patterns from Non-Responders

M Zhou, K Streater Smith, P Carver, S Falzarano, L Wood, B Rini, C Magi-Galluzzi. Cleveland Clinic, Cleveland, OH; New York University, New York.

Background: The tyrosine-kinase inhibitor sunitinib has emerged as one of the standards of care for metastatic clear cell renal cell carcinoma (mCCRCC). However, lack of therapeutic benefit and significant toxicity are seen in a significant proportion of patients receiving the treatment. Therefore, identification of biomarkers that predict clinical benefit is critical. Recent studies have shown that microRNAs (miRNAs) play critical roles in the development and metastasis of human cancers. We aimed to study whether miRNA expression patterns may predict response to sunitinib in patients with mCCRCC.

Design: Twenty-three patients with mCCRCC were treated with sunitinib and categorized as "responders" (duration of disease control on sunitinib > 12 months) and "non-responders" (lack of any disease control on sunitinib). Whole cell RNA was extracted from formalin-fixed paraffin-embedded (FFPE) pre-treatment nephrectomy specimens. Using high-throughput real-time PCR-based miRNA microarrays, the expression profiles of 768 miRNAs were compared in these two groups.

Results: The expression levels of 12 (1.6%) miRNAs were significantly different between the responders and non-responders ($p<0.05$). The fold change was greater than 2 for 7 miRNAs. MiRNAs miR-187, miR-191*, miR-302c, miR-632, miR-19a*

and miR-1257 were significantly overexpressed in sunitinib responders compared with non-responders and the fold change was 2.1, 2.3, 1.9, 1.9, 1.5 and 1.8, respectively (p values all <0.05). MiRNAs miR-9, miR-138, miR-9*, miR-376a*, miR-144* and miR-223* were significantly down-regulated in sunitinib responders, and the fold change was 0.20, 0.23, 0.21, 0.53, 0.49 and 0.44, respectively (p values all <0.036).

Conclusions: By whole genome miRNA screening, 12 miRNAs were found to have differential expression patterns between CCRCC that responded to sunitinib treatment and non-responders. Several of these miRNAs were reported in the literature to affect the maturation of immune regulatory bone marrow derived dendritic cells (miR-223) and hypoxia inducible pathways (miR-138). These findings suggest that miRNAs could be informative biomarkers for predicting response to tyrosine kinase inhibitors in patients with mCCRCC.

1080 Immunohistochemical Expression of HER2 in Urothelial Carcinoma of the Bladder (UC): Comparison of the Breast Cancer (BC) and Gastric Cancer (GC) HER2 Scoring Systems

B Zhu, X Lin, S Rohan, M Zhong, R Goyal, E Gersbach, X Yang. Northwestern University, Chicago.

Background: Immunohistochemistry (IHC) for HER2 expression is important for determining prognosis and treatment in several types of cancer. HER2 protein expression has been described in UC, ranging from 5% to 98%. The criteria for scoring HER2 IHC expression in BC and GC are well established but differ significantly. In this study, we compare HER2 IHC expression using the GC and BC scoring systems in UC of various grades and micropapillary UC (MPUC) of different stages.

Design: 20 MPUC, 57 high grade UC (HGUC) and 21 low grade UC (LGUC) were evaluated. IHC for HER2 was performed on paraffin-embedded tissues and expression was evaluated using the BC and GC scoring systems. The BC system requires at least 30% tumor cells with complete membrane staining, and is scored as 0 (absent staining), 1+ (faint intensity), 2+ (moderate intensity), and 3+ (strong intensity). The GC system requires at least 10% tumor cells with basolateral staining, and is scored as 0 (absent staining), 1+ (faint intensity), 2+ (moderate intensity), and 3+ (strong intensity).

Results: See tables.

Table1. HER2 expression in MPUC, HGUC and LGUC

Subtypes	BC System		GC System	
	Mean±SD	T test	Mean±SD	T test
MPUC (n=20)	1.65±0.81	*0.668, **0.049	2.15±1.09	*0.069, **0.002
HGUC (n=57)	1.54±1.25	^0.091	1.60±1.27	^0.063
LGUC (n=21)	1.05±1.07		1.05±1.07	

*: MPUC vs. HGUC. **: MPUC vs LGUC. ^: HGUC vs. LGUC

Table2. HER2 expression in different stages of MPUC

Stages	BC System		GC System	
	Mean±SD	T test	Mean±SD	T test
T1 (n=4)	0.75±0.5	*0.059, **0.005	1.00±0.81	*0.16, **0.003
T2 (n=8)	1.63±0.93	^0.183	1.88±1.13	^0.025
T3 (n=8)	2.13±0.35		3.00±0.00	

*:T1 vs. T2 **: T1 vs. T3. ^: T2 vs. T3

Conclusions: 1. Regardless of the scoring system used, there was a trend towards higher expression of HER2 in HGUC compared to LGUC, and in MPUC compared to both HGUC and LGUC. In addition, overexpression of HER2 is seen in higher stage MPUC. These data suggest that HER2 overexpression may be prognostically significant. 2. The GC scoring system appears to correlate better with tumor stage grade than the BC system. The true prognostic and therapeutic relevance of this finding, however, will be dependent upon further studies comparing IHC scoring systems in conjunction with gene amplification studies and the potential clinical trial of HER2-target therapy.

1081 Decreased p63 Expression Is Common in Micropapillary Urothelial Carcinoma (MPUC) and High Grade Urothelial Carcinoma (HGUC)

B Zhu, X Lin, S Rohan, M Zhong, R Goyal, E Gersbach, X Yang. Northwestern University, Chicago.

Background: In normal human tissues strong nuclear p63 protein expression is present in the basal layer of stratified squamous and transitional epithelia. Immunohistochemistry (IHC) for p63 is frequently used in clinical practice to aid in diagnosing urothelial carcinoma (UC). However, loss of p63 expression has been described in high stage UC. Micropapillary urothelial carcinoma (MPUC) is a variant of bladder cancer with an aggressive behavior that frequently presents at an advanced stage. The aim of our study was to investigate p63 IHC in MPUC in comparison to conventional UC of different grades and stages.

Design: IHC for p63 expression was performed on paraffin embedded tissue sections of 23 cases of HGUC, 20 cases of low grade urothelial carcinoma (LGUC) and 20 cases of MPUC. IHC staining was scored semiquantitatively as follows: 0 (no reactivity); 1+ (< 10% cells labeling); 2+ (10 – 50% cells labeling); 3+ (50 – 75% positive); 4+ (75 – 90% positive); and 5+ (> 90% positive). Only nuclear labeling was considered positive.

Results: p63 expression was identified in non-neoplastic surface urothelium in all MPUC cases, however, the MPUC tumor cells were negative for p63 (Table 1). 22% of high stage (pT2 or pT3) HGUC were also negative for p63. Additionally, 22% of pT2 or pT3 HGUC showed only 1+ labeling. In contrast, 60% of low stage (pT1 or pT1) HGUC exhibited more than 3+ labeling. Finally, 70% of LGUC exhibited 5+ (more than 90% tumor cells) labeling for p63.

Table1. P63 staining in MPUC and HGUC

P63 staining	MPUC (n = 20)	Conventional UC (n = 23)
positive	0	19
negative	20	4

Table 2. P63 staining in HGUC

% of tumor cells	pT1s (n = 2)	pT1 (n = 3)	pT2 (n = 15)	pT3 (n = 3)	Total (n = 23)	percentage
negative	0	0	4	0	4	17%
< 10% positive	0	1	3	1	5	21%
10-50% positive	0	1	3	1	5	21%
50-70% positive	0	1	3	0	4	17%
75-90% positive	1	0	1	1	3	13%
> 90% positive	1	0	1	0	2	9%

Conclusions: Our study indicates that p63 IHC is negative in the majority of MPUC cases. Additionally, 44% of high stage (≥ pT2) HGUC exhibited no more than focal (<10% of cells) labeling for p63. All of our LGUCs were positive for p63. Our findings suggest that decreased p63 expression in UC is more common in tumors with aggressive features. Future studies evaluating the utility of p63 as a prognostic marker in UC are warranted.

1082 Micropapillary Urothelial Carcinoma: A Clinicopathological Study of the Experience of One Academic Center

B Zhu, X Lin, S Rohan, M Zhong, R Goyal, E Gersbach, X Yang. Northwestern University, Chicago.

Background: Micropapillary variant of urothelial carcinoma (MPUC) is a rare UC variant. MPUC have been reported in the urinary bladder, ureter and renal pelvis. Its prognosis and treatment is controversial in the literature. Some studies showed the overall prognosis for MPUC is poor and suggest the early treatment with cystectomy. Whereas one study demonstrated that there is no considerable difference between micropapillary pattern positive and negative groups according to the progression rates in non-muscle-invasive and muscle-invasive groups. In this study, we tried to study the clinicopathological correlation of MPUC, particularly comparison to conventional urothelial carcinoma with same grades and same stages.

Design: 23 MPUC, 135 low grade (LG) and 92 high grade (HG) UC are retrieved. The tumor stage, lymphatic invasion and metastasis including lymph node and distant organs are evaluated. Clinical follow-up is up to 8 years.

Results: See tables.

Table 1. The tumor stage of UC

	Non-invasive	Stage T1	Stage T2	Stage ≥ T3	Median
MPUC (n=23)	1 (4%)	6 (26%)	8 (35%)	8 (35%)	T2/≥ T3
HGUC (n=89)	21 (23%)	25 (27%)	27 (29%)	16 (17%)	T2
LGUC (n=135)	132 (98%)	3 (2%)	0 (0%)	0 (0%)	Non-invasive
Total (N = 247)	155 (62%)	33 (13%)	35 (14%)	24 (10%)	Non-invasive

Table 2. Lymphovascular invasion and distant metastasis of UC

	Lymphovascular Invasion	P Value	Distant Metastasis	P Value
Total	MPUC (n=23) 14 (61%)	< 0.001	12 (52%)	< 0.001
	HGUC (n=89) 8 (9%)		6 (7%)	
T1	MPUC (n=6) 2 (33%)	< 0.001	1 (17%)	< 0.001
	HGUC (n=25) 0 (0%)		0 (0%)	
T2	MPUC (n=8) 5 (63%)	< 0.001	6 (75%)	< 0.001
	HGUC (n=27) 1 (4%)		3 (11%)	
≥ T3	MPUC (n=8) 8 (100%)	0.023	6 (75%)	0.004
	HGUC (n=16) 7 (44%)		3 (19%)	

Fisher exact test.

Conclusions: Micropapillary urothelial carcinoma tends to invade deeper (higher stage), and associated with significantly higher incidence of lymphovascular invasion and distant metastasis than conventional high grade urothelial carcinoma, indicating that this variant should be recognized and reported to facilitate studies to understand its molecular mechanism and develop better treatment.

Gynecologic & Obstetrics

1083 Adequacy of Lymphadenectomy in Endometrial Cancer: A Threshold Change Is Needed

G Aggarwal, A Malpica, ED Euscher, P Ramalingam. Georgia Health Sciences University, Augusta; UT MD Anderson Cancer Center, Houston.

Background: Adequate pelvic lymph node (PLN) dissection has been arbitrarily determined, by some authors, as yielding >10 LNs and paraaortic (PALN) dissection as yielding >5LNs. Others have suggested that thorough PLN and PALN dissection should yield a median of 35 and 17 LNs respectively. Recent studies from a large institution have shown that the median yield is 11 for PLN and 6 for PALN in completely submitted tissue. The aim of this study is to assess if this was consistent among a cohort of cases in which LNs and adipose tissue were entirely submitted for histologic evaluation.

Design: We reviewed endometrial carcinomas (EC) from 2007 to present, in which pelvic and/or para-aortic lymph node sampling was performed, including the submission of remaining adipose tissue in entirety, if present. The histologic subtype, FIGO grade and pathologic stage were evaluated for all cases. Total number of LNs in entirely submitted cases as well as presence of additional LNs when the remaining adipose tissue was submitted was recorded. The presence of metastasis if any, in LNs in remaining adipose tissue was determined.

Results: 45 EC with entirely submitted LNs were identified. The patients' age ranged from 34-83 yrs (median 64yrs) and tumor size from 1.0 -8.0cm (median 7.25cm). 32 were endometrioid carcinomas, and 13 were non-endometrioid carcinomas (2 serous carcinomas, 9 mixed carcinomas, 1 clear cell carcinoma and 1 sarcomatoid carcinoma). 29 were FIGO grade 1-2 and 16 were grade 3. Pathologic stage was as follows: 31 pT1, 8 pT2, and 6 pT3. Total number of PLN ranged from 0-22 (median 5) and PALN 1-11 (median 4). Remainder of adipose tissue was submitted in 1-9 cassettes (median 2). Additional LNs were identified 21/45 (47%) cases in which remainder of adipose tissue